

**„Untersuchungen zur Rolle der Glutaminyl-Cyclase bei der pathologischen
Bildung von Pyroglutamyl-Peptiden“**

K u m u l a t i v e D i s s e r t a t i o n

zur Erlangung des akademischen Grades

doctor rerum naturalium (Dr. rer. nat.)

vorgelegt der

Naturwissenschaftlichen Fakultät I

Biowissenschaften

der Martin-Luther-Universität Halle-Wittenberg

von

Herrn Dipl.-Biol. Holger Cynis

geb. am: 05.09.1978 in: Wippra

Gutachter:

1. Prof. Dr. Milton T. Stubbs
2. Prof. Dr. Hans-Ulrich Demuth
3. Prof. Dr. Thomas A. Bayer

Halle (Saale), den 26.01.2009

Inhaltsverzeichnis

	Seite
Abkürzungsverzeichnis.....	3
1 Einleitung und Ziel der Arbeit.....	5
2 Die N-terminale pGlu-Modifikation von Peptiden und Proteinen.....	6
2.1 Vorkommen, Funktion.....	6
2.2 Glutaminyl-Cyclase (QC): Vorkommen, Reaktion.....	11
2.3 Identifizierung und Charakterisierung von Isoenzymen der Säuger-QCs.....	15
3 Glutaminyl-Cyclase - Zielenzym für die Wirkstoffforschung.....	18
3.1. Die mutmaßliche Funktion der QC bei kardiovaskulären Erkrankungen am Beispiel von Restenose.....	18
3.2 Potentielle Rolle der QC bei der Alzheimerschen Erkrankung.....	22
4 Zusammenfassung.....	31
5 Literatur.....	32
6 Angefügte Publikationen und Manuskripte.....	46

Anhang

Abkürzungsverzeichnis

A β	Amyloid- β -Peptid
AAS	Atomabsorptionsspektroskopie
ABri	Amyloid-Peptid der Familiären Britischen Demenz
AD	Alzheimersche Demenz
ADan	Amyloid-Peptid der Familiären Dänischen Demenz
ApoE	Apolipoprotein E
ApP	Aminopeptidase P
APP	„Amyloid Precursor Protein“; Amyloid Präkursor Protein
CCR	„CC-Chemokin“-Rezeptor
CSF	„cerebrospinal fluid“; <i>Liquor cerebrospinalis</i> ; Hirnwasser
CTF	„c-terminal fragment“; C-terminales Fragment
D	Asparaginsäure
DES	„drug-eluting stent“; wirkstofffreisetzender Stent
DP4	Dipeptidylpeptidase 4
E	Glutaminsäure
EDTA	Ethylendiamintetraessigsäure
eNOS	„epithelial nitric oxide synthase“; epitheliale Stickoxidsynthase
ER	Endoplasmatisches Retikulum
FBD	„familial british dementia“; Familiäre Britische Demenz
FDD	„familial danish dementia“; Familiäre Dänische Demenz
FPP	„Fertilization Promoting Peptide“
FSH	Follikel-stimulierendes Hormon
Glu	Glutamat
GnRH	„gonadotropin-releasing hormone“; Gonadoliberin
H	Histidin
HDL	„high density lipoprotein“
LDL	„low density lipoprotein“
LH	Luteinisierendes Hormon
Maldi-TOF-MS	„matrix-assisted laser desorption/ionization time-of-flight“- Massenspektrometrie
MCP-1	„monocyte chemoattractant protein 1“; Monozyten-anlockendes Protein 1

MMP-1	Matrixmetalloproteinase 1
PAM	Peptidylglyzin- α -amidierende Monooxygenase
PS	„presenilin“; Präsenilin
pGlu, pE	Pyroglutamat, Pyroglutamyl-
QC, QPCT	Glutaminyl-Cyclase, „Glutaminyl-Peptide Cyclotransferase“
TRH	„thyrotropin-releasing hormone“; Thyreoliberin
TSH	Thyroidea-stimulierendes Hormon
TXRF	Röntgenfluoreszenz – Totalreflexionsspektroskopie
u.a.	unter anderem
Zn	Zink

1 Einleitung und Ziel der Arbeit

Posttranslationale Modifikationen wie Glykosylierung, Amidierung oder Phosphorylierung spielen eine wichtige Rolle bei der Reifung und Regulation von Proteinen und beeinflussen deren Aktivität und Stabilität im Organismus. So führt die C-terminale Amidierung von Peptiden durch Peptidylglyzin- α -amidierende-Monooxygenase (PAM) zum Schutz vor proteolytischem Abbau durch Carboxypeptidasen und zur Entfaltung der biologischen Aktivität (Eipper et al., 1983; Gale et al., 1988). Neben der C-terminalen Modifizierung von Peptiden ist die Bildung eines N-terminalen pGlu-Restes für eine Reihe von Hormonen und sezernierten Proteinen beschrieben worden. Die pGlu-Modifikation geht aus der intramolekularen Zyklisierung von Glutamin hervor und bildet den N-Terminus von z.B. Thyreoliberin (TRH), Gonadoliberin (GnRH), Neurotensin und Fibronectin (Awade et al., 1994; Blomback, 1967). Die Reaktion wird sowohl im Pflanzenreich als auch bei tierischen Organismen von Glutaminyl-Cyclasen (QC; EC 2.3.2.5) katalysiert (Messer, 1963; Fischer und Spiess, 1987). In Analogie zur C-terminalen Amidierung ist die N-terminale pGlu-Bildung wichtig für die Stabilität und biologische Aktivität der entsprechenden Peptide (Van Damme et al., 1999; Abraham und Podell, 1981). Analysen von Genpolymorphismen in verschiedenen Patientenpopulationen deuten auf eine Verbindung des QPCT-Locus mit der Entstehung von rheumatoider Arthritis (Batliwalla et al., 2005), Osteoporose (Ezura et al., 2004) und Bluthochdruck (Yamada et al., 2007) hin. Des Weiteren sind Pyroglutamyl-Peptide in eine Reihe von neuropathologischen und inflammatorischen Prozessen involviert (Charo und Taubman, 2004; Ogata et al., 1997; Saido et al., 1995). So weisen 25 – 50 % des in der Alzheimerschen Erkrankung abgelagerten β -amyloiden Peptids ($A\beta$) einen N-terminalen pGlu-Rest auf (Saido et al., 1995). Aufgrund zahlreicher Hinweise, dass pGlu-Peptide in verschiedenen pathologischen Prozessen eine Rolle spielen, stellt QC ein potentielles Zielenzym der Wirkstoffforschung dar.

Ziel dieser Arbeit war die Untersuchung der QC-Funktion bei der Generierung der pGlu-Peptide $A\beta_{3(pE)-x}$ und CCL2. Anhand der Bildung von pGlu- $A\beta$ sollten Wege der zellulären Glutamatzyklisierung von $A\beta$ -Peptiden aufgezeigt und die Wirksamkeit neu entwickelter Inhibitoren der QC (Buchholz et al., 2006) nachgewiesen werden. Weitere Untersuchungen waren der Rolle des N-terminalen pGlu-Restes des humanen Chemokins CCL2 und der Wirksamkeit eines QC-Inhibitors in einem inflammatorischen Tiermodell gewidmet.

2 Die N-terminale pGlu-Modifikation von Peptiden und Proteinen

2.1 Vorkommen und Funktion

Einhergehend mit der Verbreitung von Glutaminy-Cyclasen in Invertebraten und Vertebraten sind eine Vielzahl von pGlu-Peptiden in diesen Organismen beschrieben worden, welche sehr unterschiedliche Funktionen erfüllen. Die niedersten Metazoa, in denen pGlu-Peptide nachgewiesen werden konnten, zählen zu den Cnidaria. So weisen die Seeanemonen der Spezies *Anthopleura elegantissima* eine Reihe von Neuropeptiden auf, die einen N-terminalen pGlu-Rest tragen (Tabelle 2.1). Einige dieser pGlu-Neuropeptide lösen bei Muskelpräparationen der Seeanemone *Calliactis parasitica* Kontraktionen aus und werden daher als Neurotransmitter bzw. -modulator betrachtet (Schmutzler et al., 1992). In der maritimen Schnecke *Aplysia californica* sind ebenfalls pGlu-Peptide beschrieben worden. Auch hier handelt es sich um Neuropeptide, welche aus dem abdominalen Ganglion dieser Tiere isoliert werden konnten. Die Funktionen der pGlu-Neuropeptide in *Aplysia californica* sind weitestgehend unbekannt (Garden et al., 1999).

Des Weiteren findet man in Arthropoden eine größere Anzahl verschiedener pGlu-Proteine und -Peptide, denen vielfältige Wirkmechanismen zugeordnet werden. So ist Attacin-C ein Bestandteil der Immunantwort in *Drosophila melanogaster* (Hultmark et al., 1983). Das Adipokinetische Hormon, welches in verschiedenen Arthropoden identifiziert wurde, ist wiederum ein Neuropeptid und Teil der Energiehomöostase. Es wird vermehrt beim Insektenflug ausgeschüttet, bewirkt die Mobilisierung von Fetten und Kohlenhydraten aus dem Fettkörper und stellt so die Deckung des hohen Energiebedarfs während des Fluges sicher. (Oudejans et al., 1999) (Tabelle 2.1). N-terminal modifizierte pGlu-Proteine wurden außerdem im Gift von Spinnentieren nachgewiesen. So wird Discrepin, ein irreversibler Kaliumkanalblocker, durch den Stich eines Skorpions der Gattung *Tityus discrepans* in die Beute injiziert. Discrepin hemmt Kaliumströme von zerebellaren Körnerzellen der Ratte und ist somit ein wirksamer Bestandteil des injizierten Giftgemisches (D'Suze et al., 2004). Die brasilianische Wanderspinnne *Phoneutria nigriventer* injiziert ebenfalls ein sehr potentes Gift, in dem durch massenspektrometrische Analysen eine Reihe von pGlu-Peptiden identifiziert werden konnten, welche strukturell mit Tachykininen verwandt sind. Obwohl eine genauere Untersuchung der Wirkung der injizierten pGlu-Peptide noch aussteht, konnte gezeigt werden, dass sie unter anderem die Kontraktion des Dünndarms eines Meerschweinchens hervorrufen können, eine Eigenschaft, die ebenfalls für Tachykinin beschrieben wurde

(Pimenta et al., 2005) (Tabelle 2.1). Die Rolle des N-terminalen pGlu-Restes der aufgeführten Peptide ist nicht bekannt.

Tabelle 2.1: Ausgewählte pGlu-Peptide und –Proteine aus verschiedenen Stämmen der Invertebraten

Stamm	Art	pGlu-Peptid	Funktion
Cnidaria	<i>Anthopleura elegantissima</i>	Antho-RFamide pE-G-R-F-NH ₂	Neuropeptid
Mollusca	<i>Aplysia californica</i>	R3-14 Peptide pE-E-V-F-D-D-26	Neuropeptid
Arthropoda	<i>Drosophila melanogaster</i>	Attacin-C pE-R-P-Y-T-Q-218	Immunabwehr
	<i>Locusta migratoria</i>	Adipokinetisches Hormon pE-L-N-F-T-P-41	Energiehomöostase
	<i>Tityus discrepans</i>	Discrepin pE-I-D-T-N-V-38	Toxin Irreversibler Kaliumkanalblocker
	<i>Phoneutria nigriventer</i>	PnTkP-XIII pE-K-K-D-K-K-13	Bestandteil des Giftes Wirkung unbekannt

Neben dem Vorkommen von pGlu-Peptiden in Invertebraten sind auch in Vertebraten Proteine beschrieben, welche N-terminal einen pGlu-Rest aufweisen. So werden in den Giftdrüsen von Giftschlangen wie der Braunen Nachtbaumnatter (*Boiga irregularis*) oder der Mangroven-Nachtbaumnatter (*Boiga dendrophila*) verschiedene pGlu-Peptide gebildet, die beim Biss in die Beute injiziert werden (Pawlak and Manjunatha, 2006). Offensichtlich ist das Vorkommen N-terminal blockierter pGlu-Peptide in tierischen Giften evolutionär in verschiedenen Tierstämmen konserviert.

Tabelle 2.2: Ausgewählte humane pGlu-Peptide sowie deren physiologische und pathophysiologische Funktion

Gruppe	pGlu-Peptid	Funktion
Neuropeptide	<u>TRH</u> pE-H-P-NH ₂	Hypophysäre Freisetzung von Prolaktin und TSH Neurotransmitter / -modulator
	<u>GnRH</u> pE-H-W-S-Y-G-L-R-P-G-NH ₂	Hypophysäre Sekretion der Gonadotropine LH und FSH
Hormone	<u>FPP</u> pE-E-P-NH ₂	Spermienreifung
	<u>Gastrin-17</u> pE-G-P-W-L-E-17	Stimulation der HCl-Freisetzung im Magen
Chemokine	<u>CCL2 (MCP-1)</u> pE-P-D-A-I-N-76	Anlockung von Monozyten
	<u>CCL7 (MCP-3)</u> pE-P-V-G-I-N-76	Anlockung von eosinophilen Granulozyten
	<u>CCL8 (MCP2)</u> pE-P-D-S-V-S-76	Anlockung von Monozyten, Lymphozyten, basophilen und neutrophilen Granulozyten
	<u>CCL13 (MCP-4)</u> pE-P-D-A-L-N-75	Anlockung von Monozyten, Lymphozyten, basophilen und eosinophilen Granulozyten
Andere	<u>Fibronektin</u> pE-A-Q-Q-M-V-2355	Zelladhäsionsprotein
	<u>α-Amylase</u> pE-Y-S-S-N-T-496	Speichelprotein Spaltung von α1,4 O-glykosidischen Bindungen
Amyloid	<u>β-amyloid Peptid (Aβ)</u> pE-F-R-H-D-S-40/42	Charakteristisches Peptid von Ablagerungen der Alzheimerschen Erkrankung Aggregation und Ablagerung in amyloiden Plaques
	<u>ABri</u> pE-A-S-N-C-F-...N-I-I-E-E-N-34	Amyloides Peptid der Familiären Britischen Demenz
	<u>ADan</u> pE-A-S-N-C-F-...S-Q-E-K-H-Y-34	Amyloides Peptid der Familiären Dänischen Demenz

Als bekannteste Vertreter der pGlu-Neuropeptide sind TRH und GnRH zu nennen (Awade et al., 1994) (Tabelle 2.2). Diese werden im Hypothalamus gebildet und stellen übergeordnete Schlüsselpeptide der hormonellen Regulation dar. TRH stimuliert zum einen im Hypophysenvorderlappen die Freisetzung von Prolaktin und TSH, ist aber auch als Neurotransmitter oder Neuromodulator beschrieben worden (Nilni and Sevarino, 1999). Der

N-terminale pGlu-Rest des TRH ist essentiell für die Funktion (Abraham and Podell, 1981). GnRH stimuliert die Freisetzung von FSH und LH und gilt somit als übergeordneter Regulator der hypothalamo-hypophysär-gonadalen Achse. Der N-terminale pGlu-Rest hat offensichtlich keinen direkten Einfluss auf die Aktivität von GnRH, jedoch erhöht die pGlu-Bildung die Stabilität von GnRH in humanem Plasma (Morty et al., 2006). Weitere humane pGlu-Neuropeptide sind z.B. Neurotensin (Moore und Black, 1991) und Orexin A (Spinazzi et al., 2006).

Neben pGlu-Hormonen wie Gastrin-17, welches die Salzsäureproduktion im Magen stimuliert (Smith and Watson, 2000) und FPP, einem TRH-Analogen, welches eine Rolle bei der Spermienreifung inne hat (Khan et al., 1992; Green et al., 1996) (Tabelle 2.2), stellen pGlu-Chemokine eine wichtige Gruppe mit zentraler Bedeutung in der Immunabwehr dar.

Im Menschen zählt die Gruppe der „monocyte chemoattractant proteins“ (MCPs) (Tabelle 2.2) sowie Fraktalkin zu den pGlu-modifizierten Chemokinen. Chemokine weisen ein charakteristisches Cystein-Motiv im N-terminalen Bereich auf, welches als Merkmal zur Einteilung in die Klassen „C-“, „CC-“, „CXC-“ und „CX₃C-“ verwendet wird. MCPs gehören zu den „CC-Chemokinen“, für die 2 direkt benachbarte Cysteine charakteristisch sind. Fraktalkin ist dagegen der einzige Vertreter der „CX₃C-Chemokine“, bei dem die Cysteinreste durch 3 weitere Aminosäuren voneinander getrennt sind (Graves und Jiang, 1995; Van Coillie et al., 1999). Chemokine sind Proteine, welche die Anlockung von Immunzellen zu entzündeten Geweben vermitteln. MCP-1 (CCL2) zeigt dabei das höchste Potential zur Rekrutierung von Monozyten (Ugucioni et al., 1995). Es ist jedoch beschrieben, dass MCPs nicht ausschließlich eine Aktivität auf Monozyten besitzen, sondern eine Reihe weiterer Immunzellen anlocken (Tabelle 2.2). In Analogie zur Nomenklatur der „CC-Chemokin“-Liganden werden deren Rezeptoren als CCRs bezeichnet. MCP-1 kann auf einen inflammatorischen Stimulus hin von einer Vielzahl von Zelltypen ausgeschüttet werden. So ist dies unter anderem für Endothelzellen, Fibroblasten, Zellen der glatten Muskulatur und neuronale Zellen beschrieben worden. Nach der Sekretion in den extrazellulären Raum wird MCP-1 von Glukosaminoglykanen der extrazellulären Matrix gebunden. Somit baut sich mit zunehmender Entfernung vom Sekretionsort ein MCP-1-Gradient auf, der in Richtung der entzündeten Stelle weist (Lau et al., 2004; Proudfoot et al., 2003). Des Weiteren wird MCP-1 am Endothel der Blutgefäße gebunden und vermittelt somit die Rekrutierung von Immunzellen, z.B. Monozyten, aus der Blutzirkulation (Ni et al., 2004). MCP-1 induziert weiterhin die Expression des „Scavenger Receptors“ und damit die Differenzierung von Monozyten zu Makrophagen (Tabata et al., 2003).

Für MCP-2 (CCL-8) wurde beschrieben, dass die Bildung des N-terminalen pGlu-Restes essentiell für dessen chemotaktische Potenz ist (Van Coillie et al., 1998). Dies konnte jedoch im Rahmen dieser Arbeit nicht bestätigt werden (Cynis et al., in Vorbereitung, siehe Anhang). Vielmehr legen die Untersuchungen eine stabilisierende Funktion des pGlu-Restes im Falle aller MCPs nahe. Dies ist von besonderem Interesse, da die humanen MCPs nach Spaltung des Sekretionssignals ein N-terminales Gln-Pro-Motiv aufweisen, welches wiederum von Dipeptidylpeptidase 4 (DP4) gespalten werden kann (Van Damme et al., 1999). Jedoch benötigen viele Aminopeptidasen eine protonierte N-terminale Aminogruppe für die Substratbindung. Native MCPs sind daher vor Proteolyse durch Aminopeptidasen, insbesondere DP4, geschützt (Van Coillie et al., 1998) (Cynis et al., in Vorbereitung, siehe Anhang).

Im Gegensatz zu den bisher beschriebenen pGlu-Proteinen, deren N-Terminus durch Zyklisierung eines Glutaminylrestes gebildet wird (Schilling et al., 2003a), stellen die humanen Amyloidpeptide A β , ADan und ABri (Tabelle 2.2) Ausnahmen dar, da in diesen Fällen der Präkursor ein N-terminaler Glutamatrest ist. Obgleich wenig erforscht, ist die enzymkatalysierte Zyklisierung von N-terminalem Glutamat durch einige Beispiele belegt. So können neuronale Extrakte aus *Aplysia californica* Glutamylpeptide zu pGlu umsetzen, nicht jedoch die hitzeinaktivierten Kontrollen. Daher wurde spekuliert, dass es sich hierbei um eine enzymatisch katalysierte Reaktion handelt (Garden et al., 1999). Diese Reaktion ist ebenfalls für zwei Peptide, die aus der Spaltung von Proopiomelanocortin des Rindes hervorgehen, beschrieben worden. So weisen β -Lipotropin und das „joining peptide“ einen teilweise (50 %) blockierten N-Terminus auf, was auf eine Zyklisierung von Glutamat zurückzuführen ist. Dem pGlu-Rest konnte jedoch keine Funktion zugeordnet werden, da die entsprechenden Peptide mit N-terminalem Glutamat ebenfalls aktiv sind (Bateman et al., 1990).

A β wird ursächlich mit der Entstehung der Alzheimerschen Erkrankung, bei der sich große Mengen des Peptides im Gehirn von Patienten ablagern, in Verbindung gebracht. *Post mortem*-Analysen der Zusammensetzung von Amyloidablagerungen im Gehirn verstorbener Patienten zeigten, dass ein großer Teil N-terminal durch pGlu modifiziert ist. Diese pGlu-A β Moleküle sind für neuronale und gliale Zellkulturen toxischer als unzyklisiertes A β (Russo et al., 2002). Des Weiteren zeichnen sich diese Varianten durch ein besonders intensives Aggregationsverhalten aus. Im Vergleich zu A $\beta_{1(D)-x}$ wurde eine bis zu 250fach beschleunigte Bildung von Ablagerungen bestimmt (Schilling et al., 2006). Somit könnte pGlu-A β eine keimbildende Spezies für die Entstehung von neurotoxischen Aggregaten darstellen. Diese Eigenschaften, in Verbindung mit einer sehr frühen Ablagerung von pGlu-A β Molekülen im

Krankheitsverlauf, lassen eine besondere Rolle von pGlu-A β bei der Initiierung der Alzheimerschen Demenz vermuten (Saido, 1998; Hosoda et al., 1998) (siehe Abschnitt 3.2). Die Annahme wird durch Untersuchungen zur Pathologie von familiärer britischer Demenz (FBD) und familiärer dänischer Demenz (FDD) gestützt. Bei diesen vererbbaeren Krankheiten führen Mutationen im „Bri“-Protein zur Bildung von amyloiden Peptiden (ABri in FBD und ADan in FDD), welche ebenfalls mit einem N-terminalen Glutamat beginnen (Vidal et al., 1999; Ghiso et al., 2001a) (Tabelle 2.2). ABri und ADan lagern sich ähnlich dem A β im Hirnparenchym ab. Dabei konnte für ABri gezeigt werden, dass der N-Terminus der abgelagerten Peptide vollständig zu pGlu zyklisiert ist, während in der Blutzirkulation ausschließlich die unzyklisierte ABri-Variante gefunden wird (Ghiso et al., 2001b). Offensichtlich vermittelt die pGlu-Bildung am N-Terminus von verschiedenen amyloiden Peptiden eine beschleunigte Ablagerung und verstärkte Toxizität. Obwohl es sich bei der N-terminalen pGlu-Modifikation um eine enzymatisch katalysierte Reaktion handeln musste (Garden et al., 1999), konnte lange Zeit kein Enzym isoliert werden, welches Glutamat zyklisiert (Shirovani et al., 2002). Kürzlich wurde jedoch mittels Maldi-TOF-MS nachgewiesen, dass QC unter schwach sauren Bedingungen in der Lage ist, N-terminales Glutamat zu pGlu umzusetzen (Schilling et al., 2004). Dadurch ist QC ein potentielles Zielenzym der Wirkstoffforschung für die Behandlung der Alzheimerschen Krankheit.

2.2 Glutaminyl-Cyclase (QC): Vorkommen, Reaktion

Glutaminyl-Cyclasen (E.C. 2.3.2.5, QC, QPCT) gehören zur Gruppe der Aminoacyltransferasen und katalysieren primär die intramolekulare Umsetzung von N-terminalen Glutaminylresten zu pGlu unter Freisetzung von Ammoniak (Fischer und Spiess, 1987; Schilling et al., 2003a) (Abbildung 2.1). Diese Reaktion ist sowohl im Pflanzen-, als auch im Tierreich bekannt. Eine pflanzliche QC wurde erstmals 1963 im Latex der tropischen Pflanze *Carica papaya* beschrieben (Messer, 1963). Erst 24 Jahre später konnte die erste Säuger-QC aus Extrakten von Rinderhypophysen isoliert werden (Fischer und Spiess, 1987). Obgleich pflanzliche und tierische QCs die gleiche Reaktion katalysieren, sind sie offenbar nicht miteinander verwandt. Während tierische QCs wahrscheinlich aus bakteriellen Aminopeptidasen hervorgegangen sind und das für diese Enzyme charakteristische α/β -Hydrolase-Faltungsmuster aufweisen, stellen pflanzliche QCs eine eigene Proteinfamilie dar (Dahl et al., 2000; Booth et al., 2004). Neben der Erstbeschreibung pflanzlicher QCs aus *Carica papaya* konnten zwischenzeitlich weitere, zur Papaya-QC homologe Gene in *Arabidopsis thaliana* und *Solanum tuberosum* identifiziert und kloniert werden (Schilling et

al., 2007b). Eine erste Charakterisierung dieser Proteine zeigte, dass sie wahrscheinlich eine Rolle bei der Pathogenabwehr spielen, da eine Reihe von Proteinen, die während einer Infektion induziert werden, einen N-terminalen pGlu-Rest tragen.

QCs der Säuger wurden bisher aus dem Rind (*Bos taurus*), der Maus (*Mus musculus*), der Ratte (*Rattus norvegicus*) und dem Menschen (*Homo sapiens*) isoliert (Pohl et al., 1991; Schilling et al., 2005; Song et al., 1994; Schilling et al., 2008a). Weiterhin wurden kürzlich QCs aus Arthropoden (*Drosophila melanogaster*) und Schlangen (*Boiga spec.*) charakterisiert (Pawlak and Manjunatha, 2006; Schilling et al., 2007a). Aufgrund der Verbreitung von pGlu-Peptiden und QCs in verschiedenen Tierstämmen wird vermutet, dass QCs in jedem tierischen Organismus konserviert sind. Die QCs der Säuger sind monomere Glykoproteine, die eine molekulare Masse von ca. 40 kDa aufweisen (Fischer und Spiess, 1987; Schilling et al., 2005). Untersuchungen zur Gewebespezifität mittels Northern Blot-Analyse zeigten eine hohe Expression der Rinder-QC in neuronalem Gewebe. So konnten besonders hohe mRNA-Mengen im zerebralen Kortex, dem Striatum und dem Hippocampus nachgewiesen werden. Des Weiteren wurde Rinder-QC ebenfalls in peripheren Organen wie dem Thymus detektiert (Pohl et al., 1991). Eine Analyse der QC-Expression in verschiedenen Gehirnregionen der Maus bestätigte die hohe Konzentration an QC-mRNA in neuronalem Gewebe (Cynis et al., 2008a). Darüber hinaus wurde QC-Aktivität in einer Reihe kultivierter Säugerzelllinien detektiert, welche aus verschiedenen Geweben hervorgegangen sind (Cynis et al., 2006). Somit wird QC offensichtlich ubiquitär aber gewebespezifisch unterschiedlich stark im Säuger exprimiert.

Säuger-QCs besitzen eine N-terminale Signalsequenz, welche den Transport in das Endoplasmatische Retikulum gewährleistet. Nach Passage des Golgi-Apparates wird das Enzym in sekretorische Granulae verpackt und nach dem Transport zur Zelloberfläche sezerniert (Pohl et al., 1991). So konnte unter anderem gezeigt werden, dass Rinder-QC in Analogie zu ihren Produkten TRH und GnRH entlang der Axone des Tractus hypothalamo-hypophysialis in sekretorischen Vesikeln transportiert wird (Bockers et al., 1995). Obgleich noch nicht für TRH oder GnRH gezeigt, ist zu vermuten, dass die QC mit den Präkursoren dieser Peptide kolokalisiert ist und deren Umsetzung in pGlu-Peptide katalysiert.

Tierische QCs sind Metalloenzyme. Bereits bei der Identifizierung der QC aus Schweinehypophyse wurde erkannt, dass der Metallchelator 1,10-Phenanthrolin die QC-Aktivität hemmt. Da EDTA jedoch keine Inhibierung der QC-Aktivität bewirkte, wurde die QC nicht als Metalloenzym klassifiziert (Booth et al., 2004). Ein Vergleich der Aminosäuresequenz der QC mit Vertretern bakterieller Aminopeptidasen des Clans MH

verdeutlichte jedoch, dass die Zn^{2+} -Ion-komplexierenden Aminosäuren dieser Peptidasen (H-D-E-D-H) ebenfalls in den Säuger-QCs konserviert sind (Schilling et al., 2005). Röntgenfluoreszenz-Totalreflexionspektroskopie (TXRF) und Atomabsorptionsspektroskopie (AAS) ergaben ein stöchiometrisches Verhältnis von einem Zn^{2+} -Ion je QC-Molekül (Schilling et al., 2003b; Schilling et al., 2005). Die Kristallisation humaner QC bestätigte anschließend, dass ein Zn^{2+} -Ion im Protein gebunden ist (Huang et al., 2005). Das Zn^{2+} -Ion im aktiven Zentrum wird durch drei Aminosäuren (D-E-H) komplexiert (Schilling et al., 2003b; Schilling et al., 2005). Im Laufe der Evolution kam es offenbar zu Änderungen im aktiven Zentrum der Aminopeptidasen, was zum Verlust einer Zinkbindungsstelle führte (Schilling et al., 2003b).

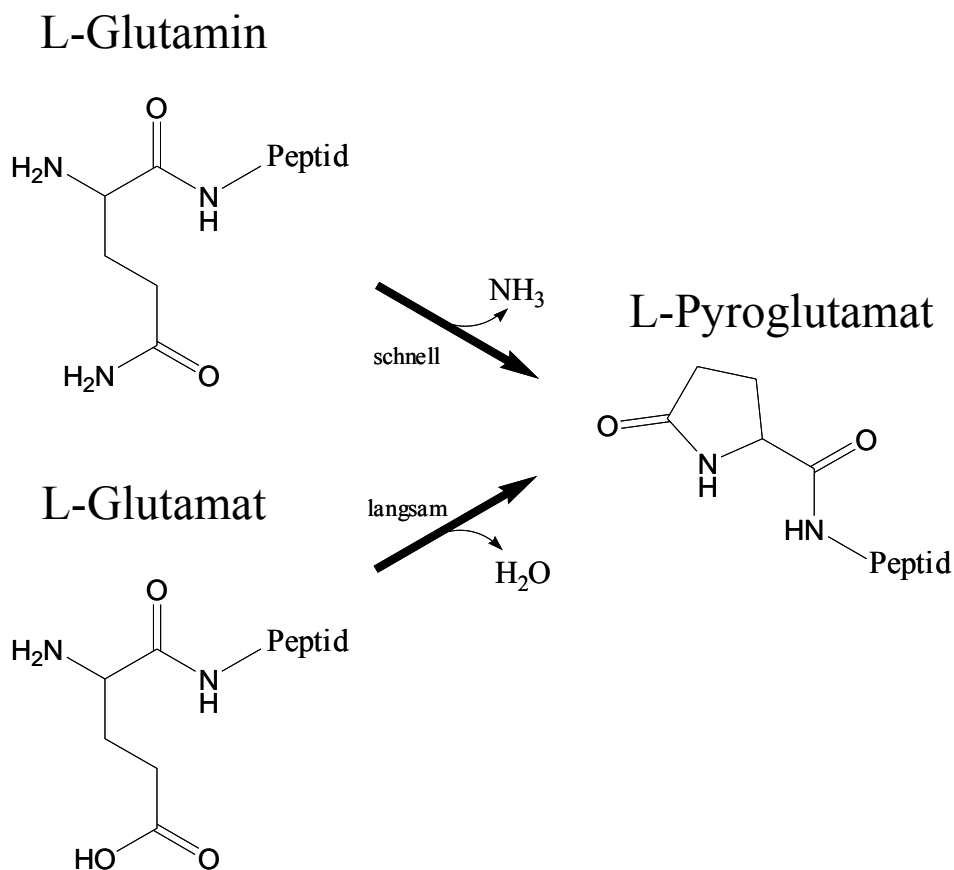


Abbildung 2.1: Schematische Darstellung der Zyklisierung von N-terminalen Glutaminyl- und Glutamylresten

Der exakte Mechanismus der QC-Katalyse ist noch nicht im Detail bekannt. Es wird jedoch vermutet, dass das Zn^{2+} -Ion im aktiven Zentrum eine Polarisierung der γ -Amidgruppe des Substrates bewirkt und im folgenden das Oxanion stabilisiert, welches durch den nukleophilen Angriff des α -Stickstoffatoms an der γ -Carbonylgruppe entsteht (Schilling et al.,

2003b). Das Zn^{2+} -Ion im aktiven Zentrum stellt auch die primäre Interaktionsstelle von kompetitiven Inhibitoren der QC dar. Bisher beschriebene Inhibitoren basieren auf metallkomplexierenden Verbindungen wie Imidazol, Benzimidazol oder Cysteamin (Buchholz et al., 2006; Schilling et al., 2005). Die Interaktion von QC-Inhibitoren mit dem Zn^{2+} -Ion im aktiven Zentrum wurde durch die Kokristallisation von humaner QC mit den Inhibitoren 1-Vinylimidazol, Benzylimidazol und *N*- ω -Acetylhistamin bestätigt (Huang et al., 2005). Eine Untersuchung der katalytischen Spezifität der humanen QC ergab, dass ein breites Spektrum von L-Glutaminylopeptiden umgesetzt wird. Humane QC akzeptiert sowohl kleine Peptidsurrogate wie z.B. H-Glutamin- β -Naphthylamin, als auch längere Substrate wie Neurotensin (13 Aminosäuren) oder MCP-1 (76 Aminosäuren). Man kann jedoch von einer relaxierten Substratspezifität sprechen, da humane QC ebenfalls N-terminales H- β -Homoglutamin umsetzt (Schilling et al., 2003a, Cynis et al., in Vorbereitung, siehe Anhang).

Wie in Abschnitt 2.1 dargelegt, resultiert die pGlu-Modifikation einiger Peptide (z.B. pGlu-A β) aus einer Zyklisierung von N-terminalem Glutamat. (Saido et al., 1995; Ghiso et al., 2001a) (Abbildung 2.1). Im Gegensatz zur schnellen spontanen Zyklisierung von N-terminalem Glutamin zyklisiert N-terminales Glutamat spontan mit einer Halbwertszeit von mehreren Jahren bis Jahrzehnten (Chelius et al., 2006; Yu et al., 2006). Eine unkatalysierte Bildung von pGlu aus einem Glutamyl-Präkursor ist unter physiologischen Bedingungen daher sehr unwahrscheinlich. In primären kortikalen Neuronen konnte eine Glutamatzyklisierung am N-Terminus von A β -Peptiden nicht nachgewiesen werden (Shirotani et al., 2002). Mittels Maldi-TOF-MS konnte später jedoch gezeigt werden, dass QC prinzipiell in der Lage ist, Glutamat zu zyklisieren. Voraussetzung dafür ist offenbar ein unprotonierter N-Terminus und eine protonierte γ -Carboxylgruppe. N-terminales Glutamat liegt bei neutralem pH-Wert überwiegend in zwitterionischer Form vor, da die pK_a -Werte der γ -Carboxylgruppe und der α -Aminogruppe 4,2 bzw. 7,5 betragen. Daher ist die γ -Carboxylgruppe bei neutralem pH-Wert nahezu vollständig deprotoniert und weist keine elektrophile Carbonylaktivität auf. Zwischen den beiden pK_a -Werten (pH 5,2-6,5) liegen beide Gruppen jedoch nur teilweise protoniert vor, was den nukleophilen Angriff der unprotonierten α -Aminogruppe auf die protonierte γ -Carboxylgruppe begünstigt. Somit kann unter schwach sauren Bedingungen N-terminales Glutamat durch QC umgesetzt werden (Schilling et al., 2004), was dem Enzym eine besondere Rolle bei der Entstehung der Alzheimerschen Erkrankung zukommen lassen könnte (siehe Abschnitt 3.2).

2.3 Identifizierung und Charakterisierung von Isoenzymen der Säuger-QCs

Für eine pharmakologische Entwicklung und Testung neuer Wirkstoffe ist es bedeutsam, verwandte Enzyme des Zielenzym in Bezug auf eine Hemmung zu charakterisieren. Kreuzreaktivitäten von Wirkstoffen mit strukturverwandten Enzymen können in der späteren klinischen Entwicklung zu Nebenwirkungen führen (Thornberry and Weber, 2007; Iezzi et al., 2007). Bereits in einer früheren Arbeit wurde vermutet, dass es im Rind unterschiedliche QC-Aktivitäten geben könnte. Diese Annahme beruhte auf Unterschieden in der Detektion von QC-mRNA und Protein im Vergleich zur QC-Aktivität in gereinigten Gewebehomogenaten der Milz und der Hirnanhangdrüse (Sykes et al., 1999). Eine entsprechende kodierende Sequenz des mutmaßlichen Isoenzym wurde jedoch nicht isoliert. Kürzlich konnten verschiedene QCs aus *Drosophila melanogaster* (Drome-QC) isoliert und charakterisiert werden (Schilling et al., 2007a). Im Rahmen dieser Arbeit wurden zur humanen QC homologe DNA-Sequenzen im Menschen und in der Maus identifiziert (Cynis et al., 2008a). Zwischen der h-isoQC und der hQC besteht eine 45 %ige Sequenzidentität. Das Zink-komplexierende Motiv (D-E-H) ist in den Isoenzymen konserviert (siehe Abbildung 2.3). Untersuchungen zur Inhibierung der h-isoQC durch heterozyklische Chelatoren belegen eine metallabhängige Aktivität des Isoenzym. Im Gegensatz zur humanen QC wird h-isoQC auch durch EDTA gehemmt, was ein Hinweis auf Unterschiede in der Architektur und Zugänglichkeit des aktiven Zentrums der h-isoQC sein könnte. Die N-terminalen Bereiche von hQC und h-isoQC weisen eine geringe Homologie auf. Dies führte zu der Annahme, dass beide Enzyme innerhalb der Zelle unterschiedlich lokalisiert sind. Während die QC der Säuger aufgrund des N-terminalen Sekretionssignals kotranslational in das Endoplasmatische Retikulum (ER) transloziert und anschließend sezerniert wird, weisen die Isoenzyme eine N-terminale Transmembranhelix auf. Diese bewirkt offenbar die Retention der h-isoQC im Golgi-Apparat.

h-isoQC zeigt eine sehr ähnliche relative Spezifität wie hQC, jedoch ist die Aktivität gegenüber der Mehrzahl der getesteten Substrate niedriger. Beide Enzyme katalysieren den Umsatz eines breiten Substratspektrums, was die Frage aufwarf, ob sie sich in Bezug auf ihre Gewebeverteilung unterscheiden. Genexpressionsanalysen in Geweben der Maus ergaben eine differentielle Expression der QC mit einer höheren Konzentration in neuronalen Geweben. Im Gegensatz dazu wird die isoQC der Maus (m-isoQC) relativ gleichmäßig in allen getesteten Organen und Geweben exprimiert. Offensichtlich erfüllen beide Enzyme unterschiedliche Funktionen innerhalb verschiedener Gewebe und möglicherweise

katalysieren QC und isoQC den Umsatz verschiedener Substrate aufgrund der unterschiedlichen Lokalisation in der Zelle.

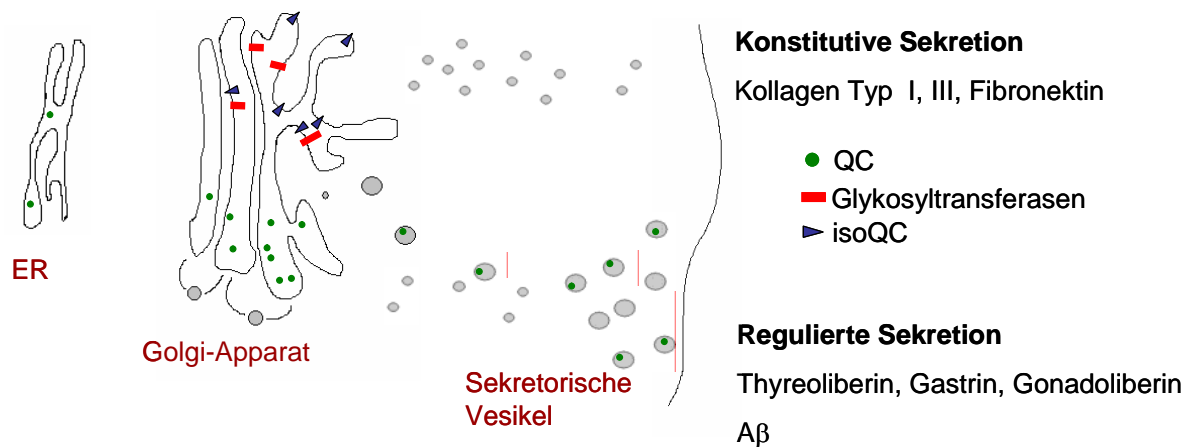


Abbildung 2.2: Schematische Darstellung der postulierten Sekretionswege von pGlu-Peptiden und -Proteinen. QC und isoQC werden post-translational in das ER transloziert und von dort in den Golgi-Apparat transportiert. Durch das N-terminale Retentionssignal der isoQC verbleibt diese im Golgi-Apparat, während QC in sekretorischen Vesikeln zur Plasmamembran transportiert und anschließend sezerniert wird. Bei einer Reihe von pGlu-Peptiden wird der N-terminale Glutaminylrest erst nach Spaltung durch Prohormonkonvertasen in den sekretorischen Vesikeln freigesetzt und ist somit ein potentielles Substrat der QC. Die Sekretion dieser pGlu-Hormone erfolgt in der Regel reguliert nach Stimulation der Zellen. Der konstitutive Sekretionsweg führt dagegen zur Sekretion von z.B. Kollagen und α -Amylase. Der N-terminale Glutaminylrest wird meist bereits im ER nach Spaltung durch Signalpeptidase freigesetzt. Diese Substrate könnten sowohl durch QC als auch durch isoQC zyklisiert werden.

Eine Reihe von pGlu-Hormonen wird aus Prohormonen durch Prohormonkonvertase-Spaltung im späten sekretorischen Weg freigesetzt. Somit kann eine pGlu-Bildung am N-Terminus der freigesetzten Hormon-Präkursoren erst in den sekretorischen Vesikeln erfolgen. Durch die Retention der isoQC im Golgi-Apparat könnte der QC eine besondere Bedeutung in der Modifikation von pGlu-Hormonen zukommen (siehe dazu auch Abbildung 2.2). Die Primärstruktur der isoQC Gene zeigt weiterhin Ähnlichkeiten zu der von Glykosyltransferasen, die ebenfalls eine N-terminale Transmembranhelix und eine luminaire katalytische Domäne besitzen. Offensichtlich stellt die isoQC neben Glykosyltransferasen und Glykanasen einen Bestandteil der enzymatischen Kaskade der Proteinreifung im Golgi-Komplex dar.


```

hQC      --MAGGRHRRVVGTLHLLLLVAALP-----WASRGVSPSASAWPEEKNYHQPAILNS
h-isoQC MEPLLPKRRLLPRVRLPLLLALAVGSAFYTIWSGWHRRTTELPLGRELRVPLIGSLPE
SgAP     -----APDIPL
VpAP     ----MPPITQQATVTAWLPQVDASQITGT-----IS

hQC      SALRQIAEGTSESEMWNLDLQPLLIERYPGSPGSYAARQHIMQR---IQRLQADWVLEID
h-isoQC  ARLRRVVGQLDPQRLWSTYLRPLLVVRTPGSPGNLQVRKFLEAT---LRSLTAGWHVLELD
SGAP     ANVKAHLTQL-----STIAANNNGNRAHGRPGYKASVDYVKAK---LDA--AGYTTTLQ
VpAP     -----SLESFTNRFYTTTSGAQASDWIASEWQALSA--SLPNASVK
                *      ..      . :      :      :      :.

hQC      TFLSQTPYGYRSFSNIIISTLNPT-AKRHLVLACHYDSKYFSHWNNR-VFVGATDDSAVPCA
h-isoQC  PFTASTPLGPVDFGNVATLDPDPR-AARHLTLACHYDSKLFPP-GST-PFVGATDDSAVPCA
SGAP     QFTSGGATGYNLIAN---WPGGD-PNKVLMAGAHLDSSVS-----SGAGINDDNGSGSA
VpAP     QVSHSGYNQ---KSVVMITIGSEAPDEWIVIGGHLDSTIGSHTNEQSVAPGADDDASGIA
                .      .      .      . . : . * **      * D . . *

hQC      MMLELARALDKKLLSLKTVSDSKPDLSLQLIFFDGEEEAFLHWSPQDSLYGSRHLAAKMAS
h-isoQC  LLELAQALD---LELSRAKQAAPVTLQLFLDGEEEALKEWGPKDSLYGSRHLAQLMES
SGAP     AVLETALAVSR-----AGYQPKHLRFAWGAEEL-----GLIGSKFYVNNLPS
VpAP     AVTEVIRVLE-----NNFQPKRSIAFMAYAAEEV-----GLRGSQDLANQYKS
                : *      .:.      .      : :      . E * * : .      *

hQC      TPHPPGARGTSQLHGMDLLVLLDLI---GAPNPTFPNFFPNSARWFERLQAIEHELHELG
h-isoQC  IPHSP---GPTRIQAIEELFMLLDLL---GAPNPTFYSHFPRTVRWFHRLRSIEKRLHRLN
SGAP     ADRS-----KLAGYLNFDMI---GSPNPGYFVYDDDPV-----IEKTFKNYF
VpAP     EGKN-----VVSALQLDMTNYKGSAQDVVFITDYTDS-----NFTQYLTQ-
                :      :      : : * :      * : . :

hQC      LLKDHSLEGRYFQNY----SYGGVIQDDHIPFLRRGVPVLLHLIP-----
h-isoQC  LLQSHPQEVMYFQPG---EPSGSVEDDHIPFLRRGVPVLLHLIS-----
SGAP     AGLNVPTEI-----ETEGDGRSDHAPFKNVGVPVGGLFTGAGYTKSAAQAQKWG
VpAP     -----LMDEYLPSLTYGFDTCGYACSDHASWHAGYPAAMPFE-----
                .      *      . * . : . * * .      :

hQC      ---SPF---PEVWHTMDDNEENLDESTIDNLNKILQVFVLEYLHL-----
h-isoQC  ---TPF---PAVWHTPADTEVNLHPPTVHNLCRILAVFLAEYLGL-----
SGAP     TAGQAF---DRCYHSSCDSLSNINDTALDR-NSDAAAHAIWTLSS--GTGEPPPT---
VpAP     ---SKFNDYNPRI-HTTQDTLANSDPTGSHA-KKFTQLGLAYAIEMGSATGDTPTPPGNQ
                *      H : * . * . .      :

```

Abbildung 2.3: Sequenzvergleich von humaner QC (hQC) und humaner isoQC (h-isoQC) mit Vertretern zinkabhängiger bakterieller Aminopeptidasen aus *Streptomyces griseus* (SGAP) und *Vibrio proteolytica* (VpAP). Das Zink-komplexierende Motiv (H-D-E-D-H) ist sowohl in den beiden menschlichen Enzymen als auch in den Vertretern bakteriellen Ursprungs vorzufinden. Im Gegensatz zu den Aminopeptidasen wird im aktiven Zentrum der Cyclasen nur ein Zn²⁺-Ion gebunden. Die Komplexierung erfolgt durch einen Aspartyl-, Glutamyl- und einen Histidylrest.

3 Glutaminyl-Cyclase - Zielenzym für die Wirkstoffforschung

3.1. Die mutmaßliche Funktion der QC bei kardiovaskulären Erkrankungen am Beispiel von Restenose

Laut Statistischem Bundesamt sind kardiovaskuläre Erkrankungen mit 48 % die Haupttodesursache in Deutschland. Dabei entfallen auf Erkrankungen der Herzkranzgefäße 21 %, Herzinfarkt 8 %, zerebrovaskuläre Erkrankungen 10 % und Schlaganfälle 6 % (Quelle: Statistisches Bundesamt 1999).

Eine Verengung des Gefäßlumens durch Fetteinlagerungen in die Gefäßwand bis hin zum Gefäßverschluß (Arteriosklerose) ist die Hauptursache für die oben aufgeführten Todesfälle. Eine Reihe von Risikofaktoren, wie z.B. Rauchen, *Diabetes mellitus* und Hyperlipidämie begünstigen die Entstehung der Erkrankung (Libby et al., 2002; Libby and Theroux, 2005; Ross, 1999). Die Ausbildung von Arteriosklerose beginnt in der Regel mit einer Funktionseinschränkung oder Verletzung des Endothels, welches die Blutgefäße auskleidet. Erhöhter Blutdruck bewirkt eine verstärkte Expression von endothelialen Adhäsionsmolekülen, wie z.B. ICAM (intercellular adhesion molecule) und VCAM (vascular cell adhesion molecule) (Ferri et al., 1999). Bedingt dadurch können sich Leukozyten anheften, welche unter normalen Bedingungen nicht an Gefäßwände adhären. Anschließend migrieren die Zellen in den subendothelialen Raum (Charo und Taubman, 2004; Libby, 2006).

Eine weitere Ursache für Arteriosklerose ist eine erhöhte Konzentration von Cholesterin im Blut. Cholesterin wird von der Leber bereitgestellt und anschließend als LDL-Cholesterin über die Bindung an Transportproteine (Apolipoprotein B) in die Peripherie transportiert. LDL-Cholesterin kann an Proteoglykane der Gefäßwand binden und dort oxidiert werden. Dieses oxidierte LDL-Cholesterin stellt einen potenten inflammatorischen Stimulus für Makrophagen und Zellen der Gefäßwand dar. Auf einen solchen Stimulus hin kommt es zur Ausschüttung von Chemokinen, insbesondere CCL2, was zu einer vermehrten Einwanderung von Immunzellen, z.B. Monozyten, in die Gefäßwand führt (Libby et al., 2002). Diese differenzieren dort zu Makrophagen und nehmen verstärkt Cholesterin auf. Mit Cholesterin gefüllte Makrophagen werden als Schaumzellen („foam cells“) bezeichnet und sind ein Hauptmerkmal arteriosklerotischer Plaques. Cholesterin wird aus den Makrophagen über Exportproteine (P-Glykoproteine) ausgeschleust und als HDL-Cholesterin (Cholesterin+Apolipoprotein A1) in die Leber transportiert. Dort finden der Abbau und der Abtransport durch Gallenflüssigkeit statt. Ein hoher Spiegel an LDL-Cholesterin wird als

Risikofaktor für Arteriosklerose betrachtet, eine hohe Konzentration von HDL-Cholesterin dagegen als protektiv (Charo und Taubman, 2004; Libby und Theroux, 2005; Libby, 2006).

Neben der Stimulation der Epithelzellen durch oxidierte Lipide können auch mechanische Reize an der Gefäßwand zu Entzündungsreaktionen führen. Die Akkumulation von Schaumzellen verengt das betroffene Gefäß bis hin zum vollständigen Verschluss und behindert so den Blutfluss. Dies hat insbesondere bei Koronararterien akut lebensbedrohliche Zustände zur Folge, da diese Gefäße in der Regel Endarterien sind, bei denen durch das Fehlen von arteriellen Anastomosen die Versorgung nicht von anderen Gefäßen übernommen werden kann. Des Weiteren können arteriosklerotische Plaques rupturieren, was zum thrombotischen Verschluss von Koronararterien führt. Die Folge ist die Unterversorgung von Herzmuskelzellen mit Sauerstoff, welche bei länger anhaltendem Sauerstoffmangel absterben. In Abhängigkeit von der Größe des nicht versorgten Areals kann dies zum Herzversagen und somit zum Tod führen (Kitamoto et al., 2003).

Eine diagnostizierte Stenose wird entweder chirurgisch mittels „Bypass“ umgangen oder durch minimalinvasive Koronarangioplastie aufgeweitet und anschließend durch Platzierung eines Drahtgeflechtes (Stent) stabilisiert. Diese Methoden führen jedoch zur Verletzung des Endothels und in der Folge zu einer Entzündungsreaktion, bei der CCL2 offenbar eine wichtige Rolle spielt. In Analogie zur Entstehung arteriosklerotischer Plaques kommt es zu einer Einwanderung von Monozyten und zur Proliferation und Migration von Zellen der glatten Muskulatur der Gefäße. Die Folge ist ein Wiederverengen (Restenose) des geweiteten Gefäßsegments, was häufig erneute Operationen notwendig macht. Restenose tritt in 20-30 % aller Angioplastien auf (Kitamoto et al., 2003). Momentane Behandlungsstrategien von Restenose basieren u.a. auf der Beschichtung von Stents mit Zytostatika aus den Wirkstoffklassen der Taxol- und Rapamycinderivate (Kastrati et al., 2005). Durch deren proliferationshemmende Eigenschaften wird jedoch die Einheilung des Stents in die Gefäßwand stark behindert. Somit stellen diese wirkstofffreisetzenden Stents („drug-eluting“ stents, DES) ein hohes Risiko für ein post-operatives Auftreten von Thrombosen dar und zeigen den Bedarf an Medikamenten auf, die wirksam das Auftreten von Restenose verhindern, ohne das Einheilen eines Stents zu behindern (Van Belle et al., 2007).

In diesem Zusammenhang konnte gezeigt werden, dass das Auftreten von Restenose mit einer dauerhaften Erhöhung des zirkulierenden CCL2 korreliert. Eine Restenose trat vor allem bei Patienten auf, bei denen sich die CCL2-Konzentration 14 Tage nach der Angioplastie nicht normalisiert hatte (Cipollone et al., 2001). CCL2 ist daher ein Zielprotein der

Wirkstoffforschung. Ein Herabsetzen der Aktivität hat potentiell Einfluss auf das Auftreten von Restenose nach Koronarangioplastie.

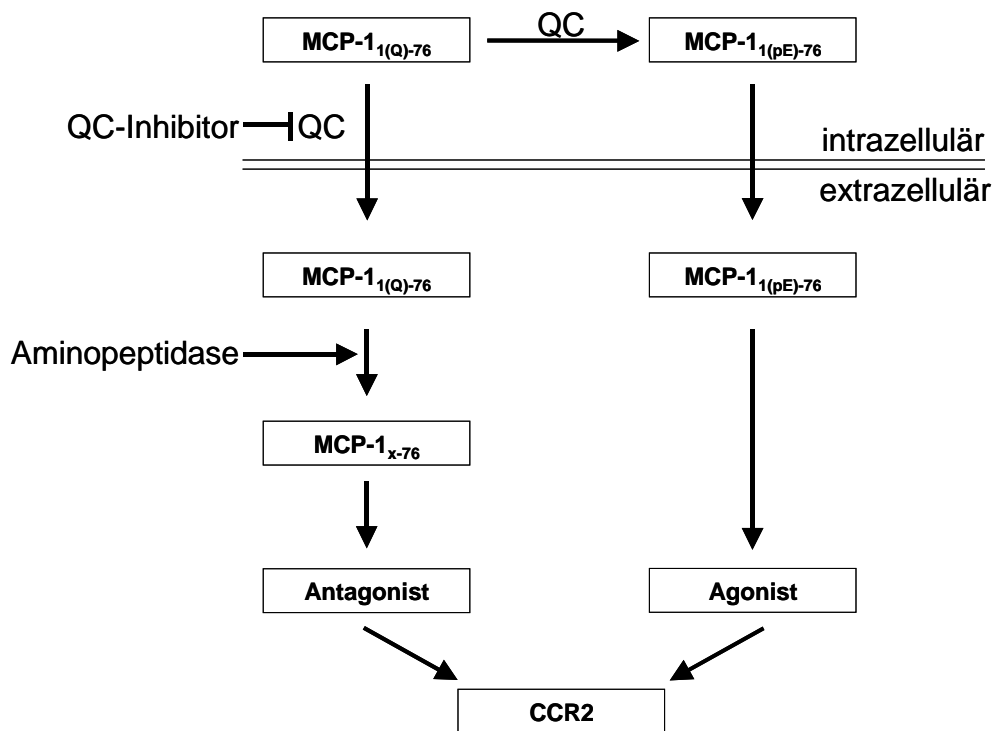


Abbildung 3.1: Wirkprinzip einer Modulation der aktiven CCL2-Konzentration durch Inhibierung der QC/isoQC. Nach Abspaltung des N-terminalen Signalpeptides von CCL2 im ER durch Signalpeptidase wird der freigesetzte Glutaminyl-Rest durch QC-Aktivität cyclisiert. Das auf diesem Wege freigesetzte CCL2_{1(pE)-76} entfaltet eine agonistische Wirkung am CCR2 und führt so zur Anlockung von Monozyten. Die Inhibierung der QC führt dagegen zur Sekretion von unreifem CCL2_{1(Q)-76}, welches durch das Fehlen des N-terminalen pGlu-Restes durch Aminopeptidasen gespalten werden kann (Cynis et al., in Vorbereitung, siehe Anhang). Die so generierten N-terminal verkürzten CCL2-Moleküle können noch an den CCR2 binden, lösen jedoch keine Chemotaxis aus (Proost et al., 1998; Zhang et al., 1994).

Im Rahmen dieser Arbeit konnte gezeigt werden, dass alle Mitglieder der humanen MCP-Familie (CCL2, 7, 8, 13) Substrate der QC sind und die N-terminale Blockierung dieser Chemokine durch einen pGlu-Rest vor Proteolyse durch Aminopeptidasen schützt. Dipeptidylpeptidase IV (DP4) wurde dabei als potentiell Enzym des Abbaus von unreifem CCL2_{1(Q)-76} in humanem Serum identifiziert. Bedingt durch das N-terminale Gln-Pro-Motiv (Tabelle 2.2) sind jedoch alle unreifen humanen MCPs mögliche Substrate für Proteasen, die N- bzw. C-terminal vom Prolin spalten können (Lambeir et al., 2003). Daher wurde die Spaltung von CCL2 durch humane Aminopeptidase P (ApP) untersucht, die den N-terminalen

Glutaminylrest von CCL2_{1(Q)-76} freisetzt. Matrixmetalloproteinase 1 (MMP-1) (McQuibban et al., 2002), welche CCL2 unabhängig von der Bildung des pGlu-Restes am N-Terminus spaltet, zeigte einen schnelleren Umsatz von CCL2_{1(Q)-76} im Vergleich zu CCL2_{1(pE)-76}. Wie in vorangegangenen Untersuchungen bereits gezeigt wurde, ist der N-Terminus von CCL2 von entscheidender Bedeutung für die Anlockung von Immunzellen (Gong and Clark-Lewis, 1995). Jede artifizielle Verlängerung bzw. Verkürzung führte zu einer Einschränkung oder zum Verlust der chemotaktischen Potenz (Abbildung 3.1). Eine Inhibierung der pGlu-Bildung von CCL2, wie hier erstmals gezeigt, führt offensichtlich zu einer Destabilisierung des Chemokins. Dadurch werden zusätzliche Abbauege im Organismus eröffnet und die chemotaktische Wirkung von CCL2 in der Folge herabgesetzt.

Die Hypothese konnte in einem krankheitsrelevanten Tiermodell, welches auf einer „Cuff“-induzierten, beschleunigten Arteriosklerose in ApoE3*Leiden Mäusen beruht, bestätigt werden (Cynis et al., in Vorbereitung, siehe Anhang). Nach Platzierung einer nicht-konstriktiven Manschette („Cuff“) um die *Arteria femoralis* kommt es in Verbindung mit der Zuführung einer cholesterinreichen Diät zu einer massiven Einwanderung von Monozyten in das operierte Gefäßsegment. Infolge dessen ist eine Ausbildung von restenotischen Parametern, z.B. erhöhte Ausschüttung von CCL2, Rekrutierung von Immunzellen und intimale Hyperplasie, zu beobachten. Die Applikation des QC-Inhibitors PBD150 zeigt in diesem Tiermodell eine spezifische Unterdrückung der Rekrutierung von Monozyten durch die Gefäßwand. Weiterhin wurden wichtige arteriosklerotische Parameter wie intimale Hyperplasie und damit verbunden die prozentuale Stenose des Gefäßlumens positiv beeinflusst.

Aufgrund der Identifizierung der isoQC im Rahmen dieser Arbeit ist jedoch unklar, welche QC-Aktivität für die pGlu-Bildung am N-Terminus von CCL2 verantwortlich ist (siehe dazu auch Abschnitt 2.3, Abbildung 2.2). Der N-terminale Glutaminylrest von CCL2 wird bereits im ER nach Spaltung der Signalpeptidase freigesetzt. Somit ist CCL2 im Gegensatz zu einigen pGlu-Hormonen, deren N-terminaler pGlu-Rest erst nach Spaltung einer Prohormonkonvertase in den sekretorischen Granulae demaskiert wird, ein potentielles Substrat sowohl für QC als auch für die isoQC.

Zukünftige Untersuchungen in „knock-out“-Mäusen werden helfen, das Zielenzym für eine Inhibierung der pGlu-Bildung am N-Terminus von CCL2 und A β zu identifizieren. Dies könnte zur Entwicklung spezifischer Inhibitoren beitragen, die gezielt die Bildung des für die jeweilige Pathologie relevanten pGlu-Peptids verhindern und nicht bzw. möglichst nur vermindert in die Reifung anderer pGlu-Peptide eingreifen.

3.2 Potentielle Rolle der QC bei der Alzheimerschen Erkrankung

Die Alzheimersche Erkrankung (AD) ist die häufigste Ursache für eine Altersdemenzkrankung in der westlichen Welt. Derzeit sind ca. 20 - 25 Millionen Menschen betroffen. Die Prävalenz erhöht sich im Alter, und aufgrund der steigenden Lebenserwartung ist in den nächsten Jahren eine weitere Verbreitung der Erkrankung zu erwarten. Frühe Symptome sind unter anderem Vergesslichkeit, zeitliche und räumliche Orientierungslosigkeit und Probleme bei der Erfüllung allgemeiner Aufgaben des täglichen Lebens. Der Verlauf der Erkrankung ist progressiv und endet mit dem Tod. Die Erkrankten bedürfen einer jahrelangen intensiven Betreuung, da in den letzten Stadien der Demenz tägliche Routineaufgaben wie Hygiene und Nahrungsaufnahme nicht mehr selbstständig vorgenommen werden können. Bisher stehen weder eine kausale noch eine wirksame palliative Therapie zur Verfügung.

Histopathologisch ist AD durch eine zunehmende Atrophie des Gehirns charakterisiert, welche molekular durch das Auftreten von extraneuronalen senilen Plaques und einem intraneuronalen neurofibrillärem Geflecht begleitet wird. Beide histopathologischen Merkmale der Demenz werden *post mortem* vor allem in kortikalen und hippocampalen Hirnarealen verstorbener Patienten beobachtet (Saido und Iwata, 2006; Selkoe, 2001). Des Weiteren ist für AD-Patienten ein Defizit des Neurotransmitters Acetylcholin beschrieben worden (Davies und Maloney, 1976). Auf der Behandlung dieser Störung basieren die meisten bisher für die AD-Therapie zugelassenen Pharmaka aus der Klasse der Acetylcholinesteraseinhibitoren (Raschetti et al., 2007), z.B. Rivastigmin, Galantamin und Donepezil. Ein weiterer Wirkstoff für die Behandlung moderater bis schwerer Alzheimerstadien ist der NMDA-Rezeptorantagonist Memantin.

Die molekularen Ursachen, die zur Entstehung der Alzheimerschen Demenz führen, sind noch nicht vollständig bekannt. Als zentraler Bestandteil der „Amyloid-Hypothese“ wird das β -amyloide Peptid ($A\beta$) betrachtet, welches den Hauptbestandteil der senilen Plaques darstellt und als Auslöser der Erkrankung angesehen wird (Selkoe, 2001). Die Primärstruktur von $A\beta$ wurde 1984 aufgeklärt (Glennner und Wong, 1984; Kang et al., 1987). Die hauptsächlichen $A\beta$ -Spezies umfassen 40 ($A\beta_{40}$) oder 42 ($A\beta_{42}$) Aminosäuren, wobei insbesondere $A\beta_{42}$ stärker zur Aggregation neigt (Kuo et al., 1996; Jarrett et al., 1993). Die Bildung der Peptide basiert auf einer sequenziellen Spaltung des "Amyloid Precursor Proteins" (APP), einem Typ I Transmembranprotein, durch β - und γ -Sekretase (Kang et al., 1987; Esler und Wolfe, 2001; Haass et al., 1992). Eine weitere Enzymaktivität (α -Sekretase) führt zur Spaltung innerhalb

der A β -Sequenz und verhindert so die amyloidogene Prozessierung von APP (Selkoe, 2001; Esler und Wolfe, 2001). Die β -Sekretase ist für die Generierung des N-Terminus von A β verantwortlich. Die Aspartatprotease BACE I (E.C. 3.4.23.46) wurde als Enzym mit β -Sekretaseaktivität isoliert und charakterisiert (Vassar et al., 1999; Cai et al., 2001). Zudem gibt es Hinweise, dass BACE I nicht das einzige Enzym ist, welches durch endoproteolytische Spaltung von APP den N-Terminus von A β freisetzen kann (Hook und Reisine, 2003). Die γ -Sekretase spaltet innerhalb der Transmembranhelix von APP und generiert die C-Termini von A β (Esler und Wolfe, 2001) (siehe Abbildung 3.2). Ein Proteinkomplex bestehend aus Nicastrin, Aph, Pen-1 und Präsenilin 1 bildet offenbar die aktive Struktur der γ -Sekretase aus, wobei Präsenilin die katalytisch aktiven Aspartatreste enthält (De Strooper, 2003).

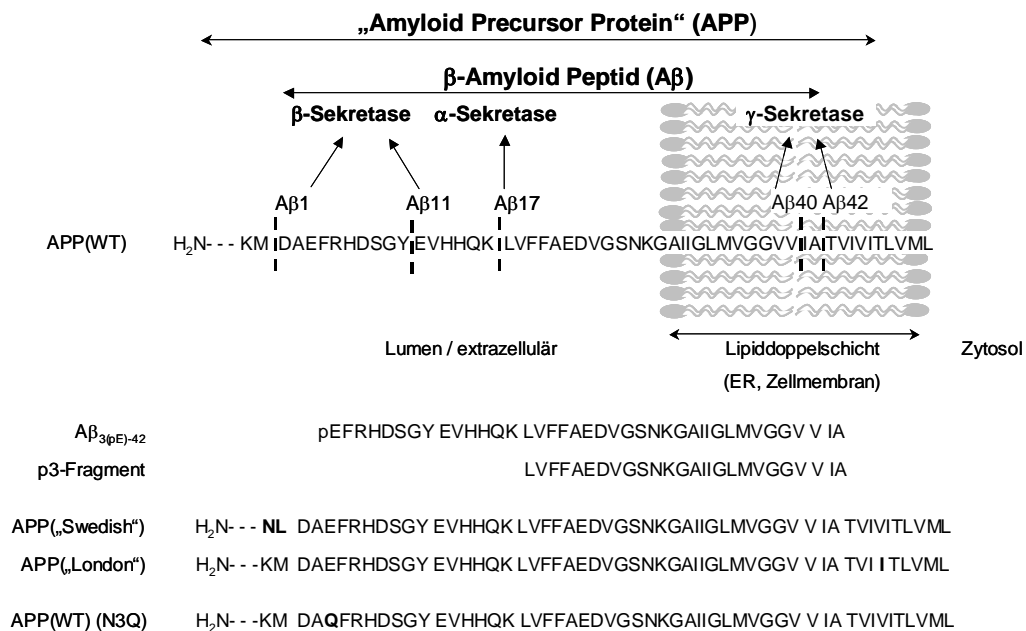


Abbildung 3.2: Die Freisetzung von A β aus APP basiert auf einer sequentiellen Spaltung durch β - und γ -Sekretase. Eine häufige Form, welche *post mortem* in humanem Gehirn detektiert werden kann, ist A β _{3(pE)-40/42}. Diese ist im Vergleich zum A β _{1(D)-40/42} N-terminal um 2 Aminosäuren verkürzt und zyklisiert. Die Spaltung innerhalb der A β -Sequenz durch α -Sekretase verhindert die A β -Bildung. Das nicht-amyloidogene Spaltprodukt von α - und γ -Sekretase wird als p3-Fragment bezeichnet. Bisher beschriebene, familiär vererbte Formen der Alzheimerschen Demenz betreffen unter anderem das APP-Gen. So wird die Doppelmutation KM596/596NL („Swedish Mutation“) innerhalb einer schwedischen Familie vererbt. Durch die Mutation wird die Spaltaktivität durch die β -Sekretase erhöht. Die „London Mutation“ V642I liegt dagegen C-terminal der γ -Sekretasespaltstelle und führt zu einer verstärkten Bildung von A β ₄₂. Zur Aufklärung des Weges, der zu N-terminal verkürzten A β -Peptiden führt, wurde im Rahmen dieser Arbeit die Punktmutation E599Q („N3Q“) eingeführt, welche als Kontrollmutation die rasche Bildung von pGlu-A β nach der Freisetzung anzeigt.

Die Aufklärung der molekularen Grundlagen von AD ist durch die Untersuchung von familiären Formen der Erkrankung beschleunigt worden. Es wurden u.a. Mutationen in den Genen APP, PS1 und PS2 mit einem frühzeitigen Ausbruch von AD in Verbindung gebracht („early-onset“ AD). Dies beruht auf einer Erhöhung der Menge von gebildetem A β bzw. einer verstärkten Bildung von A β ₄₂ (Haass et al., 1995; Sudoh et al., 1998; Scheuner et al., 1996) (Tabelle 3.1). Offensichtlich korreliert auch das ϵ 4-Allel von Apolipoprotein E mit einer familiär vererbaren Form von AD, die zwar gegenüber anderen familiär vererbaren Formen einen späten Ausbruch der Krankheit, aber im Vergleich zum Bevölkerungsdurchschnitt eine Erhöhung der Inzidenz bewirkt („late onset“ AD) (Saunders et al., 1993). Von den familiär vererbten Formen der Alzheimerschen Demenz werden die sporadischen Fälle unterschieden, welche den Hauptanteil darstellen. Studien an eineiigen Zwillingen zeigen jedoch, dass es für die Ausprägung einer Alzheimerschen Demenz in mehr als 50 % der Fälle eine genetische Prädisposition geben muss (Gatz et al., 2005). Untersuchungen an Tiermodellen zeigen weiterhin, dass die neuropathologischen Veränderungen immer an eine Bildung von A β ₄₂ geknüpft sind.

Tabelle 3.1: Ausgewählte Genmutationen, die mit vererbten Formen der Alzheimerschen Krankheit in Verbindung gebracht werden. Die Aminosäureposition ist von der APP695-Isoform abgeleitet.

Gen	Mutation	Pathologie
APP	KM595/596NL („Swedish Mutation“)	Progressive Demenz mit AD-typischen Symptomen Erhöhung der A β -Sekretion um den Faktor 6-8 Alter bei Diagnose: ca. 55 Jahre (Mullan et al., 1992; Citron et al., 1992)
	V642I („London Mutation“)	Progressive Demenz mit AD-typischen Symptomen Verschiebung der γ -Sekretasespaltung hin zur verstärkten Bildung von A β ₄₂ Alter bei Diagnose: ca. 55 Jahre (Eckman et al., 1997)
	E618G („Arctic Mutation“)	Progressive Demenz mit AD-typischen Symptomen Erhöhte Bildung von A β -Protofibrillen Alter bei Diagnose: 57 Jahre (Nilsberth et al., 2001)
	E618Q („Dutch Mutation“)	Hereditäre zerebrale Hämorrhagie mit Amyloidose, holländischer Typ A β -Ablagerungen in zerebralen Blutgefäßen in Verbindung mit Hirnblutungen Alter bei Diagnose: ca. 50-55 Jahre (Levy et al., 1990)

Gen	Mutation	Pathologie
Präsenilin 1	V261I	Progressive Demenz mit AD-typischen Symptomen Ablagerung von N-terminal verkürzten A β -Peptiden, vor allem A $\beta_{3(pE)-42}$ Alter bei Diagnose: 48 Jahre (Miravalle et al., 2005)
	M233T	Progressive Demenz mit AD-typischen Symptomen Erhöhte Bildung von A β_{42} Alter bei Diagnose: 30-35 Jahre (Kwok et al., 1997)
Präsenilin 2	M239V	Progressive Demenz mit AD-typischen Symptomen Alter bei Diagnose: 45-88 Jahre (Sherrington et al., 1996)
ApoE4	ϵ 4 Allel	Steigende Gendosis des ϵ 4 Allels von heterozygot zu homozygot erhöht das Risiko einer AD-Erkrankung von ca. 20 % auf ca. 90 % Alter bei Diagnose: 68 Jahre (Saunders et al., 1993; Corder et al., 1993)

Neben den C-terminalen Varianten unterscheiden sich die Amyloidpeptide jedoch auch am N-Terminus. Modifikationen betreffen die Aspartatreste an Position 1 und 7, welche in isomerisierter oder racemisierter Form vorliegen können, sowie die Glutamatreste an Position 3 und 11, welche durch intramolekulare Zyklisierung pGlu ausbilden (Roher et al., 1993; Saido et al., 1995). N-terminal verkürzte und pGlu-modifizierte A β -Peptide stellen die häufigste A β -Spezies im Gehirn verstorbener Patienten dar (Saido et al., 1996). Zudem gibt es Hinweise, dass A $\beta_{3(pE)-42}$ die eigentlich toxische Form in der Amyloidkaskade ist (Schilling et al., 2006; Güntert et al., 2006).

Es wurden bisher eine Reihe von Mausmodellen generiert, in denen gezielt molekulare Vorgänge der Alzheimerschen Krankheit, wie z.B. Plauepathologie durch Überexpression von mutiertem APP oder intraneuronales fibrilläres Geflecht, nachgebildet werden. Ein wichtiger Unterschied zwischen APP-transgenen Mäusen und der menschlichen Situation ist jedoch, dass in nahezu allen Modellen N-terminal verkürzte A β -Varianten nur eine unterrepräsentierte Spezies sind (Kawarabayashi et al., 2001). A $\beta_{1(D)-40/42}$ stellt in der Mehrzahl der Mausmodelle, die familiäre Varianten des humanen APP-Gens exprimieren, die Hauptspezies dar. Kürzlich beschriebene Tiermodelle, die auf einer Expression mehrerer mutierter Proteine beruhen, zeigen einen höheren Anteil von N-terminal modifiziertem A β und erstmals eine A β -bedingte Neurodegeneration (Casas et al., 2004). In der Alzheimerschen Demenz wird A $\beta_{3(pE)-42}$ sehr früh im Krankheitsverlauf abgelagert und ist toxischer für

neuronale und gliale Primärzellkulturen als $A\beta_{1(D)-40/42}$ (Russo et al., 2002; Hosoda et al., 1998). Des Weiteren trägt die pGlu-Modifikation zu einer Stabilisierung der $A\beta$ -Peptide bei, die daraufhin schlechter von kultivierten Astrozyten abgebaut werden können (Russo et al., 2002). Darüber hinaus zeigt $A\beta_{3(pE)-40/42}$ eine um das 250fache erhöhte Tendenz zur Aggregation im Vergleich zu unmodifiziertem $A\beta$. Die typische lag-Phase der Aggregation *in vitro* wurde unter schwach sauren pH-Bedingungen im Fall von pGlu- $A\beta$ nicht beobachtet, was auf eine dramatisch beschleunigte Bildung von Aggregationskeimen hindeutet. Dabei bewirkt die Aggregation offenbar auch eine Oligomerisierung anderer $A\beta$ -Peptide (Schilling et al., 2006). Somit könnte $A\beta_{3(pE)-x}$ eine keimbildende $A\beta$ -Spezies sein, die als Initiator der Amyloidkaskade der Alzheimerschen Demenz fungiert.

APP unterliegt einem sehr hohen Umsatz innerhalb eines Tages und $A\beta$ ist, obwohl es das Schlüsselpeptid für die Entstehung von AD zu sein scheint, ein physiologisches Peptid, welches ständig aus APP freigesetzt wird (Savage et al., 1998; Bateman et al., 2006). Dem Molekül konnte bisher keine Funktion zweifelsfrei zugeordnet werden. Offensichtlich stellt die Bildung und der Abbau von $A\beta$ eine Homöostase dar, welche durch das Auftreten von proteolytisch resistenten $A\beta$ -Spezies gestört wird und es so zu einer Aggregation und Ablagerung im Hirnparenchym kommen kann (Saido, 1998). Der Bildung von pGlu- $A\beta$ -Molekülen könnte hierbei eine besondere Bedeutung zukommen, da diese durch $A\beta$ -abbauende Enzyme wie Neprilysin (E.C. 3.4.24.11) schlechter gespalten werden und eine deutlich erhöhte Halbwertszeit aufweisen (Takaomi C. Saido, persönliche Kommunikation).

Die mögliche Beteiligung der QC an der Bildung von pGlu- $A\beta$ konnte im Rahmen dieser Arbeit anhand von Zellkulturuntersuchungen bestätigt werden. Eine Koexpression von QC mit verschiedenen $A\beta$ -freisetzenden Genkonstrukten bestätigte eine enzymatisch katalysierte Zyklisierung von N-terminalem Glutamat (Cynis et al., 2008b). Bedeutsam ist dabei, dass die Glutamatzyklisierung hauptsächlich intrazellulär stattfindet (Cynis et al., 2008b). Offenbar sind QC und $A\beta$ bzw. β -CTFs während des Transportes zur Plasmamembran co-lokalisiert, was mittels Immunhistochemie bestätigt werden konnte. QC und $A\beta$ könnten demnach in sekretorischen Vesikeln vorliegen, was eine hohe Konzentration von Enzym und Substrat impliziert und damit verbunden die ansonsten unter *in vitro* Bedingungen relativ langsam verlaufende Glutamatzyklisierung durch deren Kompartimentierung begünstigt (Cynis et al., 2008b). Des Weiteren ist für Vesikel des sekretorischen Weges ein schwach saurer pH-Wert beschrieben worden, der mit dem Optimum der enzymatischen Katalyse der Glutamatzyklisierung übereinstimmt. Obwohl $A\beta$ -Ablagerungen in der Regel als extrazellulär

beschrieben worden sind, gibt es einige Hinweise für eine besondere Rolle von intrazellulärem A β , welches anscheinend vor dem Auftreten der ersten extraneuronalen Plaques beobachtet werden kann (Billings et al., 2005). Damit besteht die Möglichkeit, dass intraneuronal gebildetes pGlu-A β die initialen Kristallisationskeime für die Aggregation von weiteren A β -Molekülen darstellt. Durch die hauptsächlich intrazelluläre Bildung von pGlu-A β werden die Anforderungen für QC-Inhibitoren definiert, welche eine Passage der Blut-Hirnschranke, die Penetration der entsprechenden Neurone und die Bindung an die QC unter schwach sauren Bedingungen sind.

Eine Verringerung der Bildung von pGlu-A β wurde nach Injektion von A $\beta_{3(E)-40}$ in den Kortex von Ratten bestätigt. Unter diesen Bedingungen konnte eine teilweise Umsetzung von A $\beta_{3(E)-40}$ zu A $\beta_{3(pE)-40}$ innerhalb von 24 Stunden beobachtet werden. Eine gleichzeitige Gabe eines QC-Inhibitors verringerte die Bildung von A $\beta_{3(pE)-40}$. Im Gegensatz zu vorangegangenen Zellkulturstudien, bei denen jeweils QC zur Erhöhung der Enzymkonzentration und somit zur Beschleunigung der Katalyse koexprimiert wurde, fand bei diesem Versuch die Applikation des Substrates im Überschuss statt (Schilling et al., 2008a). Eine weitere Bestätigung der QC-katalysierten pGlu-A β -Bildung wurde durch Behandlung verschiedener Mausmodelle erhalten, die eine Plauepathologie vergleichbar mit der Alzheimerschen Demenz aufweisen. Die Mausmodelle Tg2576 und T ASD-41 basieren auf der Expression von humanem APP („Swedish“) (Tabelle 3.1) bzw. humanem APP mit „Schwedischer Mutation“ und „London Mutation“ (Tabelle 3.1). Die Zusammensetzung der A β -Peptide in den Ablagerungen unterscheidet sich grundlegend von der in humanen Plaques. Die amyloiden Plaques bestehen hauptsächlich aus A $\beta_{1(D)-40/42}$, während A $\beta_{3(pE)-40/42}$ in diesen Tieren eine unterrepräsentierte Spezies ist (Kawarabayashi et al., 2001; Hutter-Paier et al., 2004). Bei prophylaktischer Applikation eines QC-Inhibitors in Tg2576, d.h. Beginn der Behandlung vor dem Auftreten von Plaques, konnten deutliche Reduktionen sowohl im Gehalt an pGlu-A β , als auch an A $\beta_{1(D)-40/42}$ detektiert werden. Diese Veränderungen gingen ebenfalls mit einer Herabsetzung der Mikro- und Astroglie in den Hirnen von Tg2576 einher. Die Behandlung resultierte in einer Verbesserung der Gedächtnisleistung der entsprechenden Tiere. Die akute Applikation eines QC-Inhibitors, d.h. Beginn der Behandlung nach Einsetzen der Plauebildung, führte jedoch zu keiner Verbesserung. Die Ergebnisse wurden in T ASD-41 Mäusen bestätigt. Die Studien stützen die Hypothese, dass pGlu-A β trotz der geringen Bildung einen entscheidenden Beitrag zur Ablagerung von A β leistet. Offensichtlich bewirkt pGlu-A β aufgrund seiner dramatischen Neigung zur Aggregation eine Keimbildung für die Ablagerung von A β auch im Mausmodell. Die Hemmung der pGlu-Bildung am N-Terminus

von A β stellt somit eine Strategie zur Verminderung der A β -Ablagerung dar (Schilling et al., 2008b).

Die molekularen Prozesse, die zur Freisetzung von N-terminal verkürzten A β -Peptiden führen, sind bisher nicht bekannt. Die Insertion einer neuen APP-Mutation (E599Q) in die APP-Sequenz sollte Aufschluss darüber geben, ob während des Zellmetabolismus N-terminal verkürzte A β -Moleküle entstehen (Abbildung 3.2). Die Punktmutation E599Q bewirkt eine rasche Umsetzung von N-terminal verkürztem A β durch QC und zeigt somit die Entstehung von N-terminalen A β -Varianten an. Theoretisch sind mehrere Möglichkeiten der Freisetzung von A $\beta_{3(E)}$ denkbar: 1. BACE 1 setzt A $\beta_{1(D)}$ frei, welches daraufhin von Aminopeptidasen zu A $\beta_{3(E)}$ verkürzt wird oder 2. die direkte Freisetzung über einen bisher noch nicht beschriebenen Mechanismus oder 3. eine sequentielle endoproteolytische Spaltung von APP. Die Expression der APP(E599Q)-Varianten lieferte den Beweis, dass der Vorläufer von A $\beta_{3(pE)}$, d.h. A $\beta_{3(Q)}$ während des normalen Zellmetabolismus entsteht. Des Weiteren deuteten diese Experimente auf eine besondere Rolle der Wildtypsequenz an der β -Sekretasespaltstelle hin. So entstehen N-terminal verkürzte A β -Moleküle hauptsächlich nach Expression von APP(WT) und APP(London) und nur zu einem geringen Teil nach Expression von APP(„Swedish“) und APP(„Swedish“/London) (Cynis et al., 2008b). Die Ergebnisse zwischen der Expression von WT- und Schwedischer Mutation weisen auf eine alternative Freisetzung von N-terminal verkürzten A β -Peptiden hin. Weiterhin konnte durch die Unterschiede in der Zusammensetzung N-terminal verkürzter A β -Peptide in Abhängigkeit von der Sequenz an der β -Sekretasespaltstelle erstmals die A $\beta_{3(pE)}$ -Bildung durch Co-Expression von APP(WT) und humaner QC nachgewiesen werden (Cynis et al., 2008b). Diese Ergebnisse könnten richtungsweisend für eine weitere Entwicklung von neuen Medikamenten zur Behandlung der Alzheimerschen Demenz und deren Ursachen sein. Wichtige Mausmodelle zur Erforschung der Mechanismen der AD-Entstehung basieren auf der Expression von APP(„Swedish“). Die so gewonnenen Ergebnisse müssen im Lichte der hier präsentierten Daten vorsichtig bewertet werden, da im Vergleich zum Mausmodell unterschiedliche Wege zur Entstehung von humanem Alzheimer existieren könnten.

Die Alzheimersche Erkrankung ist neben der pathologischen Ablagerung von A β -Peptiden und der intrazellulären Akkumulation von hyperphosphoryliertem Tau-Protein durch das Auftreten von neuroinflammatorischen Prozessen charakterisiert (Akiyama et al., 2000). Astrozyten und Mikrogliazellen akkumulieren um extraneuronale Plaques. Vor allem die vermehrte Anzahl und Aktivierung von Mikroglia ist typisch für einen entzündlichen Prozess im Gehirn, obgleich der Zusammenhang zwischen Mikrogliaaktivierung und

Plauepathologie noch nicht vollständig geklärt ist, da $CCR2^{-/-}$ in Mäusen ebenfalls zu einer verstärkten Pathologie führt (El Khoury et al., 2007). Es konnte jedoch gezeigt werden, dass A β die Sekretion von Zytokinen und Chemokinen, unter anderem CCL2, durch Immunzellen stimuliert (Janelsins et al., 2005; Szczepanik et al., 2001). Offensichtlich führt die Ablagerung von A β zu einer immunologischen Reaktion, in Folge dessen Mikroglia und Astrozyten aktiviert werden und in Richtung der A β -Ablagerungen migrieren (Meda et al., 1995). Es konnte weiterhin bewiesen werden, dass Mikroglia A β phagozytieren (Frautschy et al., 1992). Es ist jedoch nicht klar, ob diese Phagozytose zu einer Linderung oder Verschlimmerung der Krankheitssymptome führt. Allgemein wird die Reduzierung der Plauepathologie als Ziel der Wirkstoffforschung betrachtet, obgleich die Neurotoxizität von Plaues noch unklar ist und deren Anzahl nicht mit dem Verlust von Neuronen korreliert (Selkoe, 2001). Ein zentraler Bestandteil der Entfernung von Plaues sind A β -phagozytierende Mikroglia, die u.a. in Folge einer Vakzinierung A β -Peptide vermehrt aufnehmen (Lemere et al., 2006). Die Phagozytose von A β durch Mikroglia könnte jedoch vor allem zur Bildung von A $\beta_{3(pE)-40/42}$ aus dem gesamten extrazellulären A β -Gemisch beitragen und ebenso zu einer Generierung von toxischen A β -Spezies führen. Diese Annahme begründet sich auf die Entdeckung, dass die Zyklisierung von Glutamat ein hauptsächlich intrazellulärer Prozess ist (Cynis et al., 2008b). Des Weiteren konnte bereits gezeigt werden, dass die Kreuzung von Tg2576 mit CCL2-überexpremierenden Mäusen zu einer Verstärkung der Plauepathologie führt und dass CCL2 in frühen Stadien der Alzheimerschen Erkrankung vermehrt im CSF von Patienten detektiert wird (Yamamoto et al., 2005; Galimberti et al., 2006). Falls CCL2 einen negativen Einfluss auf die Entstehung der Alzheimerschen Erkrankung hat, könnten QC-Inhibitoren als duale Medikamente, welche 2 verschiedene aber ursächlich pathologische Mechanismen der Alzheimerschen Erkrankung adressieren würden, Verwendung finden. Durch Reduktion von pGlu-A β könnte die Entstehung der keimbildende A β -Spezies verhindert werden, während parallel die Migration und Aktivierung von Mikroglia und Astrozyten unterdrückt werden würde (Abbildung 3.3).

Erste Hinweise für einen möglichen dualen Mechanismus konnten aus einer Behandlung von Tg2576 mit PBD150 abgeleitet werden. Die Gabe des QC-Inhibitors verringerte nicht nur die pGlu-A β Konzentration dosisabhängig, sondern reduzierte auch die Astrogliose/Mikrogliose (Schilling et al., 2008b). Dies könnte auf eine parallele Reduktion von pGlu-A β und aktivem CCL2 zurückzuführen sein. Weitere Analysen müssen jedoch den genauen Mechanismus der reduzierten Neuroinflammation nach Gabe von QC-Inhibitoren aufklären. Des Weiteren erfordert die Rolle der hier erstmals beschriebenen isoQC besonderes Augenmerk, da

insbesondere der Einfluss dieses Isoenzym auf die Generierung von pGlu-CCL2 noch nicht endgültig geklärt werden konnte.

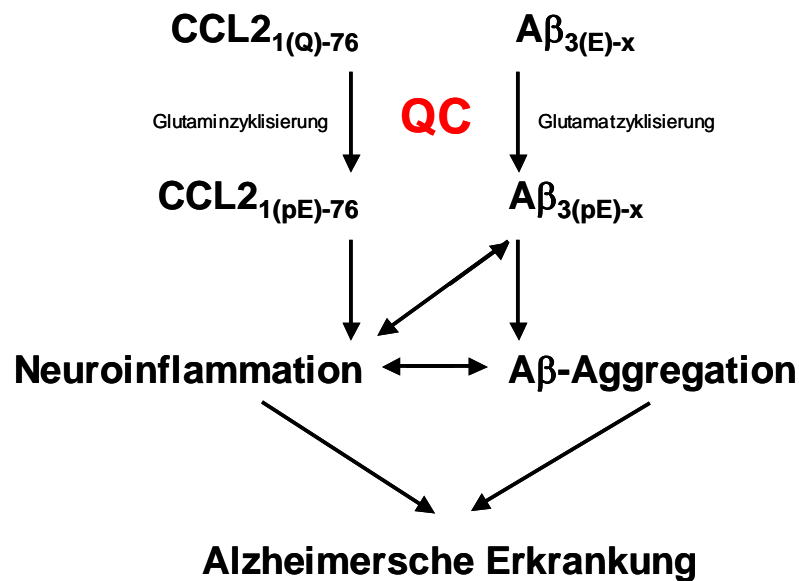


Abbildung 3.3: Postulierte, duale Rolle von QC in der Alzheimer'schen Erkrankung. Durch die Zyklisierung von Glutaminylresten am N-Terminus von CCL2 und Glutamyresten am N-Terminus von A β nimmt QC eine Schlüsselfunktion bei der Bildung dieser krankheitsrelevanten Peptide ein. CCL2 ist ein Schlüsselpепid der Neuroinflammation, A $\beta_{3(pE)-x}$ stellt eine besonders amyloidogene und hoch toxische A β -Spezies dar. Zukünftige Studien müssen klären, ob A $\beta_{3(pE)-x}$ allein bereits in der Lage ist eine Entzündungsreaktion im Gehirn auszulösen oder ob dies durch A β -Aggregate verursacht wird, die durch die hohe Neigung von A $\beta_{3(pE)-x}$ zur Oligomerisierung entstehen. Sowohl Neuroinflammation als auch A β -Aggregation werden als Ursachen des Nervenzellverlustes bei der Alzheimer'schen Erkrankung betrachtet. Eine Inhibierung der QC könnte eine Veränderung beider pathophysiologischen Prozesse bewirken.

Basierend auf den hier vorgelegten Daten ist eine Substanzentwicklung spezifischer QC-Inhibitoren geplant, die sowohl peripher auftretende, monozytengesteuerte Entzündungsprozesse über die Modulation der CCL2-Aktivität adressiert, als auch die Entwicklung hirnpentrierender Substanzen zur Behandlung der Alzheimer'schen Erkrankung.

4 Zusammenfassung

Eine Reihe von pathophysiologischen Veränderungen gehen mit einer Bildung von Pyroglutamylpeptiden einher. Diese werden durch QC-vermittelte Zyklisierung von Glutaminyl- und Glutamyresten gebildet. Ziel dieser Arbeit war die Untersuchung der QC-vermittelten Bildung von pGlu-A β in der Alzheimerschen Demenz sowie die Rolle des N-terminalen pGlu-Restes für die Funktion von CCL2. Anhand der Ergebnisse sollten mögliche Behandlungsstrategien, welche auf der Hemmung von QC beruhen, evaluiert werden. Wesentliche Ergebnisse waren:

- QC katalysiert die Zyklisierung von Glutamat am N-Terminus von A β -Peptiden nach amyloidogener und Prohormonkonvertase-vermittelter Prozessierung.
- Die Applikation eines spezifischen QC-Inhibitors verringert sowohl die Glutaminyl- als auch die Glutamylyzyklisierung *in vitro*, *in situ* und *in vivo*.
- Die QC-katalysierte pGlu-A β Bildung ist ein intrazellulärer Prozess.
- Der pGlu-Rest hat einen Einfluss auf die Stabilität und somit auf die chemotaktische Potenz von CCL2.
- Die Applikation eines QC-Inhibitors beeinflusste die arteriosklerotischen Veränderungen im Modell der „cuff“-induzierten Arteriosklerose.
- Es konnten Isoenzyme der humanen und murinen QC erstmals isoliert und charakterisiert werden.

Auf Grund der stabilisierenden Wirkung des pGlu-Restes für den N-Terminus verschiedener Proteine hat die Inhibierung von QC eine proteolysefördernde und dadurch aktivitätsmodulierende Wirkung. Neben der proteolytischen Stabilität und Amyloidogenität von pGlu-A β ist auch die N-terminale Integrität für CCL2 von entscheidender Bedeutung. Da die anabole und katabole Homöostase durch Auftreten resistenter Peptidspezies gestört werden kann, eröffnet die QC-Inhibierung eine Möglichkeit der beschleunigten proteolytischen Degradation dieser Peptide. Dies könnte der Behandlung verschiedener Krankheitssymptome dienen, welche durch das Auftreten von stabilen pGlu-Peptiden entstehen. Insofern sind die im Rahmen dieser Arbeit gewonnenen Erkenntnisse für die Entwicklung spezifischer QC-Inhibitoren zur Behandlung einer Reihe von pGlu-Protein-abhängigen Erkrankungen bedeutsam.

5 Literatur

- Abraham, G. N. und Podell, D. N. 1981. Pyroglutamic acid. Non-metabolic formation, function in proteins and peptides, and characteristics of the enzymes effecting its removal. *Mol. Cell Biochem.* 38 Spec No: 181-190.
- Akiyama, H., Barger, S., Barnum, S., Bradt, B., Bauer, J., Cole, G. M., Cooper, N. R., Eikelenboom, P., Emmerling, M., Fiebich, B. L., Finch, C. E., Frautschy, S., Griffin, W. S., Hampel, H., Hull, M., Landreth, G., Lue, L., Mrak, R., Mackenzie, I. R., McGeer, P. L., O'Banion, M. K., Pachter, J., Pasinetti, G., Plata-Salaman, C., Rogers, J., Rydel, R., Shen, Y., Streit, W., Strohmeyer, R., Tooyoma, I., Van Muiswinkel, F. L., Veerhuis, R., Walker, D., Webster, S., Wegrzyniak, B., Wenk, G., und Wyss-Coray, T. 2000. Inflammation and Alzheimer's disease. *Neurobiol. Aging* 21: 383-421.
- Awade, A. C., Cleuziat, P., Gonzales, T., und Robert-Baudouy, J. 1994. Pyrrolidone carboxyl peptidase (Pcp): an enzyme that removes pyroglutamic acid (pGlu) from pGlu-peptides and pGlu-proteins. *Proteins* 20: 34-51.
- Bateman, A., Solomon, S., und Bennett, H. P. 1990. Post-translational modification of bovine pro-opiomelanocortin. Tyrosine sulfation and pyroglutamate formation, a mass spectrometric study. *J Biol. Chem* 265: 22130-22136.
- Bateman, R. J., Munsell, L. Y., Morris, J. C., Swarm, R., Yarasheski, K. E., und Holtzman, D. M. 2006. Human amyloid-beta synthesis and clearance rates as measured in cerebrospinal fluid in vivo. *Nat. Med.* 12: 856-861.
- Batliwalla, F. M., Baechler, E. C., Xiao, X., Li, W., Balasubramanian, S., Khalili, H., Damle, A., Ortmann, W. A., Perrone, A., Kantor, A. B., Gulko, P. S., Kern, M., Furie, R., Behrens, T. W., und Gregersen, P. K. 2005. Peripheral blood gene expression profiling in rheumatoid arthritis. *Genes Immun.* 6 (5): 388-397.
- Billings, L. M., Oddo, S., Gree, K. N., McLaugh, J. L., und LaFerla, F. M. 2005. Intraneuronal A β Causes the Onset of early Alzheimer's Disease-Related Cognitive Deficits in Transgenic Mice. *Neuron* 45: 675-688.
- Blomback, B. 1967. Derivatives of Glutamine in Peptides. *Methods Enzymol.* 11: 398-411.
- Böckers, T. M., Kreutz, M. R., und Pohl, T. 1995. Glutaminyl-cyclase expression in the bovine/porcine hypothalamus and pituitary. *J Neuroendocrinol.* 7: 445-453.
- Booth, R. E., Lovell, S. C., Misquitta, S. A., und Bateman Jr., R. C. 2004. Human glutaminyl cyclase and bacterial zinc aminopeptidase share a common fold and active site. *BMC Biol.* 2: 2.

- Buchholz, M., Heiser, U., Schilling, S., Niestroj, A. J., Zunkel, K., und Demuth, H.-U. 2006. The first potent inhibitors for human glutaminyl cyclase: synthesis and structure-activity relationship. *J Med Chem* 49: 664-677.
- Cai, H., Wang, Y., McCarthy, D., Wen, H., Borchelt, D. R., Price, D. L., und Wong, P. C. 2001. BACE1 is the major beta-secretase for generation of Abeta peptides by neurons. *Nat. Neurosci.* 4: 233-234.
- Casas, C., Sergeant, N., Itier, J. M., Blanchard, V., Wirths, O., van der Kolk, N., Vingtdoux, V., van de Steeg, E., Ret, G., Canton, T., Drobecq, H., Clark, A., Bonici, B., Delacourte, A., Benavides, J., Schmitz, C., Tremp, G., Bayer, T. A., Benoit, P., und Pradier, L. 2004. Massive CA1/2 neuronal loss with intraneuronal and N-terminal truncated Abeta42 accumulation in a novel Alzheimer transgenic model. *Am. J Pathol.* 165: 1289-1300.
- Charo, I. F. und Taubman, M. B. 2004. Chemokines in the pathogenesis of vascular disease. *Circ. Res.* 95: 858-866.
- Chelius, D., Jing, K., Lueras, A., Rehder, D. S., Dillon, T. M., Vizel, A., Rajan, R. S., Li, T., Treuheit, M. J., und Bondarenko, P. V. 2006. Formation of pyroglutamic acid from N-terminal glutamic acid in immunoglobulin gamma antibodies. *Anal. Chem.* 78: 2370-2376.
- Cipollone, F., Marini, M., Fazia, M., Pini, B., Iezzi, A., Reale, M., Paloscia, L., Materazzo, G., D'Annunzio, E., Conti, P., Chiarelli, F., Cuccurullo, F., und Mezzetti, A. 2001. Elevated circulating levels of monocyte chemoattractant protein-1 in patients with restenosis after coronary angioplasty. *Arterioscler. Thromb. Vasc. Biol.* 21: 327-334.
- Citron, M., Oltersdorf, T., Haass, C., McConlogue, L., Hung, A. Y., Seubert, P., Vigo-Pelfrey, C., Lieberburg, I., und Selkoe, D. J. 1992. Mutation of the beta-amyloid precursor protein in familial Alzheimer's disease increases beta-protein production. *Nature* 360: 672-674.
- Corder, E. H., Saunders, A. M., Strittmatter, W. J., Schmechel, D. E., Gaskell, P. C., Small, G. W., Roses, A. D., Haines, J. L., und Pericak-Vance, M. A. 1993. Gene dose of apolipoprotein E type 4 allele and the risk of Alzheimer's disease in late onset families. *Science* 261: 921-923.
- Cynis, H., Rahfeld, J.-U., Stephan, A., Kehlen, A., Koch, B., Wermann, M., Demuth, H.-U., und Schilling, S. 2008a. Isolation of an Isoenzyme of Human Glutaminyl Cyclase: Retention in the Golgi Complex Suggests Involvement in the Protein Maturation Machinery. *J. Mol. Biol.* 379: 966-980.

- Cynis, H., Scheel, E., Saido, T. C., Schilling, S., und Demuth, H.-U. 2008b. Amyloidogenic processing of amyloid precursor protein: evidence of a pivotal role of glutaminyl cyclase in generation of pyroglutamate-modified amyloid-beta. *Biochemistry* 47: 7405-7413.
- Cynis, H., Schilling, S., Bodnar, M., Hoffmann, T., Heiser, U., Saido, T. C., und Demuth, H.-U. 2006. Inhibition of glutaminyl cyclase alters pyroglutamate formation in mammalian cells. *Biochim. Biophys. Acta* 1764: 1618-1625.
- D'Suze, G., Batista, C. V., Frau, A., Murgia, A. R., Zamudio, F. Z., Sevcik, C., Possani, L. D., und Prestipino, G. 2004. Discrepin, a new peptide of the sub-family alpha-ktx15, isolated from the scorpion *Tityus discrepans* irreversibly blocks K⁺ -channels (IA currents) of cerebellum granular cells. *Arch. Biochem. Biophys.* 430: 256-263.
- Dahl, S. W., Slaughter, C., Lauritzen, C., Bateman Jr., R. C., Connerton, I., und Pedersen, J. 2000. Carica papaya glutamine cyclotransferase belongs to a novel plant enzyme subfamily: cloning and characterization of the recombinant enzyme. *Protein Expr. Purif.* 20: 27-36.
- Davies, P. und Maloney, A. J. 1976. Selective loss of central cholinergic neurons in Alzheimer's disease. *Lancet* 2: 1403.
- De Strooper, B. 2003. Aph-1, Pen-2, and Nicastrin with Presenilin generate an active gamma-Secretase complex. *Neuron* 38: 9-12.
- Eckman, C. B., Mehta, N. D., Crook, R., Perez-Tur, J., Prihar, G., Pfeiffer, E., Graff-Radford, N., Hinder, P., Yager, D., Zenk, B., Refolo, L. M., Prada, C. M., Younkin, S. G., Hutton, M., und Hardy, J. 1997. A new pathogenic mutation in the APP gene (I716V) increases the relative proportion of A beta 42(43). *Hum. Mol. Genet.* 6: 2087-2089.
- Eipper, B. A., Mains, R. E., und Glembotski, C. C. 1983. Identification in pituitary tissue of a peptide alpha-amidation activity that acts on glycine-extended peptides and requires molecular oxygen, copper, and ascorbic acid. *Proc. Natl. Acad. Sci. U. S. A.* 80: 5144-5148.
- El Khoury, J., Toft, M., Hickman, S. E., Means, T. K., Terada, K., Geula, C., und Luster, A. D. 2007. Ccr2 deficiency impairs microglial accumulation and accelerates progression of Alzheimer-like disease. *Nat. Med.* 13: 432-438.
- Esler, W. P. und Wolfe, M. S. 2001. A portrait of Alzheimer secretases--new features and familiar faces. *Science* 293: 1449-1454.

- Ezura, Y., Kajita, M., Ishida, R., Yoshida, S., Yoshida, H., Suzuki, T., Hosoi, T., Inoue, S., Shiraki, M., Orimo, H., and Emi, M. 2004. Association of multiple nucleotide variations in the pituitary glutaminyl cyclase gene (QPCT) with low radial BMD in adult women. *J Bone Miner. Res.* 19: 1296-1301.
- Ferri, C., Desideri, G., Valenti, M., Bellini, C., Pasin, M., Santucci, A., and De Mattia, G. 1999. Early upregulation of endothelial adhesion molecules in obese hypertensive men. *Hypertension* 34: 568-573.
- Fischer, W. H. und Spiess, J. 1987. Identification of a mammalian glutaminyl cyclase converting glutaminyl into pyroglutamyl peptides. *Proc. Natl. Acad. Sci. U. S. A.* 84: 3628-3632.
- Frautschy, S. A., Cole, G. M., and Baird, A. 1992. Phagocytosis and deposition of vascular beta-amyloid in rat brains injected with Alzheimer beta-amyloid. *Am. J. Pathol.* 140: 1389-1399.
- Gale, J. S., McIntosh, J. E., and McIntosh, R. P. 1988. Peptidyl-glycine alpha-amidating mono-oxygenase activity towards a gonadotropin-releasing-hormone C-terminal peptide substrate, in subcellular fractions of sheep brain and pituitary. *Biochem. J.* 251: 251-259.
- Galimberti, D., Fenoglio, C., Lovati, C., Venturelli, E., Guidi, I., Corra, B., Scalabrini, D., Clerici, F., Mariani, C., Bresolin, N., and Scarpini, E. 2006. Serum MCP-1 levels are increased in mild cognitive impairment and mild Alzheimer's disease. *Neurobiol. Aging* 27: 1763-1768.
- Garden, R. W., Moroz, T. P., Gleeson, J. M., Floyd, P. D., Li, L., Rubakhin, S. S., and Sweedler, J. V. 1999. Formation of N-pyroglutamyl peptides from N-Glu and N-Gln precursors in *Aplysia* neurons. *J Neurochem.* 72: 676-681.
- Gatz, M., Fratiglioni, L., Johansson, B., Berg, S., Mortimer, J. A., Reynolds, C. A., Fiske, A., and Pedersen, N. L. 2005. Complete ascertainment of dementia in the Swedish Twin Registry: the HARMONY study. *Neurobiol. Aging* 26: 439-447.
- Ghiso, J. A., Revesz, T., Holton, J., Rostagno, A., Lashley, T., Houlden, H., Gibb, G., Anderton, B., Bek, T., Bojsen-Moller, M., Wood, N., Vidal, R., Braendgaard, H., Plant, G., and Frangione, B. 2001a. Chromosome 13 dementia syndromes as models of neurodegeneration. *Amyloid.* 8: 277-284.

- Ghisso, J. A., Holton, J., Miravalle, L., Calero, M., Lashley, T., Vidal, R., Houlden, H., Wood, N., Neubert, T. A., Rostagno, A., Plant, G., Revesz, T., und Frangione, B. 2001b. Systemic amyloid deposits in familial British dementia. *J. Biol. Chem.* 276: 43909-43914.
- Glenner, G. G. und Wong, C. W. 1984. Alzheimer's disease: initial report of the purification and characterization of a novel cerebrovascular amyloid protein. *Biochem. Biophys. Res. Commun.* 120: 885-890.
- Gong, J. H. und Clark-Lewis, I. 1995. Antagonists of monocyte chemoattractant protein 1 identified by modification of functionally critical NH2-terminal residues. *J Exp. Med* 181: 631-640.
- Graves, D. T. und Jiang, Y. 1995. Chemokines, a family of chemotactic cytokines. *Crit Rev. Oral Biol. Med.* 6: 109-118.
- Green, C. M., Cockle, S. M., Watson, P. F., und Fraser, L. R. 1996. Fertilization promoting peptide, a tripeptide similar to thyrotrophin-releasing hormone, stimulates the capacitation and fertilizing ability of human spermatozoa in vitro. *Hum. Reprod.* 11: 830-836.
- Güntert, A., Dobeli, H., und Bohrmann, B. 2006. High sensitivity analysis of amyloid-beta peptide composition in amyloid deposits from human and PS2APP mouse brain. *Neuroscience* 143 (2) 461-475.
- Haass, C., Lemere, C. A., Capell, A., Citron, M., Seubert, P., Schenk, D., Lannfelt, L., und Selkoe, D. J. 1995. The Swedish mutation causes early-onset Alzheimer's disease by beta-secretase cleavage within the secretory pathway. *Nat. Med* 1: 1291-1296.
- Haass, C., Schlossmacher, M. G., Hung, A. Y., Vigo-Pelfrey, C., Mellon, A., Ostaszewski, B. L., Lieberburg, I., Koo, E. H., Schenk, D., Teplow, D. B., und Selkoe, D. J. 1992. Amyloid beta-peptide is produced by cultured cells during normal metabolism. *Nature* 359: 322-325.
- Hook, V. Y. und Reisine, T. D. 2003. Cysteine proteases are the major beta-secretase in the regulated secretory pathway that provides most of the beta-amyloid in Alzheimer's disease: role of BACE 1 in the constitutive secretory pathway. *J Neurosci. Res.* 74: 393-405.
- Hosoda, R., Saido, T. C., Otvos Jr., L., Arai, T., Mann, D. M., Lee, V. M., Trojanowski, J. Q., und Iwatsubo, T. 1998. Quantification of modified amyloid beta peptides in Alzheimer disease and Down syndrome brains. *J Neuropathol. Exp. Neurol.* 57: 1089-1095.

- Huang, K. F., Liu, Y. L., Cheng, W. J., Ko, T. P., and Wang, A. H. 2005. Crystal structures of human glutaminyl cyclase, an enzyme responsible for protein N-terminal pyroglutamate formation. *Proc. Natl. Acad. Sci. U. S. A.* 102: 13117-13122.
- Hultmark, D., Engstrom, A., Andersson, K., Steiner, H., Bennich, H., and Boman, H. G. 1983. Insect immunity. Attacins, a family of antibacterial proteins from *Hyalophora cecropia*. *EMBO J.* 2: 571-576.
- Hutter-Paier, B., Huttunen, H. J., Puglielli, L., Eckman, C. B., Kim, D. Y., Hofmeister, A., Moir, R. D., Domnitz, S. B., Frosch, M. P., Windisch, M., and Kovacs, D. M. 2004. The ACAT inhibitor CP-113,818 markedly reduces amyloid pathology in a mouse model of Alzheimer's disease. *Neuron* 44: 227-238.
- Iezzi, A., Ferri, C., Mezzetti, A., and Cipollone, F. 2007. COX-2: friend or foe? *Curr. Pharm. Des* 13: 1715-1721.
- Janelins, M. C., Mastrangelo, M. A., Oddo, S., LaFerla, F. M., Federoff, H. J., and Bowers, W. J. 2005. Early correlation of microglial activation with enhanced tumor necrosis factor-alpha and monocyte chemoattractant protein-1 expression specifically within the entorhinal cortex of triple transgenic Alzheimer's disease mice. *J Neuroinflammation.* 2: 23.
- Jarrett, J. T., Berger, E. P., and Lansbury Jr., P. T. 1993. The carboxy terminus of the beta amyloid protein is critical for the seeding of amyloid formation: implications for the pathogenesis of Alzheimer's disease. *Biochemistry* 32: 4693-4697.
- Kang, J., Lemaire, H. G., Unterbeck, A., Salbaum, J. M., Masters, C. L., Grzeschik, K. H., Multhaup, G., Beyreuther, K., and Müller-Hill, B. 1987. The precursor of Alzheimer's disease amyloid A4 protein resembles a cell-surface receptor. *Nature* 325: 733-736.
- Kastrati, A., Mehilli, J., von Beckerath, N., Dibra, A., Hausleiter, J., Pache, J., Schühlen, H., Schmitt, C., Dirschinger, J., and Schomig, A. 2005. Sirolimus-eluting stent or paclitaxel-eluting stent vs balloon angioplasty for prevention of recurrences in patients with coronary in-stent restenosis: a randomized controlled trial. *JAMA* 293: 165-171.
- Kawarabayashi, T., Younkin, L. H., Saido, T. C., Shoji, M., Ashe, K. H., and Younkin, S. G. 2001. Age-dependent changes in brain, CSF, and plasma amyloid (beta) protein in the Tg2576 transgenic mouse model of Alzheimer's disease. *J Neurosci.* 21: 372-381.
- Khan, Z., Aitken, A., Garcia, J. R., and Smyth, D. G. 1992. Isolation and identification of two neutral thyrotropin releasing hormone-like peptides, pyroglutamylphenylalanineproline amide and pyroglutamylglutamineproline amide, from human seminal fluid. *J. Biol. Chem.* 267: 7464-7469.

- Kitamoto, S., Egashira, K., and Takeshita, A. 2003. Stress and vascular responses: anti-inflammatory therapeutic strategy against atherosclerosis and restenosis after coronary intervention. *J Pharmacol Sci.* 91: 192-196.
- Kuo, Y. M., Emmerling, M. R., Vigo-Pelfrey, C., Kasunic, T. C., Kirkpatrick, J. B., Murdoch, G. H., Ball, M. J., and Roher, A. E. 1996. Water-soluble A β (N-40, N-42) oligomers in normal and Alzheimer disease brains. *J Biol. Chem* 271: 4077-4081.
- Kwok, J. B., Taddei, K., Hallupp, M., Fisher, C., Brooks, W. S., Broe, G. A., Hardy, J., Fulham, M. J., Nicholson, G. A., Stell, R., George Hyslop, P. H., Fraser, P. E., Kakulas, B., Clarnette, R., Relkin, N., Gandy, S. E., Schofield, P. R., and Martins, R. N. 1997. Two novel (M233T and R278T) presenilin-1 mutations in early-onset Alzheimer's disease pedigrees and preliminary evidence for association of presenilin-1 mutations with a novel phenotype. *Neuroreport* 8: 1537-1542.
- Lambeir, A. M., Durinx, C., Scharpe, S., and De Meester, I. 2003. Dipeptidyl-peptidase IV from bench to bedside: an update on structural properties, functions, and clinical aspects of the enzyme DPP IV. *Crit Rev. Clin. Lab Sci.* 40: 209-294.
- Lau, E. K., Paavola, C. D., Johnson, Z., Gaudry, J. P., Geretti, E., Borlat, F., Kungl, A. J., Proudfoot, A. E., and Handel, T. M. 2004. Identification of the glycosaminoglycan binding site of the CC chemokine, MCP-1: implications for structure and function in vivo. *J Biol. Chem* 279: 22294-22305.
- Lemere, C. A., Maier, M., Jiang, L., Peng, Y., and Seabrook, T. J. 2006. Amyloid-beta immunotherapy for the prevention and treatment of Alzheimer disease: lessons from mice, monkeys, and humans. *Rejuvenation. Res.* 9: 77-84.
- Levy, E., Carman, M. D., Fernandez-Madrid, I. J., Power, M. D., Lieberburg, I., van Duinen, S. G., Bots, G. T., Luyendijk, W., and Frangione, B. 1990. Mutation of the Alzheimer's disease amyloid gene in hereditary cerebral hemorrhage, Dutch type. *Science* 248: 1124-1126.
- Libby, P. 2006. Inflammation and cardiovascular disease mechanisms. *Am. J. Clin. Nutr.* 83: 456S-460S.
- Libby, P., Ridker, P. M., and Maseri, A. 2002. Inflammation and atherosclerosis. *Circulation* 105: 1135-1143.
- Libby, P. and Theroux, P. 2005. Pathophysiology of coronary artery disease. *Circulation* 111: 3481-3488.

- McQuibban, G. A., Gong, J. H., Wong, J. P., Wallace, J. L., Clark-Lewis, I., and Overall, C. M. 2002. Matrix metalloproteinase processing of monocyte chemoattractant proteins generates CC chemokine receptor antagonists with anti-inflammatory properties in vivo. *Blood* 100: 1160-1167.
- Meda, L., Cassatella, M. A., Szendrei, G. I., Otvos Jr., L., Baron, P., Villalba, M., Ferrari, D., und Rossi, F. 1995. Activation of microglial cells by beta-amyloid protein and interferon-gamma. *Nature* 374: 647-650.
- Messer, M. 1963. Enzymatic cyclization of L-glutamine and L-glutaminy peptides. *Nature* 197: 1299.
- Miravalle, L., Calero, M., Takao, M., Roher, A. E., Ghetti, B., und Vidal, R. 2005. Amino-terminally truncated Abeta peptide species are the main component of cotton wool plaques. *Biochemistry* 44: 10810-10821.
- Moore, M. R. und Black, P. M. 1991. Neuropeptides. *Neurosurg. Rev.* 14: 97-110.
- Morty, R. E., Bulau, P., Pelle, R., Wilk, S., und Abe, K. 2006. Pyroglutamyl peptidase type I from *Trypanosoma brucei*: a new virulence factor from African trypanosomes that de-blocks regulatory peptides in the plasma of infected hosts. *Biochem. J* 394: 635-645.
- Mullan, M., Crawford, F., Axelman, K., Houlden, H., Lilius, L., Winblad, B., und Lannfelt, L. 1992. A pathogenic mutation for probable Alzheimer's disease in the APP gene at the N-terminus of beta-amyloid. *Nat. Genet.* 1: 345-347.
- Ni, W., Kitamoto, S., Ishibashi, M., Usui, M., Inoue, S., Hiasa, K., Zhao, Q., Nishida, K., Takeshita, A., und Egashira, K. 2004. Monocyte chemoattractant protein-1 is an essential inflammatory mediator in angiotensin II-induced progression of established atherosclerosis in hypercholesterolemic mice. *Arterioscler. Thromb. Vasc. Biol.* 24: 534-539.
- Nilni, E.A. und Sevarino, K A. 1999. The biology of pro-thyrotropin-releasing hormone-derived peptides. *Endocr. Rev.* 20: 599-648.
- Nilsberth, C., Westlind-Danielsson, A., Eckman, C. B., Condron, M. M., Axelman, K., Forsell, C., Sten, C., Luthman, J., Teplow, B. D., Younkin, S. G., Naslund, J., und Lannfelt, L. 2001. The 'Arctic' APP mutation (E693G) causes Alzheimer's disease by enhanced Abeta protofibril formation. *Nat. Neurosci.* 4: 887-893.
- Ogata, H., Takeya, M., Yoshimura, T., Takagi, K., und Takahashi, K. 1997. The role of monocyte chemoattractant protein-1 (MCP-1) in the pathogenesis of collagen-induced arthritis in rats. *J Pathol.* 182: 106-114.

- Oudejans, R. C., Harthoorn, L. F., Diederens, J. H., and Van der Horst, D. J. 1999. Adipokinetic hormones. Coupling between biosynthesis and release. *Ann. N. Y. Acad. Sci.* 897: 291-299.
- Pawlak, J. and Manjunatha, K. R. 2006. Snake venom glutaminyl cyclase. *Toxicon* 48: 278-286.
- Pimenta, A.M., Rates, B., Bloch Jr., C., Gomes, P. C., Santoro, M. M., de Lima, M. E., Richardson, M., and Cordeiro, M. N. 2005. Electrospray ionization quadrupole time-of-flight and matrix-assisted laser desorption/ionization tandem time-of-flight mass spectrometric analyses to solve micro-heterogeneity in post-translationally modified peptides from *Phoneutria nigriventer* (Aranea, Ctenidae) venom. *Rapid Commun. Mass Spectrom.* 19: 31-37.
- Pohl, T., Zimmer, M., Mugele, K., and Spiess, J. 1991. Primary structure and functional expression of a glutaminyl cyclase. *Proc. Natl. Acad. Sci. U. S. A* 88: 10059-10063.
- Proost, P., Struyf, S., Couvreur, M., Lenaerts, J. P., Conings, R., Menten, P., Verhaert, P., Wuyts, A., and Van Damme, J. 1998. Posttranslational modifications affect the activity of the human monocyte chemotactic proteins MCP-1 and MCP-2: identification of MCP-2(6-76) as a natural chemokine inhibitor. *J Immunol* 160: 4034-4041.
- Proudfoot, A. E., Handel, T. M. Johnson, Z., Lau, E. K., LiWang, P., Clark-Lewis, I., Borlat, F., Wells, T. N., and Kosco-Vilbois, M. H. 2003. Glycosaminoglycan binding and oligomerization are essential for the in vivo activity of certain chemokines. *Proc. Natl. Acad. Sci. U. S. A* 100: 1885-1890.
- Raschetti, R., Albanese, E., Vanacore, N., and Maggini, M. 2007. Cholinesterase inhibitors in mild cognitive impairment: a systematic review of randomised trials. *PLoS. Med.* 4: e338.
- Roher, A. E., Lowenson, J. D., Clarke, S., Wolkow, C., Wang, R., Cotter, R. J., Reardon, I. M., Zurcher-Neely, H. A., Heinrikson, R. L., Ball, M. J., and Greenberg, B. D. 1993. Structural alterations in the peptide backbone of beta-amyloid core protein may account for its deposition and stability in Alzheimer's disease. *J. Biol. Chem.* 268: 3072-3083.
- Ross, R. 1999. Atherosclerosis is an inflammatory disease. *Am. Heart J.* 138: S419-S420.

- Russo, C., Violani, E., Salis, S., Venezia, V., Dolcini, V., Damonte, G., Benatti, U., D'Arrigo, C., Patrone, E., Carlo, P., and Schettini, G. 2002. Pyroglutamate-modified amyloid beta-peptides--A β N3(pE)--strongly affect cultured neuron and astrocyte survival. *J Neurochem.* 82: 1480-1489.
- Saido, T. C. 1998. Alzheimer's disease as proteolytic disorders: anabolism and catabolism of beta-amyloid. *Neurobiol. Aging* 19: S69-S75.
- Saido, T. C. und Iwata, N. 2006. Metabolism of amyloid beta peptide and pathogenesis of Alzheimer's disease. Towards presymptomatic diagnosis, prevention and therapy. *Neurosci. Res.* 54:235-253.
- Saido, T. C., Iwatsubo, T., Mann, D. M., Shimada, H., Ihara, Y., und Kawashima, S. 1995. Dominant and differential deposition of distinct beta-amyloid peptide species, A β N3(pE), in senile plaques. *Neuron* 14: 457-466.
- Saido, T. C., Yamao-Harigaya, W., Iwatsubo, T., und Kawashima, S. 1996. Amino- and carboxyl-terminal heterogeneity of beta-amyloid peptides deposited in human brain. *Neurosci. Lett.* 215: 173-176.
- Saunders, A. M., Strittmatter, W. J., Schmechel, D., George-Hyslop, P. H., Pericak-Vance, M. A., Joo, S. H., Rosi, B. L., Gusella, J. F., Crapper-MacLachlan, D. R., Alberts, M. J., Hulette, C., Crain, B., Goldgaber, D., und Roses, A. D. 1993. Association of apolipoprotein E allele epsilon 4 with late-onset familial and sporadic Alzheimer's disease. *Neurology* 43: 1467-1472.
- Savage, M. J., Trusko, S. P., Howland, D. S., Pinsker, L. R., Mistretta, S., Reaume, A. G., Greenberg, B. D., Siman, R., und Scott, R. W. 1998. Turnover of amyloid beta-protein in mouse brain and acute reduction of its level by phorbol ester. *J Neurosci.* 18: 1743-1752.
- Scheuner, D., Eckman, C., Jensen, M., Song, X., Citron, M., Suzuki, N., Bird, T. D., Hardy, J., Hutton, M., Kukull, W., Larson, E., Levy-Lahad, E., Viitanen, M., Peskind, E., Poorkaj, P., Schellenberg, G., Tanzi, R., Wasco, W., Lannfelt, L., Selkoe, D. J., und Younkin, S. 1996. Secreted amyloid beta-protein similar to that in the senile plaques of Alzheimer's disease is increased in vivo by the presenilin 1 and 2 and APP mutations linked to familial Alzheimer's disease. *Nat. Med* 2: 864-870.

- Schilling, S., Appl, T., Hoffmann, T., Cynis, H., Schulz, K., Jagla, W., Friedrich, D., Wermann, M., Buchholz, M., Heiser, U., von Hörsten, S., und Demuth H.-U. 2008a. Inhibition of glutaminyl cyclase prevents pGlu-Abeta formation after intracortical/hippocampal microinjection in vivo/in situ. *J. Neurochem.* 106: 1225-1236.
- Schilling, S., Cynis, H., von Bohlen, A., Hoffmann, T., Wermann, M., Heiser, U., Buchholz, M., Zunkel, K., und Demuth, H.-U. 2005. Isolation, Catalytic Properties, and Competitive Inhibitors of the Zinc-Dependent Murine Glutaminyl Cyclase. *Biochemistry* 44: 13415-13424.
- Schilling, S., Hoffmann, T., Manhart, S., Hoffmann, M., und Demuth, H.-U. 2004. Glutaminyl cyclases unfold glutamyl cyclase activity under mild acid conditions. *FEBS Lett.* 563: 191-196.
- Schilling, S., Lauber, T., Schaupp, M., Manhart, S., Scheel, E., Böhm, G., und Demuth, H.-U. 2006. On the seeding and oligomerization of pGlu-amyloid peptides (in vitro). *Biochemistry* 45: 12393-12399.
- Schilling, S., Lindner, C., Koch, B., Wermann, M., Rahfeld, J.-U., von Bohlen, A., Rudolph, T., Reuter, G., und Demuth, H.-U. 2007a. Isolation and Characterization of Glutaminyl Cyclases from Drosophila: Evidence for Enzyme Forms with Different Subcellular Localization. *Biochemistry* 46 (38) 10921-10930.
- Schilling, S., Manhart, S., Hoffmann, T., Ludwig, H.-H., Wasternack, C., und Demuth, H.-U. 2003a. Substrate specificity of glutaminyl cyclases from plants and animals. *Biol. Chem* 384: 1583-1592.
- Schilling, S., Niestroj, A. J., Rahfeld, J.-U., Hoffmann, T., Wermann, M., Zunkel, K., Wasternack, C., und Demuth, H.-U. 2003b. Identification of human glutaminyl cyclase as a metalloenzyme. Potent inhibition by imidazole derivatives and heterocyclic chelators. *J Biol. Chem* 278: 49773-49779.
- Schilling, S., Stenzel, I., von Bohlen, A., Wermann, M., Schulz, K., Demuth, H.-U. und Wasternack, C. 2007b. Isolation and characterization of the glutaminyl cyclases from *Solanum tuberosum* and *Arabidopsis thaliana*: implications for physiological functions. *Biol. Chem.* 388: 145-153.

- Schilling, S., Zeitschel, U., Hoffmann, T., Heiser, U., Francke, M., Kehlen, A., Holzer, M., Hutter-Paier, B., Prokesch, M., Windisch, M., Jagla, W., Schlenzig, D., Lindner, C., Rudolph, T., Reuter, G., Cynis, H., Montag, D., Demuth, H.-U., und Rossner, S. 2008b. Glutaminyl cyclase inhibition attenuates pyroglutamate Aβ and Alzheimer's disease-like pathology. *Nat. Med.* 14: 1106-1111.
- Schmutzler, C., Darmer, D., Diekhoff, D., und Grimmeliikhuijzen, C. J. 1992. Identification of a novel type of processing sites in the precursor for the sea anemone neuropeptide Antho-RFamide (<Glu-Gly-Arg-Phe-NH₂) from *Anthopleura elegantissima*. *J Biol. Chem* 267: 22534-22541.
- Selkoe, D.J. 2001. Alzheimer's disease: genes, proteins, and therapy. *Physiol Rev.* 81: 741-766.
- Sherrington, R., Froelich, S., Sorbi, S., Campion, D., Chi, H., Rogaeva, E. A., Levesque, G., Rogaev, E. I., Lin, C., Liang, Y., Ikeda, M., Mar, L., Brice, A., Agid, Y., Percy, M. E., Clerget-Darpoux, F., Piacentini, S., Marcon, G., Nacmias, B., Amaducci, L., Frebourg, T., Lannfelt, L., Rommens, J. M., und George-Hyslop, P. H.,. 1996. Alzheimer's disease associated with mutations in presenilin 2 is rare and variably penetrant. *Hum. Mol. Genet.* 5: 985-988.
- Shirotani, K., Tsubuki, S., Lee, H. J., Maruyama, K., und Saido, T. C. 2002. Generation of amyloid beta peptide with pyroglutamate at position 3 in primary cortical neurons. *Neurosci. Lett.* 327: 25-28.
- Smith, A. M. und Watson, S. A. 2000. Review article: gastrin and colorectal cancer. *Aliment. Pharmacol Ther.* 14: 1231-1247.
- Song, I., Chuang, C. Z., und Bateman Jr., R. C. 1994. Molecular cloning, sequence analysis and expression of human pituitary glutaminyl cyclase. *J Mol. Endocrinol.* 13: 77-86.
- Spinazzi, R., Andreis, P. G., Rossi, G. P., und Nussdorfer, G. G. 2006. Orexins in the regulation of the hypothalamic-pituitary-adrenal axis. *Pharmacol Rev.* 58: 46-57.
- Sudoh, S., Kawamura, Y., Sato, S., Wang, R., Saido, T. C., Oyama, F., Sakaki, Y., Komano, H., und Yanagisawa, K. 1998. Presenilin 1 mutations linked to familial Alzheimer's disease increase the intracellular levels of amyloid beta-protein 1-42 and its N-terminally truncated variant(s) which are generated at distinct sites. *J Neurochem.* 71: 1535-1543.
- Sykes, P. A., Watson, S. J., Temple, J. S., und Bateman Jr., R. C. 1999. Evidence for tissue-specific forms of glutaminyl cyclase. *FEBS Lett.* 455: 159-161.

- Szczepanik, A. M., Funes, S., Petko, W., und Ringheim, G. E., 2001. IL-4, IL-10 and IL-13 modulate A beta(1--42)-induced cytokine and chemokine production in primary murine microglia and a human monocyte cell line. *J Neuroimmunol.* 113: 49-62.
- Tabata, T., Mine, S., Kawahara, C., Okada, Y., und Tanaka, Y. 2003. Monocyte chemoattractant protein-1 induces scavenger receptor expression and monocyte differentiation into foam cells. *Biochem. Biophys. Res. Commun.* 305: 380-385.
- Thornberry, N. A. und Weber, A. E. 2007. Discovery of JANUVIA (Sitagliptin), a selective dipeptidyl peptidase IV inhibitor for the treatment of type 2 diabetes. *Curr. Top. Med. Chem.* 7: 557-568.
- Uguccioni, M., D'Apuzzo, M., Loetscher, M., Dewald, B., und Baggiolini, M. 1995. Actions of the chemotactic cytokines MCP-1, MCP-2, MCP-3, RANTES, MIP-1 alpha and MIP-1 beta on human monocytes. *Eur J Immunol* 25: 64-68.
- Van Belle, E., Susen, S., Jude, B., und Bertrand, M. E. 2007. Drug-eluting stents: trading restenosis for thrombosis? *J. Thromb. Haemost.* 5 Suppl 1: 238-245.
- Van Coillie, E., Proost, P., Van Aelst, I., Struyf, S., Polfliet, M., de Meester, I., Harvey, D. J., Van Damme, J., und Opdenakker, G. 1998. Functional comparison of two human monocyte chemotactic protein-2 isoforms, role of the amino-terminal pyroglutamic acid and processing by CD26/dipeptidyl peptidase IV. *Biochemistry* 37: 12672-12680.
- Van Coillie, E., Van Damme, J., und Opdenakker, G. 1999. The MCP/eotaxin subfamily of CC chemokines. *Cytokine Growth Factor Rev.* 10: 61-86.
- Van Damme, J., Struyf, S., Wuyts, A., Van Coillie, E., Menten, P., Schols, D., Sozzani, S., de Meester, I., und Proost, P. 1999. The role of CD26/DPP IV in chemokine processing. *Chem Immunol* 72: 42-56.
- Vassar, R., Bennett, B. D., Babu-Khan, S., Kahn, S., Mendiaz, E. A., Denis, P., Teplow, D. B., Ross, S., Amarante, P., Loeloff, R., Luo, Y., Fisher, S., Fuller, J., Edenson, S., Lile, J., Jarosinski, M. A., Biere, A. L., Curran, E., Burgess, T., Louis, J. C., Collins, F., Treanor, J., Rogers, G., und Citron, M. 1999. Beta-secretase cleavage of Alzheimer's amyloid precursor protein by the transmembrane aspartic protease BACE. *Science* 286: 735-741.
- Vidal, R., Frangione, B., Rostagno, A., Mead, A., Revesz, T., Plant, G., und Ghiso, J. 1999. A stop-codon mutation in the BRI gene associated with familial British dementia. *Nature* 399: 776-781.

- Yamada, Y., Ando, F., und Shimokata, H. 2007. Association of gene polymorphisms with blood pressure and the prevalence of hypertension in community-dwelling Japanese individuals. *Int. J. Mol. Med.* 19: 675-683.
- Yamamoto, M., Horiba, M., Buescher, J. L., Huang, D., Gendelman, H. E., Ransohoff, R. M., und Ikezu, T. 2005. Overexpression of Monocyte Chemoattractant Protein-1/CCL2 in {beta}-Amyloid Precursor Protein Transgenic Mice Show Accelerated Diffuse {beta}-Amyloid Deposition. *Am. J Pathol.* 166: 1475-1485.
- Yu, L., Vizel, A., Huff, M. B., Young, M., Remmele Jr., R. L., und He, B. 2006. Investigation of N-terminal glutamate cyclization of recombinant monoclonal antibody in formulation development. *J. Pharm. Biomed. Anal.* 42: 455-463.
- Zhang, Y.J., Rutledge, B. J., und Rollins, B. J. 1994. Structure/activity analysis of human monocyte chemoattractant protein-1 (MCP-1) by mutagenesis. Identification of a mutated protein that inhibits MCP-1-mediated monocyte chemotaxis. *J Biol. Chem* 269: 15918-15924.

6 Angefügte Publikationen und Manuskripte

Schilling, S., **Cynis, H.**, von Bohlen, A., Hoffmann, T., Wermann, M., Heiser, U., Buchholz, M., Zunkel, K., und Demuth, H.-U. (2005). Isolation, catalytic properties, and competitive inhibitors of the zinc-dependent murine Glutaminyl Cyclase. *Biochemistry* 44 (40), 13415-13424.

Cynis, H., Schilling, S., Bodnar, M., Hoffmann, T., Heiser, U., Saido, T.C., und Demuth, H.-U. (2006). Inhibition of glutaminyl cyclase alters pyroglutamate formation in mammalian cells. *Biochim. Biophys. Acta* 1764, 1618-1625.

Cynis, H., Rahfeld, J.-U., Stephan, A., Kehlen, A., Koch, B., Wermann, M., Demuth, H.-U., und Schilling, S. (2008). Isolation of an isoenzyme of human glutaminyl cyclase: Retention in the Golgi complex suggests involvement in the protein maturation machinery. *J. Mol. Biol.* 379, 966-980.

Cynis, H., Scheel, E., Saido, T.C., Schilling, S., und Demuth, H.-U. (2008). Amyloidogenic Processing of Amyloid Precursor Protein: Evidence of a pivotal role of Glutaminyl Cyclase in generation of pyroglutamate-modified amyloid- β . *Biochemistry* 47 (28) 7405-7413

Schilling, S., Appl, T., Hoffmann, T., **Cynis, H.**, Schulz, K., Jagla, W., Friedrich, D., Wermann, M., Buchholz, M., Heiser, U., von Hörsten, S., und Demuth, H.-U. (2008) Inhibition of Glutaminyl Cyclase prevents pGlu-A β formation after intracortical/hippocampal microinjection *in vitro* / *in situ*. *J. Neurochem.* 106 (3) 1225-1236

Schilling, S., Zeitschel, U., Hoffmann, T., Heiser, U., Francke, M., Kehlen, A., Holzer, M., Hutter-Paier, B., Prokesch, M., Windisch, M., Jagla, W., Schlenzig, D., Lindner, C., Rudolph, T., Reuter, G., **Cynis, H.**, Montag, D., Demuth, H.-U., und Rossner, S. (2008) Glutaminyl Cyclase inhibition attenuates pyroglutamate A β and Alzheimer's disease-like pathology. *Nat. Med.* 14 (10) 1106-1111

Cynis, H., Hoffmann, T., Manhart, S., Gans, K., Kleinschmidt, M., Rahfeld, J.-U., Sedlmeier, R., Müller, A., Graubner, S., Heiser, U., Kehlen, A., Friedrich, D., Wolf, R., Quax, P. H. A., Thomsen, M., Schilling, S., und Demuth, H.-U. Enhancing a chemokines fate for degradation: a novel therapy for cardiovascular disease. *In Vorbereitung*

Isolation, Catalytic Properties, and Competitive Inhibitors of the Zinc-Dependent Murine Glutaminyl Cyclase[†]

Stephan Schilling,[‡] Holger Cynis,[‡] Alex von Bohlen,[§] Torsten Hoffmann,[‡] Michael Wermann,[‡] Ulrich Heiser,[‡] Mirko Buchholz,[‡] Katrin Zunkel,[‡] and Hans-Ulrich Demuth^{*‡}

Probiodrug AG, Weinbergweg 22, 06120 Halle/Saale, Germany, and ISAS-Institute for Analytical Sciences, Bunsen-Kirchhoff-Strasse 11, 44139 Dortmund, Germany

Received June 14, 2005; Revised Manuscript Received August 11, 2005

ABSTRACT: Murine glutaminyl cyclase (mQC) was identified in the insulinoma cell line β -TC 3 by determination of enzymatic activity and RT-PCR. The cloned cDNA was expressed in the secretory pathway of the methylotrophic yeast *Pichia pastoris* and purified after fermentation using a new three-step protocol. mQC converted a set of various substrates with very similar specificity to human QC, indicating a virtually identical catalytic competence. Furthermore, mQC was competitively inhibited by imidazole derivatives. A screen of thiol reagents revealed cysteamine as a competitive inhibitor of mQC bearing a K_i value of $42 \pm 2 \mu\text{M}$. Substitution of the thiol or the amino group resulted in a drastic loss of inhibitory potency. The pH dependence of catalysis and inhibition support that an uncharged nitrogen of the inhibitors and the substrate is necessary in order to bind to the active site of the enzyme. In contrast to imidazole and cysteamine, the heterocyclic chelators 1,10-phenanthroline, 2,6-dipicolinic acid, and 8-hydroxyquinoline inactivated mQC in a time-dependent manner. In addition, citric acid inactivated the enzyme at pH 5.5. Inhibition by citrate was abolished in the presence of zinc ions. A determination of the metal content by total reflection X-ray fluorescence spectrometry and atomic absorption spectroscopy in mQC revealed stoichiometric amounts of zinc bound to the protein. Metal ion depletion appeared to have no significant effect on protein structure as shown by fluorescence spectroscopy, suggesting a catalytic role of zinc. The results demonstrate that mQC and probably all animal QCs are zinc-dependent catalysts. Apparently, during evolution from an ancestral protease, a switch occurred in the catalytic mechanism which is mainly based on a loss of one metal binding site.

Several bioactive hormones, e.g., thyrotropin-releasing hormone (TRH) or gastrin, possess an N-terminal pyroglutamic acid residue, which is generated from glutamine during prohormone maturation (1–3). Glutaminyl cyclases (QCs) have been identified to catalyze the cyclization of N-terminal glutaminyl residues in plants and animals (4–6). However, recent results suggest that these enzymes are also capable of catalyzing the cyclization of N-terminal glutamic acid, liberating a water molecule instead of ammonia (7). In the last years, analysis of amyloidotic peptides deposited in familial British dementia, familial Danish dementia, and Alzheimer's disease revealed that these peptides bear pGlu in a considerable amount, likely influencing the degradation and neurotoxicity of these peptides (8–10). In contrast to the peptide hormones, however, glutamic acid precedes pGlu formation at the N-terminus of these amyloidotic peptides. It was assumed that cyclization of glutamic acid is a spontaneous process (11). The specificity of human QC, however, raises the possibility that pGlu-amyloid peptides are generated by enzymatic catalysis (7).

The first tissue distribution studies of mammalian QCs revealed that they are mainly expressed in brain and some peripheral glands, e.g., thyroid and thymus (12, 13). It is expected that the enzyme is directed to the regulated secretory pathway of the expressing cells where the hormone maturation process takes place (13, 14). Upon stimulation, QCs appear to be secreted from the cells together with the mature hormones (15).

QCs from bovine and human sources are the only mammalian enzymes that were isolated so far. The open reading frames of both enzymes consist of 361 amino acids with an overall sequence identity of about 90%. The mature proteins are glycosylated and exhibit a molecular mass of about 40 kDa (13, 16, 17). Human QC has been shown to be highly specific for the L-configuration of glutamine in the N-terminal amino acid position. Free glutamine was not converted. Other restrictions, however, were not observed, implying that the enzyme is responsible for N-terminal conversion of the very heterogeneous group of pGlu hormones (18). Initial mechanistic studies on human QC pointed to an involvement of histidinyl residues in the binding and conversion of the substrate as indicated by diethyl pyrocarbonate inhibition and site-directed mutagenesis (19). Later evidence showed that mammalian QCs are structurally related to zinc-dependent aminopeptidases and that the residues for complexation of the active site metal ions are also conserved

[†] This work was supported by the Federal Ministry of Education and Research of Germany (BMBF), Grant 0313185, to H.-U.D.

^{*} To whom correspondence should be addressed. Tel: 49 345 5559900. Fax: 49 345 5559901. E-mail: Hans-Ulrich.Demuth@probiodrug.de.

[‡] Probiodrug AG.

[§] ISAS-Institute for Analytical Science.

in human QC (20, 21). Furthermore, the metal chelators 1,10-phenanthroline, dipicolinic acid, and imidazole inhibited human QC, implying a metal-dependent catalysis of the enzyme (20). Other potential complexing inhibitors, such as EDTA, peptide thiols, or butaneboronic acid, which inactivate the related aminopeptidases of the clan MH, appeared to be inactive on human QC. In addition, initial attempts to determine the metal content in QC resulted in less than stoichiometric amounts of zinc bound to the enzyme (21).

Due to these apparent discrepancies, it was the aim of the present study to isolate mQC¹ in order to gain further insight into general characteristics of the mammalian QCs. Furthermore, the scope of the study focused on the clarification, whether mammalian QCs are metal-dependent catalysts. Answering this question might give a basic picture of the mechanistic background of mammalian QC catalysis.

EXPERIMENTAL PROCEDURES

Materials. The *Escherichia coli* strain DH5 α was applied for all plasmid constructions and propagation. *Pichia pastoris* strain X33 (AOX1, AOX2) was used for the expression of mQC. Yeast was grown, transformed, and analyzed according to the manufacturer's instructions (Invitrogen). Glutamyl peptides were obtained from Bachem (Bubendorf, Switzerland) or synthesized as described in another study (18). Streamline SP XL and butyl-Sepharose 4 Fast Flow were obtained from Pharmacia Biotech (Uppsala, Sweden). Pyroglutamyl aminopeptidase from *Bacillus amyloliquefaciens* was purchased from Qiagen (Hilden, Germany). Imidazole and cysteamine derivatives were from Acros and Sigma. All other materials used were of analytical grade.

Cloning Procedures. The primers for isolation of the open reading frame of mQC were designed using PubMed nucleotide entry AK017598, encoding the putative mQC. The primer sequences were as follows: sense, 5' ATATGCATGCATGGCAGGCAGCGAAGACAAGC; antisense, 5'-ATAAGCTTTTACAAGTGAAGATATTCCAACACAAA-GAC. Total RNA was isolated from murine insulinoma cell line β -TC 3 cells using the RNeasy mini kit (Qiagen) and reversely transcribed by SuperScriptII (Invitrogen). Subsequently, mQC cDNA was amplified on a 1:12.5 dilution of generated product in a 50 μ L reaction with Herculase enhanced DNA polymerase (Stratagene), inserted into the PCR Script CAM cloning vector (Stratagene) and verified by sequencing. The cDNA fragment encoding the mature mQC was amplified using the primers 5' ATACTC-GAGAAAAGAGCCTGGACGCAGGAGAAG (*Xho*I, sense) and 5' ATATCTAGATTACAAGTGAAGATATTCCAAC (*Xba*I, antisense). The digested fragment was ligated into the vector pPICZ α B, propagated in *E. coli* and verified by sequencing of the sense and antisense strand. Finally, the expression plasmid was linearized using *Pme*I, precipitated, and stored at -20°C .

Transformation of *P. pastoris* and Miniscale Expression. Plasmid DNA (1–2 μ g) was applied for transformation of competent *P. pastoris* cells by electroporation according to the manufacturer's instructions (Bio-Rad). Selection was

done on plates containing 100 μ g/mL zeocin. To test the recombinant yeast clones upon mQC expression, recombinants were grown for 24 h in 10 mL conical tubes containing 2 mL of BMGY. Afterward, the yeast was centrifuged and resuspended in 2 mL of BMMY containing 0.5% methanol. This concentration was maintained by addition of methanol every 24 h for about 72 h. Subsequently, QC activity in the supernatant was determined. Clones that displayed the highest activity were chosen for further experiments and fermentation.

Large-Scale Expression and Purification. The expression of mQC was performed in a 5 L reactor (Biostad B; B. Braun Biotech, Melsungen, Germany), essentially as described elsewhere (17). Briefly, fermentation was carried out in basal salt medium supplemented with trace salts at pH 5.5. Initially, biomass was accumulated in a batch and a fed batch phase with glycerol as the sole carbon source for about 28 h. Expression of mQC was initiated by methanol feeding according to a three-step profile recommended by Invitrogen for an entire fermentation time of approximately 65 h. Subsequently, cells and turbidity were removed from the mQC-containing supernatant by two sequential centrifugation steps at 6000g and 38000g for 15 min and 4 h, respectively. For purification, the fermentation broth was diluted with water to a conductivity of about 5 mS/cm and applied in reversed flow direction (15 mL/min) onto a Streamline SP XL column (2.5 \times 100 cm), equilibrated with 0.05 M phosphate buffer, pH 6.4. After a washing step in reversed flow direction with equilibration buffer for 2 column volumes, proteins were eluted at a flow rate of 8 mL/min using 0.15 M Tris-HCl buffer, pH 7.6, containing 1.5 M NaCl in forward direction. QC-containing fractions were pooled, and ammonium sulfate was added to a final concentration of 1 M. The resulting solution was applied onto a butyl-Sepharose FF column (1.6 \times 13 cm) at a flow rate of 4 mL/min. Bound mQC was washed with 0.05 M phosphate buffer, pH 6.8, containing 0.75 M ammonium sulfate for 5 column volumes and eluted in reversed flow direction with 0.05 M phosphate buffer, pH 6.8. The fractions containing mQC were pooled and desalted overnight by dialysis against 0.025 M Tris-HCl, pH 7.5. Afterward, the pH was adjusted to 8.0 by addition of NaOH and applied (4.0 mL/min) onto an Uno Q column (Bio-Rad), equilibrated with 0.02 M Tris-HCl, pH 8.1. After a washing step using equilibration buffer, mQC was eluted using the same buffer containing 0.18 M NaCl. Fractions exhibiting QC activity were pooled, and the pH was adjusted to 7.4 by addition of 1 M Bis-Tris buffer, pH 6.0. mQC was stable at 4 $^{\circ}\text{C}$ for up to 1 month. For long-term storage at -20°C , 50% glycerol was added.

Enzyme Assays and Analysis. For determination of mQC during the expression and purification, activity was evaluated using H-Gln- β NA at 30 $^{\circ}\text{C}$, essentially as described (22). Briefly, the samples consisted of 0.2 mM fluorogenic substrate, 0.1 unit of pyroglutamyl aminopeptidase in 0.05 M Tris-HCl, pH 8.0, and an appropriately diluted aliquot of QC in a final volume of 250 μ L. The excitation/emission wavelength was 320/405 nm. The assay reactions were initiated by addition of QC. One unit is defined as the amount of QC catalyzing the formation of 1.0 μ mol of pGlu- β NA from H-Gln- β NA per minute under the described conditions. In the fermentation broth, little interfering aminopeptidatic activity was observed sometimes, depending on the fermenta-

¹ Abbreviations: AAS, atomic absorption spectroscopy; GdmCl, guanidinium chloride; ICP-MS, inductively coupled plasma mass spectrometry; H-Gln-AMC, L-glutamyl-4-methylcoumarinylamide; H-Gln- β NA, L-glutamyl-2-naphthylamide; mQC, murine glutaminyl cyclase; TXRF, total reflection X-ray fluorescence spectrometry.

tation process. Unspecific cleavage of the QC substrate was determined by omitting the auxiliary enzyme. If necessary, the unspecific cleavage was subtracted from QC activity.

For inhibitor testing, the sample composition was the same as described above, except for the added putative inhibitory compound. Due to the pronounced substrate inhibition by Gln- β NA, inhibitory constants were determined using H-Gln-AMC at a concentration range between 0.25 and 4 K_M . The excitation/emission wavelength was adjusted to 380/460 nm. In contrast to H-Gln- β NA, substrate inhibition by H-Gln-AMC is negligible in the substrate concentration range applied and therefore does not interfere with the kinetic evaluation. The fluorometric assay using H-Gln-AMC was also applied to investigate the pH dependence of the catalytic parameters and inhibitory constants. In these studies, however, the reaction buffer consisted of 0.075 M acetic acid, 0.075 M Mes, and 0.15 M Tris-HCl, adjusted to the desired pH using HCl or NaOH. This buffer provides a constant ionic strength over a very broad pH range (23). Evaluation of the acquired enzyme kinetic data was performed using the equations:

$$k_{\text{cat}}(\text{pH}) = k_{\text{cat}}(\text{limit}) \quad (1)$$

$$K_M(\text{pH}) = K_M(\text{limit})(1 + [\text{H}^+]/K_{\text{HS}} + K_{\text{E1}}/[\text{H}^+] + K_{\text{E1}}/[\text{H}^+]K_{\text{E2}}/[\text{H}^+]) \quad (2)$$

$$k_{\text{cat}}/K_M(\text{pH}) = k_{\text{cat}}/K_M(\text{limit})[1/(1 + [\text{H}^+]/K_{\text{HS}} + K_{\text{E1}}/[\text{H}^+] + K_{\text{E1}}/[\text{H}^+]K_{\text{E2}}/[\text{H}^+])] \quad (3)$$

$$K_i(\text{pH}) = K_i(\text{limit})(1 + [\text{H}^+]/K_{\text{HI}} + K_{\text{E1}}/[\text{H}^+] + K_{\text{E1}}/[\text{H}^+]K_{\text{E2}}/[\text{H}^+]) \quad (4)$$

in which the left expression denotes the pH-dependent (observed) kinetic parameters. The parameters denoted with limit stand for the pH-independent ("limiting") values. K_{HS} , K_{HI} , K_{E1} , and K_{E2} denote the dissociation constants of the substrate amino group, the basic nitrogen of the imidazole-based inhibitor, and two dissociating groups of the enzyme, respectively. The data of the pH dependencies of the mQC inhibition by cysteamine derivatives were analyzed by assuming one dissociating group. The measurements were performed with a Novostar (BMG Labtechnologies, Germany) or a SpectraFluor Plus (TECAN, Switzerland) reader for microplates.

For investigation of the substrate specificity, mQC activity was studied spectrophotometrically utilizing glutamic dehydrogenase as the auxiliary enzyme (18). In contrast to the fluorometric assays, a variety of substrates can be analyzed because of the conversion of ammonia in the coupled reaction. Samples consisted of varying concentrations of the QC substrate (0.25–10 K_M), 0.3 mM NADH, 14 mM α -ketoglutaric acid, and 30 units/mL glutamic dehydrogenase in a final volume of 250 μL . The reaction buffer was 0.05 M Tris-HCl, pH 8.0. Reactions were started by addition of QC and pursued by monitoring of the decrease in absorbance at 340 nm for 8–15 min. The initial velocities were evaluated, and the enzymatic activity was determined from a standard curve of ammonia obtained under assay condi-

tions. All samples were measured at 30 °C, using the Sunrise reader for microplates (TECAN, Switzerland).

Pyroglutamyl aminopeptidase was assayed as described elsewhere (24). All kinetic data were evaluated using GraFit software (version 5.0.4 for Windows; Erithacus Software Ltd., Horley, U.K.).

The titrimetric determination of the $\text{p}K_a$ values of the amino groups of dimethylcysteamine and cysteamine was carried out at 30 °C using a DL50 Graphix titrator (Mettler-Toledo, Giessen, Germany). Six independent determinations were conducted in order to determine each $\text{p}K_a$ value.

mQC Inactivation/Reactivation. Murine QC was inactivated by addition of 2 mM 8-hydroxyquinoline in 50 mM Tris-HCl, pH 8.0 (final mQC concentration 50 $\mu\text{g}/\text{mL}$). Afterward, the sample was dialyzed against four changes [1000-fold excess (v/v), three cycles for 2 h, last cycle overnight] of 0.1 M Bis-Tris, pH 6.8, containing 1 mM EDTA. As controls, native enzyme samples were treated in the same way, except for addition of 8-hydroxyquinoline (control + EDTA) and additionally by omitting 8-hydroxyquinoline and EDTA in the dialysis buffer (control – EDTA). Addition of EDTA was necessary to avoid reactivation of the mQC during dialysis by traces of metal ions present in the buffer.

Reactivation experiments were performed at room temperature using Zn^{2+} , Mn^{2+} , Ni^{2+} , Ca^{2+} , and Co^{2+} ions at final concentrations of 1 mM in 0.1 M Bis-Tris, pH 6.8. A sample of dialyzed QC was added to the respective metal (1/1 v/v) and diluted 10-fold in 0.05 M Tris-HCl, pH 8.0, containing 1 mM EDTA, and the QC activity was determined.

TXRF and AAS Measurements. After purification of mQC as described before, mQC was desalted by size-exclusion chromatography using a Sephadex G-25 fast desalting column (1.0 \times 10 cm) which was pre-equilibrated in 10 mM Tris-HCl, pH 7.6. The QC-containing fractions were collected, the protein was concentrated to 3 mg/mL by ultrafiltration, and the metal content was analyzed. The elution buffer was used as a background control. Element analysis was performed using TXRF. The method offers excellent performance for the simultaneous quantitative determination of the multielement composition (for elements with atomic number $Z \geq 14$) of microsamples (25). An Extra II TXRF module containing molybdenum and tungsten primary X-ray sources (Seifert, Ahrensburg, Germany) connected to a Link QX 2000 detector/analyzed device (Oxford Instruments, New Wycombe, U.K.) was used. The X-ray sources were operated at 50 kV and 38 mA. Like all X-ray techniques, TXRF works basically without sample consumption.

Five microliters of undiluted sample solution or control buffer was applied onto the TXRF quartz glass sample support and dried under IR radiation. Afterward, 5 μL of diluted Se aqueous standard solution (internal standard, Aldrich) was added to each sample and dried again. The signals of X-ray fluorescence were allowed to be collected in 100 s. In the case of scarce sample amounts, only a single preparation was analyzed by TXRF in some cases; otherwise, three replicates were used.

With a view toward validation of the results, an independent method was chosen to corroborate the Zn values obtained by TXRF in the samples as well as in the buffer. A state of the art Z-8000 FAAS device (Hitachi, Japan) was used for this purpose. Zn analyses were performed with

Table 1: Purification Scheme of Recombinant Murine QC (mQC) Following Expression in *P. pastoris*

purification step	protein (mg)	QC activity (units)	specific QC activity (units/mg)	yield (%)
fermentation broth	2358	837	0.4	100
cation-exchange chromatography	45	231	5.1	27
hydrophobic interaction chromatography	23.7	156	6.6	19
anion-exchange chromatography	7.5	84	11.2	10

standard parameters using a set of aqueous standard solutions for calibration.

RESULTS

Cloning and Expression of mQC. The murine insulinoma cell line β -TC 3 was identified to express mQC by determination of enzymatic activity and by RT-PCR using primers derived from a putative mQC cDNA which was deposited in the nucleotide database as entry AK017598 (not shown). Subsequently, a cDNA encoding the mature mQC was cloned into pPICZ α B. Due to cloning, the signal peptide of murine QC was exchanged by the vector-encoded α -leader of *Saccharomyces cerevisiae* which has been shown to direct heterologous proteins efficiently into the secretory pathway of yeast. *P. pastoris* cells were transformed with the plasmid construct, and the medium was checked on QC activity after growing the cells on methanol. The best expressing clones were subjected to fermentation in a 5 L reactor. For purification, a three-step protocol was established consisting of an initial expanded bed adsorption on a cation-exchange resin, followed by a hydrophobic interaction chromatography and a final anion-exchange chromatography step. The purification process after a typical fermentation is described in Table 1. Usually, 10–20 mg of mQC was isolated after fermentation, corresponding to a yield of about 10%. Fairly homogeneous mQC was obtained after purification, as shown by SDS–PAGE analysis (Figure 1). Protein identity was also characterized by N-terminal sequencing and MALDI-TOF analysis (not shown). Deglycosylation of the protein using endoglycosidase H resulted in a shift of the mQC band in SDS–PAGE corresponding to a mass of about 2 kDa, indicating the mQC is a glycoprotein (not shown).

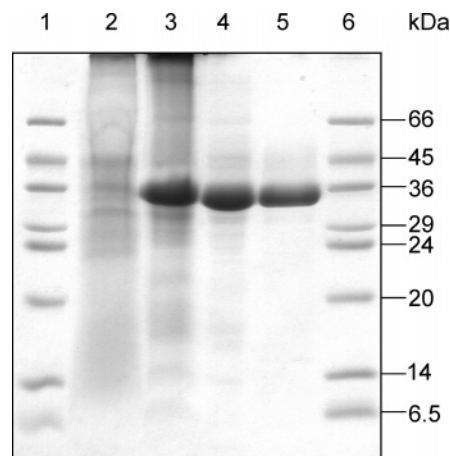


FIGURE 1: SDS–PAGE analysis of the chromatographic steps used to purify murine QC (mQC). Lanes: 1, molecular mass standards (kDa); 2, fermentation broth after centrifugation; 3, the QC-containing fraction after expanded bed adsorption on a cation-exchange resin; 4, purified mQC after hydrophobic interaction chromatography; 5, purified mQC after anion-exchange chromatography; 6, molecular mass standards. Proteins were visualized by Coomassie staining.

Substrate and Inhibitor Specificity. Recently, the substrate specificity of human QC was characterized in detail (18). For comparison, the kinetic parameters of conversion of some of these substrates by mQC were also determined (Table 2). The specificity constants for most of the substrates were somewhat lower compared to human QC. These differences are mainly based on higher K_M values; the turnover rates were virtually identical to human QC (18, 20), indicating little differences in substrate binding. As previously observed for human QC (18), low specificities were found for dipeptides, especially if they possess small or negatively charged residues in the second amino acid position as, e.g., seen for H-Gln-Gly-OH or H-Gln-Glu-OH. For longer peptides, a slight increase in specificity could be observed. Highest specificities were found for peptides with large hydrophobic residues in the second amino acid position or for dipeptide surrogates.

Imidazole derivatives inhibited the mQC catalysis in a competitive manner (not shown). The K_i values for four inhibitors were analyzed (Table 2). As was previously observed for inhibition of human QC, 1-substituents in-

Table 2: Kinetic Parameters of Substrate Conversion and Inhibition of QC^a

compound	murine QC				human QC ^b	
	K_M (mM)	k_{cat} (s ⁻¹)	K_i (mM)	k_{cat}/K_M (mM ⁻¹ s ⁻¹)	k_{cat}/K_M (mM ⁻¹ s ⁻¹)	K_i (mM)
substrates						
H-Gln-AMC	0.048 ± 0.003	6.0 ± 0.2	5.9 ± 0.7 ^d	125 ± 4	98 ± 2	nd ^c
H-Gln-βNA	0.040 ± 0.004	22 ± 1	1.77 ± 0.18 ^d	550 ± 30	294 ± 6	1.21 ± 0.07 ^d
H-Gln-Gly-OH	0.41 ± 0.03	12.4 ± 0.2		30 ± 2	53 ± 1	
H-Gln-Ala-OH	0.4 ± 0.02	42 ± 1		105 ± 3	247 ± 4	-
H-Gln-Gln-OH	0.15 ± 0.01	32 ± 1		213 ± 8	140 ± 2	
H-Gln-Glu-OH	0.8 ± 0.06	29 ± 1		36 ± 1	58 ± 1	
H-Gln-Gly-Pro-OH	0.17 ± 0.01	21.6 ± 0.2		127 ± 6	195 ± 7	
H-Gln-Trp-Ala-NH ₂	0.072 ± 0.005	41 ± 1		569 ± 26	940 ± 24	
H-Gln-Arg-Gly-Ile-NH ₂	0.32 ± 0.02	34 ± 1		106 ± 4	234 ± 4	
H-Gln-Asn-Gly-Ile-NH ₂	0.36 ± 0.03	68 ± 2		189 ± 10	329 ± 7	
H-Gln-Thr-Gly-Ile-NH ₂	0.16 ± 0.02	23 ± 1		144 ± 12	nd	
inhibitors						
imidazole			0.16 ± 0.01			0.103 ± 0.004
benzimidazole			0.192 ± 0.003			0.138 ± 0.005
methylimidazole			0.023 ± 0.001			0.030 ± 0.001
benzylimidazole			0.0064 ± 0.0007			0.0071 ± 0.0003

^a Reactions were carried out in 0.05 M Tris-HCl, pH 8.0, at 30 °C. ^b Data from refs 18 and 20. ^c nd, not determined. ^d Substrate inhibition.

creased the inhibitory potency of imidazole. For the core structures imidazole and benzimidazole, the determined K_i values were slightly higher as compared to human QC. Two 1-substituted imidazole derivatives, methylimidazole and benzylimidazole, however, showed similar inhibitory potency against both enzymes.

The only little differences in selectivity of mQC for various substrates and the imidazole-based competitive inhibitors compared to human QC reflect the high degree of sequential and hence structural conservation of mammalian QCs.

Inhibition by Chelators. The inhibition of porcine QC by the heterocyclic chelator 1,10-phenanthroline was reported already in one of the first studies on QC (1). Recently, we performed an extended study on the inhibitory specificity of human QC (20). Besides 1,10-phenanthroline, also dipicolinic acid inhibited the QC catalysis in a time-dependent manner. EDTA, however, did not inactivate the enzyme even at concentrations above 20 mM. These findings were also corroborated with mQC (not shown). Additionally, we tested another heterocyclic chelator, 8-hydroxyquinoline, as inhibitor of mQC catalysis. As was observed for the other inhibitory active heterocyclics, addition of 8-hydroxyquinoline to the QC assay resulted in time-dependent inhibition of substrate conversion (Figure 2A). Due to treatment of the enzyme with the chelator, it was possible to isolate inactive mQC after dialysis against buffer containing 1.0 mM EDTA. The isolated enzyme could be fully reactivated by addition of $ZnSO_4$. Significant reactivation was also observed with cobalt and nickel ions (Figure 2B). Addition of EDTA during dialysis was necessary in order to avoid a reactivation of the enzyme by transition metals present in the buffer solutions. EDTA had no influence on QC activity during dialysis (Figure 2B).

Inactivation of mQC was also observed by incubation in citrate buffer at pH 5.5 (Figure 2C). In contrast, at neutral pH, mQC activity was fairly stable during the time of incubation. Furthermore, inactivation by citric acid could be prevented by addition of $ZnSO_4$, indicating an inhibition due to release of zinc from mQC.

Inhibition by Cysteamine Derivatives. The only potent competitive inhibitors of QC known thus far base on an imidazole or imidazole-related core structure. The putatively related bacterial aminopeptidases are inhibited competitively by peptide thiols (26). An inhibition of human QC by one of these compounds, however, could not be detected (20). In contrast, a screening run of several thiols available revealed a potent competitive inhibition of mQC by cysteamine, exhibiting a K_i value of $42 \pm 2 \mu M$. The plot of the slopes obtained from the Lineweaver–Burk evaluation was strictly linear, effectively ruling out mixed-type inhibition (Figure 3). An initial investigation of structurally related compounds revealed a necessity of both amino and thiol group for potent inhibition (Table 3). Modification of the thiol group resulted in a drastic drop of inhibitory potency as shown for ethylenediamine and ethanolamine. In addition, the amino group of cysteamine plays a crucial role for inhibitor binding. However, its modification did not lead to a complete loss of inhibition, as indicated by mercaptoethanol or ethylmercaptan.

Interestingly, N-alkylation appears to be beneficial for binding as revealed by the potent inhibition of mQC by dimethyl- and diethylcysteamine (Table 3).

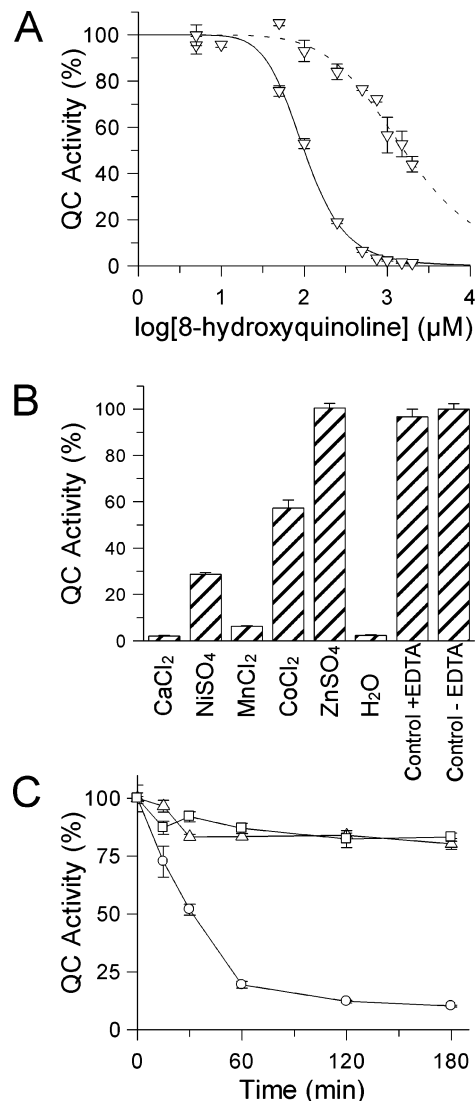


FIGURE 2: Influence of chelating agents and metal ions on mQC activity. (A) Time-dependent inhibition of mQC by 8-hydroxyquinoline. mQC activity was determined at 30 °C using H-Gln-AMC in 0.05 M Tris-HCl, pH 8.0. Varying concentrations of the chelator were added to mQC, and activity was determined immediately (dotted trace) or after 15 min of incubation (continuous trace). (B) Reactivation of mQC with divalent metals. Prior to reactivation, mQC was inactivated to a residual activity of 1–2% by addition of 1 mM 8-hydroxyquinoline in 0.05 M sodium phosphate, pH 7.5. Subsequently, the enzyme was subjected to dialysis against 0.05 M Bis-Tris, pH 6.8, containing 1 mM EDTA. Reactivation of mQC was investigated by addition of a 2 mM stock solution of different metal ions to the inactivated enzyme (dilution, 1:2 v/v). Controls are given by enzyme samples that were not inactivated but also dialyzed against EDTA solution as the inactivated enzyme (+EDTA) and by enzyme samples that were dialyzed against buffer solutions without adding EDTA (–EDTA). (C) Inactivation of mQC by citric acid. mQC was incubated in 0.15 M sodium citrate buffer at pH 5.5 (circles). At the indicated times, enzyme samples were removed, and the QC activity was determined using H-Gln-AMC in 0.05 M Tris-HCl, pH 8.0, containing 1.0 mM EDTA. EDTA was added to the reaction buffer in order to avoid a rapid reactivation of mQC by traces of zinc present in buffer solutions. Inactivation of mQC by citrate could be halted by addition of 100 μM $ZnSO_4$ during incubation (squares). Also, incubation of mQC in 0.05 M Bis-Tris, pH 6.8, for the same time did not result in significant inactivation (triangles).

pH Dependence of Catalysis and Inhibition. On the basis of the continuous coupled QC assays we described previously (22), the first detailed pH dependence study for conversion

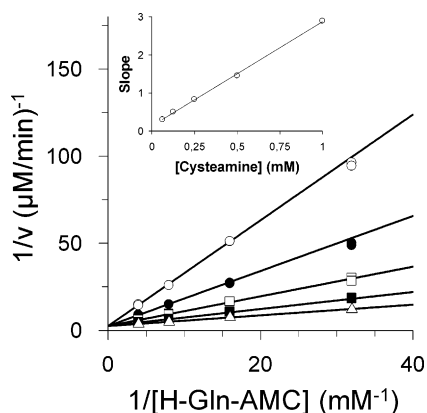


FIGURE 3: Lineweaver–Burk plot for mQC-catalyzed cyclization of H-Gln-AMC in the presence of various concentrations of cysteamine between 0.0625 and 1.0 mM. The inset shows a plot of the determined slope versus the inhibitor concentrations. The reactions were carried out in 0.05 M Tris-HCl, pH 8.0, at 30 °C.

Table 3: Inhibition of mQC by Cysteamine Derivatives and Derived Compounds^{a,b}

Compound	K_i -value (μM)	Structure
cysteamine	42 ± 2	<chem>NCCCS</chem>
N-dimethylcysteamine	29 ± 2	<chem>CN(C)CCS</chem>
N-diethylcysteamine	10.9 ± 0.3	<chem>CCN(CC)CCS</chem>
mercaptoethanol	2580 ± 160	<chem>OCCS</chem>
ethylmercaptane	n.d. ^c	<chem>CCS</chem>
ethylenediamine	22000 ± 1500	<chem>NCCN</chem>
ethanolamine	19300 ± 1100	<chem>NCCO</chem>
ethylamine	n.i.	<chem>CCN</chem>

^a Reactions were carried out in 0.05 M Tris-HCl, pH 8.0, at 30 °C.
^b ni, no inhibition detected at $[S] = K_M$ and $[I] = 10$ mM; nd, not determined. ^c 60% residual mQC activity at $[S] = 4K_M$ and $[I] = 10$ mM.

of H-Gln-AMC by a mammalian QC was performed using mQC (Figure 4A–C). Prior to analysis, we examined the pH-dependent stability of mQC and the auxiliary enzyme pyroglutamyl aminopeptidase. Both enzymes were stable in the pH range between 5.5 and 9.0 for 30 min at 30 °C (not shown). At pH values below or above, mQC was inactivated rapidly. By addition of 20 μM ZnSO_4 , denaturation in the acidic range could be partially prevented. However, we detected an inhibition of the auxiliary enzyme by trace

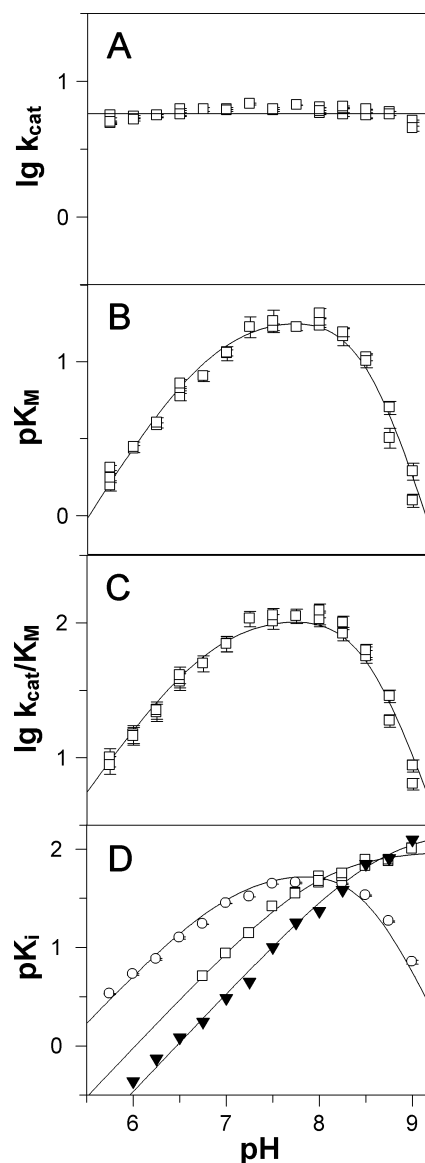


FIGURE 4: pH dependence of the kinetic parameters for the mQC-catalyzed cyclization of H-Gln-AMC and for the inhibition of this cyclization by three competitive inhibitors. (A) pH dependence of k_{cat} . Data points are well described by the assumption of pH independence. (B) pH dependence of K_M . The theoretical curve was calculated using eq 2, with $\text{p}K_{\text{HS}} = 6.83$, $\text{p}K_{\text{E1}} = 8.9$, $\text{p}K_{\text{E2}} = 8.1$, and $K_M(\text{limit}) = 0.047$ mM. (C) pH dependence of k_{cat}/K_M . The theoretical curve was calculated using eq 3 with the same values used for the constants as in the theoretical curve of (B) and $k_{\text{cat}}/K_M(\text{limit}) = 123$ $\text{mM}^{-1} \text{s}^{-1}$. (D) pH dependence of K_i for the inhibitors 1-methylimidazole (circles), cysteamine (triangles), and *N,N*-dimethylcysteamine (squares). The theoretical curve for 1-methylimidazole was calculated using eq 4, with $\text{p}K_{\text{HI}} = 7.05$, $\text{p}K_{\text{E1}} = 8.9$, $\text{p}K_{\text{E2}} = 8.1$, and $K_i(\text{limit}) = 0.015$ mM. The pH dependencies of inhibition by the cysteamine derivatives were fitted according to single dissociation curves. Fitting results were $\text{p}K_a = 8.7 \pm 0.1$ and $K_i(\text{limit}) = 0.006 \pm 0.001$ mM for cysteamine and $\text{p}K_a = 8.00 \pm 0.03$ and $K_i(\text{limit}) = 0.0104 \pm 0.0004$ mM for *N,N*-dimethylcysteamine.

amounts of zinc. Therefore, the range of analysis was limited to pH 5.5–9.0.

As shown in Figure 4A, the turnover number of mQC was virtually unchanged in the pH range of analysis. A slight decrease of k_{cat} was observed in the basic region, which might imply a decrease of k_{cat} due to deprotonation of an essential group of the enzyme or a change in the rate-determining

step of catalysis. However, the small number of data points collected in this pH range prevented a reliable determination of the corresponding putative dissociation constant. Because of the independence of k_{cat} on pH, the shapes of the curves of the kinetic parameters K_M and k_{cat}/K_M are characterized by the same dissociation constants in the pH range between 5.5 and 9.0 (Figure 4B,C). In the acidic range, the slopes of both curves indicate dependence of substrate binding on the unprotonated substrate H-Gln-AMC as suggested by the dissociation constant of 6.85, which is in good agreement with the pK_a of the substrate amino group [6.83 ± 0.01 (20)]. In the basic range above pH >8.25, K_M increases (Figure 4B). The inflections of the curve can be interpreted by deprotonation of two dissociating groups of the enzyme possessing pK_a values of 8.1 and 8.9.

Interestingly, the pH dependence of inhibition by cysteamine, dimethylcysteamine, and 1-methylimidazole showed conspicuous differences (Figure 4D). While the pH dependencies in the acidic range for all inhibitors tested show one inflection of a corresponding pK_a value that is close to the respective pK_a of the unprotonated nitrogen, only 1-methylimidazole causes a pH-dependent increase of the K_i value in the basic pH region. Apparently, imidazole derivatives interact with the active site of mQC in a different manner than cysteamine and its derivatives.

Determination of the Metal Content of mQC. The time dependency of the inactivation of mQC by different chelators and the efficient reactivation of the apoenzyme by zinc ions suggest the necessity of bound zinc for the catalysis of the enzyme. The stoichiometry of zinc binding by QC, however, is not addressed by these experiments. Therefore, we used mQC purified from several fermentations and analyzed the enzyme samples using TXRF. This method offers the chance to analyze complex mixtures in parallel, requiring only minute quantities of sample.

Several elements were detected in the enzyme samples. Some of these are originally contained in the buffer used, e.g., Cl, K, Ca, Fe, and Br. They do not differ significantly in their concentrations in the controls as well as in the enzyme samples. In addition to these elements, some traces of the elements Ni and Cu and appreciable amounts of S and Zn could be detected in mQC-containing samples (Figure 5). In contrast, the elution buffer control did not display a zinc signal at all. Quantification of the zinc content of three independent enzyme samples resulted in a zinc content of 0.94 ± 0.09 mol of zinc/mol of enzyme. This result was entirely corroborated by the parallel determination of the samples using AAS, yielding 0.9 ± 0.1 mol of zinc/mol of mQC (not shown).

Influence of Zinc Release on the Protein Structure. To investigate the influence of zinc release on the structure of mQC, fluorescence spectra of the enzyme were recorded. In the presence of $300 \mu\text{M}$ heterocyclic chelator 2,6-dipicolinic acid, mQC was inactivated to a residual activity of 3% at pH 7.2 (Figure 6A). The same experimental conditions were applied for an investigation of putative structural changes caused by the release of the metal ion by dipicolinic acid. During the time of inactivation, fluorescence emission spectra were recorded after excitation at 295 nm (Figure 6B). Interestingly, mQC inactivation appears to be accompanied only by little structural changes, as indicated by a slight decrease in fluorescence intensity after 2 h of incubation.

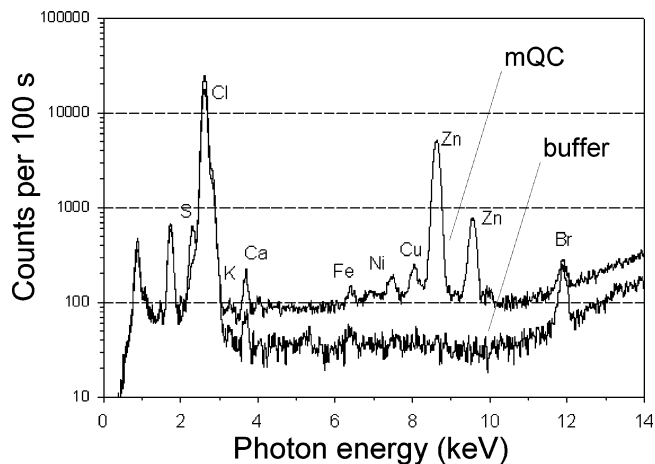


FIGURE 5: Superposition of total reflection X-ray fluorescence (TXRF) spectra of a mQC preparation and of elution buffer. mQC was purified as shown in Figure 1 and desalted by size-exclusion chromatography. The elution buffer (10 mM Tris-HCl, pH 7.6) is shown as a background control. The evaluation of the measurements reveals equimolar amounts of zinc bound to the enzyme.

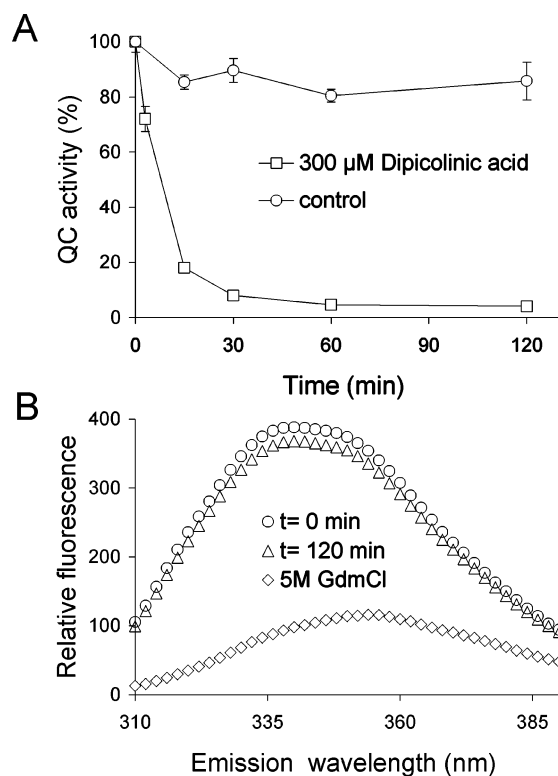


FIGURE 6: Influence of zinc depletion on mQC structure. (A) mQC was inactivated using $300 \mu\text{M}$ dipicolinic acid in 50 mM Mops buffer and 300 mM NaCl, pH 7.2 (squares). At the times indicated, residual activity was determined using H-Gln- β NA in 50 mM Tris-HCl, pH 8.0, containing 1 mM EDTA under standard conditions. Residual activity dropped to 3% after 2 h of incubation. mQC was stable in the absence of the chelating agent (circles). (B) Fluorescence emission spectra of mQC ($0.2 \mu\text{M}$) after excitation at 295 nm. The protein was dissolved in 50 mM Mops buffer, 300 mM NaCl, and $300 \mu\text{M}$ dipicolinic acid, and spectra were recorded directly after addition of the chelating agent (circles, $t = 0$ min) and after 2 h of incubation (triangles, $t = 120$ min). A spectrum of unfolded mQC was obtained in 50 mM Mops, pH 7.2, containing 5 M GdmCl (squares).

Furthermore, the fluorescence emission maximum remained unchanged at 340 nm, indicating that the environment of the tryptophanyl residues did not change significantly upon

```

Murine QC  MAGSEDKRVVGTLLHLLQLATVLSLTAGNLSLVSAAWTQEKNNHQPALHNSSSLQVVAEG
Human QC  MAGGRHRRVVGTLHLLLLVA-ALPWASRGVSPSASAWPEEKNYHQPAILNNSALRQIAEG
Bovine QC  MAGCRDPRVVDLHLLLLVA-VLPLAVSGVRRGAVDWTQEKNYHQPALLNVSSLRQVAEG
*** .. ***.***** * .*. : .: : *.:***:*** ** *.:*:*:***

SGAP  -----AP-DIPLA-----NPKAHL
      . :. : . *

Murine QC  TSISEMWQNDLRPLLIERYPGSPGSYARQHIMQRIQLQAEWVVEVDTFLSRTPYGYRS
Human QC  TSISEMWQNDLQPLLIERYPGSPGSYAARQHIMQRIQLQADWVLEIDTFLSQTGYRS
Bovine QC  TSISEMWQNDLRPLLIERYPGSPGSFAARQHIMQRIQLQADWVLEVDTFLSQTPYGYRS
*****.:*****.:*****.:*.:*.:*****:*****

SGAP  TQLSTIAANNG---NRAHGRPGYKASVDYVKAQLD--AAGYTTTLQOFTSGGATGYNL
*.:* : * : * * * * : : : : * . . : * * . * .

Murine QC  FSNIISTLNPEAKRHLVLACHYDSKYFRWDSRVFVGATDSAVPCAMMLELARALDKKLH
Human QC  FSNIISTLNPTAKRHLVLACHYDSKYFHWNNRVFVGATDSAVPCAMMLELARALDKKLH
Bovine QC  FSNIISTLNPTAKRHLVLACHYDSKYFPHWDDRVFVGATDSAVPCAMMLELARALDKQLF
***** *****.:*.:*****.:*****.:*

SGAP  IAN---WPGGDPNKVLMAGAHLDSV-----SSGAGINDNGSGSAAVLETALAVSR---
:.* . :.: * : .* ** . * . * . * * : * * * * :.:

Murine QC  SLKDVSGSKPDLSQLIFFDGEEAFHHWSPQDSLYGSRHLAQKMASSPHPPGSRGTNQLD
Human QC  SLKTVSDSKPDLSQLIFFDGEEAFLHWSPQDSLYGSRHLAAKMASTPHPPGARGTSQLH
Bovine QC  SLKNIISDRPDLSQLIFFDGEEAHLWSPQDSLYGSRHLASKMASTPHPPGARDTNQLH
** :*.:*****.***** ***** ***** * * : * * * * * . * . * .

SGAP  ----AGYQPKHLRFAWGAEEL-----GLIGSKFYVNNLPSADRSLAGYLN---
.: ** * : : . : * * . * * : . : . :

Murine QC  GMDLLVLLDLIGAANPTFPNFFPKTRWFNRLQAIIEKELYELGLLKDHSLERKYFQNFY
Human QC  GMDLLVLLDLIGAPNPTFPNFFPNSARWFERLQAIIEHELHELGLLKDHSLEGRYFQNSY
Bovine QC  GMDLLVLLDLIGAPFPFPNFFPNTARWFGRLQAIIEHGLRELGLLKDHSSEYFRNYSY
*****. *****.:** **:*: * ***** * **:*.*

SGAP  -----FDMIGSPNGY--FVYDDDPVIEK--TFKNYFAGLNVPTIETE-----
:*:*:. * : * . : : : : * : . : . *

Murine QC  GNIIQDDHIPFLRKGVPVLHLIASP-----FPEVWHTMDNEENLH
Human QC  GGVIQDDHIPFLRRGVPVLHLIISP-----FPEVWHTMDNEENLD
Bovine QC  GGVIQDDHIPFLRRGVPVLHLISSP-----FPEVWHTMDNEENLD
*.:*****.:*****.* * *****.

SGAP  -GDGRSDHAPFKNVGVVGGVGLFTGAGYTKSAAQAQKWGGTAGQAFDRCYHSSCDSLNSIN
. :.* * * . * * * * :. . . * . :.: * . * :.

Murine QC  ASTIDNLNKIIQVFVLEYLHL-----
Human QC  ESTIDNLNKILQVFVLEYLHL-----
Bovine QC  RTTIDNLNKILQVFVLEYLHL-----
:*****.:*****

SGAP  DTALDR-NSDAAAHAIWTLSSGTGEPPT
:.*. * . . : . *

```

FIGURE 7: Sequence alignment of the primary structures of QCs from a bovine (361 amino acids), human (361 amino acids), and murine (362 amino acids) origin. Sequence identity is about 80% between all proteins. Differences are mainly evident in the N-terminal signal sequences that direct the proteins to the secretory pathway. In contrast to human and bovine QC, which contain two N-glycosylation sites located at asparagines 49 and 296 or 183, respectively, murine QC has only one such site (asparagine 50). Sequence alignment was extended by the aminopeptidase of *S. griseus*, a family type member of the aminopeptidase family M28A, in which QCs are deposited in the MEROPS database. The residues of zinc complexation (bold) are conserved in all mammalian QCs.

inactivation of mQC. The impact of unfolding of mQC is illustrated by the emission spectrum obtained in 5 M GdmCl (Figure 6B). Upon unfolding, the fluorescence intensity drops drastically and is accompanied by a change in the fluorescence emission maximum to 355 nm, which is characteristic for tryptophan in aqueous solution.

DISCUSSION

Our recent studies were focused on comparison of the QCs from plants and mammals and revealed that the proteins from these origins show similarities neither in terms of structure nor in inhibitory specificity (18, 20, 27). In contrast, mammalian QCs display a high homology of their primary

structure, as revealed by a sequence alignment of the human, murine, and bovine QC, the proteins that were cloned until now (Figure 7). As shown in the present study, this conservation in sequence is well reflected by the almost identical substrate and inhibitory specificity of mQC and human QC (Table 2). The specificity constants for conversion of each substrate differed by far less than 2-fold between human and murine QC. Similarity between both proteins is even more evident in the case of the K_i values of imidazole-based inhibitors, suggesting virtually identical modes of inhibitor binding and substrate conversion.

On the basis of the inhibitory specificity and the similarity of the primary structure to bacterial aminopeptidases of the

clan MH, a zinc-dependent catalysis was proposed previously for human QC (20). Some debate, however, was raised after the determination of the zinc content of human QC by ICP-MS (21). Additionally, the authors based their conclusion of a metal-independent mechanism of mammalian QCs on the finding that EDTA and peptide thiols, chelators that inhibit the related aminopeptidases of the clan MH, do not inhibit QC (20, 26). In fact, we also could not detect an inhibition of mQC by EDTA. However, there are several examples known of zinc-dependent aminopeptidases that are not susceptible to inactivation by EDTA but which are sensitive to heterocyclic chelators (28, 29). Moreover, as shown in Figure 7, the zinc-binding motif of the aminopeptidase of *Streptomyces griseus*, the prototype peptidase of family M28B of the metalloaminopeptidases, in which QC is deposited in the MEROPS database (www.merops.sanger.uk), is conserved in all mammalian QCs that were cloned to date. Finally, the inactivation of mQC by the chelators 1,10-phenanthroline, 2,6-dipicolinic acid, 8-hydroxyquinoline, and citrate, the potent reactivation by zinc ions, and the stoichiometric amounts of zinc found in mQC using TXRF and AAS clearly suggest mQC being a metalloenzyme (Figures 2 and 4).

In addition to clarifying the metal dependence of QC, our efforts to further characterize the inhibitory specificity of mammalian QCs resulted in the identification of cysteamine and cysteamine derivatives as a second class of potent competitive inhibitors (Figure 3 and Table 3). Substitution of either functional group of the compounds results in a drop of inhibitory potency (Table 3), indicating a specific binding of the inhibitors to the active site of mQC mediated by interactions of both groups. Interestingly, inhibition by cysteamine depends strongly on presence of both the thiol and the amino group. However, the thiol group appears more important for binding, since modification results in a more drastic decrease in inhibitory potency as exemplified by aminoethanol, ethylenediamine, and ethylamine. Substitution of the amino group yielded inhibitory compounds with only about 100-fold reduced potency, e.g., mercaptoethanol and ethylmercaptan. Thus, apparently the thiol of the inhibitors provides a dominating contribution to binding. In contrast to cysteamine, however, the inhibitory potency of imidazole was thought to depend only on the interaction of the basic nitrogen with the active site of QC (20).

Differences of the binding mode between cysteamine derivatives and imidazoles become also evident comparing the pH dependence of QC inhibition by cysteamine, dimethylcysteamine, and 1-methylimidazole (Figure 4). While the K_i values in the case of the cysteamine derivatives appear to depend only on the protonation status of the inhibitor, the K_i value of 1-methylimidazole is also influenced by the protonation status of the mQC active site, similar to that seen by the pH dependencies of the substrate H-Gln-AMC and the inhibitor 1-methylimidazole in the basic pH region (Figure 4B,D). Obviously, deprotonation of two dissociating groups of the enzyme leads to diminished binding of the substrate and the imidazole-based inhibitor. Reduction in affinity might be caused by deprotonation and subsequent alterations in the active site structure leading to disruption of a binding site, e.g., the hydrophobic interaction to the imidazole ring and the hydrophobic AMC residue of the substrate. Similar results were obtained with butaneboronic

acid and one of the related aminopeptidases (30). In contrast to 1-methylimidazole, no drop of inhibitory potency was observed with the cysteamine derivatives in the basic pH region (Figure 4D), demonstrating differences in the binding mode of the competitive inhibitors. Besides these differences, the pH dependencies for the binding of the inhibitors and the substrates also show similarities. All require an unprotonated nitrogen for binding to the active site; i.e., they must be free of positive charge, as indicated by the acidic shapes of the pH dependencies.

In light of the proven zinc content of mQC and the results of the investigations regarding the pH dependence and structural requirements for inhibition, it is tempting to speculate that, in the case of the cysteamine-derived inhibitors, the thiol and, in the case of the imidazole derivatives, a ring nitrogen interact with the active site zinc ion. Probably, binding of the amino group of cysteamine accords then to the binding mode of the substrate amino group. This, in turn, would implicate that the γ -carbonyl of the substrate glutaminy residue interacts with the active site zinc, which enforces the polarity of the carbonyl and accelerates the nucleophilic attack of the amino group, as suggested previously for human QC (20).

A catalytic role of zinc is further implicated by the structural integrity of mQC after removal of the zinc ion, demonstrating that zinc is not required for stabilizing the overall structure of the protein (Figure 6). Furthermore, this is suggested by the homology to the aminopeptidases that require zinc for their catalytic activity. The peptidases of the clan MH, however, contain two zinc ions in the active site in order to exert their catalytic function. Thus, apparently during evolution of QC from an ancestral protease there was a possible switch of the catalytic mechanism that is mainly based on disruption of one zinc binding site. It is still unclear, however, which residues ligate the zinc ion in the active site. As shown in Figure 7, apparently all five residues coordinating the two zinc ions in the aminopeptidase of *S. griseus* (SgAP) are also found in mammalian QCs. Initial studies using site-directed mutagenesis point to a crucial role of the two histidines and glutamic acid residues, which are responsible for zinc binding in clan MH proteins, for catalytic activity of human QC (19, 21). In contrast, mutagenesis of the two aspartic acid residues was reported to have no effect on catalysis (21). Thus, in mammalian QCs possibly one of the glutamic acid residues and the two histidines are responsible for zinc complexation. Although these results are still the subject of further studies, the present results suggest a substantial change in zinc-complexation geometry during evolution of these enzymes. Final clarification might only be achieved by the solution of the protein crystal structure.

In conclusion, our results obtained with the newly cloned and analyzed murine QC support that all mammalian QCs are zinc-dependent catalysts. Obviously, the QCs evolved from aminopeptidases by a reorganization of the active site, accompanied by a loss of one zinc ion binding site. Further analysis of the catalytic mechanism and the zinc ion binding mode in QCs will give interesting insights into the evolutionary mechanisms that were required to provoke a change from an zinc-dependent hydrolase into a zinc-dependent transferase.

ACKNOWLEDGMENT

We thank Dr. J.-U. Rahfeld and J. Eggert for critical reading of the manuscript.

NOTE ADDED IN PROOF

During final processing of this paper, Huang et al. (31) published the 3D structure of human QC. The work reveals hQC as a zinc-dependent enzyme proving previous results obtained with hQC (20) and strongly backing our conclusion of the current article that all mammalian QCs are stoichiometric metal binding catalysts. Moreover, the work also supports our discovery (7) of plant and mammalian QCs as catalysts of glutamate cyclization and inhibition as a potential new therapeutic approach to treating pyroglutamate-peptide mediated amyloidosis.

REFERENCES

- Busby, W. H. J., Quackenbush, G. E., Humm, J., Youngblood, W. W., and Kizer, J. S. (1987) An enzyme(s) that converts glutaminyl-peptides into pyroglutaminyl-peptides. Presence in pituitary, brain, adrenal medulla, and lymphocytes, *J. Biol. Chem.* 262, 8532–8536.
- Garavelli, J. S. (2000) The RESID database of protein structure modifications: 2000 update, *Nucleic Acids Res.* 28, 209–211.
- Goren, H. J., Bauce, L. G., and Vale, W. (1977) Forces and structural limitations of binding of thyrotrophin-releasing factor to the thyrotrophin-releasing receptor: the pyroglutamic acid moiety, *Mol. Pharmacol.* 13, 606–614.
- Messer, M. (1963) Enzymatic cyclization of L-glutamine and L-glutaminyl peptides, *Nature* 4874, 1299.
- Messer, M., and Ottesen, M. (1964) Isolation and properties of glutamine cyclotransferase of dried papaya latex, *Biochim. Biophys. Acta* 92, 409–411.
- Fischer, W. H., and Spiess, J. (1987) Identification of a mammalian glutaminyl cyclase converting glutaminyl into pyroglutaminyl peptides, *Proc. Natl. Acad. Sci. U.S.A.* 84, 3628–3632.
- Schilling, S., Hoffmann, T., Manhart, S., Hoffmann, M., and Demuth, H.-U. (2004) Glutaminyl cyclases unfold glutaminyl cyclase activity under mild acid conditions, *FEBS Lett.* 563, 191–196.
- Saido, T. C., Iwatsubo, T., Mann, D. M., Shimada, H., Ihara, Y., and Kawashima, S. (1995) Dominant and differential deposition of distinct beta-amyloid peptide species, A beta N3(pE), in senile plaques, *Neuron* 14, 457–466.
- Horigaya, Y., Saido, T. C., Eckman, C. B., Prada, C.-J., Shoji, M., and Younkin, S. G. (2000) Amyloid β protein starting pyroglutamate at position 3 is a major component of the amyloid deposits in the Alzheimer's disease brain, *Biochem. Biophys. Res. Commun.* 276, 422–427.
- Ghiso, J., Revesz, T., Holton, J., Rostagno, A., Lashley, T., Houlden, H., Gibb, G., Anderton, B., Bek, T., Bojsen-Moller, M., Wood, N., Vidal, R., Braendgaard, H., Plant, G., and Frangione, B. (2001) Chromosome 13 dementia syndromes as models of neurodegeneration, *Amyloid* 8, 277–284.
- Hashimoto, T., Wakabayashi, T., Watanabe, A., Kowa, H., Hosoda, R., Nakamura, A., Kanazawa, I., Arai, T., Takio, K., Mann, D. M., and Iwatsubo, T. (2002) CLAC: a novel Alzheimer amyloid plaque component derived from a transmembrane precursor, CLAC-P/collagen type XXV, *EMBO J.* 21, 1524–1534.
- Sykes, P. A., Watson, S. J., Temple, J. S., and Bateman, R. C., Jr. (1999) Evidence for tissue-specific forms of glutaminyl cyclase, *FEBS Lett.* 455, 159–161.
- Pohl, T., Zimmer, M., Mugele, K., and Spiess, J. (1991) Primary structure and functional expression of a glutaminyl cyclase, *Proc. Natl. Acad. Sci. U.S.A.* 88, 10059–10063.
- Weisz, O. A. (2003) Acidification and protein traffic, *Int. Rev. Cytol.* 226, 259–319.
- Bockers, T. M., Kreutz, M. R., and Pohl, T. (1995) Glutaminyl-cyclase expression in the bovine/porcine hypothalamus and pituitary, *J. Neuroendocrinol.* 7, 445–453.
- Song, I., Chuang, C. Z., and Bateman, R. C., Jr. (1994) Molecular cloning, sequence analysis and expression of human pituitary glutaminyl cyclase, *J. Mol. Endocrinol.* 13, 77–86.
- Schilling, S., Hoffmann, T., Rosche, F., Manhart, S., Wasternack, C., and Demuth, H.-U. (2002) Heterologous expression and characterization of human glutaminyl cyclase: evidence for a disulfide bond with importance for catalytic activity, *Biochemistry* 41, 10849–10857.
- Schilling, S., Manhart, S., Hoffmann, T., Ludwig, H.-H., Wasternack, C., and Demuth, H.-U. (2003) Substrate specificity of glutaminyl cyclases from plants and animals, *Biol. Chem.* 384, 1583–1592.
- Bateman, R. C., Temple, J. S., Misquitta, S. A., and Booth, R. E. (2001) Evidence for essential histidines in human pituitary glutaminyl cyclase, *Biochemistry* 40, 11246–11250.
- Schilling, S., Niestroj, A. J., Rahfeld, J.-U., Hoffmann, T., Wermann, M., Zunkel, K., Wasternack, C., and Demuth, H.-U. (2003) Identification of human glutaminyl cyclase as a metalloenzyme: Inhibition by imidazole derivatives and heterocyclic chelators, *J. Biol. Chem.* 278, 49773–49779.
- Booth, R. E., Lovell, S. C., Misquitta, S. A., and Bateman, R. C., Jr. (2004) Human glutaminyl cyclase and bacterial zinc aminopeptidase share a common fold and active site, *BMC Biol.* 2, 2.
- Schilling, S., Hoffmann, T., Wermann, M., Heiser, U., Wasternack, C., and Demuth, H.-U. (2002) Continuous spectrometric assays for glutaminyl cyclase activity, *Anal. Biochem.* 303, 49–56.
- Ellis, K. J., and Morrison, J. F. (1982) Buffers of constant ionic strength for studying pH-dependent processes, *Methods Enzymol.* 87, 405–426.
- Fujiwara, K., and Tsuru, D. (1978) New chromogenic and fluorogenic substrates for pyrrolidonyl peptidase, *J. Biochem.* 83, 1145–1149.
- Klockenkämper, R., and von Bohlen, A. (2001) Total reflection X-ray fluorescence moving towards nanoanalysis: a survey, *Spectrochim. Acta B* 56, 2005–2018.
- Huntington, K. M., Bienvenue, D. L., Wei, Y., Bennett, B., Holz, R. C., and Pei, D. (1999) Slow-binding inhibition of the aminopeptidase from *Aeromonas proteolytica* by peptide thiols: synthesis and spectroscopic characterization, *Biochemistry* 38, 15587–15596.
- Dahl, S. W., Slaughter, C., Lauritzen, C., Bateman, R. C., Jr., Connerton, I., and Pedersen, J. (2000) Carica papaya glutamine cyclotransferase belongs to a novel plant enzyme subfamily: cloning and characterization of the recombinant enzyme, *Protein Expression Purif.* 20, 27–36.
- Allary, M., Schrevel, J., and Florent, I. (2002) Properties, stage-dependent expression and localization of *Plasmodium falciparum* M1 family zinc-aminopeptidase, *Parasitology* 125, 1–10.
- Auld, D. S. (1995) Removal and replacement of metal ions in metallopeptidases, *Methods Enzymol.* 248, 228–242.
- Baker, J. O., and Prescott, J. M. (1983) *Aeromonas* aminopeptidase: pH dependence and a transition-state-analogue inhibitor, *Biochemistry* 22, 5322–5331.
- Huang, K.-F., Liu, Y.-L., Cheng, W.-J., Ko, T.-P., and Wang, A. H.-J. (2005) Crystal structures of human glutaminyl cyclase, an enzyme responsible for protein N-terminal pyroglutamate formation, *Proc. Natl. Acad. Sci. U.S.A.* 102, 13117–13122.

BI051142E

Inhibition of glutaminyl cyclase alters pyroglutamate formation in mammalian cells

Holger Cynis^a, Stephan Schilling^a, Mandy Bodnár^a, Torsten Hoffmann^a, Ulrich Heiser^a, Takaomi C. Saido^b, Hans-Ulrich Demuth^{a,*}

^a Probiodrug AG, Weinbergweg 22, 06120 Halle/Saale, Germany

^b RIKEN Brain Science Institute, Laboratory for Proteolytic Neuroscience, 2-1 Hirosawa, Wako, Saitama 351-0198, Japan

Received 26 May 2006; received in revised form 29 July 2006; accepted 11 August 2006

Available online 16 August 2006

Abstract

Mammalian cell lines were examined concerning their Glutaminyl Cyclase (QC) activity using a HPLC method. The enzyme activity was suppressed by a QC specific inhibitor in all homogenates. Aim of the study was to prove whether inhibition of QC modifies the posttranslational maturation of N-glutamine and N-glutamate peptide substrates. Therefore, the impact of QC-inhibition on amino-terminal pyroglutamate (pGlu) formation of the modified amyloid peptides A β (N3E-42) and A β (N3Q-42) was investigated. These amyloid- β peptides were expressed as fusion proteins with either the pre-pro sequence of TRH, to be released by a prohormone convertase, or as engineered amyloid precursor protein for subsequent liberation of A β (N3Q-42) after β - and γ -secretase cleavage during posttranslational processing. Inhibition of QC leads in both expression systems to significantly reduced pGlu-formation of differently processed A β -peptides. This reveals the importance of QC-activity during cellular maturation of pGlu-containing peptides. Thus, QC-inhibition should impact bioactivity, stability or even toxicity of pyroglutamyl peptides preventing glutamine and glutamate cyclization.

© 2006 Elsevier B.V. All rights reserved.

Keywords: Glutaminyl Cyclase; Pyroglutamic acid; Inhibition; Amyloid- β ; Alzheimer's disease

1. Introduction

The formation of N-terminal pyroglutamic acid (pGlu) is a posttranslational modification of several hormones such as gastrin, neurotensin and GnRH [1]. For some of these peptides, e.g. thyrotropin-releasing hormone (TRH), it has been shown that this pGlu-modification is crucial for hormonal activity [2]. Glutaminyl cyclase (QC; EC 2.3.2.5) is a zinc-dependent metalloenzyme catalyzing the cyclization of amino-terminal glutamine into pGlu under concomitant liberation of ammonia. QCs have been identified in a number of animals and plants [3–

6]. Because of its broad substrate specificity, QC has a key function in posttranslational pyroglutamyl formation of presumably all pGlu-containing peptides and hormones [7]. QC is expressed in various tissues of the body with a marked abundance in different brain regions. The highest expression was observed in striatum and anterior pituitary [8]. More detailed studies on the cellular and sub-cellular distribution in porcine and bovine hypothalamic and pituitary tissue (detection of QC-immunoreactivity on secretory granules of axonal nerve endings belonging to the tractus hypothalamo hypophysialis) revealed the striking evidence, that QC is transported via the same routes as its substrates, e.g. the hormone precursors of GnRH and TRH [9].

Recently, it has been shown that QC is also capable of converting amino-terminal glutamate to pyroglutamate [10]. Therefore, QC might also play a role in amyloidotic diseases, e.g. Alzheimer's Disease (AD), Familial British Dementia (FBD) or Familial Danish Dementia (FDD), because significant amounts of the deposited peptides (A β , ABri, ADan) are N-

Abbreviations: A β , amyloid β -peptide; APP, amyloid precursor protein; β -CTF, β -C-terminal fragment of APP; DMEM, Dulbecco's modified eagle medium; GnRH, gonadotropin releasing hormone; HRP, horseradish peroxidase; pGlu, pyroglutamic acid; QC, glutaminyl cyclase; SDS-PAGE, sodium dodecylsulfate polyacrylamide gel electrophoresis; TMB, tetramethylbenzidine; mTRH, murine thyrotropin releasing hormone

* Corresponding author. Tel.: +49 345 5559900; fax: +49 345 5559901.

E-mail address: Hans-Ulrich.Demuth@probiodrug.de (H.-U. Demuth).

terminally modified by a pyroglutamyl residue resulting from glutamate cyclization [11–13]. These pGlu-containing peptide species have been suggested to be a potential target for the development of a treatment strategy due to their pronounced neurotoxicity, stability and aggregation propensity [12,14–16]. After demonstrating QC-catalyzed N-glutamate peptide cyclization *in vitro* [10], the aim of our present study was to show that QC-inhibitors prevent the pyroglutamate formation in cultured mammalian cells. Hence, we have screened a number of established cell lines in culture for QC-activity using a HPLC method. Having successfully identified several QC-containing cell lines, we were interested in suppressing QC-activity using a recently characterized highly potent QC inhibitor P150/03 [17]. Because of the lack of specific antibodies to analyze the prevention of pGlu formation at the N-terminus of a variety of potential QC peptide substrates, we decided to test P150/03 using engineered A β (N3E-42) and A β (N3Q-42) because of the availability of specific sandwich ELISAs for A β (N3pGlu-42).

2. Materials and methods

2.1. Reverse-transcription PCR

Total RNA was isolated from HEK293 and β -TC 3 cells using the Nucleospin Kit (Macherey-Nagel) and reversely transcribed by SuperScript II (Invitrogen). Subsequently, QC was amplified on a 1:12.5 dilution of generated cDNA product in a 25 μ l reaction with Herculase Enhanced DNA-Polymerase (Stratagene). The primer sequences for amplification of QC were: β -TC 3, 5'-ATATGCATGCATGGCAGGCAGCGAAGACAAGC-3' (mQC, sense) and 5'-ATATAAGCTTTTACAAGTGAAGATATCCCAACACAAAGAC-3' (mQC, antisense); HEK293, 5'-CATGGCATGGATTATTGG-3' (hQC, sense) and 5'-GACGGTATCAGATGCAGAAC-3' (hQC, antisense). The PCR products were purified utilizing the Strataprep PCR Purification Kit (Stratagene) and confirmed by sequencing.

Full-length cDNA of mTRH was isolated from primary cortical neurons (generously provided by Dr. S. Rossner, Paul Flechsig Institute for Brain Research, Leipzig, Germany) and subcloned into vector pPCR Script (Stratagene). The Primers were: 5'-ATATAAGCTTATGCAGGACCTTGGCTGATG-3' (sense) and 5'-ATATTACTCCTCCAGAGGTTCCCTG-3' (antisense). The pre-pro sequence was amplified applying the Primers: 5'-ATATAAGCTTATGCAGGACCTTGGCTGATG-3' (sense) and 5'-ATATGCATGCTGTGATC-CAGGAATCTAAGG-3' (antisense), subcloned into vector pPCR Script and confirmed by sequencing.

2.2. Cloning procedure

The cDNA of human APP695 (NLQ) was generated as described elsewhere [18]. The construct contained Swedish KM595/596NL and London V642I familial AD mutations, a deletion of amino acids D597, A598, and a point mutation of E599Q. On basis of NLQ, the sequences of A β (N3E-42), and A β (N3Q-42) were amplified and fused to the 3' end of pre-pro sequence of mTRH via an artificial *SphI* cleavage site. The sequence of mature human QC was also fused to mTRH using the artificial *SphI* cleavage site. *SphI* site was mutated to wild type to possess a lysine-arginine motif for prohormone convertase cleavage using Primers 5'-TTAGATTCCTGGATCACAAAACGC [C/G]AATTCCGACATGACTCA-3' (sense) and 5'-TGAGTCATGTCCG-GAATT[C/G]GCGTTTTGTGATCCAGGAATCTAA-3' (antisense) for A β (N3E-42) and A β (N3Q-42) and 5'-GATTCCTGGATCACAAAACGCCAT-CATCATCATCATCAT-3' (sense) and 5'-ATGATGATGATGATGATGATGGCGTTTTGTGATCCAGGAATC-3' (antisense) for human QC fusion protein. A β (N3E-42), A β (N3Q-42), human QC fusion proteins and cDNA of NLQ were ligated into the *HindIII/NotI*-site of vector pcDNA 3.1 (Invitrogen), confirmed by sequencing and isolated for cell culture purposes using the EndoFree Plasmid Maxi Kit (Qiagen).

2.3. Cell culture and transfection

Human embryonal kidney cells HEK293, murine monocyte/macrophage cell line RAW264.7, human glioma U343, murine insulinoma β -TC 3, murine fibroblast cell line L929, human cervix carcinoma HeLa and human plasma cell leukaemia cell line L-363 were cultured in appropriate cell culture media in a humidified atmosphere of 5% CO₂ at 37 °C. HEK293 cells were transfected with the APP695 (NLQ) and β -TC 3 cells were transfected with the mTRH-A β (N3Q-42) construct using Lipofectamin2000 (Invitrogen) according to the manufacturer's manual. Furthermore, β -TC 3 cells were also transfected with the mTRH-A β (N3E-42) construct alone or in combination with the mTRH-QC construct. Transiently transfected cells were grown over night and afterwards incubated for 24h with phenolred-free DMEM (Gibco) under serum-free conditions either in presence or absence of QC inhibitor 1-(3-(1*H*-imidazol-1-yl)propyl)-3-(3,4-dimethoxyphenyl)thiourea (P150/03) [17] in a concentration of 100 μ M for β -TC 3 and 10 μ M for HEK293. The next day, media were collected, readily mixed with protease inhibitor cocktail (Roche) containing additionally 1mM PefaBloc (Roth) and stored at -80 °C. Cell count of each well was determined using the CASY cell counter system (Schaefer System).

2.4. HPLC-assay

Cells were grown to confluency, pelleted, frozen on dry ice and stored until assay. Test samples were sonicated and centrifuged in buffer (10mM Tris, 100mM NaCl, 5mM EDTA, 0.5% Triton X-100, 10% Glycerol, pH 7.5) at 16.000 \times g for 30min and 4 °C. The protein concentration of the resulting supernatant was determined using the method of Bradford and used as enzyme source. The QC activity was determined applying an HPLC-assay essentially as described elsewhere [19] since continuous assay methods were hampered by aminopeptidase activities in the crude extracts. The assay is based on conversion of H-Gln- β NA to pGlu- β NA. The sample consisted of 50 μ M H-Gln- β NA or 50 μ M H-Gln- β NA/10 μ M P150/03 in 25mM MOPS, pH 7.0, 0.1mM *N*-Ethylmaleimide (NEM) and enzyme solution in a final volume of 1ml. Samples were incubated at 30 °C and constantly shaken at 300rpm in a thermomixer (Eppendorf). Test samples were removed, and the reaction stopped by boiling for 5min followed by centrifugation at 16.000 \times g for 10min. All HPLC measurements were performed using a RP18 LiChroCART HPLC-Cartridge and the HPLC system D-7000 (Merck-Hitachi). Briefly, 10 μ l of the sample were injected and separated by increasing concentration of solvent A (acetonitrile containing 0.1% TFA) from 8% to 20% in solvent B (H₂O containing 0.1% TFA). QC activity was quantified from a standard curve of pGlu- β NA (Bachem) determined under assay conditions.

2.5. Immunoblotting

HEK293 cells were transfected with APP (NLQ) or with vector alone in 6-well plates and lysed 1 day post transfection by adding 100 μ l 5 \times SDS sample buffer directly to each well. Cells were collected by scraping using rubber policeman, diluted by addition of 200 μ l PBS and sonicated for 15s. Afterwards, the sample was heated to 100 °C for 5min, cooled on ice and centrifuged at 13.000rpm for 5min. 10 μ l, 20 μ l, 40 μ l and 60 μ l of the sample were loaded onto a SDS-PAGE gel (8%) and separated. Proteins were transferred to a nitrocellulose membrane (Roth), which was blocked using 3% (w/v) dry milk in TBS-T (20mM Tris/HCl; pH 7.5; 500mM NaCl, 0.05% (v/v) Tween20). APP was detected by consecutive incubation of the blot membrane with a polyclonal APP antibody (Cell Signaling) and an anti-rabbit antibody conjugated with horseradish peroxidase (Cell Signaling) in TBS-T containing 5% (w/v) dry milk and visualized using the SuperSignal West Pico System (Pierce) according to the manufacturer's protocol.

2.6. Enzyme-linked immunosorbent assay (ELISA)

A β (42) concentration in cell culture supernatants was determined using specific sandwich ELISAs detecting either total A β (x-42) or the N-terminally pyroglutamated variant A β (N3pGlu-42) (IBL-Hamburg). Briefly, 100 μ l of the sample or adequate standard were added to 96-well microtiter-plates coated with an antibody specific for A β (42) followed by incubation over night at 4 °C. The

next day, plates were washed and incubated with antibodies detecting either A β (x-42) or A β (N3pGlu-42). Both antibodies were conjugated with horseradish peroxidase (HRP). After a final washing step, bound enzyme activity was measured using a TMB peroxidase substrate in a colorimetric reaction. The absorbance at 450nm was determined using a Sunrise plate reader (Tecan).

3. Results

3.1. Determination of QC activity in cell lines

With emphasis on QC activity, we have analyzed mammalian cell lines representing different derivations in order to select an optimal line for expression of QC substrate precursors mTRH-A β (N3E-42), mTRH-A β (N3Q-42) or APP (NLQ). Murine QC was recently isolated from mouse insulinoma cell line β -TC 3 and detected in mouse monocyte/macrophage cell line RAW264.7 [19,20]. In addition, the human cell lines HeLa, HEK293, U343 and L-363 as well as the murine cell line L929 were analyzed in the present study applying an HPLC method for determination of QC activity. Incubation of cell supernatant with Q- β NA substrate led to a linear rise in pGlu- β NA product over a time period of 60 min, as exemplarily shown for HEK293 and β -TC 3 (Fig. 1). In both cases, the activity could be completely blocked by addition of QC-specific inhibitor P150/03 at a concentration of 10 μ M. Furthermore, the enzymatic activity was also abolished by boiling the cell supernatant for 5 min before applying it to the assay (not shown), suggesting that conversion of Q- β NA to pGlu- β NA in cell supernatant is exclusively enzyme-catalyzed. Among the examined cell lines, β -TC 3 contained the highest QC activity (16.3 \pm 3.0 nmol/h/mg), followed by L-363 (11.5 \pm 0.2 nmol/h/mg), HeLa (9.5 \pm 0.4 nmol/h/mg), U343 (9.2 \pm 1.3 nmol/h/mg), L929 (8.1 \pm 0.9 nmol/h/mg), RAW264.7 (6.5 \pm 1.9 nmol/h/mg) and HEK293 (3.5 \pm 0.9 nmol/h/mg) (Fig. 2). The activity determina-

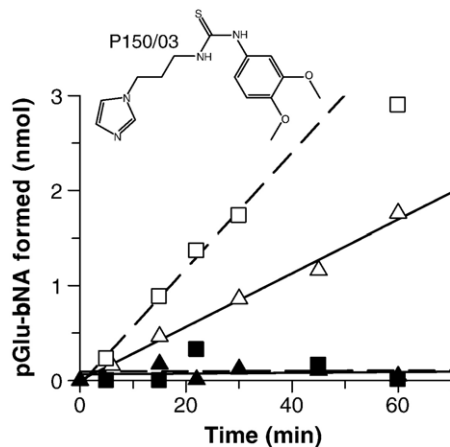


Fig. 1. Time dependent formation of pGlu- β NA in HEK293 and β -TC 3. Q- β NA (50 μ M) was incubated with cell extract in presence (HEK293—filled triangles; β -TC 3—filled squares) or absence (HEK293—open triangles; β -TC 3—open squares) of 10 μ M P150/03. Assay was carried out in 25 mM MOPS, pH 7.0, containing 0.1 mM N-Ethylmaleinimide (NEM) at 30 $^{\circ}$ C. The inset shows the chemical structure of P150/03. For data evaluation, only the phase of linear product formation was used. Therefore, the time point at 60 min for β -TC 3 was omitted.

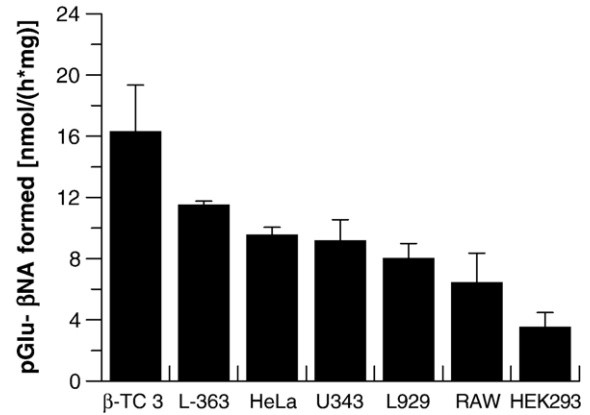


Fig. 2. Distribution of QC activity among various cell lines. Cell lines and determined QC activity were as follows: β -TC 3 (16.3 \pm 3.0 nmol/h/mg), L-363 (11.5 \pm 0.2 nmol/h/mg), HeLa (9.5 \pm 0.4 nmol/h/mg), U343 (9.2 \pm 1.3 nmol/h/mg), L929 (8.1 \pm 0.9 nmol/h/mg), RAW264.7 (6.5 \pm 1.9 nmol/h/mg), HEK293 (3.5 \pm 0.9 nmol/h/mg).

tions show that QC is present in a broad range of cells varying from neuronal-derived cells (U343, HEK293) to blood cells (RAW264.7, L-363) and even cells of peripheral tissues (HeLa, β -TC 3, L929). For further expression studies, we have chosen β -TC 3 due to its high QC content and HEK293 since this cell line is a well-established model for expression and amyloidogenic processing of APP [21,22].

3.2. Verification of QC expression in β -TC 3 and HEK293

To substantiate the findings obtained by the HPLC-assay, we have analyzed the QC expression in β -TC 3 and HEK293 using RT-PCR. These investigations were performed to prove that QC activity arises from expression of murine or human QC mRNA and not from putative isoenzymes [23]. Therefore, total-RNA was isolated from both cell lines for cDNA generation. RT-PCR yielded products for both cell lines (Fig. 3), and the QC cDNA sequence was confirmed by sequencing (not shown). We have also found QC transcripts in RAW264.7, L-929 and L-363 (not shown) whereas HeLa and U343 were not further characterized. Although these RT-PCR results do not rule out putative isoenzymes, the synopsis of the RT-PCR and QC activity

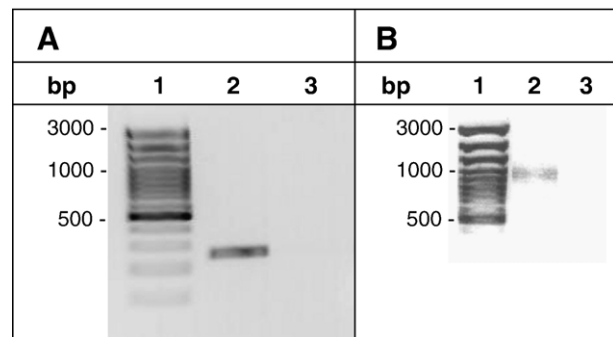


Fig. 3. Analysis of QC expression by RT-PCR. (A) Detection of QC transcripts in HEK293. Lanes: 1, DNA standard; 2, amplified PCR product of human QC; 3, negative control; (B) Detection of QC transcripts in β -TC 3. Lanes: 1, DNA standard; 2, amplified PCR product of murine QC; 3, negative control.

determinations suggests that enzymatic activity originates exclusively from QC, which is further substantiated by the complete inhibition of the cyclization activity in both cell extracts. Thus, β -TC 3 and HEK293 are suitable for expression of the QC substrate precursors and to evaluate the effect of QC inhibitors in these cell lines.

3.3. Expression of mTRH-A β (N3Q-42) in β -TC 3

For the expression of mTRH-A β (N3Q-42), the pre-pro sequence of mTRH was cloned, containing a signal peptide with an adjacent propeptide terminating at arginine76. The sequence was fused N-terminally to the A β (N3Q-42) sequence. The selection of murine insulinoma cell line β -TC 3 for transfection was based on its high QC content, reliable transfection rates, and characterization as hormone-secreting cell line. According to the well-established steps of releasing TRH from its precursor protein, it was anticipated that mTRH-A β (N3Q-42) is directed to the Endoplasmic Reticulum via the mTRH signal peptide and that A β (N3Q-42) is liberated within the secretory pathway by prohormone convertases [24]. β -TC 3 was transfected with the construct mTRH-A β (N3Q-42) or with the vector alone and the amount of A β (42) and A β (N3pGlu-42) was determined using commercially available ELISA kits. In this regard, the A β (x-42) ELISA recognizes all N-terminally truncated isoforms of the A β -peptide, but the A β (N3pGlu-42) ELISA is specific for formation of N-terminal pGlu. The expression of mTRH-A β (N3Q-42) leads to significantly elevated A β (42) levels in converted media of β -TC 3 incubated in absence of P150/03 (49.7 ± 8.9 pg/ml/ 1.5×10^6 cells) ($P < 0.05$; Student's *t*-test) or with media containing P150/03 (100 μ M) (47.7 ± 3.2 pg/ml/ 1.5×10^6 cells) ($P < 0.01$; Student's *t*-test) compared to vector-transfected controls without inhibitor (32.7 ± 1.1 pg/ml/ 1.5×10^6 cells) or with inhibitor (22.9 ± 1.8 pg/ml/ 1.5×10^6 cells) (Fig. 4A). Thus, the incubation of A β -transfected cells with P150/03 did not change the levels of A β (42) within 24h of the assay, suggesting addition of P150/03 does not affect A β (N3Q-42) expression or secretion. The significant amounts of A β (42) detected in vector-transfected controls were always observed for β -TC 3, but not for HEK293 (Fig. 4A). The N-terminal glutamine of secreted A β N3Q-42 is converted to pyroglutamic acid (63.5 ± 16.4 pg/ml/ 1.5×10^6 cells) as determined by pGlu ELISA, implying a processing of the fusion protein within the secretory pathway. Moreover, the incubation of A β (N3Q-42) expressing β -TC 3 cells with P150/03 leads to significantly reduced pGlu formation at the N-terminus of N3Q-42 (17.5 ± 4.3 pg/ml/ 1.5×10^6 cells) ($P < 0.01$; Student's *t*-test) indicating that the QC inhibitor P150/03 is capable of preventing pGlu formation within this model system (Fig. 4B).

3.4. Expression of APP (NLQ) in HEK293

To examine whether QC inhibition leads also to reduced pGlu formation at the N-terminus of A β (N3Q-42) after the amyloidogenic proteolytic processing, we expressed APP (NLQ) in HEK293 cells. HEK293 were identified to belong

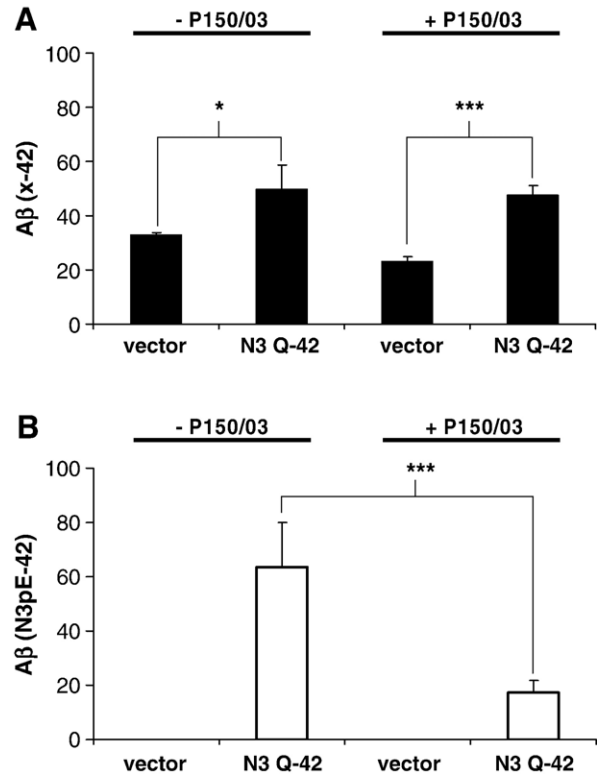


Fig. 4. (A) Determination of A β (x-42) secreted by transfected β -TC 3. Cells transfected with construct mTRH-A β (N3Q-42) or with vector alone were incubated either with (100 μ M) or without QC specific inhibitor P150/03. A β concentration measured by A β (42) specific ELISA was normalized to cell count (pg/ml/ 1.5×10^6 cells). (*, Student's *t*-test, $P < 0.05$, $n = 3$; ***, Student's *t*-test, $P < 0.001$, $n = 3$). (B) Determination of A β (N3pGlu-42) secreted by transfected β -TC 3. Cells were incubated with (100 μ M) or without P150/03. Extent of cyclization was measured by A β (N3pGlu-42) specific ELISA and normalized to cell count (pg/ml/ 1.5×10^6 cells). (**, Student's *t*-test, $P < 0.01$, $n = 3$).

to the neuronal lineage even though they are based on primary cultures of human embryonic kidney cells and they comprise a suitable cell system for expression of APP [21,22]. After transfection of HEK293 with the construct APP (NLQ), the protein is abundantly detectable in cell lysates showing two bands at 100 kDa corresponding to mature and immature forms of APP695 after 30s development time. The vector-transfected controls did not show a signal for APP in consequence of the short development time (Fig. 5). However, native APP in HEK293 can be visualized by longer development times (not shown). In analogy to the direct expression model, the extent of N-terminal cyclization of liberated A β (N3Q-42) in presence or in absence of P150/03 was determined. Thereby, it became evident that HEK293 cells appear to be more sensitive to P150/03 treatment than β -TC 3, since A β (42) was significantly reduced after inhibitor administration at a concentration of 100 μ M, indicating a toxic effect, although no toxicity was observed on β -TC 3 and HEK293 up to a concentration of 1 mM during routine determination of cytotoxicity. Due to the unspecific effect, the concentration of P150/03 was reduced by one order of magnitude to 10 μ M, which corresponds to the 200fold of the K_i value [17]. At this concentration, a putative cytotoxic effect (or a total A β (42) modulating effect) was not

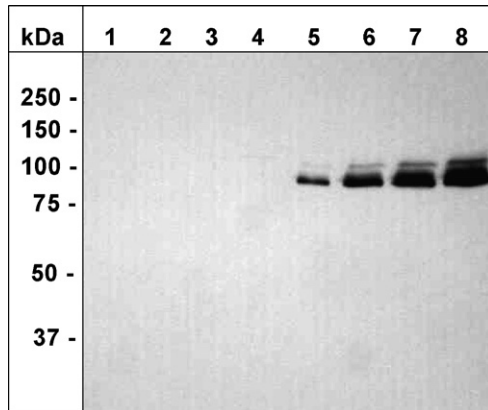


Fig. 5. Western Blot for APP (NLQ) detection in HEK293. Lanes: kDa, Protein Standard Dual Color (Bio-Rad); 1, vector 10 µl; 2, vector 20 µl; 3, vector 40 µl; 4, vector 60 µl; 5, APP(NLQ) 10 µl; 6, APP(NLQ) 20 µl; 7, APP(NLQ) 40 µl; 8, APP(NLQ) 60 µl.

observed as suggested by the Aβ(42) concentration in the cell culture supernatant of HEK293 incubated with (173.6 ± 29.6 pg/ml/1 × 10⁶ cells) or without (152.9 ± 39 pg/ml/1 × 10⁶ cells) inhibitor (Fig. 6A). However, by applying 10 µM of P150/03 to HEK293 cells expressing APP (NLQ) we significantly reduced the amount of Aβ(N3pGlu-42) by 50% (122.8 ± 13.3 pg/ml/1 × 10⁶ cells) compared to the untreated control (245.5 ± 44.4 pg/ml/1 × 10⁶ cells) (*P* < 0.001; Student's *t*-test) (Fig. 6B).

To balance the reduced concentration of the inhibitor, HEK293 were incubated with the inhibitor 3 h prior to the assay. Again, no significant differences were detected in Aβ(42) concentration between samples incubated with (202.9 ± 44.9 pg/ml/1 × 10⁶ cells) or without (192.9 ± 28.6 pg/ml/1 × 10⁶ cells) inhibitor (Fig. 6A). The amount of detectable N3pGlu-42, however, was reduced to 31% (153.9 ± 25.2 pg/ml/1 × 10⁶ cells) compared with the untreated control (485.9 ± 67 pg/ml/1 × 10⁶ cells) (*P* < 0.001; Student's *t*-test) (Fig. 6B). Surprisingly, for every Aβ(N3pGlu-42) determination a higher Aβ content was observed than determined with Aβ(x-42) specific ELISA. This might be a result of different detection antibodies in both ELISAs displaying different specificities.

3.5. Co-expression of mTRH-Aβ(N3E-42) and mTRH-QC in β-TC 3

The N-terminal pGlu modification in the disease-related proteins Aβ, ABri and ADan arises from the cyclization of glutamate and not from glutamine. To address the question, whether QC is also capable of cyclizing glutamate under physiological conditions in cell culture, the construct mTRH-Aβ(N3E-42) possessing a N-terminal glutamate after processing was expressed in β-TC 3. In accordance with the findings after expression of mTRH-Aβ(N3Q-42), the transfection of mTRH-Aβ(N3E-42) led to elevated amounts of Aβ(42) in the cell culture media (65.6 ± 4.6 pg/ml/1.5 × 10⁶ cells) but the amount of Aβ(N3pGlu-42) remained below the limit of quantification (0.13 ± 0.18 pg/ml/1.5 × 10⁶ cells). However, the QC-catalyzed cyclization of glutamate *in vitro* is slow [10,33].

Therefore, it was assumed that the QC activity in β-TC 3 might be not sufficient to produce significant Aβ(N3pGlu-42) levels within 24 h, i.e. during the time of analysis. Consequently, we co-transfected the constructs mTRH-Aβ(N3E-42) and mTRH-QC to increase the QC activity in β-TC 3. This approach led to elevated amounts of Aβ(42) (42.0 ± 1.7 pg/ml/1.5 × 10⁶ cells) and, interestingly, to significant levels of Aβ(N3pGlu-42) (2.5 ± 0.6 pg/ml/1.5 × 10⁶ cells) (*P* < 0.01; Student's *t*-test) (Fig. 7A). The over-expression of QC was monitored by activity determination in cell culture media (not shown). In consistence with the findings obtained by expression of mTRH-Aβ(N3Q-42) in β-TC 3, the application of P150/03 in a concentration of 100 µM did not change the amount of Aβ(42) detected after co-transfection of mTRH-Aβ(N3E-42) and mTRH-QC (49.7 ± 5.9 pg/ml/1.5 × 10⁶ cells vs. 48.8 ± 2.9 pg/ml/1.5 × 10⁶ cells).

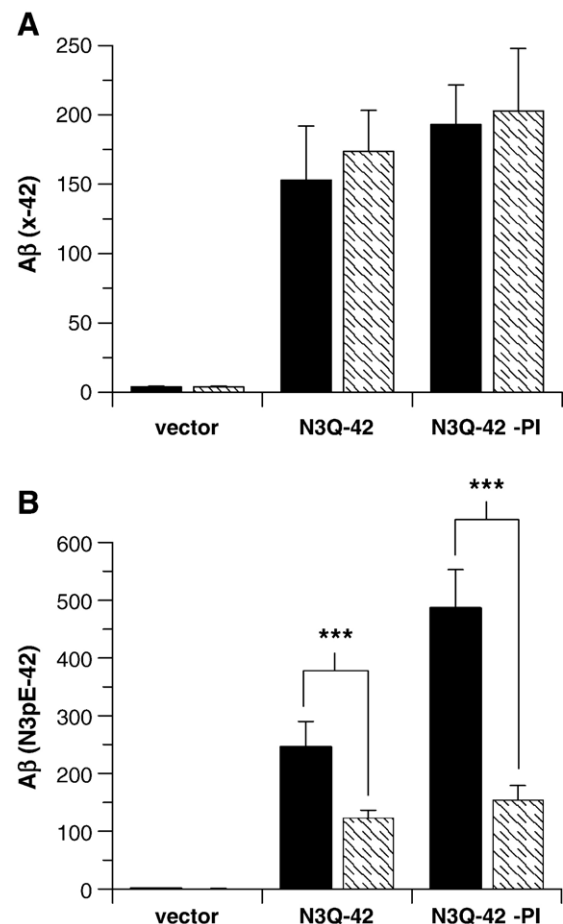


Fig. 6. (A) Analysis of Aβ(x-42) secreted by HEK293. Cells were transfected with APP (NLQ) or with vector alone in absence (closed bars) or presence (open bars) of 10 µM P150/03. Inhibitor was added to HEK293 either together with assay medium (N3Q-42, no preincubation) or cells were preincubated with inhibitor 3 h prior to the assay (N3Q-42-PI). Aβ was determined by Aβ(x-42) specific ELISA and normalized to cell count (pg/ml/1 × 10⁶ cells), (*n* = 6). (B) Analysis of Aβ(N3pGlu-42) secreted by transfected HEK293. Cells were incubated in absence (closed bars) or presence (open bars) of 10 µM P150/03. Inhibitor was added to HEK293 either together with assay medium (N3Q-42, no preincubation) or cells were preincubated with inhibitor 3 h prior to the assay (N3Q-42-PI). Aβ was determined by Aβ(N3pGlu-42) specific ELISA and normalized to cell count (pg/ml/1 × 10⁶ cells), (***) Student's *t*-test, *P* < 0.001, *n* = 6).

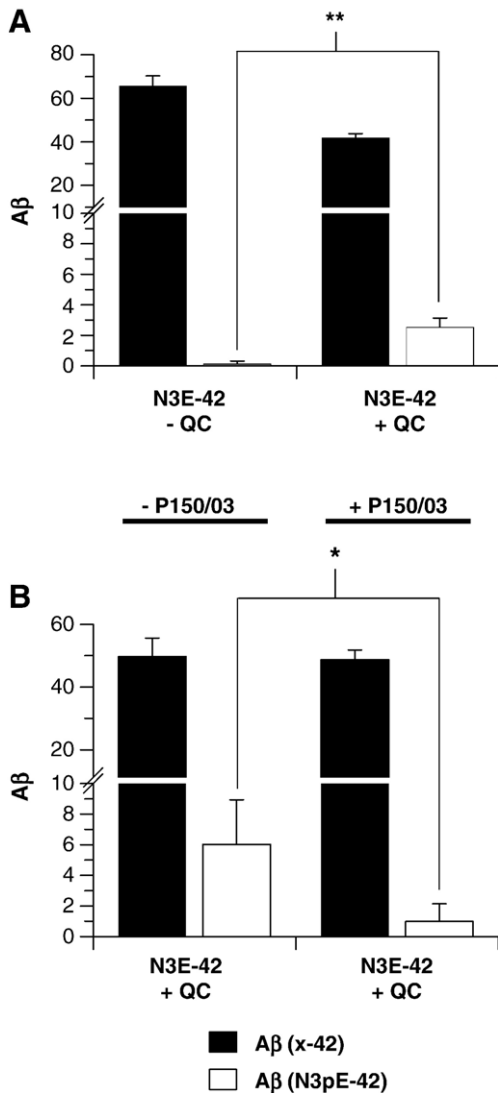


Fig. 7. (A) Determination of Aβ(x-42) (closed bars) and Aβ(N3pGlu-42) (open bars) secreted by β-TC 3. Cells were transfected with construct mTRH-Aβ(N3E-42) in absence or presence of construct mTRH-QC. Aβ concentration measured by Aβ(42) and Aβ(N3pGlu-42) specific ELISA was normalized to cell count (pg/ml/1.5 × 10⁶ cells). (**, Student's *t*-test, *P* < 0.01, *n* = 3). (B) Determination of Aβ(x-42) (closed bars) and Aβ(N3pGlu-42) (open bars) secreted by β-TC 3. Cells were transfected with constructs mTRH-Aβ(N3E-42) and mTRH-QC and incubated either with (100 μM) or without P150/03. Aβ concentrations were determined by Aβ(42) and Aβ(N3pGlu-42) specific ELISA and normalized to cell count (pg/ml/1.5 × 10⁶ cells). (*, Student's *t*-test, *P* < 0.05, *n* = 3).

However, the amount of Aβ(N3pE-42) was significantly reduced in the cell culture medium supplemented with P150/03 (0.98 ± 1.12 pg/ml/1.5 × 10⁶ cells) compared to medium without inhibitor (6.0 ± 2.9 pg/ml/1.5 × 10⁶ cells) (*P* < 0.05; Student's *t*-test) (Fig. 7B).

It is important to underline that within this study the determined Aβ(42) concentrations did not significantly differ in samples incubated with or without the inhibitor, but the extent of pGlu formation at the N-terminus of Aβ peptides was always significantly reduced. Thus, the QC-specific inhibitor P150/03 not only modulates the cyclization of glutamine but also

decreases the QC-catalyzed cyclization of glutamate at the N-terminus of artificial Aβ peptides.

4. Discussion

For several bioactive peptides, a N-terminal pyroglutamyl residue is described, which is formed post-translationally from a glutamine precursor. This pGlu formation is catalyzed by QC and pGlu-containing peptides and proteins are conserved in invertebrates like the marine snail *Aplysia californica* and the Brazilian armed spider *Phoneutria nigriventer* as well as in vertebrates like *Mus musculus*, *Bos taurus* and *Homo sapiens* [4,20,25–27]. Two major functions are attributed to the pGlu residue. It stabilizes proteins by preventing N-terminal degradation by aminopeptidases and thus prolongs their biological half-life. On the other hand, for some mammalian peptides like TRH the pGlu modification was shown to be essential for biologic activity [2]. Therefore, blockage of pGlu formation at the N-terminus of selected peptides seems to be a promising approach for modulating their activity throughout the body either by their metabolic destabilization or by their functional inactivation. Previous publications have shown that QC is expressed in various tissues, with a marked abundance in brain, e.g. cerebral cortex, hypothalamus, hippocampus and striatum, in peripheral glands like thyroid and thymus and in human B-lymphocytes [3,8,23]. The current study demonstrates that QC activity is readily detectable in mammalian cell lines from very different origins (Fig. 2). This ubiquitous occurrence within the cell lines tested was a surprising finding because it was presumed that QC is co-expressed with an adequate substrate within the secretory pathway. In fact, for almost all of those cell lines no QC substrate is described. Nevertheless, further screening of mammalian cell lines did not reveal one single cell line possessing no QC-activity (unpublished results). Seven years ago, researchers also found a ubiquitous distribution of QC activity in all tissues they examined and they have speculated that tissue-specific forms of QC might exist because of obvious discrepancies between QC expression studies using Northern Blot and QC activity determination [23]. Clearly, it is reasonable to take the existence of isoenzymes of QC into consideration. However, P150/03, an imidazole-derivative, completely blocked QC activity in cell extracts of the utilized cell lines HEK293 and β-TC 3 suggesting either a very high homology of QC and the putative isoenzyme regarding their active sites or simply the absence of such an isoenzyme. In addition, the RT-PCR revealed transcripts of QC in HEK293, β-TC 3 and in the other cell lines (not shown) indicating that the QC activity originates substantially from QC and not from a putative isoenzyme. Finally, it has been described that putative isoforms of QC are not inhibited by imidazole [23]. Moreover, it should also be noted that these cell lines represent immortalized tumor cells and it cannot be excluded that during transformation of a cancer cell QC activity is upregulated.

Having successfully identified a number of cell lines possessing QC activity, the effort was to demonstrate potency of a QC-specific inhibitor in cell culture. Because of the lack of antibodies or ELISAs specific for the N-terminal pGlu

modification of nearly all QC substrates, an expression model was used, where the QC substrate A β (N3Q-42) was expressed in β -TC 3 as fusion protein with pre–pro sequence of mTRH to mimic pGlu hormone maturation. This model is based on the generation of a native QC substrate from a prohormone precursor after prohormone convertase cleavage, its post-translational pGlu modification and the prevention of pGlu formation by a QC-specific inhibitor within the secretory pathway. We also expressed a mutant form of APP (NLQ) in HEK293, which resembles, after its secretase liberation from the larger amyloid precursor protein, the subsequent pGlu formation of the amyloidogenic species A β (N3pGlu-42). In contrast to the mTRH-A β (N3Q-42) construct which is processed within the secretory pathway, i.e. under conditions where QC is abundant, the liberation of A β from APP has been described within the endosomal/lysosomal as well as within the secretory pathway [28–30]. This in addition raises the interesting question, whether QC inhibition is capable of suppressing pGlu-A β formation despite of the potentially different sub-cellular localization of QC and A β in both experimental approaches. Finally, the expression of mTRH-A β (N3E-42) in combination with mTRH-QC was to prove the involvement of QC in glutamate cyclization in mammalian cells. As expected, after expression of mTRH-A β (N3Q-42) and mTRH-A β (N3E-42) in β -TC 3 and APP (NLQ) in HEK293, A β (42) was liberated from both different precursors by endogenous proteolysis. A β (42) levels did not differ between experiments in presence or absence of P150/03, indicating that the inhibitor exhibits no unspecific effects on the APP-processing machinery of the cell in its concentration range studied. But strikingly, the pGlu formation at the N-terminus of A β (N3Q-42) was significantly suppressed in presence of the inhibitor suggesting a specific inhibition of this post-translational modification reaction in both model systems. This is of particular interest in the case of APP processing. The generation of pGlu-A β indicates that QC and the β -secretase cleavage products, i.e. A β and β -CTF, are co-localized in the secretory pathway at least in our cell-based model system. The result supports our hypothesis of potentially intraneuronal induction of neurodegeneration by toxic pGlu-peptide species. In fact, intracellular toxic oligomer formation as perhaps causal, early event becomes more and more accepted [29,30].

N-terminal pyroglutamated A β -peptides are a major hallmark of Alzheimer's disease amyloid plaques [11,12,31], are more prone to aggregation [15,34], and more toxic to neurons and astrocytes than full length A β (42) [16]. The precursor of pGlu in disease-related peptides in amyloidotic diseases is glutamate instead of glutamine. Recently, we could show that QC is responsible for pGlu formation from glutamate at the N-terminus of A β peptides *in vitro* [10]. This study demonstrates for the first time that QC is also capable of converting glutamate into pGlu in living cultured cells. Based on our results we cannot exactly predict in which cellular compartment the pGlu-A β peptide derived from the APP-precursor is formed, but the TRH-A β -precursor is very likely processed within the secretory pathway. However, in all experimental settings, P150/03 suppresses pGlu-formation from a glutamine and a glutamate

precursor. Therefore, it is tempting to conclude, that QC inhibition has an impact on pGlu-formation independent from the pathway, in which a certain QC substrate is posttranslationally generated by convertases and/or secretases. Thus, alteration of pGlu formation using highly potent QC inhibitors comprises an interesting new tool with broader applicability.

In the present study, pGlu formation in cell culture experiments was never completely blocked (Figs. 4B, 6B) by administration of P150/03, which was in contrast to the total inhibition of QC activity observed in cell extracts. The detection of remaining A β (N3pGlu-42) despite inhibitor administration is not surprising because P150/03 is an imidazole derivative [17] and the acidic environment of secretory granules leads to the protonation of a ring nitrogen and thus, partially hinders the interaction with the active site metal of the target enzyme [6]. This assumption is substantiated by the decline of the K_i value of P150/03 from 60nM at pH 8.0 to 200nM at pH 6.0. Moreover, a significant amount of spontaneous cyclization must also to be taken into consideration. Incubation of N-glutamine peptides in absence of enzyme (100mM MES, pH 7.0, 30 °C) leads to a relatively high amount (approximately 20% within 24h) of spontaneous glutamine cyclization similar to the observations here in cell culture (F. Seifert et al., manuscript in preparation) (Figs. 4B, 6B).

In conclusion, our study verifies QC as a potential target in Alzheimer's disease. Preclinical investigations will target the formation of toxic pGlu-A β species by inhibitors of QC in different animal models. However, by administration of QC inhibitors not only the formation of toxic pGlu-A β peptides from N-glutamate substrates will be influenced but rather all native N-glutamine substrates. Thus, due to the relatively fast spontaneous cyclization of the N-glutamine peptides, partial and reversible blockage of the pGlu-formation should be beneficial, if long-term application is considered. Further investigations will concentrate also on other native QC substrates with relevance in certain diseases, e.g. the contribution of gastrin to colorectal cancer [32].

Acknowledgments

This work was supported by grants of the BMBF (grant #0313185). The authors gratefully thank Dr. Steffen Rossner (Paul Flechsig Institute for Brain Research, Leipzig, Germany) for providing cultures of murine primary cortical neurons. We thank Dr. Ingo Schulz and Mirko Buchholz for helpful discussions, Nadine Schreier for routine cytotoxicity tests and Anett Stephan for technical assistance. The help of Prof. Dr. Robert C. Bateman Jr. and Jan Eggert for critical reading of the manuscript is also gratefully acknowledged.

References

- [1] A.C. Awade, P. Cleuziat, T. Gonzales, J. Robert-Baudouy, Pyrrolidone carboxyl peptidase (Pcp): an enzyme that removes pyroglutamic acid (pGlu) from pGlu-peptides and pGlu-proteins, *Proteins* 20 (1994) 34–51.
- [2] G.N. Abraham, D.N. Podell, Pyroglutamic acid. Non-metabolic formation, function in proteins and peptides, and characteristics of the enzymes effecting its removal, *Mol. Cell. Biochem.* 38 Spec. No. (1981) 181–190.

- [3] W.H. Busby Jr., G.E. Quackenbush, J. Humm, W.W. Youngblood, J.S. Kizer, An enzyme(s) that converts glutaminyl-peptides into pyroglutaminyl-peptides. Presence in pituitary, brain, adrenal medulla, and lymphocytes, *J. Biol. Chem.* 262 (1987) 8532–8536.
- [4] W.H. Fischer, J. Spiess, Identification of a mammalian glutaminyl cyclase converting glutaminyl into pyroglutaminyl peptides, *Proc. Natl. Acad. Sci. U. S. A.* 84 (1987) 3628–3632.
- [5] M. Messer, Enzymatic cyclization of L-glutamine and L-glutaminyl peptides, *Nature* 197 (1963) 1299.
- [6] S. Schilling, A.J. Niestroj, J.U. Rahfeld, T. Hoffmann, M. Wermann, K. Zunkel, C. Wasternack, H.U. Demuth, Identification of human glutaminyl cyclase as a metalloenzyme. Potent inhibition by imidazole derivatives and heterocyclic chelators, *J. Biol. Chem.* 278 (2003) 49773–49779.
- [7] S. Schilling, S. Manhart, T. Hoffmann, H.H. Ludwig, C. Wasternack, H.U. Demuth, Substrate specificity of glutaminyl cyclases from plants and animals, *Biol. Chem.* 384 (2003) 1583–1592.
- [8] T. Pohl, M. Zimmer, K. Mugele, J. Spiess, Primary structure and functional expression of a glutaminyl cyclase, *Proc. Natl. Acad. Sci. U. S. A.* 88 (1991) 10059–10063.
- [9] T.M. Bockers, M.R. Kreutz, T. Pohl, Glutaminyl-cyclase expression in the bovine/porcine hypothalamus and pituitary, *J. Neuroendocrinol.* 7 (1995) 445–453.
- [10] S. Schilling, T. Hoffmann, S. Manhart, M. Hoffmann, H.U. Demuth, Glutaminyl cyclases unfold glutaminyl cyclase activity under mild acid conditions, *FEBS Lett.* 563 (2004) 191–196.
- [11] T.C. Saido, T. Iwatsubo, D.M. Mann, H. Shimada, Y. Ihara, S. Kawashima, Dominant and differential deposition of distinct beta-amyloid peptide species. A beta N3(pE), in senile plaques, *Neuron* 14 (1995) 457–466.
- [12] Y. Harigaya, T.C. Saido, C.B. Eckman, C.M. Prada, M. Shoji, S.G. Younkin, Amyloid beta protein starting pyroglutamate at position 3 is a major component of the amyloid deposits in the Alzheimer's disease brain, *Biochem. Biophys. Res. Commun.* 276 (2000) 422–427.
- [13] J. Ghiso, T. Revesz, J. Holton, A. Rostagno, T. Lashley, H. Houlden, G. Gibb, B. Anderton, T. Bek, M. Bojsen-Moller, N. Wood, R. Vidal, H. Braendgaard, G. Plant, B. Frangione, Chromosome 13 dementia syndromes as models of neurodegeneration, *Amyloid* 8 (2001) 277–284.
- [14] T.C. Saido, Alzheimer's disease as proteolytic disorders: anabolism and catabolism of beta-amyloid, *Neurobiol. Aging* 19 (1998) S69–S75.
- [15] W. He, C.J. Barrow, The A beta 3-pyroglutaminyl and 11-pyroglutaminyl peptides found in senile plaque have greater beta-sheet forming and aggregation propensities *in vitro* than full-length A beta, *Biochemistry* 38 (1999) 10871–10877.
- [16] C. Russo, E. Violani, S. Salis, V. Venezia, V. Dolcini, G. Damonte, U. Benatti, C. D'Arrigo, E. Patrone, P. Carlo, G. Schettini, Pyroglutamate-modified amyloid beta-peptides-AbetaN3(pE)-strongly affect cultured neuron and astrocyte survival, *J. Neurochem.* 82 (2002) 1480–1489.
- [17] M. Buchholz, U. Heiser, S. Schilling, A.J. Niestroj, K. Zunkel, H.U. Demuth, The first potent inhibitors for human glutaminyl cyclase: synthesis and structure–activity relationship, *J. Med. Chem.* 49 (2006) 664–677.
- [18] K. Shirovani, S. Tsubuki, H.J. Lee, K. Maruyama, T.C. Saido, Generation of amyloid beta peptide with pyroglutamate at position 3 in primary cortical neurons, *Neurosci. Lett.* 327 (2002) 25–28.
- [19] T. Chikuma, K. Taguchi, M. Yamaguchi, H. Hojo, T. Kato, Improved determination of bovine glutaminyl cyclase activity using precolumn derivatization and reversed-phase high-performance liquid chromatography with ultraviolet detection, *J. Chromatogr., B Anal. Technol. Biomed. Life Sci.* 806 (2004) 113–118.
- [20] S. Schilling, H. Cynis, A. von Bohlen, T. Hoffmann, M. Wermann, U. Heiser, M. Buchholz, K. Zunkel, H.U. Demuth, Isolation, catalytic properties, and competitive inhibitors of the zinc-dependent murine glutaminyl cyclase, *Biochemistry* 44 (2005) 13415–13424.
- [21] G. Shaw, S. Morse, M. Ararat, F.L. Graham, Preferential transformation of human neuronal cells by human adenoviruses and the origin of HEK 293 cells, *FASEB J.* 16 (2002) 869–871.
- [22] C. Haass, M.G. Schlossmacher, A.Y. Hung, C. Vigo-Pelfrey, A. Mellon, B.L. Ostaszewski, I. Lieberburg, E.H. Koo, D. Schenk, D.B. Teplow, Amyloid beta-peptide is produced by cultured cells during normal metabolism, *Nature* 359 (1992) 322–325.
- [23] P.A. Sykes, S.J. Watson, J.S. Temple, R.C. Bateman Jr., Evidence for tissue-specific forms of glutaminyl cyclase, *FEBS Lett.* 455 (1999) 159–161.
- [24] P. Schaner, R.B. Todd, N.G. Seidah, E.A. Nillni, Processing of prothyrotropin-releasing hormone by the family of prohormone convertases, *J. Biol. Chem.* 272 (1997) 19958–19968.
- [25] R.W. Garden, T.P. Moroz, J.M. Gleeson, P.D. Floyd, L. Li, S.S. Rubakhin, J.V. Sweedler, Formation of N-pyroglutaminyl peptides from N-Glu and N-Gln precursors in *Aplysia* neurons, *J. Neurochem.* 72 (1999) 676–681.
- [26] A.M. Pimenta, B. Rates, C. Bloch Jr., P.C. Gomes, M.M. Santoro, M.E. de Lima, M. Richardson, M.N. Cordeiro, Electrospray ionization quadrupole time-of-flight and matrix-assisted laser desorption/ionization tandem time-of-flight mass spectrometric analyses to solve micro-heterogeneity in post-translationally modified peptides from *Phoneutria nigriventer* (Aranea, Ctenidae) venom, *Rapid Commun. Mass Spectrom.* 19 (2005) 31–37.
- [27] I. Song, C.Z. Chuang, R.C. Bateman Jr., Molecular cloning, sequence analysis and expression of human pituitary glutaminyl cyclase, *J. Mol. Endocrinol.* 13 (1994) 77–86.
- [28] C. Haass, C.A. Lemere, A. Capell, M. Citron, P. Seubert, D. Schenk, L. Lannfelt, D.J. Selkoe, The Swedish mutation causes early-onset Alzheimer's disease by beta-secretase cleavage within the secretory pathway, *Nat. Med.* 1 (1995) 1291–1296.
- [29] K. Takeda, W. Araki, T. Tabira, Enhanced generation of intracellular Abeta42 amyloid peptide by mutation of presenilins PS1 and PS2, *Eur. J. Neurosci.* 19 (2004) 258–264.
- [30] A.M. Cataldo, S. Petanceska, N.B. Terio, C.M. Peterhoff, R. Durham, M. Mercken, P.D. Mehta, J. Buxbaum, V. Haroutunian, R.A. Nixon, Abeta localization in abnormal endosomes: association with earliest Abeta elevations in AD and Down syndrome, *Neurobiol. Aging* 25 (2004) 1263–1272.
- [31] L. Miravalle, M. Calero, M. Takao, A.E. Roher, B. Ghetti, R. Vidal, Amino-terminally truncated Abeta peptide species are the main component of cotton wool plaques, *Biochemistry* 44 (2005) 10810–10821.
- [32] A.M. Smith, S.A. Watson, Review article: gastrin and colorectal cancer, *Aliment. Pharmacol. Ther.* 14 (2000) 1231–1247.
- [33] K.F. Huang, Y.L. Liu, W.J. Cheng, T.P. Ko, A.H. Wang, Crystal structures of human glutaminyl cyclase, an enzyme responsible for protein N-terminal pyroglutamate formation, *Proc. Natl. Acad. Sci. U. S. A.* 102 (37) (2005) 13117–13122.
- [34] S. Schilling, T. Lauber, M. Schaupp, S. Manhart, E. Scheel, G. Bohm, H.U. Demuth, On the seeding and oligomerization of pGlu-amyloid peptides (*in vitro*), *Biochemistry* (2006) (in press).

Isolation of an Isoenzyme of Human Glutaminyl Cyclase: Retention in the Golgi Complex Suggests Involvement in the Protein Maturation Machinery

Holger Cynis, Jens-Ulrich Rahfeld, Anett Stephan, Astrid Kehlen, Birgit Koch, Michael Wermann, Hans-Ulrich Demuth* and Stephan Schilling

Probiodrug AG, Weinbergweg
22, 06120 Halle/Saale, Germany

Received 2 January 2008;
received in revised form
12 March 2008;
accepted 31 March 2008
Available online
15 April 2008

Mammalian glutaminyl cyclase isoenzymes (isoQCs) were identified. The analysis of the primary structure of human isoQC (h-isoQC) revealed conservation of the zinc-binding motif of the human QC (hQC). In contrast to hQC, h-isoQC carries an N-terminal signal anchor. The cDNAs of human and murine isoQCs were isolated and h-isoQC, lacking the N-terminal signal anchor and the short cytosolic tail, was expressed as a fusion protein in *Escherichia coli*. h-isoQC exhibits 10fold lower activity compared to hQC. Similar to hQC, h-isoQC was competitively inhibited by imidazoles and cysteamines. Inactivation by metal chelators suggests a conserved metal-dependent catalytic mechanism of both isoenzymes. A comparison of the expression pattern of m-isoQC and murine QC revealed ubiquitous expression of both enzymes. However, murine QC transcript formation was higher in neuronal tissue, whereas the amount of m-isoQC transcripts did not vary significantly between different organs. h-isoQC was exclusively localized within the Golgi complex, obviously retained by the N-terminus. Similar resident enzymes of the Golgi complex are the glycosyltransferases. Golgi apparatus retention implies a “housekeeping” protein maturation machinery conducting glycosylation and pyroglutamylation. For these enzymes, apparently similar strategies evolved to retain the proteins in the Golgi complex.

© 2008 Elsevier Ltd. All rights reserved.

Keywords: glutaminyl cyclase isoenzymes; pyroglutamate; QPCTL; Golgi complex; posttranslational protein modification

Edited by J. Karn

Introduction

Posttranslational modifications, such as amidation, sulfatation and glycosylation are common events in

the biosynthesis of a number of proteins. The formation of an N-terminal 5-oxoproline (pyroglutamate, pGlu) is a modification that is present at the N-terminus of a number of peptide hormones and secretory proteins, e.g., thyrotropin-releasing hormone (TRH), gonadotropin-releasing hormone (GnRH), neurotensin and fibronectin.^{1,2} For TRH, the pGlu residue has been shown to be crucial for hormonal activity.³ Furthermore, the pGlu residue confers resistance against proteolysis by aminopeptidases.⁴

The enzymatic formation of the N-terminal pGlu from glutamine was first described in plants.⁵ The first mammalian glutaminyl cyclase (QC) cDNA was isolated from bovine pituitary, and further work by two different groups yielded in the isolation and characterization of human (hQC) and murine QC (mQC).^{6–9} In contrast to the plant QCs, the mammalian counter-

*Corresponding author. E-mail address:

hans-ulrich.demuth@probiodrug.de.

Abbreviations used: QC, glutaminyl cyclase; isoQC, glutaminyl cyclase isoenzyme; mQC, murine QC; hQC, human QC; pGlu, pyroglutamate; TRH, thyrotropin-releasing hormone; GnRH, gonadotropin-releasing hormone; AD, Alzheimer's disease; GST, glutathione S-transferase; EDTA, ethylenediaminetetraacetic acid; Met, methionine; EGFP, enhanced green fluorescent protein; PBS, phosphate-buffered saline; SS, signal sequence.

parts represent zinc-dependent metalloenzymes.^{7,10} The active-site-bound zinc ion, which presumably exerts a role in the polarization of the γ -amide group of the substrate, represents also the primary interaction of competitive inhibitors of QC.¹¹ The tissue distribution of bovine QC revealed a marked abundance in different brain regions, with highest expression in the striatum and hippocampus.⁶ Within neurons, QC is co-localized with its products TRH and GnRH and is secreted from secretory granules into the extracellular space.¹² The localization of soluble QCs in the regulated secretory pathway, which is primarily necessary for the processing of the hormonal precursors, was also corroborated for a QC of *Drosophila* that has been isolated recently. In contrast to mammals, however, *Drosophila* apparently expresses an isoform that is translocated into mitochondria.¹³

In human disease, compelling evidence suggests an involvement of QC in conditions such as rheumatoid arthritis, osteoporosis and Alzheimer's disease (AD).^{14,15} Significant amounts of beta-amyloid (A β) peptides, deposited in amyloid plaques of AD, are N-terminally modified to possess a pGlu residue originating from glutamate cyclization.^{16,17} These pGlu-containing A β peptides are suggested to be potential targets in drug development due to their pronounced stability, neurotoxicity and aggregation propensity.^{18–22} With respect to the therapeutic intervention in those pathophysiological processes, the characterization of potential isoenzymes is important to reduce risk of cross-reactivity and, hence, side effects.^{23,24}

Here we describe the isolation and characterization of a mammalian isoenzyme of QC. The results provide evidence for a general role of glutaminyl cyclases in the protein-maturation machinery of the secretory pathway, revealing notable functional homology to glycosyltransferases. Furthermore, the results will have importance for the profiling of QC inhibitors for the treatment of QC-related disorders.

Results

Identification of human and murine glutaminyl cyclase isoenzyme

On the basis of the primary structure of human and murine QC, similarity searches using BLAST at the National Institute for Biotechnology Information were performed. The putative glutaminyl cyclase isoenzyme (isoQC) sequences were selected from nucleotide entries NM_017659 (h-isoQC) and BC058181 (m-isoQC), respectively. On the basis of the identified nucleotide sequences, specific primers for the isolation of h-isoQC and m-isoQC were deduced. The coding sequences of h-isoQC and m-isoQC were isolated from human hepatocellular carcinoma cell line Hep-G2 and murine thalamus, respectively. The generated PCR products were

subcloned and the respective sequences verified (Fig. 1a and b). The comparison of the human enzymes using ClustalW at PBIL† revealed a sequence identity of 45% and 43% for the murine enzymes (Fig. 1d). The zinc-binding motif (Asp-Glu-His)⁷ of mammalian QCs is conserved in both isoenzymes. In contrast to the QCs, however, the isoenzymes lack N-glycosylation sites. With respect to the overall primary structure, notable inhomogeneity was observed in the N-terminal region of QC and isoQC. In the QC proteins, the N-terminus contains a secretion signal that is cleaved off co-translationally by signalpeptidase.⁶ In contrast, predictions using the programs signalP²⁵ suggested the presence of an N-terminal anchor for h-isoQC (not shown). The result was corroborated by HMMTOP topology analysis,²⁶ which provided evidence for an N-terminal signal anchor in both isoenzymes (Fig. 1c). Two codons were identified at the N-terminus of the isoQCs, which might function as initiation points of translation.

Heterologous expression of h-isoQC

In order to verify that the cDNA encodes a protein possessing QC activity, the h-isoQC cDNA starting with Phe48, thus lacking N-terminal signal anchor, was inserted into vector pET41a. The h-isoQC sequence was fused in-frame with the vector-encoded glutathione S-transferase (GST) tag, a C-terminal His₆ tag was inserted and the protein was expressed in *Escherichia coli* BL21 cells (not shown). For purification, a three-step protocol was established consisting of expanded bed absorption on a Ni²⁺-chelating resin, followed by GST-affinity chromatography and a final cation-exchange chromatography. The procedure usually resulted in fairly homogenous GST-h-isoQC fusion protein, as depicted by SDS-PAGE (Fig. 2a).

For comparison with human QC (hQC)²⁷ and mQC,⁷ the substrate specificity of GST-h-isoQC was investigated for several glutaminyl peptides (Table 2). All substrates were also converted by h-isoQC, suggesting that the identified h-isoQC is substantially similar to QC. Furthermore, the determined specificity points to a similar selectivity of QC and isoQC as evidenced by the high specificity constants that were observed with the hydrophobic fluorogenic substrates. However, the specificity constant k_{cat}/K_M was always lower for h-isoQC compared to hQC, indicating an overall reduced enzymatic activity.

In analogy to QCs, h-isoQC was also inhibited by imidazole derivatives in a competitive manner (not shown). For four previously published inhibitors,^{7,10} the K_i values were determined (Table 2). The obtained K_i values are very similar for hQC and h-isoQC. For both enzymes, N-substituted imidazole derivatives are more potent inhibitors than imidazole or benzimidazole. Comparing the K_i values of imidazole, benzimidazole, methylimidazole and cysteamine ob-

† <http://npsa-pbil.ibcp.fr>

(a)

DNA: ATGCGTTCCGGGGCCGCGGGCGACCCCGCCTGCGGCTGGGGAAACGTGGCCT**CATGGAGCCACTCTTGCCGCCG** 75
 aa: **M** R S G G R G R P R L R L G E R G L **M** E P L L P P

DNA: AAGCGCCGCTGCTACCGCGGGTTCGGCTCT**GCCTCTGTTGCTGGCGCTGGCCGTGGGCTCGGCGTTCTACACC** 150
 aa: K R R L L P R V R **L L P L L L A L A V G S A F Y T**

DNA: **ATTTGGAGCGGCTGGCACCGCAGGACTGAGGAGCTGCCGCTGGGCCGGGAGCTGCGGGTCCCA**TTGATCGGAAGC 225
 aa: **I W** S G W H R R T E E L P L G R E L R V P L I G S

DNA: CTCCCGAAGCCCGCTGCGGAGGGTGGTGGGACAACCTGGATCCACAGCGTCTCTGGAGCACTTATCTGCGCCCC 300
 aa: L P E A R L R R V V G Q L D P Q R L W S T Y L R P

DNA: CTGCTGGTTGTGCGAACCCCGGCGAGCCCGGAAATCTCCAAGTCAGAAAGTTCTGGAGGCCACGCTGCGGTTCC 375
 aa: L L V V R T P G S P G N L Q V R K F L E A T L R S

DNA: CTGACAGCAGGTTGGCACGTTGGAGCTGGATCCCTTCACAGCCTCAACACCCCTGGGGCCAGTGGACTTTGGCAAT 450
 aa: L T A G W H V E L D P F T A S T P L G P V D F G N

DNA: GTGGTGGCCACACTGGACCCAAGGGGTGCCCGTCACCTCACCTTGCCTGCCATTATGACTCGAAGCTCTTCCCA 525
 aa: V V A T L D P R A A R H L T L A C H Y D S K L F P

DNA: CCCGATCGACCCCTTTGTAGGGGCCACGGATTGCGCTGTGCCCTGTGCCCTGCTGCTGGAGCTGGCCCAAGCA 600
 aa: P G S T P F V G A T D S A V P C A L L L E L A Q A

DNA: CTTGACCTGGAGCTGAGCAGGGCCAAAAACAGGCAGCCCGGTGACCCTGCAACTGCTCTTCTTGGATGGTGAA 675
 aa: L D L E L S R A K K Q A A P V T L Q L L F L D G E

DNA: GAGGCGTGAAGGAGTGGGGACCCAAGGACTCCCTTTACGGTTCCCGGCACCTGGCCCAGCTCATGGAGTCTATA 750
 aa: E A L K E W G P K D S L Y G S R H L A Q L M E S I

DNA: CCTCACAGCCCGGCCCCACCAGGATCCAGGCTATTGAGCTCTTTATGCTTCTTGATCTCTGGGAGCCCCCAAT 825
 aa: P H S P G P T R I Q A I E L F M L L D L L G A P N

DNA: CCCACCTTCTACAGCCACTTCCCTCGCACGGTCCGCTGGTTCCATCGGCTGAGGAGCATTGAGAAGCGTCTGCAC 900
 aa: P T F Y S H F P R T V R W F H R L R S I E K R L H

DNA: CGTTTGAACCTGCTGCAGTCTCATCCCCAGGAAGTGATGTACTTCCAACCCGGGAGCCCTCTGGCTCTGTGGAA 975
 aa: R L N L L Q S H P Q E V M Y F Q P G E P S G S V E

DNA: GACGACCACATCCCCTTCTCCGAGAGGGGTACCCGTGCTCCATCTCATCTCCACGCCCTTCCCTGCTGTGTTC 1050
 aa: D D H I P F L R R G V P V L H L I S T P F P A V W

DNA: CACACCCCTGCGGACACCGAGGTCAATCTCCACCCACCCACGGTACACAACCTGTGCCGATTCTCGTGTGTTTC 1125
 aa: H T P A D T E V N L H P P T V H N L C R I L A V F

DNA: CTGGCTGAATACCTGGGGCTCTAG 1049
 aa: L A E Y L G L *

Fig. 1. Nucleotide sequence (DNA) and amino acid sequence (aa) of h-isoQC isolated from human Hep-G2 cells (a) and m-isoQC isolated from murine thalamus (b). The putative start methionines and the predicted signal anchors are highlighted in bold. The primer sequences for isolation of the open reading frame using RT-PCR are underlined. (c) Topology analysis of the N-terminal 100 amino acids of h-isoQC and m-isoQC using HMMTOP showing a putative N-terminal signal anchor (bold letters) (pred, prediction; I, inside/cytosol; i, inside tail; H, transmembrane helix; O, outside/lumen; o, outside tail). (d) Sequence alignment of the primary structures of hQC (361 amino acids), mQC (362 amino acids), h-isoQC (382 amino acids) and m-isoQC (382 amino acids). The sequence identity between hQC and h-isoQC is 45% and between mQC and m-isoQC 43%. The isoenzymes possess two potential start methionines designated as MetI and MetII (bold). The residues for complexation of a zinc ion in the active site (Asp-Glu-His) (bold) are conserved in mammalian QCs and isoQCs. Major differences are depicted at the N-terminus. The QCs possess a signal sequence directing the protein to the secretory pathway, whereas h-isoQC carries a putative signal anchor (bold, italics). A further difference is the lack of N-glycosylation sites in h-isoQC and m-isoQC. In contrast, hQC possesses two such sites (bold, italics).

(b)

DNA: ATGAGTCCCGGAGCCGCGGGCGGCCCGCCGAGCGGCTCGAGGATCGTGGCCTCATGAAACCACCTCACTTTCC 75
 aa: M S P G S R G R P R Q R L E D R G L M K P P S L S

DNA: AAGCGCCGTCTTCTGCCGCGAGTGCAGTTCCTGCCCTGCTGCTGCTGGCGCTGGCTATGGGCTTGGCTTTCTAT 150
 aa: K R R L L P R V Q F L P L L L L A L A M G L A F Y

DNA: ATCGTCTGGAACAGCTGGCACCTGGGGTTGAGGAGATGTACGGAGCCGGGATCTGCGGGTCCCGTGATCCGGA 225
 aa: I V W N S W H P G V E E M S R S R D L R V P L I G

DNA: AGCCTTTCAGAAAGCAAGCTGCGGCTGGTGGTAGGGCAGCTGGATCCGACGCTCTCTGGGAACTTCTCTGCTAT 300
 aa: S L S E A K L R L V V G Q L D P Q R L W G T F L R

DNA: CCCTTATTGATGTGCGACCCCCGGTAGTTCTGGCAATCTCAAGTGAGAAAGTTCTGGAGGCTACGTTGCGGA 375
 aa: P L L I V R P P G S S G N L Q V R K F L E A T L Q

DNA: TCCCTGTGCGCAGGCTGGCATGTTGAACTGGACCCATTACGGCCTCAACCCCTTGGGGCCACTGGACTTCCGGA 450
 aa: S L S A G W H V E L D P F T A S T P L G P L D F G

DNA: AACGTGGTGGCCACACTTGACCCAGGAGCTGCCGTCACCTCACCTCGCCTGCCATTATGACTCTAAGTTCTTC 525
 aa: N V V A T L D P G A A R H L T L A C H Y D S K F F

DNA: CCTCCGGGTTGCCCCCTTTGTGGGGCCACAGATTGAGCTGTGCCCTGTGCCCTGCTTCTGGAGTTGGTCCGGA 600
 aa: P P G L P P F V G A T D S A V P C A L L L E L V Q

DNA: GCCCTTGATGCCATGCTGAGCAGAATCAAGCAGCAGGCAGCACCGGTGACCTGCAGCTGCTTTTCTGGGGGAG 675
 aa: A L D A M L S R I K Q Q A A P V T L Q L L F L G E

DNA: GAGGCACTGAAGGAGTGGGGACCAAAGGACTCCCTCTATGGCTCCCGGCACCTAGCTCAGATCATGGAGTCTATA 750
 aa: E A L K E W G P K D S L Y G S R H L A Q I M E S I

DNA: CCACACAGCCCTGGCCCCACCAGGATCCAGGCTATTGAGCTCTTTGTCCCTCCTCGACCTTCTGGGAGCATCCAGT 825
 aa: P H S P G P T R I Q A I E L F V L L D L L G A S S

DNA: CCGATCTTCTTCAGTCACTTCCCTCGCACAGCCCGCTGGTTCAGCGACTGAGGAGCATTGAGAAGCGCCTTCCAC 900
 aa: P I F F S H F P R T A R W F Q R L R S I E K R L H

DNA: CGGCTGAACCTACTGCAGTCTCACCCCCAGGAAGTGTACTTCCAACCCGGGAGCCCCCGGCCCTGTGGAA 975
 aa: R L N L L Q S H P Q E V M Y F Q P G E P P G P V E

DNA: GATGACCACATCCCCTTCCTTCCGAGAGGGTCCCGGTGCTCCACCTCATGACCAGCCCTTCCCTGCTGTGTTG 1050
 aa: D D H I P F L R R G V P V L H L I A T P F P A V L

DNA: CACACACCTGCTGACACCGAGGCCAACCTCCACCCACCCACTGTGCATAACCTGAGCCGCATCCTTGTGTGTTTC 1125
 aa: H T P A D T E A N L H P P T V H N L S R I L A V F

DNA: CTGGCCGAGTACCTGGGACTCTAG 1149
 aa: L A E Y L G L *

Fig. 1 (legend on previous page)

tained for the inhibition of both enzymes, we found hQC two- to threefold more potently inhibited by these compounds than h-isoQC. Benzylimidazole and *N*-dimethylcysteamine displayed highest inhibitory potency for both enzymes, substantiating simi-

larities in the binding modes of inhibitors from different classes.

A time-dependent inhibition of QCs from different sources has been observed with heterocyclic chelators.^{7,10} In analogy, h-isoQC was also inactivated by

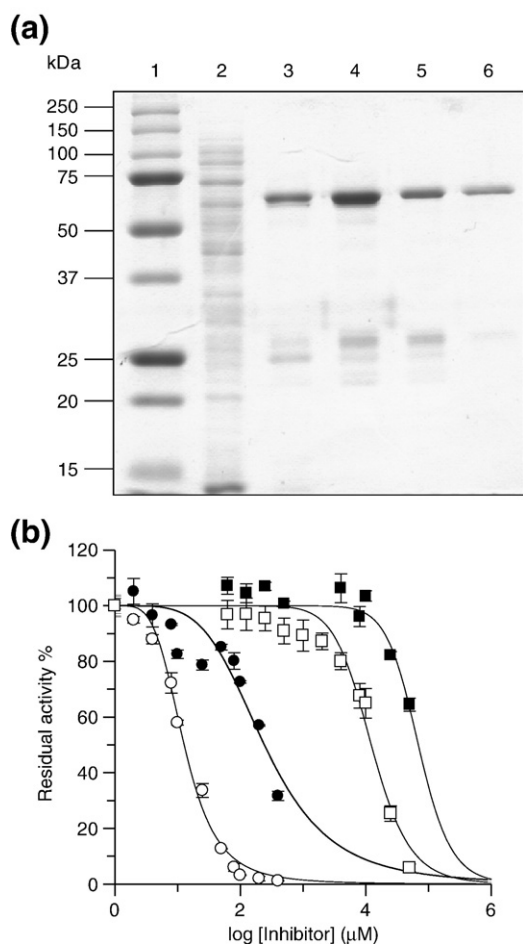


Fig. 2. Analysis of h-isoQC that was recombinant expressed in *E. coli*. (a) SDS-PAGE analysis of the chromatographic steps used to purify GST-tagged h-isoQC. Lane 1, molecular mass standards (kilodaltons) (Dual Color, Bio-Rad); lane 2, supernatant after French press and centrifugation; lane 3, GST-h-isoQC protein-containing fraction after immobilized metal-affinity chromatography (Ni^{2+} -IMAC); lane 4, GST-h-isoQC protein after GST affinity chromatography (GST); lane 5, GST-h-isoQC after gel filtration; lane 6, purified GST-h-isoQC fusion protein after cation-exchange chromatography (IEX). Proteins were visualized by Coomassie staining. (b) Time-dependent inhibition of h-isoQC by the metal-chelating compounds 1,10-phenanthroline (circles) and EDTA (squares). Residual h-isoQC activity was determined directly after addition (filled symbols) or preincubation of h-isoQC with the respective reagent for 15 min at 30 °C (open symbols).

duced. Primers 20 and 21 (Table 1) specifically amplify m-isoQC without any cross-reactivity to mQC (Fig. 3a, inset) and primers 18 and 19 (Table 1) amplify mQC without an observable cross-reactivity to m-isoQC (Fig. 3b, inset). On the basis of these results, the tissue distribution of mQC and m-isoQC was investigated by quantitative PCR. Similar expression was observed for m-isoQC in different brain regions and peripheral organs such as kidney and lung, lower expression in heart and spleen (Fig. 3a). mQC expression is apparently higher in brain tissues compared with peripheral organs. The highest mQC expression

was observed in the thalamus and hippocampus (Fig. 3b). The spleen shows also a very small amount of mQC transcripts. In general, the variation of m-isoQC among all tissues is low, compared to mQC, for which the transcript levels differ by up to one order of magnitude.

Subcellular distribution of h-isoQC

In order to investigate the subcellular localization of h-isoQC in mammalian cells and the relevance of the putative start methionines (Fig. 1), h-isoQC-(enhanced green fluorescent protein) EGFP fusions beginning either at methionine I (MetI) or at methionine II (MetII) were generated. Human LN405 cells were transiently transfected with an average transfection efficiency of 30–50% (not shown) and the subcellular localization of h-isoQC was examined using confocal laser scanning microscopy. The expression of h-isoQC (MetI)-EGFP fusion protein resulted in a distinct staining pattern close to the nucleus of virtually all cells expressing the transgene (Fig. 4a). Counterstaining of cellular mannosidase II revealed the presence of h-isoQC (MetI) exclusively within the Golgi complex. Furthermore, no additional vesicular staining was observed, suggesting retention of h-isoQC (MetI)-EGFP within the Golgi complex. An immunohistochemical staining of the mitochondria did not reveal any co-localization (Fig. 4a). Expression of h-isoQC (MetII)-EGFP fusion protein resulted in very similar fluorescence staining, which matched well with that of mannosidase II but not with that of mitochondria (Fig. 4b). Thus, the subcellular distribution of h-isoQC is independent of the N-terminal methionine.

The subcellular distribution of h-isoQC was further characterized by analysis of QC activity following cellular fractionation. h-isoQC and hQC were expressed in HEK293 cells, and the QC activity was determined using H-Gln- β NA as substrate. Little QC activity was detected in mock-transfected cells (pcDNA). In contrast, QC activity was readily detectable following transfection with h-isoQC (MetI) and h-isoQC (MetII), with the highest specific activity in the heavy membrane fraction (MetI, $40 \pm 2 \mu\text{mol min}^{-1} \text{g}^{-1}$; MetII, $36 \pm 1.5 \mu\text{mol min}^{-1} \text{g}^{-1}$) and the medium (MetI, $30 \pm 2 \mu\text{mol min}^{-1} \text{g}^{-1}$; MetII, $54 \pm 3 \mu\text{mol min}^{-1} \text{g}^{-1}$). In contrast, hQC shows the highest specific QC activity within the medium ($1339 \pm 76 \mu\text{mol min}^{-1} \text{g}^{-1}$) (Fig. 5a).

The data obtained by the expression of the native enzymes were further supported by expression of h-isoQC (MetI and MetII) and hQC possessing a C-terminal FLAG tag. Western blot analysis of the resulting FLAG-tagged proteins in comparison to marker proteins of the Golgi complex and mitochondria revealed a mainly intracellular localization of h-isoQC (MetI) and h-isoQC (MetII) within the debris and heavy membrane fraction, whereas hQC is enriched within the medium but also found within the debris and heavy membrane fraction. Visualization of marker proteins of the Golgi complex (ST1GAL3) and mitochondria confirmed the presence of these com-

Table 1. Oligonucleotides used for isolation, cloning and characterization of QC and isoQC sequences

Oligonucleotide	Sequence (5'→3'), restriction sites (underlined)	Purpose
1	ACCATGCGTTCCGGGGCCGCGGG	Isolation of h-isoQC-
2	ACGCTAGAGCCCCAGGTATTCAGCCAG	Isolation of h-isoQC
3	ATGAGTCCCCGGGAGCCGC	Isolation of m-isoQC
4	CTAGAGTCCCAGGTACTC	Isolation of m-isoQC
5	ATATACTAGTGATGACGACGACAAGTTCTACACCATTGGAGCG	Insertion of h-isoQC into pET41a
6	TATAGAATTCCTAGTGATGGTGATGGTGATGGAGCCCCAGGTATTC AGC	Insertion of h-isoQC into pET41a
7	ATATATAAGCTTATGGCAGGCGGAAGACAC	Insertion of native hQC into pcDNA 3.1
8	ATATGCGGCCGCTTACAAATGAAGATATTCC	Insertion of native hQC into pcDNA 3.1
9	ATATATGAATTCATGCGTTCGGGGGGCCGC	Amplification of h-isoQC starting with MetI
10	ATATATGAATTCATGGAGCCACTCTTGCCGCCG	Amplification of h-isoQC starting with MetII
11	ATATATGCGGCCGCTAGAGCCCCAGGTATTCAGC	Amplification of h-isoQC including the stop codon for insertion into pcDNA 3.1
12	ATATATGTCGACGAGCCCCAGGTATTCAGCCAG	Amplification of h-isoQC lacking the stop codon for insertion into vector EGFP-N3
13	ATATCTCGAGTCCATCGCCACCATGGTGAGC	Amplification of EGFP
14	ATATCTCGAGTTACTTGTACA GCTCGTCCAT	Amplification of EGFP
15	ATATGCGGCCGCTATGTCGACGCTCCAAATGGTGTAGAACGC	Amplification of h-isoQC N-terminal sequence
16	ATATGCGGCCGCTTACTTGTGCATCGTCATCCTTGTAATC CAAATGAAGATATTCCAA	Amplification of hQC C-FLAG
17	ATATGCGGCCGCTTACTTGTGCATCGTCATCCTTGTA ATCGAGCCCCAGGTATTCAGC	Amplification of h-isoQC C-Flag
18	ATCAAGAGGCACCAACCAAC	Tissue distribution of mQC
19	CTGGATAATATTCCATAG	Tissue distribution of mQC
20	CCAGGATCCAGGCTATTGAG	Tissue distribution of m-isoQC
21	TTCCACAGGGCCGGGGGGC	Tissue distribution of m-isoQC

partments within the debris and heavy membrane fraction (Fig. 5b). In addition, the 65-kDa mitochondrial protein was also detected within the soluble fraction.

Identification of a Golgi retention sequence

In order to clarify whether the predicted N-terminal signal anchor is responsible for the retention of h-isoQC within the Golgi complex, the signal peptides starting at MetI and MetII, including the putative signal anchor, were cloned in-frame with EGFP. The resulting vectors h-isoQC (MetI) signal sequence (SS) EGFP and h-isoQC (MetII) SS EGFP were expressed in LN405 cells and the expression was analyzed by confocal laser scanning microscopy. The expression of h-isoQC (MetI) SS EGFP and h-isoQC (MetII) SS EGFP led to the same Golgi complex localization that was observed for the full-length h-isoQC fusion proteins. Again, a transport of the fusion proteins to mitochondria was not observed (Fig. 6). Consequently, the N-terminal sequence of h-isoQC leads to the co-translational translocation of the protein to the membrane of the endoplasmic reticulum and to the retention within the Golgi complex. Further-

more, due to the expression of h-isoQC (MetII) SS EGFP, the Golgi retention signal can be grossly mapped between residues methionine 19 and serine 53.

Discussion

Genes encoding glutaminyl cyclases (QPCT) have been recently described in numerous species. Examples are known from the lower phyla cnidaria, mollusks and arthropods,^{13,28–30} lower vertebrates such as serpents³¹ and higher mammals such as mice,⁷ cattle⁶ and humans.⁹ In particular, the human enzyme is well characterized, since QC emerged as a potential drug target for treatment of pGlu-protein-mediated amyloidoses, such as AD.³² Although different QC activities in mammalian tissue have been observed,³³ no gene encoding a potential isoenzyme of glutaminyl cyclase has been isolated.^{6,33} However, the recent identification of a QC that is directed to mitochondria in *Drosophila*¹³ tempted us to search for isoenzymes in mammals.

On the basis of the hQC sequence, cDNAs were isolated that encode isoenzymes of QC in mice and

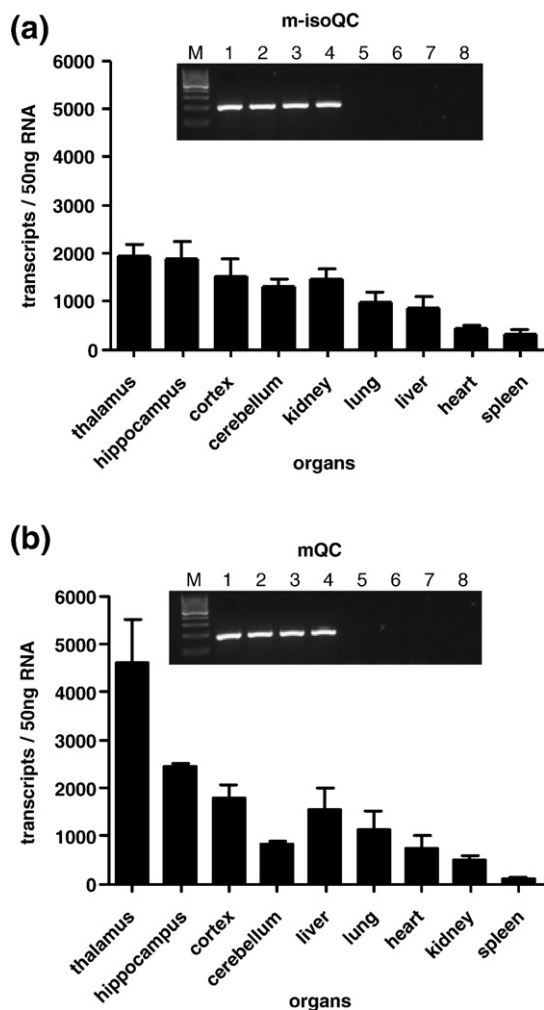


Fig. 3. Tissue distribution of mQC and m-isoQC mRNA using quantitative RT-PCR. (a) m-isoQC was analyzed in various organs of 3-6 month old C57/Bl6 mice ($n=5$). The inset shows the amplification of m-isoQC by specific primers without cross-reactivity to mQC using cloned cDNAs of mQC and m-isoQC. M, DNA standard; lane 1, m-isoQC, 286 ng/ μ l; lane 2, m-isoQC, 28.6 ng/ μ l; lane 3, m-isoQC, 2.86 ng/ μ l; lane 4, m-isoQC, 0.286 ng/ μ l; lane 5, mQC, 242 ng/ μ l; lane 6, mQC, 24.2 ng/ μ l; lane 7, mQC, 2.42 ng/ μ l; lane 8, mQC, 0.242 ng/ μ l. (b) mQC in various organs of 3- to 6-month-old C57/Bl6 mice ($n=5$). The inset shows the amplification of mQC by specific primers without cross-reactivity to m-isoQC using cloned cDNAs of mQC and m-isoQC. M, DNA standard; lane 1, mQC, 242 ng/ μ l; lane 2, mQC, 24.2 ng/ μ l; lane 3, mQC, 2.42 ng/ μ l; lane 4, mQC, 0.242 ng/ μ l; lane 5 m-isoQC, 286 ng/ μ l; lane 6, m-isoQC, 28.6 ng/ μ l; lane 7, m-isoQC, 2.86 ng/ μ l; lane 8, m-isoQC, 0.286 ng/ μ l. Values were normalized to RNA concentration.

humans. The enzymatic activity of the h-isoQC was confirmed by homologous and heterologous expression. An initial analysis of the activity revealed similar selectivity but reduced specificity against the tested substrates compared to hQC (Table 2). As described for animal QCs,^{7,10} isoQCs are also metal-dependent transferases as revealed by the potent inhibition of imidazole, cysteamines and chelators. The conserva-

tion of the zinc-binding motif (Asp-Glu-His) in QC and isoQC is in line with these observations and strongly suggests a similar architecture of the active sites. This, in turn, is corroborated by the similarities of the inhibitory potencies of cysteamine and imidazole derivatives for both enzymes, in particular by the low inhibition constants obtained with N-substituted imidazoles. With regard to the comparison of the different substrate specificities, it cannot be fully excluded that the N-terminal GST tag or the C-terminal His₆ tag of the h-isoQC fusion protein influenced the catalytic proficiency. Furthermore, the expression of hQC in *E. coli* hampered the formation of a disulfide bond between two cysteines also conserved in the isoQCs.⁸ In hQC, the lack of disulfide formation apparently exerted some influence on the turnover of the substrates. More detailed studies on the comparison of the substrate specificities between hQC and h-isoQC will be conducted with enzymes that are expressed in eukaryotic hosts.

Since QC and isoQC catalyze the same enzymatic reaction, the question arose, whether QC and isoQC are differentially expressed with respect to tissue and subcellular distribution. Interestingly, m-isoQC displayed an ubiquitous expression in neuronal and peripheral organs with little difference in the transcript concentration (Fig. 3). With mQC, in contrast, higher variances between different tissues were observed. The expression pattern of mQC is similar to the observations in earlier studies resembling the tissue distribution found for bovine QC, which revealed a marked abundance in neuronal tissues.⁶ In addition, it has been shown that QC and its products of catalysis, i.e., the hormones GnRH and TRH, are colocalized in secretory vesicles of hypothalamic neurons. The presence of QC in those vesicles becomes comprehensible from related descriptions concerning the processing of the pGlu-hormonal precursors.³⁴ The hormones are expressed as large precursors that are processed by prohormone convertases, e.g., PC1 and PC2,³⁵ in the late secretory pathway. Following initial N- and C-terminal processing, the final maturation takes place in the secretory granules.^{36,37} Formation of pGlu-hormones in the regulated secretory pathway thus requires the presence of a vesicular, soluble QC. The regulated secretory pathway has been described for neuroendocrine cells,^{38,39} which might explain the higher expression levels of QC observed in neuronal tissue.

In contrast to the hormonal precursors, numerous pGlu-peptides and proteins are generated by simple epithelial cells or fibroblasts, e.g., chemokines or fibronectin,^{40,41} or have been shown to be constitutively secreted, e.g., immunoglobulins.⁴² The N-terminal pGlu of these proteins is generated from a glutaminy residue, which is demasked directly by signalpeptidase without requirement of the complex prohormone processing machinery, which is also under-represented in those cells. These substrates are likely candidates for conversion by isoQC, which has been shown here to be a resident enzyme of the Golgi apparatus. In the Golgi complex, secretory proteins undergo a number of different posttranslational modifi-

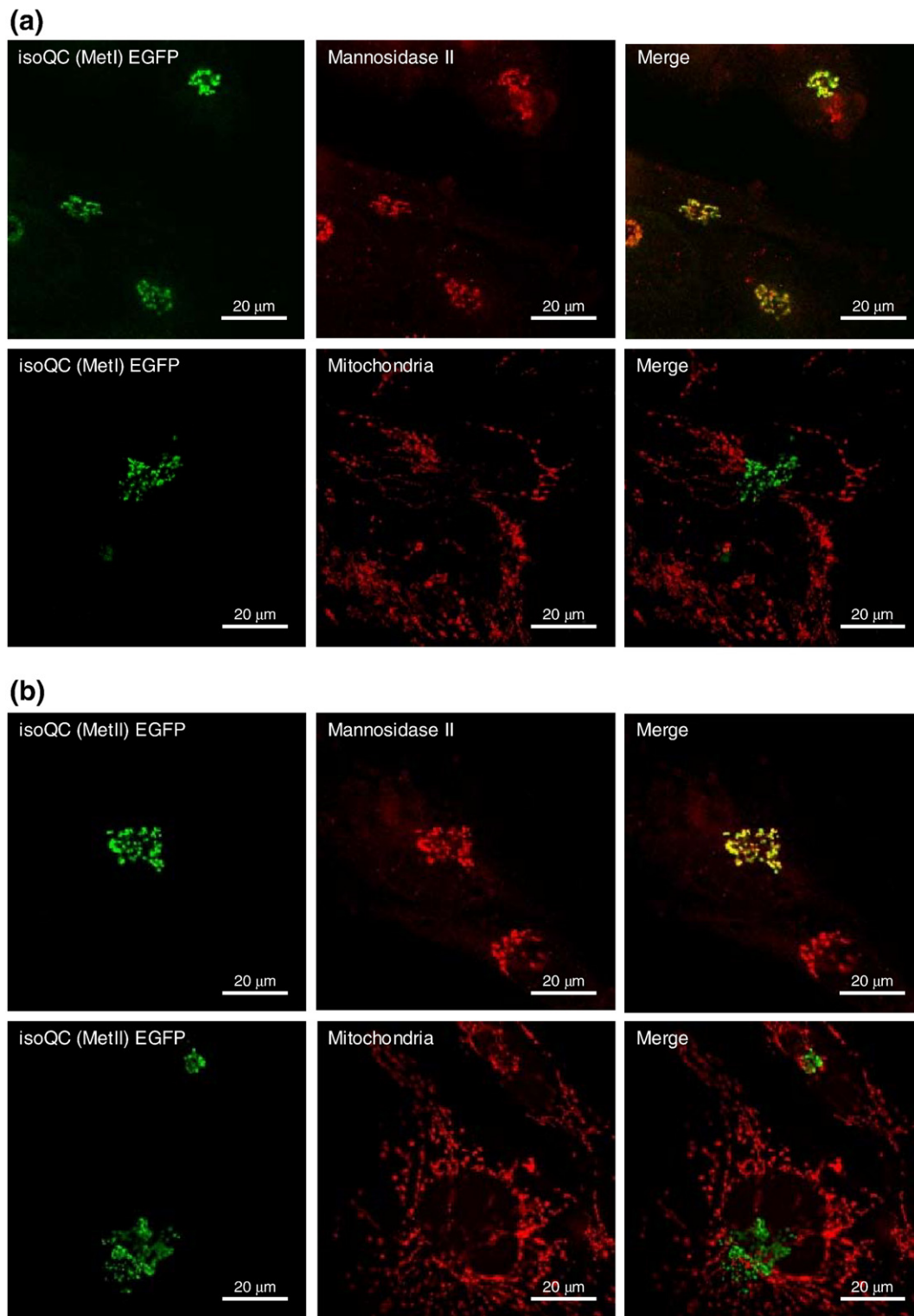


Fig. 4. Subcellular localization of h-isoQC-EGFP fusion proteins starting with (a) MetI [isoQC (MetI)-EGFP] and (b) MetII [isoQC (MetII)-EGFP]. Golgi complex was counterstained using an anti-mannosidase II antibody and human mitochondria were stained using an anti-human mitochondria antibody, detecting a 65-kDa protein of human mitochondria. Co-localization is shown by superimposition of EGFP fluorescence and Red X fluorescence (Merge).

cations, e.g., enzymatic rearrangement of sugar chains by glycosyltransferases. Intriguingly, the mammalian isoQCs reveal a structural similarity with those processing enzymes. Glycosyltransferases are type II

transmembrane proteins that possess a short cytoplasmic sequence, followed by the signal anchor and a large luminal catalytic domain (for a review, see Ref. 43). This, in turn, is essentially the same

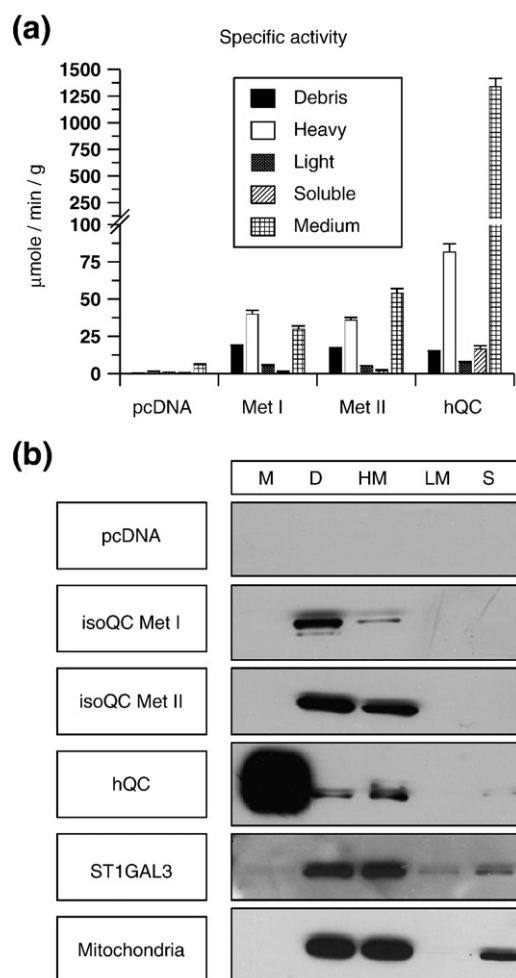


Fig. 5. Biochemical analysis of the subcellular localization of QC activity after expression of pcDNA and the native enzymes h-isoQC (MetI), h-isoQC (MetII) and hQC in HEK293 cells. (a) Specific activity within the cell fractions ($\mu\text{mol min}^{-1} \text{g}^{-1}$). (b) Expression of h-isoQC (MetI), h-isoQC (MetII) and hQC possessing a C-terminal FLAG tag in HEK293 in comparison to vector-transfected control (pcDNA) followed by Western blot analysis applying specific antibodies detecting either the FLAG-epitope, a 65-kDa protein of human mitochondria or human sialyl-transferase ST1GAL3.

structural motif that has been identified for m-isoQC and h-isoQC (Fig. 7). Similarly, for a number of glycosyltransferases the Golgi retention signal was identified to reside within the signal anchor,⁴⁴⁻⁴⁶ and truncation of the cytoplasmic tail was found to have no influence on the activity or the localization of the protein.⁴⁵ In conclusion, we suggest that common mechanisms evolved leading to retention of transmembrane proteins in the Golgi complex.

By Golgi retention of the different processing enzymes, an environment is generated that allows maturation of the glycosyl side chains and the N-terminal pGlu-blockage of common secretory proteins, which are secreted basally.

The presence of a second QC activity in neuronal cells provides further support for the potential role of

QC activity in amyloidotic diseases that are characterized by cerebral accumulation of pGlu-amyloid peptides, e.g., AD, familial Danish dementia and familial British dementia.^{17,47,48} The isolation and characterization of QC isoenzymes give implications for the development of selective inhibitors in order to prevent unwanted side effects.

Materials and Methods

Materials

E. coli strain DH5 α was used for propagation of plasmids and *E. coli* strain BL21 was used for the expression of h-isoQC. *E. coli* strains were grown, transformed and analyzed according to the manufacturer's instructions [Qiagen (DH5 α) Stratagene (BL21)].

Cultivation and transfection of mammalian cells

Human astrocytoma cell line LN405, human embryonal kidney cell line HEK293 and human hepatocellular carcinoma cell line Hep-G2 were cultured in appropriate cell culture media (Dulbecco's modified Eagle's medium, 10% fetal bovine serum for HEK293 and LN405; RPMI 1640, 10% fetal bovine serum for Hep-G2), in a humidified atmosphere of 5% CO₂ (Hep-G2, HEK293) or 10% CO₂ (LN405) at 37 °C. For transfection, LN405 and HEK293 cells were cultured in six-well dishes, grown until 80% confluency and transfected by incubation in a solution containing Lipofectamin2000 (Invitrogen) and the respective plasmids according to the manufacturer's manual. The solution was replaced with appropriate growth media after 5 h and cells were grown overnight.

Isolation of h-isoQC and m-isoQC

Full-length cDNA of h-isoQC was isolated from Hep-G2 cells and full-length cDNA of m-isoQC was isolated from murine thalamus (strain C57/Bl6) using RT-PCR. Briefly, total RNA of Hep-G2 and murine thalamus was isolated using the NucleoSpin[®] RNA II isolation kit (Macherey-Nagel) and reverse-transcribed by SuperScript II (Invitrogen). Subsequently, isoQCs were amplified on a 1:12.5 dilution of generated cDNA product in a 25- μl reaction with *Phusion* DNA-Polymerase (Finnzymes) using primers 1 (sense) and 2 (antisense) (Table 1) for h-isoQC and primers 3 (sense) and 4 (antisense) (Table 1) for m-isoQC. The resulting PCR products were subcloned into vector pPCRScript CAM SK (+) (Stratagene) and confirmed by sequencing.

Cloning procedure for expression of h-isoQC and hQC in mammalian cell culture

hQC and h-isoQC were inserted into vector pcDNA 3.1 (+) (Invitrogen) using the HindIII and NotI or EcoRI and NotI restriction sites, respectively. The respective PCR fragments were generated using the primers 7 (sense) and 8 (antisense) for hQC, primers 9 (sense) and 11 (antisense) for h-isoQC starting with MetI and primers 10 (sense) and 11 (antisense) for h-isoQC starting with an alternative MetII (Table 1). The cloning procedure for expression of C-terminally FLAG-tagged hQC and h-isoQC was essentially

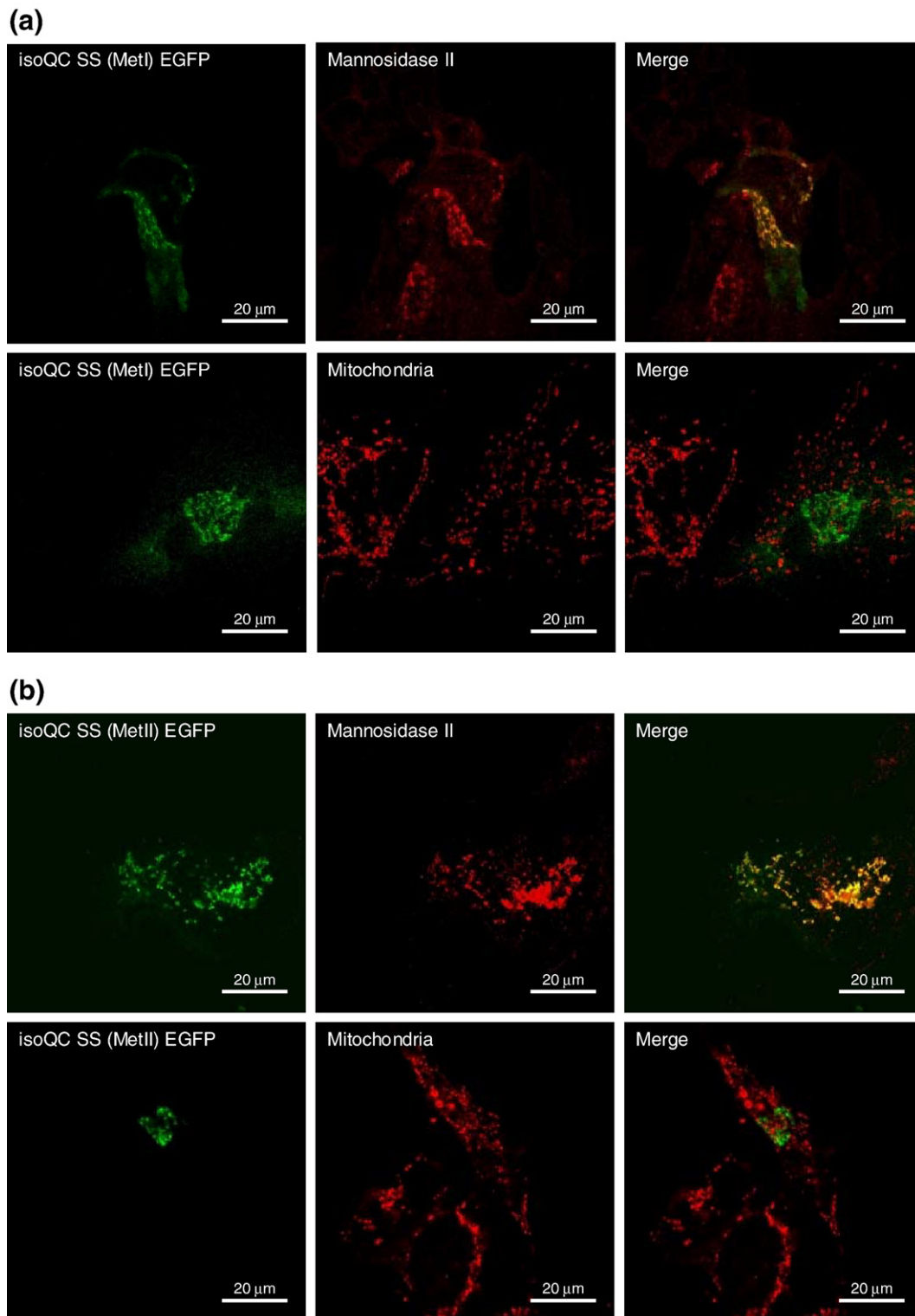


Fig. 6. Subcellular localization of h-isoQC signal sequences. (a) MetI–serine 53 and (b) MetII–serine 53 fused to EGFP. The Golgi complex was stained using an anti-mannosidase II antibody and mitochondria were stained using an antibody detecting a 65-kDA protein of human mitochondria. Co-localization is shown by superimposition of EGFP fluorescence and Red X fluorescence (Merge).

the same. Fragments were amplified using the primers 7 (sense) and 16 (antisense) for hQC, primers 9 (sense) and 17 (antisense) for h-isoQC starting with MetI and primers 10 (sense) and 17 (antisense) for h-isoQC starting with MetII (Table 1).

Cloning procedure for EGFP-tagged h-isoQC and QC

For expression of full-length h-isoQC (MetI)–EGFP and h-isoQC (MetII)–EGFP fusion protein in LN405, the vector pEGFP-N3 (Invitrogen) was applied. The cDNA of the

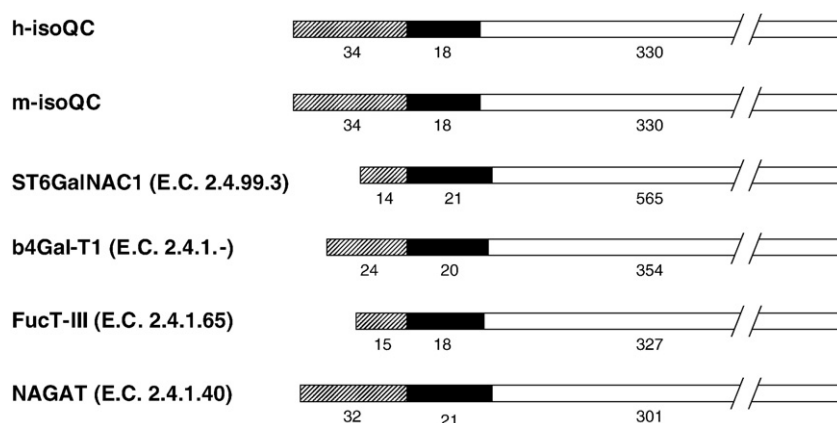


Fig. 7. Domain structure of h-isoQC and m-isoQC in comparison to published sequences of human glycosyltransferases: alpha-N-acetylgalactosaminide alpha-2,6-sialyltransferase 1 (ST6GalNAC1; E.C. 2.4.99.3); beta-1,4-galactosyltransferase 1 (b4Gal-T1, E.C. 2.4.1.-); galactoside 3 (4)-L-fucosyltransferase (FucT-III; E.C. 2.4.1.65) and glycoprotein-fucosylgalactoside alpha-N-acetylgalactosaminyl transferase (NAGAT, E.C. 2.4.1.40). The number of amino acids is listed below the columns. The cytosolic part is shaded, the signal anchor is black and the luminal part is illustrated in white.

native h-isoQC starting either at MetI or at MetII was fused C-terminally in-frame with the plasmid-encoded EGFP. The primers 9 (sense) and 12 (antisense) were used for amplification of h-isoQC starting with MetI and primers 10 (sense) and 12 (antisense) (Table 1) were used for amplification of h-isoQC starting with MetII. The fragments were inserted into vector pEGFP-N3 (Invitrogen) employing the restriction sites of EcoRI and Sall and the correct insertion was confirmed by sequencing. In addition, the EGFP sequence of vector pEGFP-N3 (Invitrogen) was introduced into vector pcDNA 3.1 (Invitrogen) using primers 13 (sense) and 14 (antisense) (Table 1) for amplification. The fragment was introduced into the XhoI site of pcDNA 3.1. The N-terminal sequences of h-isoQC beginning with MetI and II each ending at serine 53 were fused C-terminally with EGFP in vector pcDNA 3.1 using primer 9 (sense) and primer 15 (antisense) for the N-terminal fragment of h-isoQC beginning with MetI and primer 10 (sense) and primer 15 (antisense) for the N-terminal fragment of h-isoQC beginning with MetII (Table 1). Fragments were inserted into the EcoRI and NotI restriction sites of vector pcDNA 3.1. Subsequently, all vectors were isolated for cell culture purposes using the EndoFree Maxi Kit (Qiagen).

Expression and purification of h-isoQC in *E. coli* BL21

For expression of h-isoQC in *E. coli* BL21, the vector pET41a (Novagen) was used. The cDNA of the h-isoQC lacking the transmembrane region was fused in-frame with the plasmid-encoded GST tag. The amplification utilizing the primers 5 (sense) and 6 (antisense) (Table 1) introduced a C-terminal His₆ tag. After subcloning, the fragment was inserted into the expression vector employing the restriction sites of SpeI and EcoRI. The construct was transformed into *E. coli* BL21 (Stratagene) and cells were grown on selective LB agar plates at 37 °C. Protein expression was carried out in LB medium containing 1% glucose at 37 °C. After reaching an OD₆₀₀ of approximately 0.8, h-isoQC expression was induced with 20 μM IPTG for 4 h at 37 °C. Cells were separated from the medium by centrifugation (4000g, 20 min), resuspended in phosphate-buffered saline (PBS) (140 mM NaCl, 2.7 mM KCl, 10 mM Na₂HPO₄, 1.8 mM KH₂PO₄, pH 7.3) and lysed by one cycle of freezing and thawing followed by high-pressure homogenization. The cell lysate was diluted to a final volume of 1.5 l using phosphate-containing buffer (50 mM Na₂HPO₄, 500 mM NaCl, pH 7.3) and centrifuged at 13,400g at 4 °C for 1 h. The purification was initiated by Ni²⁺-IMAC

Table 2. Kinetic parameters of substrate conversion and inhibition of h-isoQC and hQC

Compound	h-isoQC				hQC	
	K_M (mM)	k_{cat} (s ⁻¹)	K_i (mM) ^a	$\frac{k_{cat}}{K_M}$ ($\times 10^3$ M ⁻¹ s ⁻¹)	$\frac{k_{cat}}{K_M}$ ($\times 10^3$ M ⁻¹ s ⁻¹)	K_i (mM) ^a
<i>Substrates</i>						
H-Gln-βNA	0.036±0.003	3.4±0.1	1.47±0.07 ^a	93±7	294±6 ^b	1.21±0.07 ^a
H-Gln-AMC	0.017±0.001	1.07±0.03	5.73±0.81 ^a	63±6	98±2 ^b	nd
H-Gln-Gln-OH	0.115±0.027	2.72±0.03		25±4	140±2 ^b	
H-Gln-Glu-OH	0.705±0.136	2.65±0.21		4±0.6	58±1 ^b	
H-Gln-Gly-OH	0.424±0.041	1.66±0.04		4±0.3	53±1 ^b	
H-Gln-Gly-Pro-OH	0.214±0.016	4.02±0.14		19±1	195±7 ^b	
<i>Inhibitors</i>						
Imidazole			0.219±0.0009			0.103±0.004 ^b
Benzimidazole			0.199±0.008			0.138±0.005 ^b
Methylimidazole			0.079±0.0047			0.030±0.001 ^b
Benzylimidazole			0.0073±0.0005			0.0071±0.0003 ^b
Cysteamine			0.068±0.0015			0.038±0.001
N-Dimethylcysteamine			0.022±0.0013			0.019±0.00005

Reactions were carried out in 0.05 mM Tris-HCl, pH 8.0, at 30 °C. nd, not determined.

^a Substrate inhibition.

^b Data from Refs. 38 and 39.

(immobilized metal-affinity chromatography) in reverse-flow direction using a Streamline SP XL column (GE Healthcare) as gel matrix. After a washing step [10 column volumes (CV)], proteins were eluted with PBS containing 100 mM histidine (1.5 CV). The h-isoQC-containing fractions were pooled and further purified using a glutathione Sepharose 4 Fast Flow (GE Healthcare) column. Bound protein was eluted with 50 mM Tris containing 10 mM reduced glutathione. Subsequently, the sample was desalted by gel filtration. Finally, cation-exchange chromatography (IEX) on a UNO S (Bio-Rad) was carried out. The h-isoQC was eluted by an increasing gradient of NaCl in 25 mM Mes (5 CV). The purified GST-h-isoQC protein was stable for months in 50% glycerol at -20°C .

QC assays

QC activity was evaluated fluorimetrically using H-Gln- β NA or H-Gln-AMC, essentially as described elsewhere.⁷ Briefly, the samples consisted of 0.2 mM fluorogenic substrate, 0.25 U pyroglutamyl aminopeptidase (Qiagen, Hilden, Germany) in 0.05 M Tris-HCl, pH 8.0, and an appropriately diluted aliquot of sample in a final volume of 250 μl . A spectrophotometric assay was used to determine the kinetic parameters for most of the QC substrates²⁷ utilizing glutamic dehydrogenase as auxiliary enzyme. Samples consisted of the respective QC substrate, 0.3 mM NADH, 14 mM α -ketoglutaric acid and 30 U/ml glutamic dehydrogenase in a final volume of 250 μl . All reactions were carried out at 30°C , using either the NovoStar (BMG Labtechnologies) or the Sunrise (TECAN) reader for microplates.

Tissue distribution

For tissue distribution studies of m-isoQC, organs from 3- to 6-month-old C57/Bl6 mice were used. The total RNA from 30 mg of each tissue was isolated and 1 μg of total RNA was reverse-transcribed using the SuperScript II (Invitrogen). The cDNA was stored at -80°C until analysis. The expression of mQC and m-isoQC was investigated using a Rotorgene3000 quantitative PCR cyclor (Corbett Research) and the QuantiTect SYBR Green PCR system (Qiagen), applying primers 18 (sense) and 19 (antisense) for mQC and primers 20 (sense) and 21 (antisense) for m-isoQC (Table 1). For quantification of the transcript concentration, a standard curve was prepared on the basis of plasmids containing the isolated cDNAs. The number of transcripts was normalized to 50 ng RNA. The specificity of primer pairs 18/19 (mQC) and 20/21 (m-isoQC) was analyzed using PCR testing various concentrations of plasmids containing mQC and m-isoQC, respectively.

Histochemical analysis

LN405 cells were grown in six-well dishes containing a coverslip. One day after transfection, cells were washed twice with D-PBS (Invitrogen) and fixed using ice-cold methanol for 10 min at -20°C , followed by three washing steps of D-PBS for 10 min at room temperature. For staining of the Golgi complex, LN405 cells were incubated with rabbit anti-mannosidase II polyclonal antibody (Chemicon) in a 1:50 dilution of antibody in D-PBS for 3 h. For staining of mitochondria, cells were incubated with mouse anti-human mitochondria monoclonal antibody (Chemicon) in a 1:100 dilution of antibody in D-PBS for 3 h at room temperature. Subsequently, the cells were washed three

times with D-PBS for 10 min. Cells stained for the Golgi complex or mitochondria were incubated with goat anti-rabbit IgG secondary antibody conjugated with Rhodamin-RedX (Dianova) or goat anti-mouse IgG secondary antibody conjugated with Rhodamin-RedX (Dianova), respectively, at room temperature in the dark for 45 min. Afterwards, the samples were washed three times with D-PBS for 5 min and the coverslips were mounted on a microscope slide with citiflour. Cells were observed with a confocal laser scanning microscope (Carl-Zeiss).

Cell fractionation

Cell fractionation was employed to characterize the sub-cellular distribution of h-isoQC activity. One day following transfection, expressing HEK293 cells were washed with D-PBS and collected by centrifugation at 500g for 5 min at 4°C . Subsequently, D-PBS was discarded and the cells were resuspended in 1 ml of homogenization buffer (50 mM Tris, 50 mM KCl, 5 mM EDTA, 2 mM MgCl_2 , pH 7.6) and cracked by 30 crushes in a Potter cell homogenizer. The suspension was centrifuged at 700g for 10 min at 4°C . The obtained pellet was resuspended in 300 μl of homogenization buffer and designated as debris fraction (d). The supernatant was further centrifuged at 20,000g for 30 min at 4°C . The pellet represented the heavy membrane (HM) fraction and was resuspended in 200 μl of homogenization buffer. The resulting supernatant was centrifuged at 100,000g for 1 h at 4°C . Again, the obtained pellet was resuspended in 200 μl of buffer and was termed as light membrane (LM) fraction. The supernatant was designated as soluble fraction (S). Debris, heavy membrane and light membrane fractions were sonicated for 10 s and the protein content was determined⁴⁹. Subsequently, fractions were analyzed for QC activity or subjected to Western blot analysis.

Immunoblotting

After cell fractionation, FLAG-tagged h-isoQC, hQC or respective marker proteins were loaded onto a Tris-glycine 4–20% gradient SDS-PAGE gel (Serva) and separated. Under semidry conditions, proteins were transferred onto a nitrocellulose membrane (Roth), which was blocked using 3% (w/v) dry milk in TBS-T [20 mM Tris/HCl (pH 7.5), 500 mM NaCl, 0.05% (v/v) Tween 20]. The FLAG tag was detected using a rabbit anti-DYKDDDDK-tag polyclonal antibody (Cell Signaling); the Golgi complex was stained using a mouse anti-ST1GAL3 polyclonal antibody (Abnova), detecting ST3 β -galactoside α -2,3-sialyltransferase 1. In addition, enrichment of mitochondria was detected by a monoclonal antibody that is directed against human mitochondria (Chemicon). Blots were developed by applying horseradish peroxidase-conjugated secondary antibodies (anti-rabbit for FLAG tag and anti-mouse for human mitochondria and ST1GAL3, Cell Signaling) and the SuperSignal West Pico System (Pierce) according to the manufacturer's protocol.

Acknowledgements

The authors are grateful to Dr. Ingo Schulz for helpful discussion and Daniel Friedrich for providing the mouse organs. The authors also thank Dr.

Steffen Rossner (Paul-Flechsig Institute for Brain Research, Leipzig) for the access to the confocal laser scanning microscope.

References

- Awade, A. C., Cleuziat, P., Gonzales, T. & Robert-Baudouy, J. (1994). Pyrrolidone carboxyl peptidase (Pcp): an enzyme that removes pyroglutamic acid (pGlu) from pGlu-peptides and pGlu-proteins. *Proteins*, **20**, 34–51.
- Blomback, B. (1967). Derivatives of glutamine in peptides. *Methods Enzymol.* **11**, 398–411.
- Abraham, G. N. & Podell, D. N. (1981). Pyroglutamic acid. Non-metabolic formation, function in proteins and peptides, and characteristics of the enzymes effecting its removal. *Mol. Cell Biochem.* **38**(Spec. No.), 181–190.
- Van Coillie, E., Proost, P., Van Aelst, I., Struyf, S., Polfliet, M., De Meester, I. *et al.* (1998). Functional comparison of two human monocyte chemotactic protein-2 isoforms, role of the amino-terminal pyroglutamic acid and processing by CD26/dipeptidyl peptidase IV. *Biochemistry*, **37**, 12672–12680.
- Messer, M. (1963). Enzymatic cyclization of L-glutamine and L-glutaminyl peptides. *Nature*, **197**, 1299.
- Pohl, T., Zimmer, M., Mugele, K. & Spiess, J. (1991). Primary structure and functional expression of a glutaminyl cyclase. *Proc. Natl Acad. Sci.* **88**, 10059–10063.
- Schilling, S., Cynis, H., von Bohlen, A., Hoffmann, T., Wermann, M., Heiser, U. *et al.* (2005). Isolation, catalytic properties, and competitive inhibitors of the zinc-dependent murine glutaminyl cyclase. *Biochemistry*, **44**, 13415–13424.
- Schilling, S., Hoffmann, T., Rosche, F., Manhart, S., Wasternack, C. & Demuth, H. U. (2002). Heterologous expression and characterization of human glutaminyl cyclase: evidence for a disulfide bond with importance for catalytic activity. *Biochemistry*, **41**, 10849–10857.
- Song, I., Chuang, C. Z. & Bateman, R. C., Jr. (1994). Molecular cloning, sequence analysis and expression of human pituitary glutaminyl cyclase. *J. Mol. Endocrinol.* **13**, 77–86.
- Schilling, S., Niestroj, A. J., Rahfeld, J. U., Hoffmann, T., Wermann, M., Zunkel, K. *et al.* (2003). Identification of human glutaminyl cyclase as a metalloenzyme. Potent inhibition by imidazole derivatives and heterocyclic chelators. *J. Biol. Chem.* **278**, 49773–49779.
- Buchholz, M., Heiser, U., Schilling, S., Niestroj, A. J., Zunkel, K. & Demuth, H. U. (2006). The first potent inhibitors for human glutaminyl cyclase: synthesis and structure–activity relationship. *J. Med. Chem.* **49**, 664–677.
- Bockers, T. M., Kreutz, M. R. & Pohl, T. (1995). Glutaminyl-cyclase expression in the bovine/porcine hypothalamus and pituitary. *J. Neuroendocrinol.* **7**, 445–453.
- Schilling, S., Lindner, C., Koch, B., Wermann, M., Rahfeld, J. U., Bohlen, A. V. *et al.* (2007). Isolation and characterization of glutaminyl cyclases from *Drosophila*: evidence for enzyme forms with different subcellular localization. *Biochemistry*, **46**(38), 10921–10930.
- Batliwalla, F. M., Baechler, E. C., Xiao, X., Li, W., Balasubramanian, S., Khalili, H. *et al.* (2005). Peripheral blood gene expression profiling in rheumatoid arthritis. *Genes Immun.* **6**(5), 388–397.
- Ezura, Y., Kajita, M., Ishida, R., Yoshida, S., Yoshida, H., Suzuki, T. *et al.* (2004). Association of multiple nucleotide variations in the pituitary glutaminyl cyclase gene (QPCT) with low radial BMD in adult women. *J. Bone Miner. Res.* **19**, 1296–1301.
- Harigaya, Y., Saido, T. C., Eckman, C. B., Prada, C. M., Shoji, M. & Younkin, S. G. (2000). Amyloid beta protein starting pyroglutamate at position 3 is a major component of the amyloid deposits in the Alzheimer's disease brain. *Biochem. Biophys. Res. Commun.* **276**, 422–427.
- Saido, T. C., Iwatsubo, T., Mann, D. M., Shimada, H., Ihara, Y. & Kawashima, S. (1995). Dominant and differential deposition of distinct beta-amyloid peptide species. A beta N3(pE), in senile plaques. *Neuron*, **14**, 457–466.
- He, W. & Barrow, C. J. (1999). The A beta 3-pyroglutamyl and 11-pyroglutamyl peptides found in senile plaque have greater beta-sheet forming and aggregation propensities *in vitro* than full-length A beta. *Biochemistry*, **38**, 10871–10877.
- Russo, C., Violani, E., Salis, S., Venezia, V., Dolcini, V., Damonte, G. *et al.* (2002). Pyroglutamate-modified amyloid beta-peptides—AbetaN3(pE)—strongly affect cultured neuron and astrocyte survival. *J. Neurochem.* **82**, 1480–1489.
- Saido, T. C. (1998). Alzheimer's disease as proteolytic disorders: anabolism and catabolism of beta-amyloid. *Neurobiol. Aging*, **19**, S69–S75.
- Saido, T. C. & Iwata, N. (2006). Metabolism of amyloid beta peptide and pathogenesis of Alzheimer's disease. Towards presymptomatic diagnosis, prevention and therapy. *Neurosci. Res.* **54**, 235–253.
- Schilling, S., Lauber, T., Schaupp, M., Manhart, S., Scheel, E., Bohm, G. & Demuth, H. U. (2006). On the seeding and oligomerization of pGlu-amyloid peptides (*in vitro*). *Biochemistry*, **45**, 12393–12399.
- Iezzi, A., Ferri, C., Mezzetti, A. & Cipollone, F. (2007). COX-2: friend or foe? *Curr. Pharm. Des.* **13**, 1715–1721.
- Thornberry, N. A. & Weber, A. E. (2007). Discovery of JANUVIA (Sitagliptin), a selective dipeptidyl peptidase IV inhibitor for the treatment of type 2 diabetes. *Curr. Top. Med. Chem.* **7**, 557–568.
- Bendtsen, J. D., Nielsen, H., von Heijne, G. & Brunak, S. (2004). Improved prediction of signal peptides: SignalP 3.0. *J. Mol. Biol.* **340**, 783–795.
- Tusnady, G. E. & Simon, I. (2001). The HMMTOP transmembrane topology prediction server. *Bioinformatics*, **17**, 849–850.
- Schilling, S., Manhart, S., Hoffmann, T., Ludwig, H. H., Wasternack, C. & Demuth, H. U. (2003). Substrate specificity of glutaminyl cyclases from plants and animals. *Biol. Chem.* **384**, 1583–1592.
- Bateman, A., Solomon, S. & Bennett, H. P. (1990). Post-translational modification of bovine pro-opiomelanocortin. Tyrosine sulfation and pyroglutamate formation, a mass spectrometric study. *J. Biol. Chem.* **265**, 22130–22136.
- Pimenta, A. M., Rates, B., Bloch, C., Jr., Gomes, P. C., Santoro, M. M., de Lima, M. E. *et al.* (2005). Electrospray ionization quadrupole time-of-flight and matrix-assisted laser desorption/ionization tandem time-of-flight mass spectrometric analyses to solve microheterogeneity in post-translationally modified peptides from *Phoneutria nigriventer* (Aranea, Ctenidae) venom. *Rapid Commun. Mass Spectrom.* **19**, 31–37.
- Schmutzler, C., Darmer, D., Diekhoff, D. & Grimmlikhuijzen, C. J. (1992). Identification of a novel type of processing sites in the precursor for the sea anemone neuropeptide Antho-RFamide (<Glu-Gly-Arg-Phe-NH₂) from *Anthopleura elegantissima*. *J. Biol. Chem.* **267**, 22534–22541.

31. Pawlak, J. & Manjunatha, K. R. (2006). Snake venom glutaminyl cyclase. *Toxicon*, **48**, 278–286.
32. Cynis, H., Schilling, S., Bodnar, M., Hoffmann, T., Heiser, U., Saido, T. C. & Demuth, H. U. (2006). Inhibition of glutaminyl cyclase alters pyroglutamate formation in mammalian cells. *Biochim. Biophys. Acta*, **1764**, 1618–1625.
33. Sykes, P. A., Watson, S. J., Temple, J. S. & Bateman, R. C., Jr. (1999). Evidence for tissue-specific forms of glutaminyl cyclase. *FEBS Lett.* **455**, 159–161.
34. Nillni, E. A. & Sevarino, K. A. (1999). The biology of pro-thyrotropin-releasing hormone-derived peptides. *Endocr. Rev.* **20**, 599–648.
35. Friedman, T. C., Loh, Y. P., Cawley, N. X., Birch, N. P., Huang, S. S., Jackson, I. M. & Nillni, E. A. (1995). Processing of prothyrotropin-releasing hormone (ProTRH) by bovine intermediate lobe secretory vesicle membrane PC1 and PC2 enzymes. *Endocrinology*, **136**, 4462–4472.
36. Nillni, E. A., Sevarino, K. A. & Jackson, I. M. (1993). Identification of the thyrotropin-releasing hormone-prohormone and its posttranslational processing in a transfected AtT20 tumoral cell line. *Endocrinology*, **132**, 1260–1270.
37. Nillni, E. A., Sevarino, K. A. & Jackson, I. M. (1993). Processing of proTRH to its intermediate products occurs before the packing into secretory granules of transfected AtT20 cells. *Endocrinology*, **132**, 1271–1277.
38. Arvan, P. & Castle, D. (1998). Sorting and storage during secretory granule biogenesis: looking backward and looking forward. *Biochem. J.* **332**(Pt 3), 593–610.
39. Dannies, P. S. (1999). Protein hormone storage in secretory granules: mechanisms for concentration and sorting. *Endocr. Rev.* **20**, 3–21.
40. Koyama, S., Sato, E., Masubuchi, T., Takamizawa, A., Nomura, H., Kubo, K. *et al.* (1998). Human lung fibroblasts release chemokinetic activity for monocytes constitutively. *Am. J. Physiol.* **275**, L223–L230.
41. Stampfer, M. R., Vlodaysky, I., Smith, H. S., Ford, R., Becker, F. F. & Riggs, J. (1981). Fibronectin production by human mammary cells. *J. Natl. Cancer Inst.* **67**, 253–261.
42. Tartakoff, A., Vassalli, P. & Detraz, M. (1978). Comparative studies of intracellular transport of secretory proteins. *J. Cell Biol.* **79**, 694–707.
43. Paulson, J. C. & Colley, K. J. (1989). Glycosyltransferases. Structure, localization, and control of cell type-specific glycosylation. *J. Biol. Chem.* **264**, 17615–17618.
44. Colley, K. J., Lee, E. U. & Paulson, J. C. (1992). The signal anchor and stem regions of the beta-galactoside alpha 2,6-sialyltransferase may each act to localize the enzyme to the Golgi apparatus. *J. Biol. Chem.* **267**, 7784–7793.
45. Masibay, A. S., Balaji, P. V., Boeggeman, E. E. & Qasba, P. K. (1993). Mutational analysis of the Golgi retention signal of bovine beta-1,4-galactosyltransferase. *J. Biol. Chem.* **268**, 9908–9916.
46. Tang, B. L., Wong, S. H., Low, S. H. & Hong, W. (1992). The transmembrane domain of N-glucosaminyltransferase I contains a Golgi retention signal. *J. Biol. Chem.* **267**, 10122–10126.
47. Ghiso, J., Revesz, T., Holton, J., Rostagno, A., Lashley, T., Houlden, H. *et al.* (2001). Chromosome 13 dementia syndromes as models of neurodegeneration. *Amyloid*, **8**, 277–284.
48. Tomidokoro, Y., Lashley, T., Rostagno, A., Neubert, T. A., Bojsen-Moller, M., Braendgaard, H. *et al.* (2005). Familial Danish dementia: co-existence of Danish and Alzheimer amyloid subunits (ADan AND A{beta}) in the absence of compact plaques. *J. Biol. Chem.* **280**, 36883–36894.
49. Bradford, M. M. (1976). A rapid and sensitive method for the quantitation of microgram quantities of protein utilizing the principle of protein-dye binding. *Anal. Biochem.* **72**, 248–254.

Amyloidogenic Processing of Amyloid Precursor Protein: Evidence of a Pivotal Role of Glutaminyl Cyclase in Generation of Pyroglutamate-Modified Amyloid- β [†]

Holger Cynis,[‡] Eike Scheel,[‡] Takaomi C. Saido,[§] Stephan Schilling,^{*,‡} and Hans-Ulrich Demuth[‡]

Probiodrug AG, Weinbergweg 22, 06120 Halle/Saale, Germany, and Laboratory for Proteolytic Neuroscience, RIKEN Brain Science Institute, 2-1 Hirosawa, Wako, Saitama 351-0198, Japan

Received February 12, 2008; Revised Manuscript Received April 29, 2008

ABSTRACT: Compelling evidence suggests that N-terminally truncated and pyroglutamyloxy-modified amyloid- β ($A\beta$) peptides play a major role in the development of Alzheimer's disease. Posttranslational formation of pyroglutamic acid (pGlu) at position 3 or 11 of $A\beta$ implies cyclization of an N-terminal glutamate residue rendering the modified peptide degradation resistant, more hydrophobic, and prone to aggregation. Previous studies using artificial peptide substrates suggested the potential involvement of the enzyme glutaminyl cyclase in generation of pGlu- $A\beta$. Here we show that glutaminyl cyclase (QC) catalyzes the formation of $A\beta_{3(pE)-40/42}$ after amyloidogenic processing of APP in two different cell lines, applying specific ELISAs and Western blotting based on urea-PAGE. Inhibition of QC by the imidazole derivative PBD150 led to a blockage of $A\beta_{3(pE)-42}$ formation. Apparently, the QC-catalyzed formation of N-terminal pGlu is favored in the acidic environment of secretory compartments, which is also supported by double-immunofluorescence labeling of QC and APP revealing partial colocalization. Finally, initial investigations focusing on the molecular pathway leading to the generation of truncated $A\beta$ peptides imply an important role of the amino acid sequence near the β -secretase cleavage site. Introduction of a single-point mutation, resulting in an amino acid substitution, APP(E599Q), i.e., at position 3 of $A\beta$, resulted in significant formation of $A\beta_{3(pE)-40/42}$. Introduction of the APP KM595/596NL "Swedish" mutation causing overproduction of $A\beta$, however, surprisingly diminished the concentration of $A\beta_{3(pE)-40/42}$. The study provides new cell-based assays for the profiling of small molecule inhibitors of QC and points to conspicuous differences in processing of APP depending on sequence at the β -secretase cleavage site.

Alzheimer's disease (AD)¹ has emerged as the major cause of dementia in the developed world, affecting approximately 20–25 million patients (1). Neurofibrillary tangles and senile plaques, which are found *post mortem* in cortical and hippocampal brain sections of AD patients, represent the major histopathological hallmarks of the disease. According to the amyloid cascade hypothesis, amyloid- β ($A\beta$) peptides, the primary components of senile plaques, are key for the development of the disease (1, 2). These $A\beta_{40/42}$ peptides are liberated sequentially by proteolysis of the amyloid precursor protein (APP) by β - and γ -secretases (3, 4). $A\beta$ undergoes a high level of turnover within the brain, and its impaired degradation is presumed to be the primary cause of $A\beta$ deposition (1, 5, 6).

It has been shown that N-terminal variants of $A\beta$ are abundant in human amyloid deposits and soluble $A\beta$. Modifications affect the aspartic acids at positions 1 and 7, which are isomerized or racemized (7–10), or the glutamic acid residues at position 3 and 11, which are found to be cyclized into pyroglutamic acid (pGlu) after liberation by peptidases. In this regard, the most prominent N-terminal variant has been identified as $A\beta_{3(pE)-42}$ (7, 11–15). The $A\beta_{3/11(pE)-40/42}$ peptides are suggested to play a crucial role in the development of AD, since deposition occurs early in AD and $A\beta_{3(pE)-40/42}$ exhibited pronounced toxicity in neuronal and glial cell cultures (14, 16). In addition, pGlu-modified $A\beta$ species exhibit an up to 250-fold accelerated initial rate of aggregation compared to that of unmodified $A\beta$, suggesting these peptides as potential seeding species for neurotoxic aggregate formation *in vivo* (17, 18). Importantly, in healthy and pathologically aged brains, profound plaque pathology without signs of dementia has been observed, which is accompanied by $A\beta_{3(pE)-42}$ at low levels (19). Finally, the occurrence of intracellular N-truncated $A\beta$ species correlates with hippocampal neuron loss in a mouse model (20), supporting a decisive role of pGlu- $A\beta$ in the development of AD.

Human glutaminyl cyclase (QC) was recently shown to convert N-terminal glutamate residues into pyroglutamic acid *in vitro* (21, 22). In the study presented here, the glutam(in)yl cyclase-mediated pGlu formation was analyzed in detail in cultures of human cell lines HEK293 and LN2308. The aim of the work was to investigate the generation of $A\beta_{3(pE)-42}$ in

[†] This work was supported by a grant from the German Federal Department of Education, Science and Technology, BMBF 0313185 to H.-U.D.

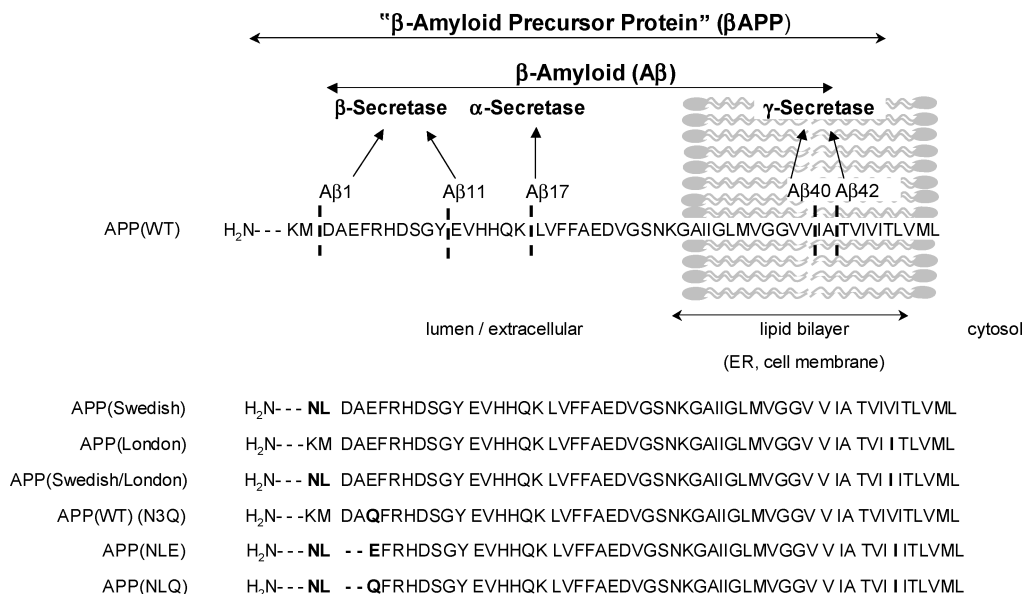
* To whom correspondence should be addressed: Probiodrug AG, Weinbergweg 22, 06120 Halle, Germany. Telephone: +49 (345) 5559900. Fax: +49 (345) 5559901. E-mail: stephan.schilling@probiodrug.de.

[‡] Probiodrug AG.

[§] RIKEN Brain Science Institute.

¹ Abbreviations: $A\beta$, β -amyloid peptide; AD, Alzheimer's disease; APP, amyloid precursor protein; ELISA, enzyme-linked immunosorbent assay; FBD, familial British dementia; FDD, familial Danish dementia; H-Gln- β NA, glutamine β -naphthylamine; PAGE, polyacrylamide gel electrophoresis; pGlu, pyroglutamic acid; QC, glutaminyl cyclase; TMB, tetramethylbenzidine; WT, wild type.

Scheme 1: APP695 constructs used in this study, including APP(WT), APP(Swedish) (KM595/596NL), APP(London) (V642I), and APP(Swedish/London) (KM595/596NL, V642I)^a



^a All APP constructs were also tested, containing additionally a N3Q mutation (E599Q). For example, APP(WT) (N3Q) is shown. For investigating glutamate cyclization by human glutaminyl cyclase, the constructs APP(NLE) (KM595/596NL, ΔD597, ΔA598, V642I) and APP(NLQ) (KM595/596NL, ΔD597, ΔA598, E599Q, V642I) were used.

mammalian cell culture by expression of APP and QC to show whether QC is capable of generating Aβ_{3(pE)-42} following amyloidogenic processing of APP. The results, thus, should provide new cell-based screening systems for small molecule QC inhibitors and validate QC inhibition as a strategy for preventing pGlu-Aβ formation.

EXPERIMENTAL PROCEDURES

Peptides. Aβ peptides were purchased from AnaSpec (San Jose, CA) or synthesized as described previously (17).

Vectors. The cDNAs of human APP695(Swedish/London), APP(NLE), and APP(NLQ) was generated as described previously (22, 23). The E599Q point mutation was introduced into the FAD- and WT-containing APP cDNAs. The cDNAs were ligated into the *NotI* site of vector pcDNA 3.1(+) (Invitrogen) (Scheme 1). Additionally, the human QC was inserted into vector pcDNA 3.1(+) using *HindIII* and *NotI* restriction sites. For generation of a human QC-EGFP fusion protein, the enhanced green fluorescent protein was inserted into the *XhoI* site of vector pcDNA 3.1(+) and subsequently fused to human QC cDNA lacking the stop codon using the *HindIII* and *NotI* sites. All constructs were confirmed by sequencing and isolated for cell culture purposes using the EndoFree Plasmid Maxi Kit (Qiagen).

Cell Culture and Transfection. Human embryonic kidney cells (HEK293) and human glioma cell line LN2308 were cultured in DMEM (10% FBS) in a humidified atmosphere of 5% CO₂ at 37 °C. Cells were transfected with APP695 variants with Lipofectamine2000 (Invitrogen), essentially as described previously (22). The next day, cells were either analyzed for APP expression using Western blotting and immunohistochemistry or incubated for 24 h in assay medium (DMEM, without phenol red, without FBS). The supernatant was collected and readily mixed with Complete Mini protease inhibitor cocktail (Roche) supplemented with additional 1 mM AEBFS (Roth)

to prevent unspecific degradation by proteases. The samples were stored at −80 °C until the assay.

Concentration of Aβ Peptides. Prior to Western blot analysis of Aβ, the conditioned media were collected. Aβ was concentrated using Hydrosart centricons (Sartorius) with a 1 kDa cutoff. For immunoprecipitation, monoclonal antibody 4G8 (Chemicon), detecting total Aβ, was added to the cell culture medium and the mixture incubated under continuous shaking for 24 h at 4 °C. The next day, sheep anti-mouse IgG dyanalbeads (Invitrogen) were added to the solution and the mixture was incubated for an additional 24 h at 4 °C. Afterward, Aβ peptides were dislodged by boiling in urea-PAGE gel buffer for 5 min and analyzed by Western blotting. For ELISA detection, the beads were incubated in a methanol/formic acid solution for 1 h. The supernatant was neutralized by addition of 200 mM phosphate buffer (pH 8.0) and EIA ELISA diluent buffer (IBL-Hamburg) and subsequently probed on the desired ELISA plate.

Western Blot Analysis. The detection of APP was performed applying Tris-glycine-PAGE as described previously (22). The electrophoretic separation of N-terminally modified Aβ peptides was carried out using 15% urea-PAGE gels (24). Proteins were transferred to a nitrocellulose membrane under semidry conditions. Subsequently, the membrane was blocked using 3% (w/v) dry milk in TBS-T [20 mM Tris-HCl (pH 7.5), 500 mM NaCl, and 0.05% (v/v) Tween 20]. APP and Aβ were detected using a polyclonal anti-APP antibody (Cell Signaling) and monoclonal anti-Aβ(1–16) antibody 6E10 (Chemicon), respectively. Pyroglutamylyl-modified Aβ was detected applying antibody 8E1 (IBL-Hamburg). For visualization, blot membranes were incubated with secondary antibodies (anti-rabbit for APP and anti-mouse for Aβ), both conjugated with horseradish peroxidase (Cell Signaling) in TBS-T containing 5% (w/v) dry milk, and subsequently developed using the SuperSignal West Pico System (Pierce) according to the manufacturer's protocol.

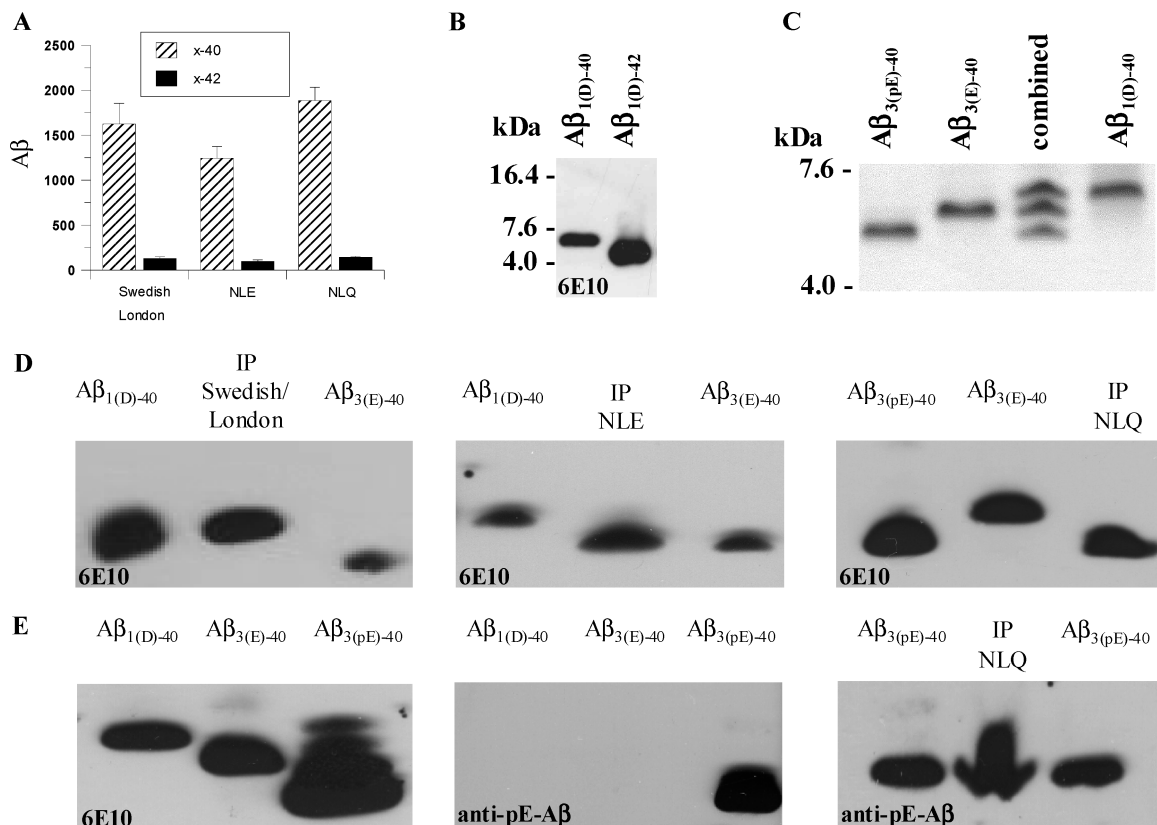


FIGURE 1: (A) Analysis of A β_{x-40} (hatched bars) and A β_{x-42} (black bars) secreted by HEK293 cells, which were transfected with APP(Swedish/London), APP(NLE), and APP(NLQ) using an ELISA detecting either A β_{x-40} or A β_{x-42} (total A β). The A β concentration was normalized to cell count (picograms per milliliter per 1×10^6 cells) ($n = 6$). (B) Urea-PAGE followed by Western blot analysis of 10 ng of A $\beta_{1(D)-40}$ in comparison to 10 ng of A $\beta_{1(D)-42}$ standard peptides. (C) Urea-PAGE followed by Coomassie staining of different N-terminal variants of A β_{40} (3 μ g each). (D) Western blot of A β species secreted by HEK293 cells expressing APP(Swedish/London), APP(NLE), and APP(NLQ) in comparison to 10 ng of standard A β peptides. (E) In addition, an antibody specific for A $\beta_{3(pE)-x}$ was implemented, showing the generation of A $\beta_{3(pE)-40}$ after expression of APP(NLQ), compared to A $\beta_{3(pE)-40}$ standard peptides (10 ng).

Immunohistochemistry. Cells were washed twice with D-PBS (Invitrogen) and fixed using ice-cold methanol for 10 min, followed by three washing steps using D-PBS for 10 min at room temperature. For staining of the Golgi complex, HEK293 cells were incubated with rabbit anti-mannosidase II polyclonal antibody (Chemicon), applying a 1:50 dilution of the antibody in D-PBS at room temperature for 3 h. For APP and A β staining, HEK293 cells were incubated at room temperature with mouse anti- β -amyloid monoclonal antibody 6E10 (Calbiochem) for 3 h using a 1:50 dilution of the antibody in D-PBS. Subsequently, the cells were washed three times with D-PBS for 10 min. The immunostained Golgi complex and APP were tagged by applying IgG secondary antibodies, which were conjugated with Rhodamin-RedX (Dianova). The samples were incubated at room temperature in the dark for 45 min. Afterward, cells were washed three times with D-PBS for 5 min at room temperature. Finally, the fixed and stained samples were mounted with citiflour and covered with a microscope slide. The cells were observed with oil immersion using a confocal laser scanning microscope (Carl-Zeiss).

Quantification of A β Peptides and QC Activity. Glutaminyll cyclase activity was measured using the substrate H-Gln- β NA as described previously (25). The assay reaction was started by addition of the QC-containing cell culture supernatant and evaluated using a Novostar reader for microplates (BMG-Labtechnologies). QC activity was determined from a standard curve of β -naphthylamine under assay conditions.

A β_{40} and A β_{42} concentrations were determined using specific sandwich ELISAs detecting total A β_{x-40} and A β_{x-42} , full-length A $\beta_{1(D)-40}$ and A $\beta_{1(D)-42}$, or the N-terminally pyroglutaminated variants A $\beta_{3(pE)-40}$ and A $\beta_{3(pE)-42}$ (all IBL-Hamburg) according to the manufacturer's instructions.

Investigation of Intracellular pGlu Formation. HEK293 cells were transfected with vector APP(NLE) alone or in combination with a vector encoding the native human QC. Additionally, HEK293 cells were transfected with APP(NLE) alone, and recombinant human QC was added to the cell culture medium. After 24 h, samples were collected and the A β concentration was determined using ELISAs.

RESULTS

Generation of A $\beta_{3(pE)-40/42}$ Peptides in Cell Culture. On the basis of several different APP constructs (Scheme 1), the N- and C-terminal heterogeneity of A β peptides generated by HEK293 cells was assessed. Expression of all APP variants led to a significant increase in the A β_{x-40} and A β_{x-42} concentration (not shown), which was in good agreement with previous findings (26, 27), suggesting that the HEK293 expression system is well-suited for analysis of A $\beta_{x-40/42}$ formation. The A β concentrations were negligible in conditioned media of untransfected or mock transfected cells.

To prove QC-mediated pGlu-A β formation occurred after amyloidogenic processing of APP, we expressed APP(Swedish/London) and its modified variants APP(NLE) and

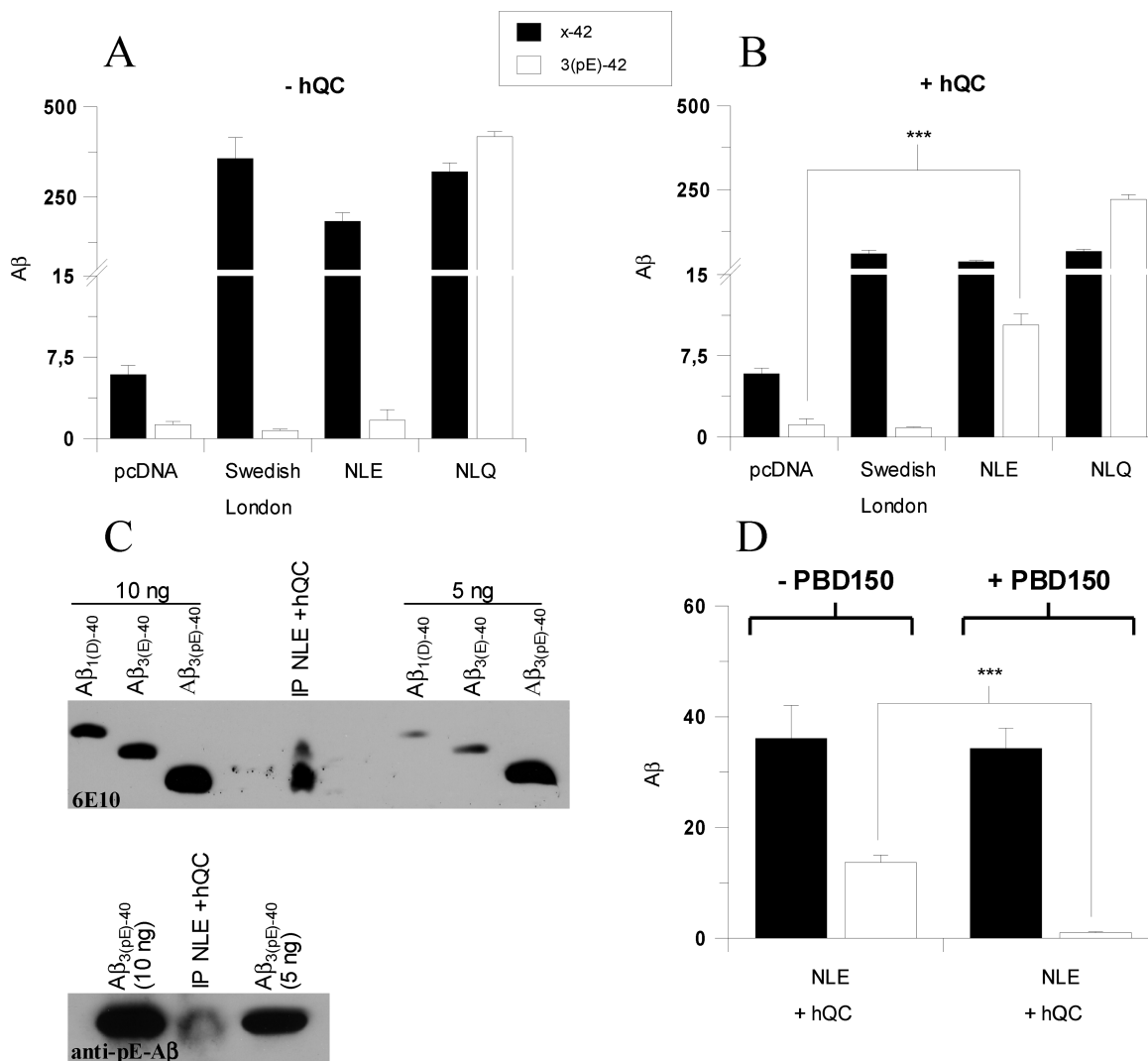


FIGURE 2: Analysis of pGlu formation after expression of vectors pcDNA, APP(Swedish/London), APP(NLE), and APP(NLQ) in HEK293 cells using an ELISA in the absence (A) or presence (B) of cotransfection with human QC. $A\beta$ concentrations were normalized to cell count (picograms per milliliter per 1×10^6 cells) (asterisks, $P < 0.001$; Student's t test; $n = 3$). (C) QC-dependent pGlu formation of APP(NLE) was corroborated using Western blot analysis detecting total- $A\beta$ (6E10) or pGlu-modified $A\beta$ (anti-pE- $A\beta$) (application in comparison to standard $A\beta$ peptides). (D) The formation of $A\beta_{3(pE)-42}$ after cotransfection of APP(NLE) with human QC was inhibited by application of the QC-specific inhibitor PBD150 ($10 \mu\text{M}$). $A\beta$ concentrations were normalized to cell count (picograms per milliliter per 1×10^6 cells) (asterisks, $P < 0.001$; Student's t test; $n = 6$).

APP(NLQ) (Scheme 1) in HEK293 cells. The processing of the latter constructs should result in rapid liberation of $A\beta_{3(E)-40/42}$ and $A\beta_{3(Q)-40/42}$, i.e., precursors of $A\beta_{3(pE)-40/42}$. The expression of APP(Swedish/London), APP(NLE), and APP(NLQ) resulted in comparable $A\beta_{x-40/42}$ concentrations in the cell culture supernatant (Figure 1A). In addition, the secreted $A\beta$ peptides were analyzed using urea-PAGE according to the method of Kalfki et al. (24), followed by Western blot analysis. In agreement with the earlier observations using urea-PAGE, $A\beta_{1(D)-42}$ migrates faster than $A\beta_{1(D)-40}$ (Figure 1B). Furthermore, the method enables the separation of $A\beta_{1(D)-40}$, $A\beta_{3(E)-40}$, and $A\beta_{3(pE)-40}$ (Figure 1C). According to the Western blot analysis, the expression of APP(Swedish/London) led to $A\beta$ peptides starting with aspartate 1 [$A\beta_{1(D)-40/42}$]. In contrast, transfection of APP(NLE) resulted primarily in $A\beta_{3(E)-40/42}$, as revealed by the faster migration in urea-PAGE, whereas the transfection of APP(NLQ) exclusively generated $A\beta_{3(pE)-40/42}$ (Figure 1D). The dominant formation of $A\beta_{3(pE)}$ by expression of APP(NLQ) is most likely caused by rapid QC-catalyzed cycliza-

tion of $A\beta_{3(Q)-40/42}$, possibly accompanied by spontaneous cyclization of glutamine (Figure 1E) (22, 23). In conclusion, the results suggest that β - and γ -secretase appropriately process the APP variants APP(NLE) and APP(NLQ).

$A\beta_{3(pE)}$ Formation Is Catalyzed by QC. Since the expression of APP(Swedish/London) and its derivatives APP(NLE) and APP(NLQ) led to the secretion of $A\beta$ peptides starting with distinct N-terminal amino acids (aspartic acid, glutamic acid, or glutamine), these vectors were analyzed for $A\beta_{x-40/42}$ and $A\beta_{3(pE)-40/42}$ generation after transfection into HEK293 cells. Again, expression of APP(Swedish/London), APP(NLE), and APP(NLQ) resulted in generation of $A\beta_{x-40/42}$ peptides, but significant $A\beta_{3(pE)-40/42}$ formation could be detected only in the case of APP(NLQ), which is catalyzed by endogenous QC, present in HEK293 cells (22) (Figures 1E and 2A). However, formation of $A\beta_{3(pE)-42}$ was observed after cotransfection of APP(NLE) with human QC (Figure 2B). This finding was further corroborated by Western blot analysis after immunoprecipitation of $A\beta$ peptides from the cell culture supernatant of HEK293 cells coexpressing

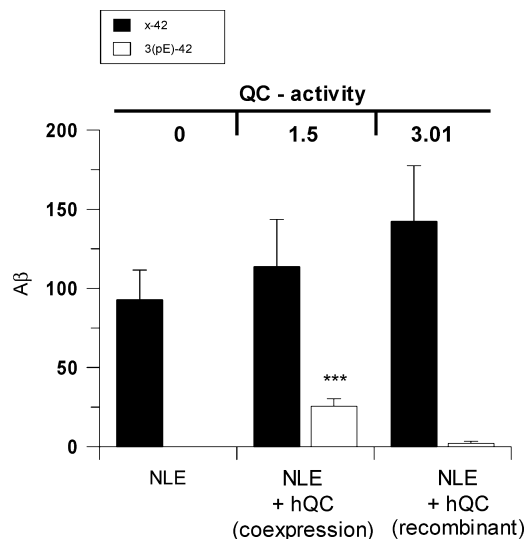


FIGURE 3: Determination of QC-dependent intracellular and extracellular A $\beta_{3(pE)-42}$ formation in HEK293 cells. Expression of APP(NLE) in the absence or presence of coexpression with native human QC or expression of APP(NLE) and subsequent application of recombinant human QC to the cell culture medium. Determination of the amount of A β_{x-42} (black bars) and A $\beta_{3(pE)-42}$ (white bars) by an ELISA. QC activity (in micromolar per minute per 1×10^6 cells) was measured using a fluorescence assay (asterisks, $P < 0.001$; Student's t test; $n = 6$).

APP(NLE) and human QC (Figure 2C). The detection of A $\beta_{3(pE)-42}$ after cotransfection of APP(NLE) and human QC typically resulted in 5–20% pGlu formation at the N-terminus of A β (Figure 2B, replication not shown). Interestingly, if the A β peptides were immunoprecipitated, the

A $\beta_{3(pE)}$ band was more prominent than the unmodified A $\beta_{3(E)}$ signal, when using antibody 6E10 for detection. However, when the anti-pE-A β antibody was applied, a rather weak pGlu-A β signal was obtained (Figure 2C).

In an accompanying experiment, the efficacy of the QC inhibitor PBD150 in suppressing the formation of A $\beta_{3(pE)}$ was evaluated. Therefore, APP(NLE) and human QC were coexpressed in the absence and presence of 10 μ M PBD150. The inhibitor did not affect the secretion of total A β_{x-42} . However, the extent of A $\beta_{3(pE)-42}$ generation was significantly lower, when PBD150 was applied (Figure 2D).

QC-Dependent A $\beta_{3(pE)}$ Formation Is Favored Intracellularly. Previous investigations of the pH dependency of QC-catalyzed cyclization of glutamic acid in vitro revealed an optimum under mildly acidic conditions. Localizing the environment under which the cyclization occurs in the cell-based system was another goal. Cotransfection of APP(NLE) with human QC led to N-terminal cyclization of glutamate and, because of secretion of the enzyme, to an increased QC activity within the cell culture medium (not shown). Therefore, there was a need for elucidation of whether an intracellular colocalization of human QC and APP(NLE) was required for A $\beta_{3(pE)}$ formation or the QC activity within the medium was responsible. The APP(NLE) construct was expressed either singly or in combination with human QC. In parallel samples, recombinant human QC (28) was applied to the culture medium of cells expressing APP(NLE) to clarify whether extracellular QC activity contributes to the glutamate cyclization. As expected, the single expression of APP(NLE) led only to the detection of A β_{x-42} . In contrast, cotransfection of APP(NLE) with human QC resulted in

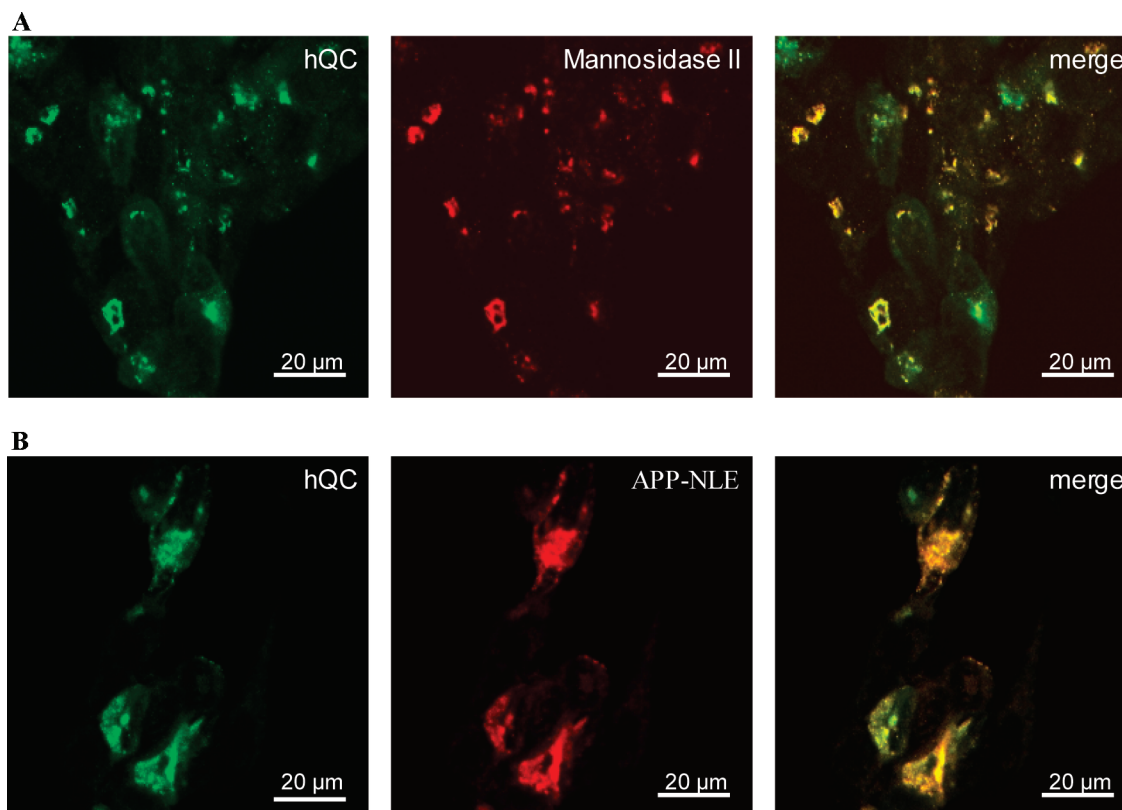


FIGURE 4: (A) Immunohistochemical staining of Mannosidase II (red) in HEK293 cells for identification of the Golgi zone and comparison to the expression pattern obtained with the hQC-EGFP fusion protein (green) in HEK293. An overlay of hQC and Mannosidase II suggests colocalization within the Golgi zone (merge). (B) Expression of hQC-EGFP protein (green) and APP(NLE) (red) in HEK293 cells. An overlay of hQC and APP(NLE) suggests a colocalization at least within the Golgi compartment (merge).

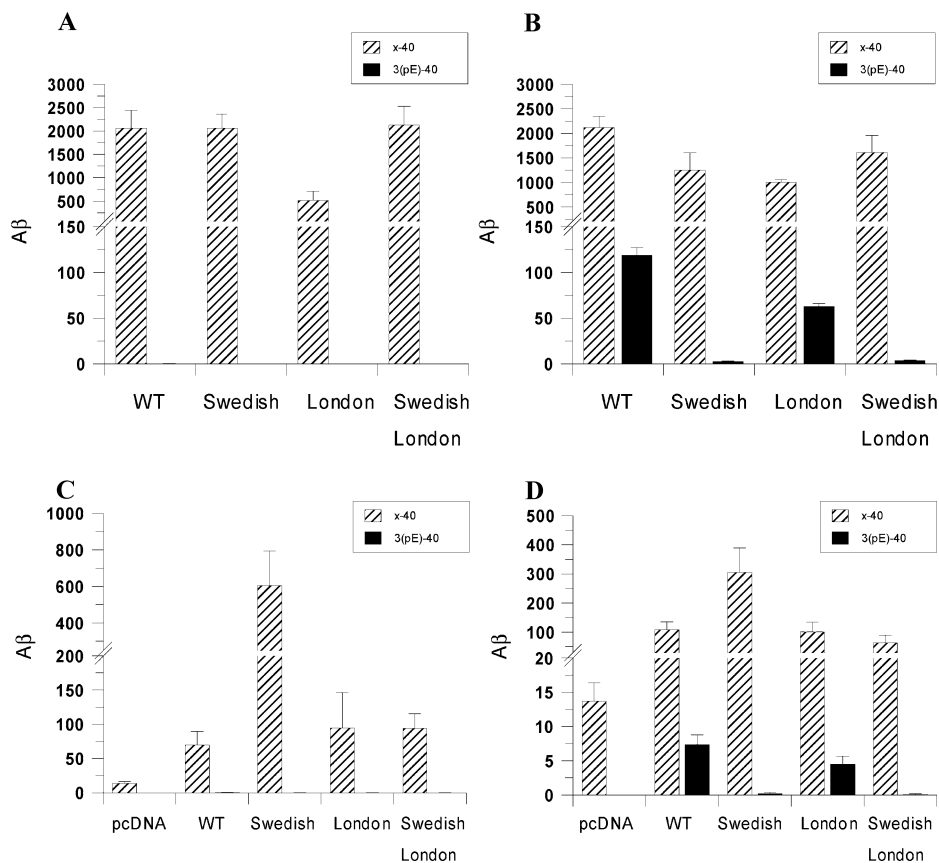


FIGURE 5: N-Terminal variants generated by the expression of FAD mutants and APP(WT) in HEK293 cells (A and B) and LNZ308 cells (C and D). The formation of $A\beta_{3(pE)-40}$ was investigated in the absence (A and C) and presence (B and D) of an E599Q (N3Q) mutation. The $A\beta$ concentration was determined using ELISAs specific for $A\beta_{x-40}$ and $A\beta_{3(pE)-40}$ and normalized to cell count (picograms per milliliter per 1×10^6 cells).

formation of $A\beta_{3(pE)-42}$. Furthermore, the addition of recombinant human QC to the cell culture medium of APP(NLE)-expressing cells generated only minor amounts of $A\beta_{3(pE)-42}$ compared to the human QC cotransfection (Figure 3). The determination of QC activity after incubation for 24 h on the cells showed a 2-fold higher activity, when recombinant QC was applied, in comparison to the coexpression of APP(NLE) and human QC. This result supports the assumption that cyclization of glutamate is favored in intracellular compartments. This was further substantiated by an immunohistochemical analysis of the subcellular distribution of human QC and APP(NLE) in HEK293 cells. A cDNA construct was generated encoding human QC, which was fused to the enhanced green fluorescent protein (EGFP). The expression of the QC-EGFP fusion protein led to a vesicular staining within the expressing cells. HEK293 cells were counterstained using an anti-Mannosidase II antibody as a marker protein for the Golgi complex. Superimpositions of the resulting images show that human QC colocalizes within the Golgi complex with Mannosidase II, substantiating the localization of QC in the secretory compartments (Figure 4A). Coexpression of human QC-EGFP fusion protein with APP(NLE) clearly supports partial colocalization in the secretory pathway, as revealed by a counterstaining with anti- β -amyloid antibody 6E10 (Figure 4B).

Formation of N-Truncated $A\beta$ Peptides Is Influenced by the β -Secretase Cleavage Site. The removal of the dipeptide Asp-Ala from the N-terminus of $A\beta_{1(D)-x}$ must precede the formation of $A\beta_{3(pE)}$ in vivo. It remains unclear whether the

pGlu precursor $A\beta_{3(E)}$ is sequentially liberated by β -secretase and an aminopeptidase or is generated directly by endoproteolysis of APP by a yet unknown mechanism. The impact of FAD mutations on the N-terminal composition of $A\beta$ peptides was investigated using ELISAs, which discriminate between intact N-terminal $A\beta_{1(D)-40/42}$ or N-truncated $A\beta_{x-40/42}$ peptides. Introduction of the KM595/596NL Swedish mutation into the APP695 sequence led preferentially to the generation of $A\beta$ molecules possessing an intact N-terminus. However, the K595/M596 WT sequence at the β -secretase cleavage site produced prominent amounts of $A\beta$ peptides differing from $A\beta_{1(D)}$ at the N-terminus. Only 21% of $A\beta_{x-40}$ corresponded to $A\beta_{1(D)-40}$ and 46% of $A\beta_{x-42}$ to $A\beta_{1(D)-42}$, if APP(WT) was expressed. In contrast, the Swedish mutation within the APP sequence provoked generation of $A\beta$ peptides with an intact N-terminus (not shown).

To investigate the influence of the β -cleavage on $A\beta_{3(pE)-42}$ formation, we introduced a novel E599Q (N3Q) point mutation into APP(WT), APP(Swedish), APP(London), and APP(Swedish/London), allowing the sensitive and specific detection of $A\beta$ species, which are N-terminally truncated. Upon N-terminal cleavage, glutamine is readily cyclized to pGlu as observed with the APP(NLQ) construct (Figure 2A,B). Thus, the N3Q mutation within the applied FAD-APP mutants and APP(WT) serves as a monitoring mutation for the generation of N-truncated $A\beta$ peptides starting with a pGlu residue in position 3. All APP variants were expressed in the absence (Figure 5A,C) and presence (Figure 5B,D) of the N3Q mutation in HEK293 cells (Figure 5A,B) and

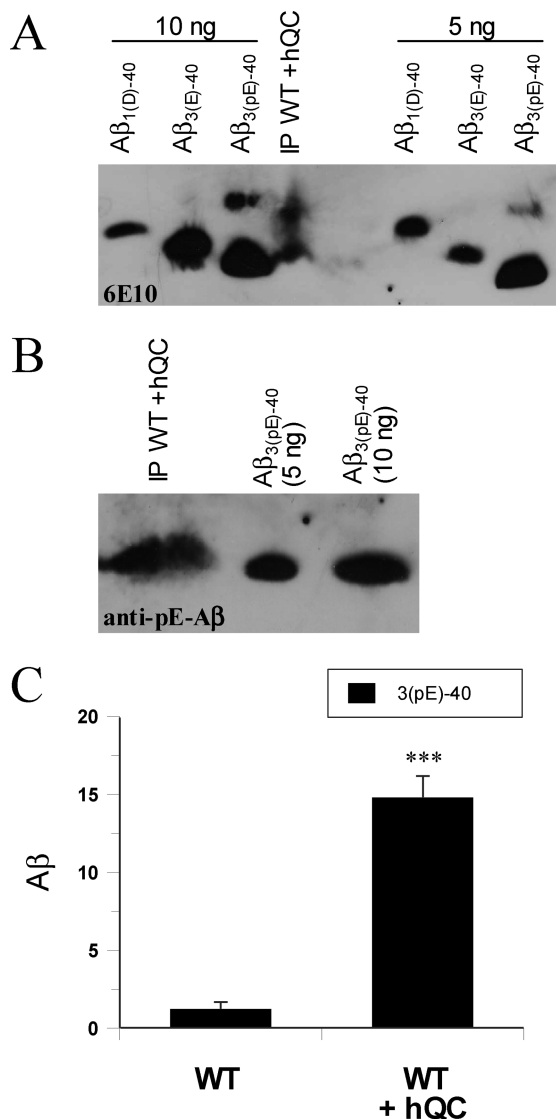


FIGURE 6: QC-dependent pGlu formation of APP(WT) was investigated by Western blotting after immunoprecipitation of A β peptides (application in comparison to standard A β peptides) using antibody 6E10, detecting total-A β (A) and antibody detecting pGlu-modified A β (B). (C) QC-dependent pGlu formation investigated using an ELISA after concentration of A β -containing cell media using centrifugal devices [single transfection of APP(WT) or cotransfection of APP(WT) with hQC] (A β concentration in picograms per milliliter) (asterisks, $P < 0.001$; Student's t test; $n = 5$).

LNZ308 cells (Figure 5C,D). The cell culture medium was analyzed for potential A $\beta_{3(pE)-40}$ formation. Intriguingly, the expression of APP variants containing the N3Q mutation led only in the case of APP(WT) and APP(London) to significant amounts of A $\beta_{3(pE)-40}$, whereas the presence of the Swedish mutation resulted only in scarce amounts of A $\beta_{3(pE)-40}$. This result was also observed when A $\beta_{3(pE)-42}$ was analyzed, pointing to differences in the liberation of A β peptides from APP molecules bearing the APP(WT) and APP(Swedish) sequence at the β -secretase cleavage site.

These significant differences in the liberation of N-truncated A β peptides prompted us to investigate the formation of A $\beta_{3(pE)}$ from APP(WT). As described for the APP(NLE) construct, cotransfection of APP(WT) and human QC was implemented to facilitate the formation of A $\beta_{3(pE)}$. On the basis of the urea-PAGE Western blot analysis, two different A β forms were detected (Figure 6A). The lower

band corresponds to A $\beta_{3(pE)-40}$, whereas the upper band migrates slower than A $\beta_{1(D)-40}$, again suggesting an N-terminus differing from that of full-length A β , observed for APP(WT) expression. In addition, the results obtained by IP-Western blot analysis were validated by application of a pGlu-specific antibody (Figure 6B) and by concentration of the supernatant in centrifugal devices, followed by an ELISA, revealing significant A $\beta_{3(pE)-40}$ formation after cotransfection of APP(WT) and human QC (Figure 6C).

DISCUSSION

The A β peptides of amyloid deposits in brains of patients with Alzheimer's disease display a profound N- and C-terminal heterogeneity (7, 11, 29). Cleavage of γ -secretase causes primarily the C-terminal differences. Because neuritic plaques are mainly composed of A β_{42} , and the deposition of A β_{42} precedes that of A β_{40} , A β_{42} is thought to be more amyloidogenic than A β_{40} (27, 30). The role and formation of N-terminal modifications, however, are more poorly understood. In particular, it is known that truncated A β peptides possessing a pGlu residue at the N-terminus are highly abundant in affected brains of patients with Alzheimer's disease and Down syndrome (11, 12, 14). Furthermore, the amyloidogenic peptides ABri in familial British dementia (FBD) and ADan in familial Danish dementia (FDD) possess an N-terminal pGlu residue, and pGlu formation appears to be crucial for the deposition of the ADan peptides in vivo (31, 32). Moreover, these pGlu-modified peptides have been shown to seed the aggregation of A $\beta_{1(D)-42}$ (17). Therefore, the prevention of pGlu formation might represent a new concept for the causal treatment of Alzheimer's disease and other pGlu-related amyloidoses.

However, the generation of pGlu peptides in AD, FBD, and FDD remained elusive, leaving room for speculation about their generation. In addition, despite evidence of an early role of pGlu-A β in the development of Alzheimer's disease, the formation of pGlu-A β peptides is frequently considered as a spontaneous secondary reaction occurring late in the progression of the disease (33). It should be noted that the uncatalyzed cyclization of N-terminal glutamic acid occurs exceptionally slowly, with half-lives of years to decades under in vivo conditions (43, 44). In addition, since A β anabolism and catabolism make up a homeostasis showing a high rate of daily turnover, it is conceivable to assume an enzyme-catalyzed formation of pGlu-A β peptides. On the basis of artificial peptide substrates, recent in vitro studies provided the first evidence that glutamate cyclization at the N-terminus of A β might be due to catalysis of QC (21, 22). These results are highlighted here by the proof that the formation of A $\beta_{3(pE)-40/42}$ from glutamate occurs after amyloidogenic processing of APP. Most importantly, we describe for the first time the generation of A $\beta_{3(pE)}$ after expression of APP(WT), which is present in the vast majority of all AD cases, substantiating the assumption that QC might be a novel drug target for the treatment of pGlu-related amyloidoses.

According to the previous investigations of substrate specificity, the QC-catalyzed cyclization of glutamate requires a protonated γ -carboxyl group and an unprotonated α -amino group. The highest concentrations of these species are found under mildly acidic conditions around pH 6.0 (21). Similar pH conditions have been described for the secretory compartments

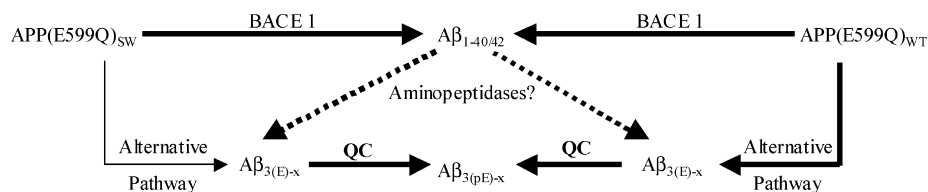


FIGURE 7: Proposed mechanism for the generation of N-terminally truncated Aβ peptides. Aβ is naturally liberated by N-terminal proteolysis due to BACE I, leading to Aβ_{1(D)-40/42}. This full-length Aβ species can be truncated by aminopeptidases. However, significant differences were observed for the generation of Aβ_{3(pE)-x} between APP(E599Q)_{WT} and APP(E599Q)_{SW}. Obviously, an alternative pathway exists, which is more pronounced for the APP(E599Q)_{WT} variant. This leads to the generation of N-truncated Aβ_{3(E)-x} species, which can be further cyclized by QC to obtain Aβ_{3(pE)-x}. Whether the alternative pathway represents different subcellular sites of BACE I-mediated Aβ liberation or a BACE I-independent mechanism has to be further addressed.

(37). As summarized in Figure 4, APP and QC are colocalized at least within the Golgi complex, where a spatially high concentration of both QC and Aβ or the respective β-CTFs can be expected (34–36). In this regard, these data suggest that the colocalization of QC and Aβ enhances pGlu-Aβ formation (Figure 3) and further support a catalyzed generation of this peptide species. In addition, the accumulation of pGlu-Aβ might also contribute to the intracellular aggregation of Aβ, which is frequently detected in patients with Down syndrome and Alzheimer's disease (38–41), in terms of generating the initial insoluble seeds for further Aβ deposition. The seeding capability of pGlu-Aβ was recently investigated *in vitro*, supporting the possibility that pGlu-Aβ can initiate seeding of full-length Aβ peptides (17).

Although these results strongly imply a QC-catalyzed formation of Aβ_{3(pE)}, a molecular pathway of APP processing leading finally to the substrate Aβ_{3(E)-x} has never been investigated in detail. To examine the generation of Aβ_{3(pE)} from APP processing, we introduced a novel monitoring mutation [APP(E599Q)], which leads to instant pGlu formation following the release of the N-terminal amino acids of Aβ. Intriguingly, the results suggest that the WT sequence at the β-secretase cleavage results in the production of N-truncated Aβ species, whereas the Swedish mutation leads preferentially to full-length Aβ_{1(D)-x} peptides (Figure 7). Apparently, the endoproteolytic processing of APP(WT) and APP(Swedish) by β-secretase differs not only in our analyzed model system. Data from studies in transgenic animals overexpressing the APP(Swedish) mutation, e.g., Tg2576, have revealed conspicuous differences with regard to the Aβ composition (42). AD patients display up to 50% of pGlu-Aβ deposited as an early Aβ species. These mouse models, in stark contrast, show only minor amounts of pGlu-Aβ [up to 0.5% (unpublished data)] occurring late in the life span of Tg2576 (12–15 months of age) (S. Schilling et al., manuscript in preparation). Most intriguingly, Tg2576 shows only mild, if any, cognitive deficits, whereas animal models accumulating larger amounts of pGlu-Aβ display strong cognitive decline and hippocampal neuron loss (20).

In conclusion, the data presented here provide for the first time evidence that (i) cyclization of glutamic acid generating Aβ_{3(pE)-40/42} is facilitated by QC after amyloidogenic processing of APP, (ii) the localization of QC and APP and the significant formation of Aβ_{3(pE)-40/42} after coexpression point to a primarily intracellular pGlu generation, and (iii) the generation of N-truncated Aβ, accounting for the majority of Aβ in AD and DS, is possibly mediated by an alternative pathway of APP processing. The latter result is reflected in the unexpected finding of tremendous Aβ_{3(pE)-40/42} formation in an APP(E599Q) variant, suggesting that the WT sequence

at the β-cleavage site leads to Aβ molecules that are prone to cyclization by QC (Figure 7).

The results thus strongly imply that the majority of the pGlu peptides deposited in AD and DS brains are formed by enzymatic catalysis following processing of APP(WT). QC activity, mediated by the neurotoxic potential of Aβ_{3(pE)-40/42}, might be involved in the first intracellular events of the amyloid cascade, potentially driving the aggregation process of Aβ. The enhanced aggregation propensity and stability of pyroglutamated Aβ, in turn, might trigger the aggregation of other Aβ species, which are generated by β- and γ-secretase at higher levels. Accordingly, the prevention of pGlu-Aβ formation might represent a novel concept for a causal treatment of Alzheimer's disease.

ACKNOWLEDGMENT

We thank Dr. Torsten Hoffmann for helpful discussion and Anett Stephan for technical assistance. We also thank Dr. Steffen Rossner (Paul-Flechsig Institut for Brain Research, Leipzig, Germany) for the access to the laser-scanning microscope. The help of Jan Eggert in critically reading the manuscript is also gratefully acknowledged.

REFERENCES

- Saido, T. C., and Iwata, N. (2006) Metabolism of amyloid β peptide and pathogenesis of Alzheimer's disease. Towards presymptomatic diagnosis, prevention and therapy. *Neurosci. Res.* 54, 235–253.
- Selkoe, D. J. (2001) Alzheimer's disease: Genes, proteins, and therapy. *Physiol. Rev.* 81, 741–766.
- Esler, W. P., and Wolfe, M. S. (2001) A portrait of Alzheimer secretases: New features and familiar faces. *Science* 293, 1449–1454.
- Haass, C., Schlossmacher, M. G., Hung, A. Y., Vigo-Pelfrey, C., Mellon, A., Ostaszewski, B. L., Lieberburg, I., Koo, E. H., Schenk, D., Teplow, D. B., and Selkoe, D. J. (1992) Amyloid β-peptide is produced by cultured cells during normal metabolism. *Nature* 359, 322–325.
- El Mouedden, M., Vandermeeren, M., Meert, T., and Mercken, M. (2006) Reduction of Aβ levels in the Sprague Dawley rat after oral administration of the functional γ-secretase inhibitor, DAPT: A novel non-transgenic model for Aβ production inhibitors. *Curr. Pharm. Des.* 12, 671–676.
- Saido, T. C. (1998) Alzheimer's disease as proteolytic disorders: Anabolism and catabolism of β-amyloid. *Neurobiol. Aging* 19, S69–S75.
- Saido, T. C., Yamao-Harigaya, W., Iwatsubo, T., and Kawashima, S. (1996) Amino- and carboxyl-terminal heterogeneity of β-amyloid peptides deposited in human brain. *Neurosci. Lett.* 215, 173–176.
- Sergeant, N., Bombois, S., Ghestem, A., Drobecq, H., Kostanjevecki, V., Missiaen, C., Watzet, A., David, J. P., Vanmechelen, E., Sergheraert, C., and Delacourte, A. (2003) Truncated β-amyloid peptide species in pre-clinical Alzheimer's disease as new targets for the vaccination approach. *J. Neurochem.* 85, 1581–1591.
- Jarrett, J. T., Berger, E. P., and Lansbury, P. T., Jr. (1993) The carboxy terminus of the β amyloid protein is critical for the seeding

- of amyloid formation: Implications for the pathogenesis of Alzheimer's disease. *Biochemistry* 32, 4693–4697.
10. Roher, A. E., Palmer, K. C., Yurewicz, E. C., Ball, M. J., and Greenberg, B. D. (1993) Morphological and biochemical analyses of amyloid plaque core proteins purified from Alzheimer disease brain tissue. *J. Neurochem.* 61, 1916–1926.
 11. Saido, T. C., Iwatsubo, T., Mann, D. M., Shimada, H., Ihara, Y., and Kawashima, S. (1995) Dominant and differential deposition of distinct β -amyloid peptide species, A β N3(pE), in senile plaques. *Neuron* 14, 457–466.
 12. Russo, C., Saido, T. C., DeBusk, L. M., Tabaton, M., Gambetti, P., and Teller, J. K. (1997) Heterogeneity of water-soluble amyloid β -peptide in Alzheimer's disease and Down's syndrome brains. *FEBS Lett.* 409, 411–416.
 13. Russo, C., Salis, S., Dolcini, V., Venezia, V., Song, X. H., Teller, J. K., and Schettini, G. (2001) Amino-terminal modification and tyrosine phosphorylation of carboxy-terminal fragments of the amyloid precursor protein in Alzheimer's disease and Down's syndrome brain. *Neurobiol. Dis.* 8, 173–180.
 14. Hosoda, R., Saido, T. C., Otvos, L., Arai, T., Mann, D. M., Lee, V. M., Trojanowski, J. Q., and Iwatsubo, T. (1998) Quantification of modified amyloid β peptides in Alzheimer disease and Down syndrome brains. *J. Neuropathol. Exp. Neurol.* 57, 1089–1095.
 15. Harigaya, Y., Saido, T. C., Eckman, C. B., Prada, C. M., Shoji, M., and Younkin, S. G. (2000) Amyloid β protein starting pyroglutamate at position 3 is a major component of the amyloid deposits in the Alzheimer's disease brain. *Biochem. Biophys. Res. Commun.* 276, 422–427.
 16. Russo, C., Violani, E., Salis, S., Venezia, V., Dolcini, V., Damonte, G., Benatti, U., D'Arrigo, C., Patrone, E., Carlo, P., and Schettini, G. (2002) Pyroglutamate-modified amyloid β -peptides—A β N3-(pE)—strongly affect cultured neuron and astrocyte survival. *J. Neurochem.* 82, 1480–1489.
 17. Schilling, S., Lauber, T., Schupp, M., Manhart, S., Scheel, E., Bohm, G., and Demuth, H. U. (2006) On the seeding and oligomerization of pGlu-amyloid peptides (in vitro). *Biochemistry* 45, 12393–12399.
 18. He, W., and Barrow, C. J. (1999) The A β 3-pyroglutamy and 11-pyroglutamyl peptides found in senile plaque have greater β -sheet forming and aggregation propensities in vitro than full-length A β . *Biochemistry* 38, 10871–10877.
 19. Piccini, A., Russo, C., Gliozzi, A., Relini, A., Vitali, A., Borghi, R., Giliberto, L., Armirotti, A., D'Arrigo, C., Bachi, A., Cattaneo, A., Canale, C., Torrassa, S., Saido, T. C., Markesbery, W., Gambetti, P., and Tabaton, M. (2005) β -Amyloid is different in normal aging and in Alzheimer's disease. *J. Biol. Chem.* 280, 34186–34192.
 20. Casas, C., Sergeant, N., Itier, J. M., Blanchard, V., Wirths, O., van der, K. N., Vingtdeux, V., van de, S. E., Ret, G., Canton, T., Drobecq, H., Clark, A., Bonici, B., Delacourte, A., Benavides, J., Schmitz, C., Tremp, G., Bayer, T. A., Benoit, P., and Pradier, L. (2004) Massive CA1/2 neuronal loss with intraneuronal and N-terminal truncated A β 42 accumulation in a novel Alzheimer transgenic model. *Am. J. Pathol.* 165, 1289–1300.
 21. Schilling, S., Hoffmann, T., Manhart, S., Hoffmann, M., and Demuth, H. U. (2004) Glutaminyll cyclases unfold glutamyl cyclase activity under mild acid conditions. *FEBS Lett.* 563, 191–196.
 22. Cynis, H., Schilling, S., Bodnar, M., Hoffmann, T., Heiser, U., Saido, T. C., and Demuth, H. U. (2006) Inhibition of glutaminyll cyclase alters pyroglutamate formation in mammalian cells. *Biochim. Biophys. Acta* 1764, 1618–1625.
 23. Shirovani, K., Tsubuki, S., Lee, H. J., Maruyama, K., and Saido, T. C. (2002) Generation of amyloid β peptide with pyroglutamate at position 3 in primary cortical neurons. *Neurosci. Lett.* 327, 25–28.
 24. Klafki, H. W., Wiltfang, J., and Staufenbiel, M. (1996) Electrophoretic separation of β A4 peptides (1–40) and (1–42). *Anal. Biochem.* 237, 24–29.
 25. Schilling, S., Hoffmann, T., Wermann, M., Heiser, U., Wasternack, C., and Demuth, H. U. (2002) Continuous spectrometric assays for glutaminyll cyclase activity. *Anal. Biochem.* 303, 49–56.
 26. Citron, M., Oltersdorf, T., Haass, C., McConlogue, L., Hung, A. Y., Seubert, P., Vigo-Pelfrey, C., Lieberburg, I., and Selkoe, D. J. (1992) Mutation of the β -amyloid precursor protein in familial Alzheimer's disease increases β -protein production. *Nature* 360, 672–674.
 27. Suzuki, N., Cheung, T. T., Cai, X. D., Odaka, A., Otvos, L., Jr., Eckman, C., Golde, T. E., and Younkin, S. G. (1994) An increased percentage of long amyloid β protein secreted by familial amyloid β protein precursor (β APP717) mutants. *Science* 264, 1336–1340.
 28. Schilling, S., Hoffmann, T., Rosche, F., Manhart, S., Wasternack, C., and Demuth, H. U. (2002) Heterologous expression and characterization of human glutaminyll cyclase: Evidence for a disulfide bond with importance for catalytic activity. *Biochemistry* 41, 10849–10857.
 29. Kuo, Y. M., Emmerling, M. R., Woods, A. S., Cotter, R. J., and Roher, A. E. (1997) Isolation, chemical characterization, and quantitation of A β 3-pyroglutamyl peptide from neuritic plaques and vascular amyloid deposits. *Biochem. Biophys. Res. Commun.* 237, 188–191.
 30. Iwatsubo, T., Odaka, A., Suzuki, N., Mizusawa, H., Nukina, N., and Ihara, Y. (1994) Visualization of A β 42(43) and A β 40 in senile plaques with end-specific A β monoclonals: Evidence that an initially deposited species is A β 42(43). *Neuron* 13, 45–53.
 31. Tomidokoro, Y., Lashley, T., Rostagno, A., Neubert, T. A., Bojsen-Moller, M., Braendgaard, H., Plant, G., Holton, J., Frangione, B., Revesz, T., and Ghiso, J. (2005) Familial Danish dementia: Co-existence of Danish and Alzheimer amyloid subunits (ADan AND A β) in the absence of compact plaques. *J. Biol. Chem.* 280, 36883–36894.
 32. Ghiso, J., Revesz, T., Holton, J., Rostagno, A., Lashley, T., Houlden, H., Gibb, G., Anderton, B., Bek, T., Bojsen-Moller, M., Wood, N., Vidal, R., Braendgaard, H., Plant, G., and Frangione, B. (2001) Chromosome 13 dementia syndromes as models of neurodegeneration. *Amyloid* 8, 277–284.
 33. Hashimoto, T., Wakabayashi, T., Watanabe, A., Kowa, H., Hosoda, R., Nakamura, A., Kanazawa, I., Arai, T., Takio, K., Mann, D. M., and Iwatsubo, T. (2002) CLAC: A novel Alzheimer amyloid plaque component derived from a transmembrane precursor, CLAC-P/collagen type XXV. *EMBO J.* 21, 1524–1534.
 34. Greenfield, J. P., Tsai, J., Gouras, G. K., Hai, B., Thinakaran, G., Checler, F., Sisodia, S. S., Greengard, P., and Xu, H. (1999) Endoplasmic reticulum and trans-Golgi network generate distinct populations of Alzheimer β -amyloid peptides. *Proc. Natl. Acad. Sci. U.S.A.* 96, 742–747.
 35. Hartmann, T., Bieger, S. C., Bruhl, B., Tienari, P. J., Ida, N., Allsop, D., Roberts, G. W., Masters, C. L., Dotti, C. G., Unsicker, K., and Beyreuther, K. (1997) Distinct sites of intracellular production for Alzheimer's disease A β 40/42 amyloid peptides. *Nat. Med.* 3, 1016–1020.
 36. Fischer, W. H., and Spiess, J. (1987) Identification of a mammalian glutaminyll cyclase converting glutaminyll into pyroglutamyl peptides. *Proc. Natl. Acad. Sci. U.S.A.* 84, 3628–3632.
 37. Demaurex, N., Furuya, W., D'Souza, S., Bonifacino, J. S., and Grinstein, S. (1998) Mechanism of acidification of the trans-Golgi network (TGN). In situ measurements of pH using retrieval of TGN38 and furin from the cell surface. *J. Biol. Chem.* 273, 2044–2051.
 38. Gouras, G. K., Almeida, C. G., and Takahashi, R. H. (2005) Intraneuronal A β accumulation and origin of plaques in Alzheimer's disease. *Neurobiol. Aging* 26, 1235–1244.
 39. Mori, C., Spooner, E. T., Wisniewski, K. E., Wisniewski, T. M., Yamaguchi, H., Saido, T. C., Tolan, D. R., Selkoe, D. J., and Lemere, C. A. (2002) Intraneuronal A β 42 accumulation in Down syndrome brain. *Amyloid* 9, 88–102.
 40. Gouras, G. K., Tsai, J., Naslund, J., Vincent, B., Edgar, M., Checler, F., Greenfield, J. P., Haroutunian, V., Buxbaum, J. D., Xu, H., Greengard, P., and Relkin, N. R. (2000) Intraneuronal A β 42 accumulation in human brain. *Am. J. Pathol.* 156, 15–20.
 41. Gyure, K. A., Durham, R., Stewart, W. F., Smialek, J. E., and Troncoso, J. C. (2001) Intraneuronal A β -amyloid precedes development of amyloid plaques in Down syndrome. *Arch. Pathol. Lab. Med.* 125, 489–492.
 42. Kawarabayashi, T., Younkin, L. H., Saido, T. C., Shoji, M., Ashe, K. H., and Younkin, S. G. (2001) Age-dependent changes in brain, CSF, and plasma amyloid β protein in the Tg2576 transgenic mouse model of Alzheimer's disease. *J. Neurosci.* 21, 372–381.
 43. Yu, L., Vize, A., Huff, M. B., Young, M., Remmele, R. L., Jr., and He, B. (2006) Investigation of N-terminal glutamate cyclization of recombinant monoclonal antibody in formulation development. *J. Pharm. Biomed. Anal.* 42, 455–463.
 44. Chelius, D., Jing, K., Lueras, A., Rehder, D. S., Dillon, T. M., Vize, A., Rajan, R. S., Li, T., Treuheit, M. J., and Bondarenko, P. V. (2006) Formation of pyroglutamic acid from N-terminal glutamic acid in immunoglobulin γ antibodies. *Anal. Chem.* 78, 2370–2376.

Inhibition of glutaminyl cyclase prevents pGlu-A β formation after intracortical/hippocampal microinjection *in vivo/in situ*

Stephan Schilling,* Thomas Appl,† Torsten Hoffmann,* Holger Cynis,* Katrin Schulz,* Wolfgang Jagla,‡ Daniel Friedrich,* Michael Wermann,* Mirko Buchholz,* Ulrich Heiser,* Stephan von Hörsten† and Hans-Ulrich Demuth*·‡

*Probiodrug AG, Halle (Saale), Germany

†University of Erlangen-Nürnberg, Franz-Penzoldt-Center, Experimental Therapy, Palmsanlage, Erlangen, Germany

‡Ingenium Pharmaceuticals GmbH, Martinsried, Germany

Abstract

Modified amyloid β (A β) peptides represent major constituents of the amyloid deposits in Alzheimer's disease and Down's syndrome. In particular, N-terminal pyroglutamate (pGlu) following truncation renders A β more stable, increases hydrophobicity and the aggregation velocity. Recent evidence based on *in vitro* studies suggests that the cyclization of glutamic acid, leading to pGlu-A β , is catalyzed by the enzyme glutaminyl cyclase (QC) following limited proteolysis of A β at the N-terminus. Here, we studied the pGlu-formation by rat QC *in vitro* as well as after microinjection of A β (1–40) and A β (3–40) into the rat cortex *in vivo/in situ* with and without

pharmacological QC inhibition. Significant pGlu-A β formation was observed following injection of A β (3–40) after 24 h, indicating a catalyzed process. The generation of pGlu-A β from A β (3–40) was significantly inhibited by intracortical microinjection of a QC inhibitor. The study provides first evidence that generation of pGlu-A β is a QC-catalyzed process *in vivo*. The approach *per se* offers a strategy for a rapid evaluation of compounds targeting a reduction of pGlu formation at the N-terminus of amyloid peptides.

Keywords: Alzheimer's disease, amyloid, glutamine cyclotransferase, glutaminyl cyclase, pyroglutamic acid.
J. Neurochem. (2008) **106**, 1225–1236.

Amyloid β (A β) peptides are the major constituent of amyloid plaques, one of the pathological hallmarks of Alzheimer's disease (AD). A β is produced from the large transmembrane precursor protein (APP) by consecutive catalysis of β - and γ -secretase generating the N- and C-terminus, respectively (Selkoe 2001). Numerous studies of the past decade revealed A β 42 as highly amyloidogenic and crucial for development of the disease (Jarrett *et al.* 1993; Iwatsubo *et al.* 1994; McGowan *et al.* 2005). Also, various N-terminal modifications have been described for the A β peptides. Besides N-terminal truncation, the aspartic acid residues at positions 1 and 7 are isomerized and racemized in amyloid deposits (Mori *et al.* 1992; Roher *et al.* 1993; Iwatsubo *et al.* 1996). Most prominent modifications are related to N-truncated peptides, which carry a pyroglutamyl-modified N-terminus, which is formed by cyclization of glutamic acid at positions 3 and 11 (Saido *et al.* 1995), while the process of limited proteolysis resulting in A β (3–40) is unknown. However, those pyroglutamate (pGlu)-A β species readily built up to 50% of the total amyloid in senile plaques

and vascular deposits (Lemere *et al.* 1996; Saido *et al.* 1996; Kuo *et al.* 1997). In addition, recent evidence suggests that the presence of pGlu-modified peptides correlates with the severity of the disease, and, in particular, pGlu-A β is detected in subjects carrying mutations in the presenilin genes 1 and 2 (Russo *et al.* 2000; Miravalle *et al.* 2005; Guntert *et al.* 2006). Furthermore, the presence of

Received January 31, 2008; revised manuscript received April 28, 2008; accepted April 30, 2008.

Address correspondence and reprint requests to Hans-Ulrich Demuth, Probiodrug AG, Weinbergweg 22, Biocenter, D-06120 Halle (Saale), Germany. E-mail: hans-ulrich.demuth@probiodrug.de or Stephan von Hörsten, University of Erlangen-Nürnberg, Franz-Penzoldt-Center, Experimental Therapy, Palmsanlage 5, 91054 Erlangen, Germany. E-mail: stephan.v.hoersten@ze.uni-erlangen.de

Abbreviations used: AD, Alzheimer's disease; APP, amyloid precursor protein; A β , amyloid- β ; BSA, bovine serum albumin; DAB, diaminobenzidine; FDD, familial Danish dementia; HEK, human embryonic kidney cell; PBS, phosphate-buffered saline; pGlu, pyroglutamate; QC, glutaminyl cyclase; RT, room temperature; SDS, sodium dodecyl sulfate; TBS-T, Tris-buffered saline Tween.

pGlu-modified peptides has been described in diffuse plaques of Down syndrome subjects, indicating an early formation in an AD-like deposition process (Iwatsubo *et al.* 1996; Saido *et al.* 1996).

Thus, in spite of the established contribution of pGlu-amyloid in the disease process, the formation of the pGlu-residue from glutamic acid itself is still a subject of speculation. To this end, the cyclization of glutamyl residues via a spontaneous release of water from glutamic acid has been suggested (Hashimoto *et al.* 2002). In contrast, more recently, we were able to show that the enzyme glutaminyl cyclase (QC), which is involved in the pGlu-formation from N-terminal glutamine of neuropeptides, also is capable to catalyze the formation of pGlu-residues from N-terminal glutamic acid in A β species *in vitro* (Schilling *et al.* 2004). Subsequently, this was supported by findings showing that QC-inhibitors suppress the pGlu-A β formation in mammalian cell culture (Cynis *et al.* 2006).

Consequently, as a next step, we here studied the faith of human A β species after intracortical microinjection in rats trying to monitor the formation of pGlu-A β *in vivo*, potentially resulting in a rapid screening model system for QC-inhibitor lead candidates.

Materials and methods

A β peptides

A β (3–40), A β (1–40), and pGlu-A β (3–40) were synthesized as described previously (Schilling *et al.*, 2006). For sample preparation the crude peptides were treated with hexafluoro isopropanol (HFIP) and dissolved in acetonitrile-containing water. Insoluble material was removed by centrifugation prior to injection into the HPLC. Preparative HPLC was performed with a gradient of acetonitrile in water (10–65% acetonitrile, 0.04% trifluoro acetic acid over 40 min) on a 250 \times 20 Luna RP18 column (Phenomenex, Aschaffenburg, Germany). Peptide-containing fractions were further purified to get oligomer-free amyloid peptide: After lyophilization, 1–4 mg of amyloid peptide were dissolved in a buffer consisting of 10 mM Tris, 2.5 mM dithiothreitol, 5 mM EDTA, 2% sodium dodecyl sulfate (SDS), pH 9.0, followed by centrifugation and injection of the supernatant to a 150 \times 4.6 Source 5RPC ST column (5 μ m, Amersham, Uppsala, Sweden). A gradient mixed from solvent A (0.1% NH₃ in H₂O, pH 9) and solvent B (60% acetonitrile, 40% solvent A) was used for purification. The resulting peptide could be easily solved in 0.15 M Tris buffer, pH 8.8 at a concentration of 10 mg/mL. Peptide purity and identity was confirmed by analytical HPLC (150 \times 4.6, 5 μ m Source or Gemini) and matrix-assisted laser-desorption ionization mass spectrometry (MALDI-MS).

Cloning and characterization of rat QC

The cDNA sequence of rat QC was obtained from nucleotide entry XM_233812. Mature rat QC was isolated from cDNA of PC12 cells using the primers 5'-CGCTGTTGCCTGGACGCAGG-3' (sense) and 5'-ATATAAGCTTTTACAAGTGAAGATATTCC-3' (antisense). The cDNA was cloned into the yeast expression vector

pPIC α B, which is suited for expression of recombinant proteins in the yeast *Pichia pastoris*. The system was already applied for isolation of murine QC (Schilling *et al.* 2005). Rat QC was purified to apparent homogeneity from the supernatant after fermentation of *Pichia*, applying two chromatographic steps, an expanded bed absorption on a cation exchange resin followed by a hydrophobic interaction chromatography step on a Butyl-Sepharose resin (see also supplementary information). Usually, approximately 20 mg of protein was isolated from a typical 5 L fermentation. QC activity was assayed as described previously (Schilling *et al.* 2002, 2003a,b).

Animals, surgery and injection procedure

Female Sprague–Dawley rats (12 weeks of age, 220 \pm 14 g BW; four per group and time point) were used. Injection of pGlu-A β (3–40) served as positive control and to establish injection coordinates, injection, fixations, immunohistochemistry and ELISA. For each compound, two time points (24 and 48 h) were tested and in each case the contralateral side served as negative control. Animals were anesthetized using i.p. injection of Dormitor® (Pfizer, Karlsruhe, Germany) and Ketamine® (Albrecht, Aulendorf, Germany) (0.09 + 0.3 mL/270 g BW), the skull was shaved, a midline incision set, bregma targeted, and coordinates [bregma (Z): –4.0 mm; lateral right (X): –3.0 mm; caudal (Y): –3.0 mm] according to the Paxinos Atlas were used for deep cortical/intrahippocampal injection. Surgery and microinjections were conducted as previously described (Kask *et al.* 2001), the general approach being adapted from Shin *et al.* (1997), and all research and animal care procedures were approved by the local authorities and performed according to international guidelines for the use of laboratory animals. The lyophilized A β samples were freshly solubilized to 10 mg/mL in 0.15 M Tris buffer, pH 8.8, filtered (0.22 μ m), immediately before each injection. Five microliters of the solution was injected into the right side of the deep cerebral cortex and/or hippocampus. In case of the co-injection experiments, A β injection was preceded by injection of either vehicle (5 μ L, control) or PBD150 (5 μ mol, dissolved in saline).

Cultivation, transfection, and immunostaining of rat QC in HEK293 cells

Human embryonic kidney cell line (HEK) 293 was cultured in Dulbecco's modified Eagle's medium, 10% fetal bovine serum in a humidified atmosphere of 5% CO₂ at 37°C. For transfection, cells were cultured in six-well dishes, grown until 80% confluency and transfected by incubation in a solution containing Lipofectamine 2000 (Invitrogen, Carlsbad, CA, USA) and the respective plasmids according to the manufacturer's manual. Appropriate growth media replaced the solution after 5 h and cells were grown overnight. For subsequent immunostaining, cells were grown in six-well dishes containing a coverslip. One day after transfection, cells were washed twice with Dulbecco–phosphate-buffered saline (PBS) (Invitrogen) and fixed using ice-cold methanol for 10 min at –20°C, followed by three washing steps of Dulbecco–PBS for 10 min at 23°C. The slices were treated sequentially with 0.5% H₂O₂, 0.3% TX-100, and 2% normal goat serum for 10 min, 10 min, and 1 h, respectively. Application of the primary QC-specific antibody [1 : 2000 in 1% bovine serum albumin (BSA)] was followed by visualization of immunoreactive products with the avidin–biotin complex kit (Vector

ABC Elite, Burlingame, CA, USA) using the substrate diaminobenzidine (DAB). For immunoblotting, proteins were loaded onto a Tris-glycine 4–20% gradient SDS-polyacrylamide electrophoresis gel (Serva, Heidelberg, Germany), separated and transferred onto a nitrocellulose membrane under semi-dry conditions. The membrane was blocked using 3% (w/v) dry milk in Tris-buffered saline Tween (TBS-T) [20 mM Tris/HCl; pH 7.5; 500 mM NaCl, 0.05% (v/v) Tween-20]. QC was detected applying primary antibody A01 (1 : 750 in TBS-T; Abnova Inc., Taipei City, Taiwan). Blots were developed using horseradish peroxidase-conjugated secondary antibodies and the SuperSignal West Pico System (Pierce, Rockford, IL, USA) according to the manufacturer's protocol.

Histochemistry and immunohistochemistry

After different post-injection survival times, the brains were removed from the rats, fixed in 70% ethanol/0.15 M NaCl and embedded in paraffin as reported by Shin *et al.* (1993, 1994). Paraffin blocks were sectioned at 6 and 10 μ m thickness through the injection side, which is visible by inspection by eye during cutting. After de-paraffination and mounting, sections were treated for 30 min with formic acid, 10 min with H₂O₂ (3%), followed again by a TBS rinse. This was either followed either by cresyl violet (Nissl) and congo red stainings according to standard procedures, or by incubation (6 h at 4°C) with primary antibodies for immunohistochemistry, the latter using several different antibodies that specifically recognize different epitopes of A β .

For immunohistochemistry on paraffin sections, the 4G8 (Chemicon, Temecula, CA, USA) [1 : 100 (mouse) in PBS + 5% rabbit serum + 0.3% TX-100] and anti-N3 (pE) (Assay Designs, Ann Harbor, MI, USA) (1 : 500 rabbit, in PBS + 5% Goat serum + 0.3% TX-100) antibodies were used. The primary antibodies were detected by anti-mouse bio (1 : 200 in PBS + 5% rabbit serum + 0.3% TX-100) or anti-rabbit bio (1 : 200 in PBS + 5% goat serum + 0.3% TX-100) antibodies. The immunoreactive products were visualized with the avidin-biotin complex kit (Vector ABC Elite) consisting of the following steps as previously described (von Horsten *et al.* 2003): A Tris-HCl rinse was followed by ABC kit (according to instruction), TBS-T rinse, substrate (DAB) solution for 15 min, and a series of isopropanol and xylol steps, finally completed by coverslipping in paramount or eukitt media. For immunohistochemistry of QC in the rat brain, animals were deeply anesthetized as described above and transcardially perfused through the ascending aorta with 200 mL ice-cold 0.9% NaCl, followed by at least 300 mL ice-cold fixation solution that consisted of 4% paraformaldehyde in 0.1 N PBS. Brains were removed, post-fixed for 4 h in the fixation solution, cryoprotected in 30% sucrose solution (5 days) and shock-frozen in petrolether. Coronal cryosections (30 μ m) were processed free-floating for substrate-based immunohistochemistry (3',3-diaminobenzidine tetrahydrochloride solution, DAB). Between incubation steps, all washing of sections were done three times (each 10 min) in 0.1 N PBS. Briefly, for inhibition of endogenous peroxidase, sections were incubated in 1.5% H₂O₂ in 20% v/v methanol, 0.1 N PBS (5 min, 23°C). This was followed by pre-incubation in 5% BSA solution (0.3% Triton, 0.1 N PBS, 45 min, 23°C) and consecutive incubation

with the polyclonal mouse anti-QPCT antibody (A01, Abnova Inc.) (diluted 1 : 1000 in 0.3% Triton, 0.1 N PBS, overnight, 4°C). Subsequently, sections were incubated in donkey anti-mouse antibody biotinylated (Jackson Immuno-Research Inc., West Grove, PA, USA) (1 : 200, diluted in 0.1 N PBS, 2% BSA, 1 h, 23°C) and followed by incubation in the avidin-biotin complex kit (30 min, 23°C) (Vector ABC Elite). Finally, sections were reacted with DAB as a chromogen (SK-4100, Vector Laboratories) (6 min, 23°C), mounted onto object slides, air-dried and coverslipped with DPX Mountant (Fluka Chemie GmbH, Buchs, Switzerland). Pre-absorption experiments: for evaluation of the specificity of the QC antibody A01, the immunogenic peptide Q01 was spotted (2 μ L) in 10-fold excess onto a nitrocellulose membrane. Membranes were repeatedly incubated in the antibody working dilution. Efficacy of pre-absorbed antibodies was tested by visualization of bound antibodies onto the membrane using a suitable peroxidase-coupled secondary antibody and processing of chemiluminescence by conventional enhanced chemiluminescence plus detection system (Amersham).

For double-labeling immunofluorescence, sections were blocked in 10% normal donkey serum containing 0.3% Triton X-100 in PBS for 1 h, and incubated with the 4G8 (1 : 200 in PBS + 5% rabbit serum + 0.3% TX-100) and anti-N3 (pE) (1 : 1000 in PBS + 5% goat serum + 0.3% TX-100). Following subsequent washes, sections were labeled using Cy-2- and Cy-3-coupled secondary antibodies (1 : 200, 2 h, 23°C) (Jackson Immuno-Research Laboratories), each diluted in PBS and 3% normal donkey serum. In some case 4', 6-diamidino-2-phenylindole (DAPI) nuclear staining was applied according to standard procedures. After washing with PBS, sections were mounted in Vectashield-DAPI mounting medium (Vector).

All sections were analyzed using a Nikon light microscope (Eclipse 80i; Nikon, Tokyo, Japan), Nikon objectives (Plan Apo, VC series), motorized specimen stage for automatic sampling (Märzhäuser, Wetzlar, Germany), electronic microcator (Heidenhain, Traunreut, Germany), a dedicated Nikon HiSN fluorescence system, a Nikon cooled DS-5Mc camera, and imaging software (Stereo Investigator; MicroBrightField, Williston, VT, USA). Controls consisted in omitting primary antibodies and yielded lack of specific stainings.

ELISA analysis

Sequential A β extraction was performed, essentially as described (Kawarabayashi *et al.* 2001). At every stage of the extraction procedure, the homogenized tissue was subjected to sonification (Bandelin sonoplus, Berlin, Germany). Briefly, frozen hemispheres without cerebellum were homogenized in 2.5 mL TBS using a dounce homogenizer, sonicated and centrifuged at 75 500 g for 1 h. The supernatant was then subjected to two further homogenizations in 2.5 mL 2% SDS and 0.5 mL formic acid. The final fraction was neutralized using 19.5 mL 1 M Tris, pH 9.0. The vast majority (> 90%) of A β was extracted by 2% SDS. The assay samples were diluted 1 : 10 at least prior to ELISA analysis.

A β (x-40) sandwich ELISA (IBL, Hamburg, Germany) was performed according to the manufacturer's manual. pGlu-A β (3-40) was assayed applying a novel established ELISA. The horseradish peroxidase-conjugated antibody directed against pGlu-A β (IBL)

was applied in combination with microplates that were pre-coated with an A β 40 – detecting antibody known from the A β (x-40) assay kit. Ratios of each individual data set (treated/untreated) were evaluated using unpaired Student's *t*-tests. Significant values are shown in figures.

Results

Isolation and enzymatic characterization of rat QC

The sequence of the putative rat QC was obtained by database mining. On the basis of the primary structure of human QC, nucleotide entry XM_233812 was identified encoding the rat QC (Fig. S1). Rat and human QC share 83% sequence identity. The mature rat QC was isolated from a cDNA library of PC12 cells, expressed in *P. pastoris* and purified to homogeneity from the supernatant after fermentation (Fig. S2).

As revealed by the conversion of various peptide substrates and dipeptide surrogates, rat QC displays a very similar catalytic specificity compared with human QC (Table 1). The functional homology of the QC proteins from mammalian origins is also reflected by the inhibition by imidazole derivatives (Table 1). Virtually identical K_i -values were obtained with several imidazoles and the specific QC-inhibitor PBD150. The inhibition mode was linear competitive for all compounds (not shown).

The characterization of the newly isolated QC from rat clearly demonstrates conserved enzymatic mechanisms and

modes of inhibitor binding, thus enabling QC-inhibitor studies, which exhibit highly predictive potential for the human target enzyme.

Immunohistochemical analysis of rat QC

Initial expression analysis of a bovine QC revealed transcript levels in all brain regions (Pohl *et al.* 1991). To prove the expression of rat QC in the cortex, which was intended as injection site of the A β peptides, QC was immunohistochemically labeled using a polyclonal antibody for human QC. The reactivity with recombinant rat QC was verified applying western blot analysis of HEK293 cells expressing rat QC (Fig. 1a). Furthermore, the specificity of the antibody was characterized applying immunocytological labeling of the fixed cells (Fig. 1c) and also in rat cortex (Fig. 1e). Applying a pre-absorption with the antigenic QC-related peptide, the staining was abolished (Fig. 1b, d, f). Thus, the data clearly support a high selectivity of the antibody for QC and demonstrate that the procedure is suitable for immunodetection of rat QC. In fact, a prominent immunostaining was obtained with the polyclonal QC-antiserum in the cortex of the rat (Fig. 2a). The pattern clearly suggests a high expression of QC in neurons of several cell layers of the cortex and hippocampus (Fig. 2b). Higher magnifications give rise to the assumption that the protein is localized in soma and axons of the expressing cells (Fig. 2c, d). This, in turn, suggests a secretion of the QC into the extracellular space, which was also suggested

Table 1 Kinetic parameters of substrate conversion and inhibition of rat QC

Compound	Rat QC			Human QC ^a		
	K_M (mM)	k_{cat} (s ⁻¹)	K_i (mM)	k_{cat}/K_M (mM ⁻¹ *s ⁻¹)	k_{cat}/K_M (mM/s)	K_i (mM)
Substrates						
H-Gln-AMC	0.049 ± 0.001	4.0 ± 0.2	4.5 ± 0.4 ^b	81.5 ± 0.4	98 ± 2	ND
H-Gln- β NA	0.050 ± 0.004	12 ± 1	1.3 ± 0.1 ^b	234 ± 21	294 ± 6	1.21 ± 0.07 ^b
H-Gln-Gly-OH	0.30 ± 0.01	3.0 ± 0.2	–	10.1 ± 0.6	53 ± 1	–
H-Gln-Gln-OH	0.20 ± 0.01	8.1 ± 0.2	–	41 ± 3	140 ± 2	–
H-Gln-Glu-OH	0.51 ± 0.05	7.7 ± 0.1	–	15 ± 1	58 ± 1	–
H-Gln-Gly-Pro-OH	0.19 ± 0.01	7.3 ± 0.1	–	39 ± 3	195 ± 7	–
H-Gln-Phe-Arg-His-NH ₂	0.05 ± 0.01	16 ± 1	–	324 ± 53	–	–
Inhibitors						
Imidazole	–	–	0.116 ± 0.004	–	–	0.103 ± 0.004
Benzimidazole	–	–	0.130 ± 0.004	–	–	0.138 ± 0.005
N-Methylimidazole	–	–	0.013 ± 0.001	–	–	0.030 ± 0.001
Benzylimidazole	–	–	0.0035 ± 0.001	–	–	0.0071 ± 0.0003
PBD150	–	–	1 × 10 ⁻⁴ ± 5 × 10 ⁻⁶	–	–	6 × 10 ⁻⁵ ± 2 × 10 ⁻⁷

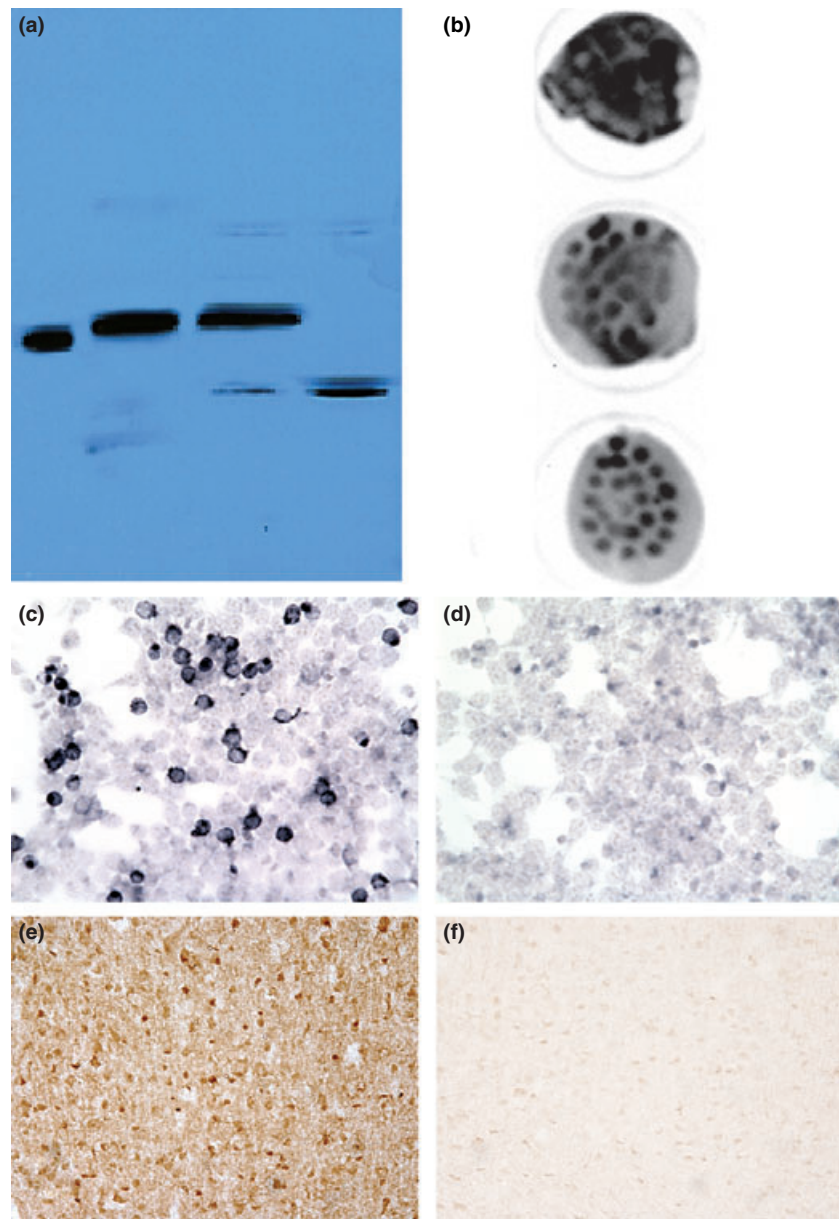
Reactions were carried out in 0.05 M Tris/HCl, pH 8.0 at 30°C.

^aData from Refs Schilling *et al.* 2003a, b and Buchholz *et al.* 2006.

^bSubstrate inhibition.

QC, glutaminyl cyclase; ND, not determined.

Fig. 1 Characterization of a polyclonal antibody raised against human glutaminy cyclase (QC) used in this study. (a) Western blot analysis of proteins present in conditioned media and cells of line human embryonic kidney cell (HEK) 293. Naturally, HEK293 expresses only minor amounts of QC activity (Cynis *et al.* 2006). Lanes are (from the left to the right): 1, recombinant human QC expressed in yeast; 2, concentrated medium of HEK cells expressing rat QC; 3, cell pellet following expression of rat QC in HEK cells; 4, cell pellet of mock-transfected HEK cells. (b) Illustration of the pre-absorption event performed before IHC staining depicted in images (d) and (f). The peptide Q01 was spotted on a nitrocellulose membrane and the antibody working solution applied consecutively for three times. The pre-absorption was followed by enhanced chemiluminescence staining of the spots. (c) Immunohistochemical staining (antibody A01, DAB) of HEK cells, which transiently express rat QC. QC-positive cells are identified by the dark-brown coloration. (d) Cells as described in (c), with pre-absorbed antibody using the QC-derived peptide Q01. (e and f) Immunohistochemical localization of QC in the rat brain representing deeper cortical layers. Incubation of cryosections with the QC antibody A01 shows a QC immunoreactivity in the cortex. Pre-absorption of the primary antibody with the appropriate antigenic peptide decreases staining intensity and served as negative control.



from other studies in the bovine hypothalamus (Bockers *et al.* 1995).

Establishment of a pGlu-A β (3–40) ELISA

To quantify the formation of pGlu-A β (3–40) after injection of A β (1–40) and A β (3–40), an ELISA was established based on commercially available antibodies and microplates (IBL, Hamburg, Germany). In the assay, the microplate-bound primary antibody binds to the C-terminus of A β . The secondary antibody (monoclonal N3pE, IBL) recognizes specifically the N-terminus of pGlu-A β . The A β -standard was synthesized and the peptide concentration determined by spectrophotometry. A fairly linear

dependence of absorption was obtained in the concentration range between 1 and 500 pg/mL (Fig. 3). In addition, the cross-reactivity of the ELISA against A β (1–40) and A β (3–40) was assessed, revealing a reactivity for A β (3–40) and A β (1–40) of < 0.5% (Fig. 3, inset) compared with pGlu-A β (3–40). Thus, the method was well suited for the intended trial.

Immunohistochemistry of pGlu-A β after deep cortical injection of pGlu-A β (3–40), A β (3–40) and A β (1–40)

To investigate the pGlu-A β formation under *in situ* conditions, human A β (1–40) and human A β (3–40) were injected into the deep cortex of the rat. The brains were removed and

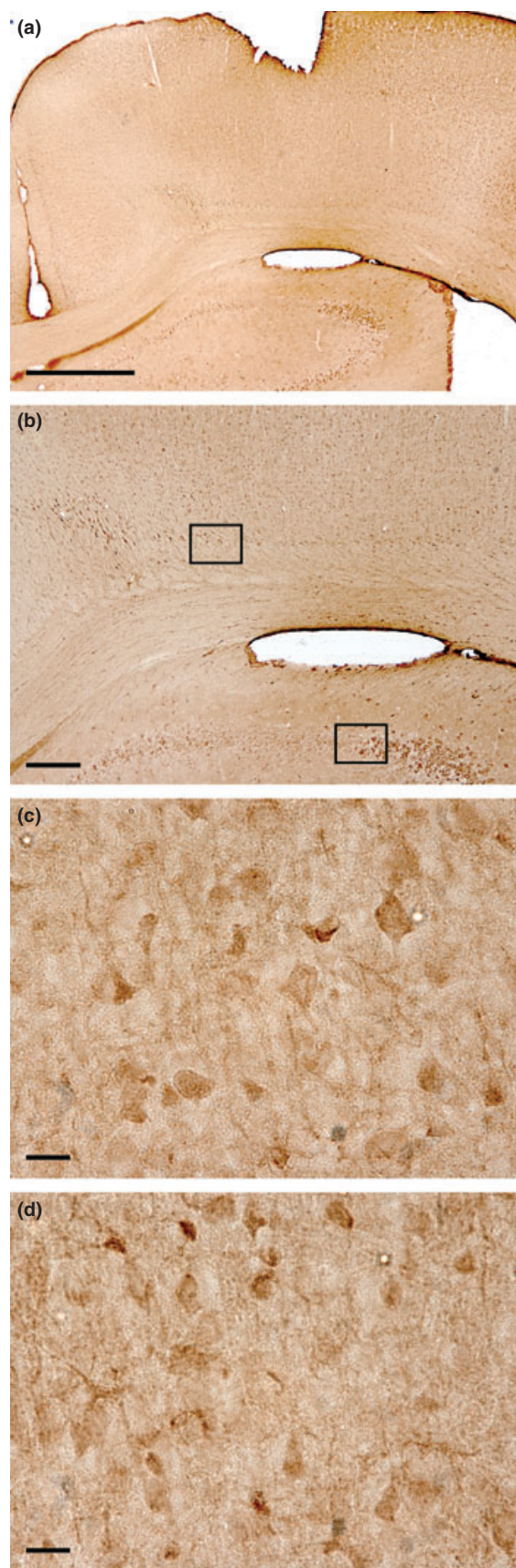


Fig. 2 Immunohistochemical staining of glutaminyl cyclase (QC) in cortical layers and hippocampal formation of the rat brain (a and b). A representative brain section (bregma -2.04 mm according to the brain atlas of Paxinos and Watson, 2007) showed strong QC immunoreactivity within several cortical regions such as the primary motor cortices, retrosplenial granular cortex and cingulum (b, upper rectangle). In addition, moderate QC immunoreactivity was anatomically defined in subcortical regions including pyramidal cell layers and CA3 field of the hippocampal formation (b, lower rectangle). Under a higher magnification, immunostaining for QC was not restricted to cell somata within cortical neurons, but was also observed in axons and processes (c). Punctuate, cytoplasmic staining was observed in hippocampal neurons (d). Scale bars: (a) $1000 \mu\text{m}$, (b) $100 \mu\text{m}$, (c and d) $10 \mu\text{m}$.

the A β composition analyzed in histochemical stainings applying monoclonal pGlu-A β antibody, monoclonal 4G8 antibody detecting total A β and thioflavin S. Corresponding specific immunoreactivity was found in the deep cortical areas as well as in the cingulum, alveolus of the hippocampus, external capsule, fibriae of the hippocampus as well as rarely in hippocampal fissure, CA1 and CA2 of the hippocampus. As can be observed in Fig. 4, showing the evaluation of a representative injection experiment, 24 h after injection, prominent stainings with antibody 4G8 were observed, indicating a slow degradation of the A β 40 peptides. In the first experiments, the assay was established using pGlu-A β (3–40) as standard peptide. All A β peptides presumably form aggregates after injection, as evidenced by the congo red staining. Interestingly, the most intense 4G8 and congo red stainings were observed following injection of pGlu-A β (3–40). A pGlu-A β immunoreactivity was not observed after injection of A β (1–40). In contrast, pGlu-A β was detected 24 h after injection of A β (3–40), indicating a partial conversion of the N-terminal glutamic acid into pyroglutamic acid. The apparent differences in the stainings especially using the 4G8 and thioflavin S, e.g. highest intensities for pGlu-A β , lowest for A β (1–40), might be caused by rapid aggregation of the peptide and generation of degradation-resistant deposits. Those differences have been proven in *in vitro* experiments and potentially influence the staining intensity. The detection of pGlu-A β following injection of A β (3–40) strongly supports a catalyzed pGlu-A β formation under *in vivo* conditions.

Immunohistochemistry of pGlu-A β after deep cortical injection of A β (3–40) and co-injection of QC-inhibitor PBD150

A primary aim of the study was to prove, whether the cyclization is enzyme catalyzed, presumably by endogenous QC *in vivo*. Therefore, vehicle followed by A β (3–40) were injected into left hemisphere, as previous experiments revealed pGlu-A β within 24 h under these conditions. Into the other, right hemisphere, however, the QC-inhibitor PBD150 (1 or $5 \mu\text{mol}$) and consecutive A β (3–40) were co-injected. A rapid generation of pGlu-A β was important,

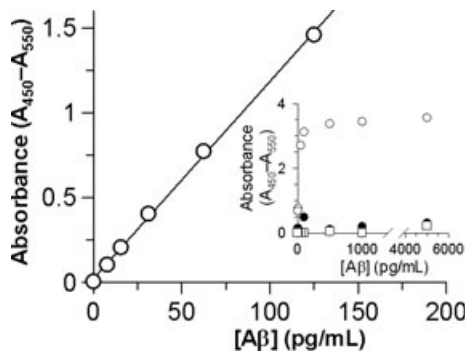


Fig. 3 Establishment of a pGlu-A β (3-40) specific ELISA. For analysis, a pGlu-A β specific monoclonal antibody and coated plates specific for A β 40 were used (both IBL). The A β peptides were synthesized as described in Materials and methods and the concentration verified by quantification of the absorbance at 275 nm. A fairly linear dependence of the absorbance was observed in a concentration range between 0 and 130 pg/mL. Moreover, as illustrated in the inset, the ELISA did not show significant cross-reactivity against A β (1-40) (dark circles) and A β (3-40) (squares), suggesting reliable quantification of pGlu-A β (3-40) under the experimental settings of the deep cortical injection of human A β .

because in control experiments, a clearance or metabolism of the inhibitor was suggested within 48 h (not shown). To avoid repeated injections of the inhibitor, the pGlu-A β formation following application of A β (3-40) was analyzed 24 h after injection of A β and PBD150. Representative sections of four brains after injection of 5 μ mol PBD150 into the right hemisphere are illustrated in Fig. 5. In the left hemispheres, where A β (3-40) was injected, prominent DAB staining was observed, illustrating significant pGlu-A β formation. In the contralateral hemispheres, a markedly reduced staining is evident, suggesting an attenuated pGlu-A β formation. Thus, the pre-injection of the QC-inhibitor PBD150 on this side exerted a significant effect on the cyclization of A β (3-40), strongly implying that QC-catalysis is responsible for the generation of the N-terminal pyroglutamic acid residue.

ELISA analysis of pGlu-A β (3-40) formation after deep cortical injection of A β (3-40) and co-injection of QC-inhibitor PBD150

To quantify the reduction of pGlu-A β by the QC-inhibitor, the A β -peptides were sequentially extracted from the brains

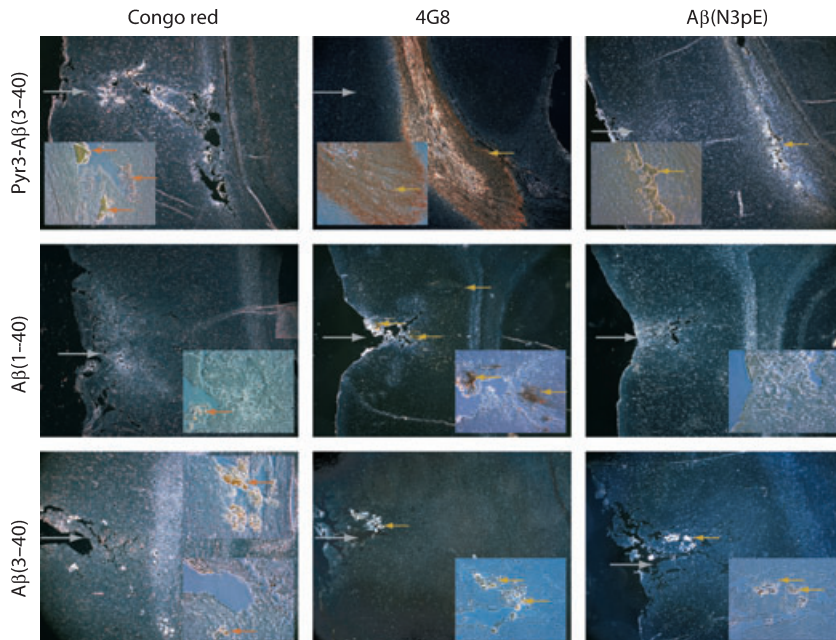


Fig. 4 Dark field microscopy of representative sections of rat brains (magnification 40 \times) stained with congo red (left column), 4G8 (middle column), and A β (N3pE) (right column) 24 h after injection of either pGlu-A β (3-40) (upper row), A β (1-40) (middle row), and A β (3-40) (lower row). Sections are rotated 90 $^\circ$, and the direction of injection is indicated by gray arrows. Small panels represent higher magnification (200 \times) of the corresponding section. The left column (congo red) illustrates that congophilic 'red-orange' (orange arrows) deposits were found after injection of all three A β peptides. However, the 'typical' change of color in polarized light (Ph2) was most convincingly

observed after injection of pGlu-A β (3-40) (green/orange deposits in upper left small panel). The middle column illustrates that 4G8 immunoreactivity (yellow arrows) was also detected after injection of all three A β peptides. The right column [A β (N3pE)] illustrates that pGlu-A β immunoreactivity (yellow arrows) was observed after injection of pGlu-A β (3-40). Although not as prominent, pGlu-A β immunoreactivity was also observed following injection of A β (3-40) peptides (see small upper right and lower right panels with yellow arrows). Positive stainings for pGlu-A β were never observed after injection of A β (1-40) (right column, panel in the middle).

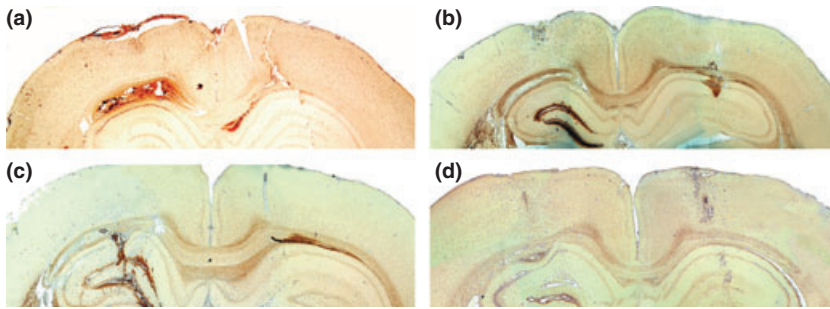


Fig. 5 Photomicroscopy of representative sections of four different rat brains 24 h after bilateral injection of either vehicle or PBD150 followed by A β (3–40). IHC-based detection of pGlu-A β (3–40), using diaminobenzidine as substrate, was performed. Panels a–d provides representative sections at the level of the injection site in all four animals.

using 2% SDS and 70% formic acid consecutively. The vast majority of the A β peptides was extracted by 2% SDS (not shown). The extracted A β peptides were quantified applying ELISAs detecting either total A β 40, i.e. N-truncated variants and also partially rodent A β , and specifically pGlu-A β (3–40). The total amounts of A β were determined and the ratio of pGlu-A β and total A β calculated. The ratio illustrates the effect of the QC-inhibitor specifically on the pGlu-A β formation and provides, in fact, the percentage of the A β , which was converted by QC.

In general, based on the ELISA analysis, only about 2–10% of the injected A β was recovered after extraction, implying a rapid clearance of the peptide after injection (not shown). Interestingly, about 2.5–5% of the recovered A β after injection of A β (3–40) was converted into pGlu-A β (Fig. 6). In comparison, the generation of pGlu-A β (3–40) from A β (1–40), however, was only marginal, substantiating

the findings of the A β -immunohistochemistry (compare with Fig. 4). Thus, apparently the removal of the first two N-terminal amino acids from A β (1–40) occurs only very slowly *in vivo* compared with N-terminal cyclization. The pGlu-content after injection of A β (1–40) increased slightly after 48 h, indicating an initial aminopeptidase driven slow removal of the first two amino acids and the subsequent generation of the A β (3–40), which is prone to cyclization. Co-injection of the inhibitor did not affect the pGlu-A β generation, most likely because of the rapid clearance of the compound after injection.

In contrast, based on the results obtained with the inhibitor PBD150, the conversion of A β (3–40) into pGlu-A β (3–40) was substantially decreased. The injection of 5 μ mol PBD150 resulted in a significant reduction in the pGlu-A β level after 24 and 48 h. In a second trial, the inhibitor was reduced to 1 μ mol (Fig. 6, inset). Consequently, the reduction in the pGlu-A β content in relation to the total extracted A β lacked statistical significance. This, in turn, indicates a dose dependency of the inhibitory effect. Notably, none of the animal deceased after injection of PBD150 solution, suggesting that the QC-inhibition does not exert acute toxic effects.

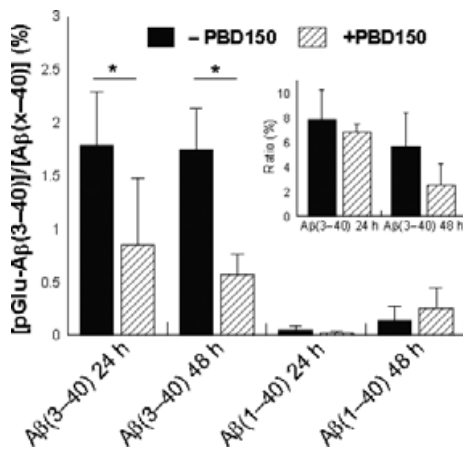


Fig. 6 Ratio of the N-terminally pGlu-modified and total A β 40 determined using ELISAs after deep cortical injection and sequential extraction of the A β peptides. Injection of A β (3–40) resulted in significant formation of pGlu-A β (3–40) 24 h after injection. In contrast, pGlu-A β formation was marginal after injection of A β (1–40). The co-injection of the inhibitor PBD150 (5 μ mol) reduced the pGlu-A β concentration significantly (hatched bars). Reduction of the compound to 1 μ mol exerted a reduced effect, suggesting a dose dependency and thus inhibitory specificity (inset) (* p < 0.05, unpaired t -test).

Double-immunofluorescence stainings following injection of A β (3–40)

The ELISA analysis suggested that A β (3–40) was only partially converted into pGlu-A β . Therefore, it was a further aim to investigate, whether pGlu-A β and A β (x–40) form common aggregates after injection. Previous studies *in vitro* suggested a generation of such deposits (Schilling *et al.*, 2006), and also studies in human AD brain support the abundance of different A β forms in amyloid plaques (Saido *et al.* 1995). In the present study, double-immunofluorescent stainings applying antibody 4G8 and the pGlu-specific antibody revealed a co-staining near the injection site (Fig. 7a–i). This, in turn, clearly substantiates that different N-terminal A β variants may form mixed aggregates also *in vivo*. According to the observation of pGlu-A β seeding *in vitro*, the QC-catalyzed formation of pGlu-A β could precede the deposition of the other peptides. As implied by the reduced staining for pGlu-A β and total A β following

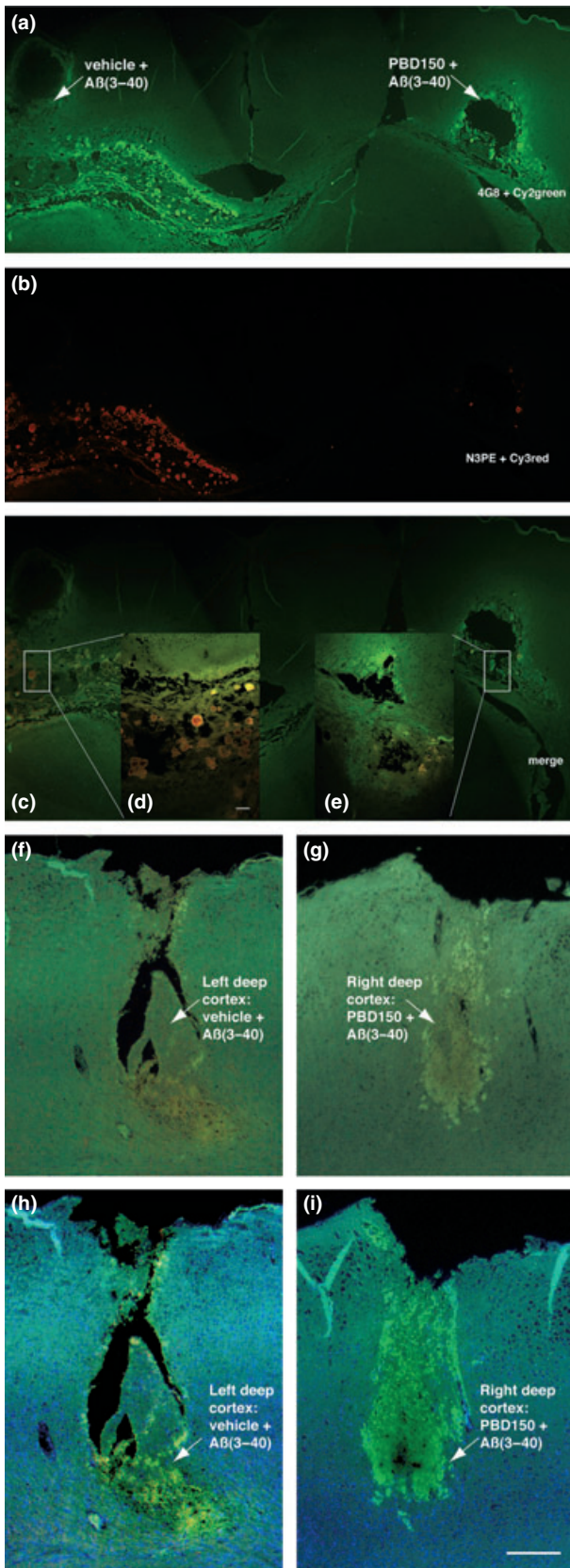


Fig. 7 Double-immunofluorescent stainings of total A β (a; 4G8, green) and pGlu-A β (b; N3pE, red) after cortical injection of A β (3–40). The overlay mode (c) suggests co-localization of the peptides, implying formation of mixed aggregates consisting of A β (x–40) and pGlu-A β (3–40) (inset d and e). The more intense staining for pGlu-A β and total A β in the hemisphere without injection of QC-inhibitor PBD150 implies abundance of A β aggregates and slower A β clearance, caused by seeding of pGlu-A β . (f–i) Staining of the injection sites of an additional injection approach as described before, however, in addition to 4G8 and N3pE, DAPI was introduced for labeling of nuclei (f–i). Corresponding images of left and right injection sites using triple-excitation-band-immunofluorescences (f and g) as well as merged single-excitation-immunofluorescence images (h and i) are given. Scale bars = 50 μ m.

PBD150 co-injection (Fig. 7a and b, comparing the hemispheres), the pGlu-formation might trigger aggregation of other, more abundant species, thus functioning as a site for accumulation of A β in deposits. Although this requires further substantiation in transgenic animal models, the present approach in an acute model might help to clarify the role of seeding A β species for deposition of A β *in vivo*.

Discussion

Although substantial efforts were made as the discovery of N-terminally truncated A β peptides in amyloid deposits of AD patients, their role in neuropathophysiology as well as their formation *in vivo* is still ambiguous. Many reports suggested, that N-terminally truncated and pGlu-modified peptides are the major constituents in amyloid plaques (Iwatsubo *et al.* 1996; Saido *et al.* 1995, 1996; Hosoda *et al.* 1998; Harigaya *et al.* 2000; Shirotani *et al.* 2002). More recently, also evidence was provided that especially pGlu-amyloid peptides might play a decisive role in disease progression, because pGlu-A β peptides were present in brains of sporadic AD patients in significantly higher amounts compared with aged-matched controls displaying amyloid deposits (Piccini *et al.* 2005). Furthermore, the potential of pGlu-modified peptides to speed the disease process becomes also evident from several studies investigating the influence of the mutations in the presenilins and their impact on the amyloid plaque composition (Russo *et al.* 2000; Miravalle *et al.* 2005). Interestingly, the pGlu-modified peptides are over-represented in FAD cases, which are caused by mutations in PS1 or PS2, likely contributing to the early onset of the disease. Support for the potential disease-provoking role of N-truncated A β peptides is also provided by the analysis of transgenic murine animal models. A model, which has shown to generate N-terminally truncated A β peptides displays massive neuron loss (Casas *et al.* 2004). Intriguingly, the signs of neuronal dysfunction appear to be coupled with the occurrence of pGlu-A β (3–42). In contrast, the more commonly used animal models generating

A β based on the over-expression of familial APP mutations, e.g. tg2576 mice, show less pGlu-modified A β peptides in the amyloid deposits and little or no neurodegeneration (Kawarabayashi *et al.* 2001; Kuo *et al.* 2001; Kalback *et al.* 2002; McGowan *et al.* 2006).

The molecular pathways leading to the generation of N-truncated amyloid peptides are only poorly understood. It has been suggested that especially aminopeptidases might cause the N-truncation of A β , thus generating A β (3–x) which is then prone to N-terminal cyclization. Originally, it was suggested that the N-terminal cyclization of glutamic acid is a spontaneous process similar to cyclization of glutamine (Hashimoto *et al.* 2002). However, also glutaminylation cyclization is enzyme catalyzed by QC *in vivo*. Furthermore, in contrast to spontaneous pGlu-formation from N-terminal glutamine, glutamic acid has been shown to cyclize extremely slow with cyclization half-lives of months to years (Chelius *et al.* 2006; Yu *et al.* 2006; Dick *et al.* 2007). This, in turn, strongly implies an enzyme catalyzed pGlu-A β formation *in vivo*. Recently, it has been shown *in vitro* that QC catalyzes the cyclization of A β (3–x) at slow rates (Schilling *et al.* 2004; Cynis *et al.* 2006). Finally, the present study clearly substantiates that the pGlu-A β formation is a QC-catalyzed process *in situ*, as evidenced by the rapid conversion of A β (3–40) into pGlu-A β (3–40) and by its prevention co-applying the QC inhibitor PBD150 intracortically. In fact, several lines of evidence are supportive for a QC-mediated pGlu-A β formation *in vivo*: (i) as shown here for the first time by immunohistochemistry, QC is expressed in brain regions that are afflicted in AD, i.e. in cortex and hippocampus; (ii) QC and APP are transported and processed in secretory compartments, and QC is secreted from the expressing cells (Pohl *et al.* 1991); (iii) several recent studies including our own point to a negligible spontaneous pGlu-formation from N-terminal glutamic acid at physiological conditions, i.e. neutral to mildly acidic pH and 37°C (Schilling *et al.* 2004; Chelius *et al.* 2006; Yu *et al.* 2006; Dick *et al.* 2007). QC-mediated pGlu-formation has been shown, in turn, to be optimal under these conditions (Schilling *et al.* 2004).

Although the compelling evidence points to the QC-catalyzed pGlu-A β formation, the role of the pGlu-modified peptides for the disease is still not fully clear. However, because of the N-terminal lactam formation, conspicuous changes of the biophysical properties occur. Caused by the pGlu-residue, the A β -peptides are stabilized against N-terminal degradation by aminopeptidases and possibly also by endopeptidases (Hosoda *et al.* 1998; Saido 1998). The stabilization is based on the loss of the basic, under physiological conditions positively charged N-terminus of the peptide, which is required for substrate recognition by most unspecific aminopeptidases. The drastically increased proteolytic stability of the pGlu-modified A β might also cause the correlation of the pGlu-A β content with severity of

the sporadic AD, which was suggested in a previous study (Guntert *et al.* 2006). The presence of pGlu-amyloid *in vivo* in relation to pathophysiological severity of neurodegeneration has been also studied recently in human and tg mouse brain tissue by imaging techniques. While *in vivo* positron emission tomography (PET) and *ex vivo* autoradiography analysis of ‘Pittsburgh Compound B’ (PIB) retention in amyloid-rich regions of human and mouse brain revealed strong correlation of PIB and pGlu-amyloid co-deposition, PIB-retention did not correlate to A β (1–40) and A β (1–42) deposition in the investigated tissue samples (Maeda *et al.* 2007).

The loss of N-terminal charged residues by truncation and cyclization, however, also causes a drastic increase in the hydrophobicity, likely provoking the enhanced tendency to aggregation that has been described for pGlu-A β (3–40/42) (He and Barrow 1999; Schilling *et al.*, 2006). Hence, QC inhibition might lead to reduction of pGlu-amyloid formation in sporadic and familial AD as well as in the inherited amyloidoses familial Danish dementia (FDD) and familial British dementia (FBD). It appears, furthermore, that the pGlu-A β aggregates differ structurally from those of full-length A β (unpublished observations). The formation of mixed aggregates consisting of pGlu-A β (3–42) and A β (1–42) has been demonstrated *in vitro* recently (Schilling *et al.*, 2006). The double-immunofluorescent stainings provided here (Fig. 7) indicate that also *in situ* mixed amyloid aggregates develop fast, further indicating that the pGlu-A β species might speed the aggregation of full-length A β , caused by their own insolubility. That pGlu-A β can serve as a nidus for and promoter of aggregation of A β 1–40/42 was shown *in vitro* (Schilling *et al.*, 2006). The data presented in Fig. 7 now support that an inhibition of pGlu-formation exerts secondary effects on the A β aggregation and accumulation *in vivo*. Considering the high amounts of A β (3–40), which were injected in the cortex, the 5% pGlu-A β formation detected by ELISA analysis might trigger accumulation and, in turn, reduced degradation as revealed by the differences in the total A β staining in both hemispheres (Fig. 7a).

Further support for the seeding theory of pGlu-modified amyloid is also provided by studies of FDD, which have been shown that ADan, amyloid peptides carrying also N-terminal pGlu, which is generated from N-terminal glutamic acid, is co-deposited with A β peptides in FDD, strongly suggesting that ADan provokes the deposition of A β . Moreover, A β aggregation by seeding of ADan could be shown *in vitro* (Schilling *et al.*, 2006). Thus, the QC-catalyzed N-terminal pGlu-formation might represent a general concept leading to amyloid peptides displaying a massive seeding capacity and stability.

It is obvious that the immunohistological characterization of the injection sites (e.g. Fig. 3) shows a certain degree of variability in the staining intensity, levels of sectioning/

staining in relation to the bilateral injection sites, and corresponding pGlu production – the latter being revealed by N3pE immunoreactivity. When considering this with regard to the potential usefulness of this assay as a pharmacological screening tool, it is conceivable that quantification is hardly to accomplish. Major obstacles are that the injected A β -species tend to flow out of the injection area, especially when the corpus callosum is close to this area and that the immunoreactivity of the primary antibody in the tissue being followed by a secondary detection system do not allow a linear (or any other) prediction of the corresponding absolute amount of a certain immunogene (in this case pGlu-A β). Focusing on the bilateral injection sites, a semi-quantitative scoring appears possible and – probably more important for the present approach – local reactivity, cellular effects (microglia activation, etc.) might well be studied using these techniques in the future. Thus, while this reasoning provides sufficient justification for the application of immunohistochemical studies at the sites of microinjection, a more reliable quantification of the pGlu-A β production will remain a domain of the ELISA-based approach established in the present work. Together, both techniques (immunohistochemistry and ELISA) provide a basis for the further establishment of this approach for medium throughput screening of compounds modulating pGlu-A β production. From this point of view, the present experimental approach provides an excellent tool to characterize the efficacy of QC-inhibitors to suppress the pGlu-A β formation *in situ* and thus enables an efficient profiling of QC inhibitors for future studies *in vivo*. The apparent conservation of the QC enzymatic properties between human and other mammalian species, as revealed here for rat QC for the first time, supports the reliability of rodent animal models for the studies aiming at the pGlu-peptide formation in general.

Acknowledgements

We thank S. Kuhlmann, S. Fassbender, and A. Stephan for their technical assistance. This work was supported by the German Federal Department of Education, Science and Technology, BMBF grant no. 3013185 to HUD.

Supplementary material

The following supplementary material is available for this article:

Fig. S1 Sequence alignment of human and rat QC.

Fig. S2 Purification of mature rat QC: rat QC was recombinantly expressed in *Pichia pastoris*.

This material is available as part of the online article from: <http://www.blackwell-synergy.com/doi/abs/10.1111/j.1471-4159.2008.05471.x> (This link will take you to the article abstract).

Please note: Blackwell Publishing are not responsible for the content or functionality of any supplementary materials supplied by the authors. Any queries (other than missing material) should be directed to the corresponding author for the article.

References

- Bockers T. M., Kreutz M. R. and Pohl T. (1995) Glutaminyl-cyclase expression in the bovine/porcine hypothalamus and pituitary. *J. Neuroendocrinol.* **7**, 445–453.
- Buchholz M., Heiser U., Schilling S., Niestroj A. J., Zunkel K. and Demuth H. U. (2006) The first potent inhibitors for human glutaminyl cyclase: synthesis and structure-activity relationship. *J. Med. Chem.* **49**, 664–677.
- Casas C., Sergeant N., Itier J. M. *et al.* (2004) Massive CA1/2 neuronal loss with intraneuronal and N-terminal truncated Abeta42 accumulation in a novel Alzheimer transgenic model. *Am. J. Pathol.* **165**, 1289–1300.
- Chelius D., Jing K., Lueras A., Rehder D. S., Dillon T. M., Vizeal A., Rajan R. S., Li T., Treuheit M. J. and Bondarenko P. V. (2006) Formation of pyroglutamic acid from N-terminal glutamic acid in immunoglobulin gamma antibodies. *Anal. Chem.* **78**, 2370–2376.
- Cynis H., Schilling S., Bodnar M., Hoffmann T., Heiser U., Saido T. C. and Demuth H. U. (2006) Inhibition of glutaminyl cyclase alters pyroglutamate formation in mammalian cells. *Biochim. Biophys. Acta* **1764**, 1618–1625.
- Dick L. W. Jr, Kim C., Qiu D. and Cheng K. C. (2007) Determination of the origin of the N-terminal pyro-glutamate variation in monoclonal antibodies using model peptides. *Biotechnol. Bioeng.* **97**, 544–553.
- Guntert A., Döbeli H. and Böhrmann B. (2006) High sensitivity analysis of amyloid-beta peptide composition in amyloid deposits from human and PS2APP mouse brain. *Neuroscience* **143**, 461–475.
- Harigaya Y., Saido T. C., Eckman C. B., Prada C.-J., Shoji M. and Younkin S. G. (2000) Amyloid β protein starting pyroglutamate at position 3 is a major component of the amyloid deposits in the Alzheimer's disease brain. *Biochem. Biophys. Res. Commun.* **276**, 422–427.
- Hashimoto T., Wakabayashi T., Watanabe A. *et al.* (2002) CLAC: a novel Alzheimer amyloid plaque component derived from a transmembrane precursor, CLAC-P/collagen type XXV. *EMBO J.* **21**, 1524–1534.
- He W. and Barrow C. J. (1999) The A beta 3-pyroglutamyl and 11-pyroglutamyl peptides found in senile plaque have greater beta-sheet forming and aggregation propensities *in vitro* than full-length A beta. *Biochemistry* **38**, 10871–10877.
- von Horsten S., Schmitt I., Nguyen H. P. *et al.* (2003) Transgenic rat model of Huntington's disease. *Hum. Mol. Genet.* **12**, 617–624.
- Hosoda R., Saido T. C., Otvos L. J., Arai T., Mann D. M., Lee V. M., Trojanowski J. Q. and Iwatsubo T. (1998) Quantification of modified amyloid beta peptides in Alzheimer disease and Down syndrome brains. *J. Neuropathol. Exp. Neurol.* **57**, 1089–1095.
- Iwatsubo T., Odaka A., Suzuki N., Mizusawa H., Nukina N. and Ihara Y. (1994) Visualization of A beta 42(43) and A beta 40 in senile plaques with end-specific A beta monoclonals: evidence that an initially deposited species is A beta 42(43). *Neuron* **13**, 45–53.
- Iwatsubo T., Saido T. C., Mann D. M., Lee V. M. and Trojanowski J. Q. (1996) Full-length amyloid-beta (1-42(43)) and amino-terminally modified and truncated amyloid-beta 42(43) deposit in diffuse plaques. *Am. J. Pathol.* **149**, 1823–1830.
- Jarrett J. T., Berger E. P. and Lansbury P. T. Jr (1993) The carboxy terminus of the beta amyloid protein is critical for the seeding of amyloid formation: implications for the pathogenesis of Alzheimer's disease. *Biochemistry* **32**, 4693–4697.
- Kalback W., Watson M. D., Kokjohn T. A. *et al.* (2002) APP transgenic mice Tg2576 accumulate Abeta peptides that are distinct from the chemically modified and insoluble peptides deposited in Alzheimer's disease senile plaques. *Biochemistry* **41**, 922–928.

- Kask A., Nguyen H. P., Pabst R. *et al.* (2001) Neuropeptide Y Y1 receptor-mediated anxiolysis in the dorsocaudal lateral septum: functional antagonism of corticotropin-releasing hormone-induced anxiety. *Neuroscience* **104**, 799–806.
- Kawarabayashi T., Younkin L. H., Saido T. C., Shoji M., Ashe K. H. and Younkin S. G. (2001) Age-dependent changes in brain, CSF, and plasma amyloid (beta) protein in the Tg2576 transgenic mouse model of Alzheimer's disease. *J. Neurosci.* **21**, 372–381.
- Kuo Y. M., Emmerling M. R., Woods A. S., Cotter R. J. and Roher A. E. (1997) Isolation, chemical characterization, and quantitation of A beta 3-pyroglutamyl peptide from neuritic plaques and vascular amyloid deposits. *Biochem. Biophys. Res. Commun.* **237**, 188–191.
- Kuo Y. M., Kokjohn T. A., Beach T. G. *et al.* (2001) Comparative analysis of amyloid-beta chemical structure and amyloid plaque morphology of transgenic mouse and Alzheimer's disease brains. *J. Biol. Chem.* **276**, 12991–12998.
- Lemere C. A., Blusztajn J. K., Yamaguchi H., Wisniewski T., Saido T. C. and Selkoe D. J. (1996) Sequence of deposition of heterogeneous amyloid beta-peptides and APO E in Down syndrome: implications for initial events in amyloid plaque formation. *Neurobiol. Dis.* **3**, 16–32.
- Maeda J., Ji B., Irie T. *et al.* (2007) Longitudinal, quantitative assessment of amyloid, neuroinflammation, and anti-amyloid treatment in a living mouse model of Alzheimer's disease enabled by positron emission tomography. *J. Neurosci.* **27**, 10957–10968.
- McGowan E., Pickford F., Kim J. *et al.* (2005) Abeta42 is essential for parenchymal and vascular amyloid deposition in mice. *Neuron* **47**, 191–199.
- McGowan E., Eriksen J. and Hutton M. (2006) A decade of modeling Alzheimer's disease in transgenic mice. *Trends Genet.* **22**, 281–289.
- Miravalle L., Calero M., Takao M., Roher A. E., Ghetti B. and Vidal R. (2005) Amino-terminally truncated Abeta peptide species are the main component of cotton wool plaques. *Biochemistry* **44**, 10810–10821.
- Mori H., Takio K., Ogawara M. and Selkoe D. J. (1992) Mass spectrometry of purified amyloid beta protein in Alzheimer's disease. *J. Biol. Chem.* **267**, 17082–17086.
- Paxinos G. and Watson C. (2007). *The Rat Brain in Stereotaxic Coordinates, Compact*, 6th ed, CD-Rom. Academic Press, San Diego, CA.
- Piccini A., Russo C., Gliozzi A. *et al.* (2005) β -Amyloid is different in normal aging and in Alzheimer disease. *J. Biol. Chem.* **280**, 34186–34192.
- Pohl T., Zimmer M., Mugele K. and Spiess J. (1991) Primary structure and functional expression of a glutaminyl cyclase. *Proc. Natl Acad. Sci. USA* **88**, 10059–10063.
- Roher A. E., Palmer K. C., Yurewicz E. C., Ball M. J. and Greenberg B. D. (1993) Morphological and biochemical analyses of amyloid plaque core proteins purified from Alzheimer disease brain tissue. *J. Neurochem.* **61**, 1916–1926.
- Russo C., Schettini G., Saido T. C., Hulette C., Lippa C., Lannfelt L., Ghetti B., Gambetti P., Tabaton M. and Teller J. K. (2000) Presenilin-1 mutations in Alzheimer's disease. *Nature* **405**, 531–532.
- Saido T. C. (1998) Alzheimer's disease as proteolytic disorders: anabolism and catabolism of beta-amyloid. *Neurobiol. Aging* **19**, S69–S75.
- Saido T. C., Iwatsubo T., Mann D. M., Shimada H., Ihara Y. and Kawashima S. (1995) Dominant and differential deposition of distinct beta-amyloid peptide species, A beta N3(pE), in senile plaques. *Neuron* **14**, 457–466.
- Saido T. C., Yamao H., Iwatsubo T. and Kawashima S. (1996) Amino- and carboxyl-terminal heterogeneity of beta-amyloid peptides deposited in human brain. *Neurosci. Lett.* **215**, 173–176.
- Schilling S., Hoffmann T., Wermann M., Heiser U., Wasternack C. and Demuth H.-U. (2002) Continuous spectrometric assays for glutaminyl cyclase activity. *Anal. Biochem.* **303**, 49–56.
- Schilling S., Manhart S., Hoffmann T., Ludwig H.-H., Wasternack C. and Demuth H.-U. (2003a) Substrate specificity of glutaminyl cyclases from plants and animals. *Biol. Chem.* **384**, 1583–1592.
- Schilling S., Niestroj A. J., Rahfeld J.-U., Hoffmann T., Wermann M., Zunkel K., Wasternack C. and Demuth H.-U. (2003b) Identification of human glutaminyl cyclase as a metalloenzyme: Inhibition by imidazole derivatives and heterocyclic chelators. *J. Biol. Chem.* **278**, 49773–49779.
- Schilling S., Hoffmann T., Manhart S., Hoffmann M. and Demuth H. U. (2004) Glutaminyl cyclases unfold glutamyl cyclase activity under mild acid conditions. *FEBS Lett.* **563**, 191–196.
- Schilling S., Cynis H., von Bohlen A., Hoffmann T., Wermann M., Heiser U., Buchholz M., Zunkel K. and Demuth H. U. (2005) Isolation, catalytic properties, and competitive inhibitors of the zinc-dependent murine glutaminyl cyclase. *Biochemistry* **44**, 13415–13424.
- Schilling S., Lauber T., Schaupp M., Manhart S., Scheel E., Bohm G. and Demuth H. U. (2006) On the seeding and oligomerization of pGlu-amyloid peptides (in vitro). *Biochemistry* **45**, 12393–12399.
- Selkoe D. J. (2001) Alzheimer's disease: genes, proteins, and therapy. *Physiol. Rev.* **81**, 741–766.
- Shin R. W., Bramblett G. T., Lee V. M. and Trojanowski J. Q. (1993) Alzheimer disease A68 proteins injected into rat brain induce codeposits of beta-amyloid, ubiquitin, and alpha 1-antichymotrypsin. *Proc. Natl Acad. Sci. USA* **90**, 6825–6828.
- Shin R. W., Lee V. M. and Trojanowski J. Q. (1994) Aluminum modifies the properties of Alzheimer's disease PHF tau proteins in vivo and in vitro. *J. Neurosci.* **14**, 7221–7233.
- Shin R. W., Ogino K., Kondo A., Saido T. C., Trojanowski J. Q., Kitamoto T. and Tateishi J. (1997) Amyloid beta-protein (Abeta) 1-40 but not Abeta1-42 contributes to the experimental formation of Alzheimer disease amyloid fibrils in rat brain. *J. Neurosci.* **17**, 8187–8193.
- Shirovani K., Tsubuki S., Lee H. J., Maruyama K. and Saido T. C. (2002) Generation of amyloid beta peptide with pyroglutamate at position 3 in primary cortical neurons. *Neurosci. Lett.* **327**, 25–28.
- Yu L., Vizel A., Huff M. B., Young M., Remmele R. L. Jr and He B. (2006) Investigation of N-terminal glutamate cyclization of recombinant monoclonal antibody in formulation development. *J. Pharm. Biomed. Anal.* **42**, 455–463.

Glutamyl cyclase inhibition attenuates pyroglutamate A β and Alzheimer's disease-like pathology

Stephan Schilling¹, Ulrike Zeitschel², Torsten Hoffmann¹, Ulrich Heiser¹, Mike Francke², Astrid Kehlen¹, Max Holzer², Birgit Hutter-Paier³, Manuela Prokesch³, Manfred Windisch³, Wolfgang Jagla⁴, Dagmar Schlenzig¹, Christiane Lindner⁵, Thomas Rudolph⁵, Gunter Reuter⁵, Holger Cynis¹, Dirk Montag⁶, Hans-Ulrich Demuth^{1,4} & Steffen Rossner²

Because of their abundance, resistance to proteolysis, rapid aggregation and neurotoxicity, N-terminally truncated and, in particular, pyroglutamate (pE)-modified A β peptides have been suggested as being important in the initiation of pathological cascades resulting in the development of Alzheimer's disease^{1–6}. We found that the N-terminal pE-formation is catalyzed by glutamyl cyclase *in vivo*. Glutamyl cyclase expression was upregulated in the cortices of individuals with Alzheimer's disease and correlated with the appearance of pE-modified A β . Oral application of a glutamyl cyclase inhibitor resulted in reduced A β _{3(pE)-42} burden in two different transgenic mouse models of Alzheimer's disease and in a new *Drosophila* model. Treatment of mice was accompanied by reductions in A β _{x-40/42}, diminished plaque formation and gliosis and improved performance in context memory and spatial learning tests. These observations are consistent with the hypothesis that A β _{3(pE)-42} acts as a seed for A β aggregation by self-aggregation and co-aggregation with A β _{1-40/42}. Therefore, A β _{3(pE)-40/42} peptides seem to represent A β forms with exceptional potency for disturbing neuronal function. The reduction of brain pE-A β by inhibition of glutamyl cyclase offers a new therapeutic option for the treatment of Alzheimer's disease and provides implications for other amyloidoses, such as familial Danish dementia.

The brains of individuals with Alzheimer's disease are characterized by the presence of neurofibrillary tangles and by deposits of A β in neocortical brain structures¹. Sequential β - and γ -secretase cleavage of the amyloid precursor protein (APP) liberates A β peptides, which have different amyloidogenicity and neurotoxicity^{1–3}. Glutamate at the N-terminus of truncated A β can be subsequently cyclized into pE, resulting in A β _{3(pE)-40/42} (refs. 4–6) and A β _{11(pE)-40/42} (refs. 7,8). This pE-modification of A β confers proteolytic resistance^{9,10} and loss of N-terminal charge, resulting in accelerated aggregation of A β _{3(pE)}

compared with unmodified A β ¹¹. In particular, A β _{3(pE)-42}, a major constituent of A β deposits in sporadic and familial Alzheimer's disease^{4,12}, is neurotoxic⁹. Thus, reduction of A β _{3(pE)-42} should promote A β proteolysis and could, in turn, prevent A β aggregation by clearance of a major nucleation factor and thereby enhance neuronal survival. Recently, we discovered that glutamyl cyclase is capable of catalyzing A β _{3(pE)-42} formation and that glutamyl cyclase inhibitors prevent A β _{3(pE)-42} generation *in vitro*^{13,14}. Here, we asked whether glutamyl cyclase expression is altered in the Alzheimer's disease brain and might therefore be involved in the generation of A β _{3(pE)} *in vivo* and whether chronic glutamyl cyclase inhibition affects A β deposition, gliosis and memory deficits in animal models of Alzheimer's disease.

Glutamyl cyclase is widely distributed in mammalian brain with considerable expression in the hippocampus and cortex^{15,16}. To assess whether glutamyl cyclase expression can be correlated with the generation of A β _{3(pE)-42} in Alzheimer's disease, we analyzed glutamyl cyclase mRNA and protein concentrations in human neocortical brain samples post mortem (Fig. 1a,b). Glutamyl cyclase mRNA and protein were upregulated in samples from individuals with Alzheimer's disease compared with samples from normal aging individuals. Moreover, significantly larger concentrations of A β _{3(pE)-42} were detected in samples from individuals with Alzheimer's disease compared with nondemented individuals, supporting a role for glutamyl cyclase in the generation of A β _{3(pE)-42} ($P < 0.05$; Fig. 1c). In contrast, ELISA analysis also revealed high total A β _{x-42} concentrations in aged controls (Fig. 1c). This observation was corroborated by immunohistochemistry (Fig. 1d). A β immunoreactivity was detected in the brain sections of all groups. In contrast, A β _{3(pE)-42} staining was absent in normal aging but was specific for Alzheimer's disease brain, where A β _{3(pE)-42} immunoreactivity was almost as high as total A β .

To substantiate the correlation of glutamyl cyclase expression and A β _{3(pE)-42} generation, we co-expressed APP and glutamyl cyclase in HEK293 cells. Glutamyl cyclase strongly accelerated the generation of A β _{3(pE)-42}. The A β _{3(pE)-42} formation is suppressed in a

¹Probiodrug AG, Weinbergweg 22, 06120 Halle/S., Germany. ²Paul Flechsig Institute for Brain Research, University of Leipzig, Jahnallee 59, 04109 Leipzig, Germany. ³JSW-CNS Research GmbH, Parkring 12, 8074 Grambach/Graz, Austria. ⁴Ingenium Pharmaceuticals GmbH, Fraunhoferstrasse 13, 82152 Munich-Martinsried, Germany. ⁵Institute of Biology, Department of Genetics, University of Halle-Wittenberg, Weinbergweg 10, 06120 Halle/S., Germany. ⁶Research Group Neurogenetics, Leibniz Institute for Neurobiology, Brennekestrasse 6, 39118 Magdeburg, Germany. Correspondence should be addressed to H.-U.D. (hans-ulrich.demuth@probiodrug.de).

Received 12 March; accepted 3 September; published online 28 September 2008; doi:10.1038/nm.1872

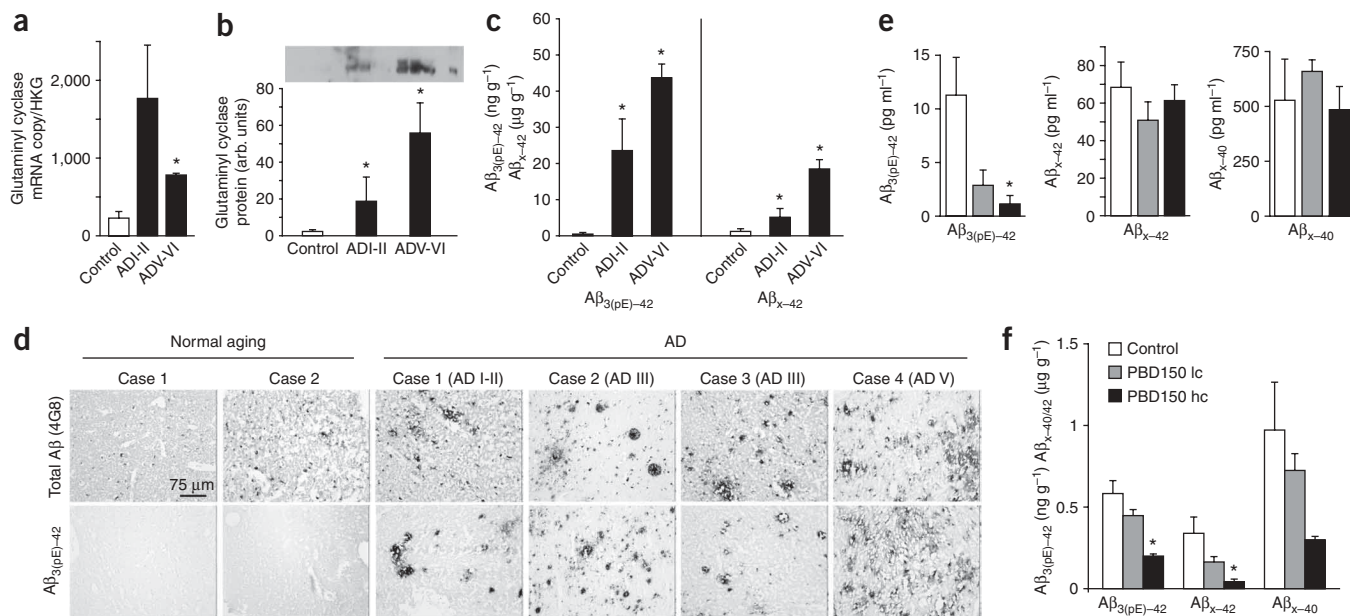


Figure 1 Glutaminyl cyclase expression and pE-A β in Alzheimer's disease: prevention of pE-A β formation by glutaminyl cyclase inhibition *in vitro* and *in vivo*. **(a)** Quantitative analysis of glutaminyl cyclase transcript levels. Total RNA from human neocortical brain samples (Brodmann area 22) was isolated from aged controls and individuals with Alzheimer's disease (Braak stages are indicated with Roman numerals). **(b)** Western blot analysis of the same cases and brain region as used for glutaminyl cyclase mRNA analysis. **(c)** Quantification of A $\beta_{3(pE)-42}$ and of A β_{1-42} concentrations from the samples in **a** and **b**, using ELISA analysis. **(d)** Immunohistochemical detection of total A β peptides with 4G8 and of A $\beta_{3(pE)-42}$ peptides in Brodmann area 22 from aged controls and individuals with Alzheimer's disease. Sparse A β plaques were detected in normal aging, but these deposits lacked A $\beta_{3(pE)-42}$ immunoreactivity. **(e)** Quantification of A β concentrations in conditioned media of HEK293 cells, which were transiently transfected with an APPsw/variant²⁹ and human glutaminyl cyclase. PBD150 was applied at 0.1 μ M (low concentration, PBD150 lc) and 1 μ M (high concentration, PBD150 hc) concentrations. The formation of A $\beta_{3(pE)-42}$, but not of A β_{x-42} and A β_{x-40} , was significantly reduced, substantiating the specificity of PBD150. **(f)** Quantification of A β concentrations in the brains of 10-month-old Tg2576 control mice and of age-matched littermates treated for 6 months with PBD150 at a concentration of 2.4 mg (PBD150 lc) or 7.2 mg (PBD150 hc) per g of food pellets. Only female mice were enrolled in the study ($n = 4$ per group). Data are expressed as mean \pm s.e.m. (* $P < 0.05$ versus control, one-way ANOVA followed by Tukey HSD).

dose-dependent manner by the glutaminyl cyclase inhibitor PBD150 (ref. 17). Notably, amyloidogenic processing was not influenced *per se*, as indicated by unchanged concentrations of A β_{x-42} and A β_{x-40} , demonstrating the specific effect of the compound on glutaminyl cyclase catalysis (Fig. 1e).

PBD150 did not affect the activities of proteases involved in A β degradation (such as insulin-degrading enzyme, neutral endopeptidase or aminopeptidase N) and in A β generation (beta-site APP cleaving enzyme1) (Supplementary Fig. 1 online).

Subsequently, we applied PBD150 orally to 4-month-old female Tg2576 mice for 6 months to study effects of glutaminyl cyclase inhibition on the concentrations of A $\beta_{3(pE)-42}$, A β_{x-42} and A β_{x-40} in the insoluble A β pool (Supplementary Fig. 1). The compound was administered via implementation into food pellets and reached brain concentrations of at least 0.02 μ g per g of body weight, which corresponds to approximately half-maximal inhibition of glutaminyl cyclase. Pharmacokinetic evaluations gave no evidence for an accumulation of the compound in brain or other organs. Similar weight gain and mortality in treated and control groups indicated that PBD150 was well tolerated (data not shown).

We found a dose-dependent decrease of A $\beta_{3(pE)-42}$ by 23% for a low dose of PBD150 and by 65% for a high dose of PBD150 (Fig. 1f). A $\beta_{3(pE)-42}$ reduction alleviated A β_{x-42} and A β_{x-40} concentrations in a dose-dependent manner (Fig. 1f). These initial findings suggest that A $\beta_{3(pE)-42}$ generation is mediated by glutaminyl cyclase *in vivo* and that there is a relationship between A $\beta_{3(pE)-42}$ and the aggregation of total A β .

To assess whether glutaminyl cyclase inhibition could abrogate the accumulation of A $\beta_{3(pE)-42}$, A β_{x-42} and A β_{x-40} , we initiated long-term treatment of Tg2576 mice at 6 months of age and continued it for 10 months. Tg2576 mice start to develop plaques by the age of 10–12 months. At the end of the study, untreated mice were expected to show profound plaque burden and behavioral impairment. The effects of PBD150 on total A β and A $\beta_{3(pE)-42}$ essentially resembled those seen in the younger mice treated from months 4 to 10. The reduction of A $\beta_{3(pE)-42}$ by 26% and 52% after application of PBD150 at a low and high dose, respectively, was accompanied by a significant and dose-dependent lowering of A β_{x-42} (by 45% and by 75%) and A β_{x-40} (by 31% and by 66%) ($P < 0.05$; Fig. 2a).

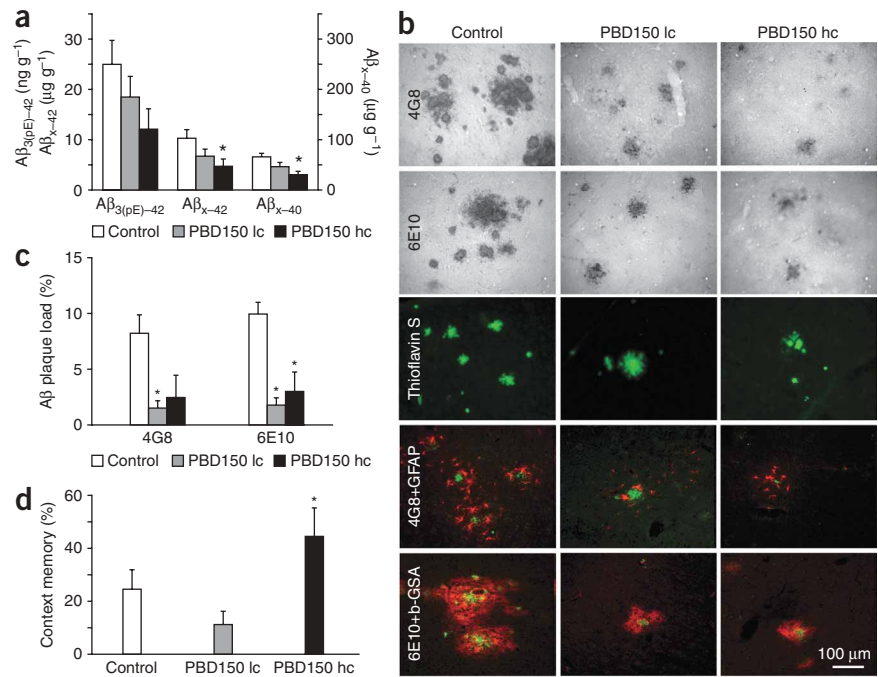
Immunohistochemistry revealed diminished cortical plaque formation after PBD150 treatment (Fig. 2b,c). Moreover, the load of cored plaques detected by thioflavin-S staining was reduced by PBD150 treatment (Fig. 2b), again supporting a modulating role for A $\beta_{3(pE)-42}$ in A β aggregation. The decrease in plaque load was accompanied by alleviated plaque-associated inflammation, involving both glial fibrillary acidic protein (GFAP)-immunoreactive astrocytes and biotin-GSA-labeled microglial cells (Fig. 2b).

Notably, no significant differences in concentrations of soluble A β_{x-40} or A β_{x-42} were observed in any of the treatment procedures (analysis of variance (ANOVA), $F_{2,27} = 0.890$, $P = 0.423$, data not shown), effectively ruling out a direct effect of PBD150 on A β production. Similarly, the expression of APP and its secretory processing were not affected by glutaminyl cyclase inhibition in Tg2576 organotypic brain slice cultures (Supplementary Fig. 2 online).

Figure 2 Effects of glutaminy cyclase inhibition on Tg2576 mice. **(a)** Quantification of A β concentrations in the brains of 16-month-old Tg2576 control mice and of age-matched littermates treated for 10 months (prophylactic treatment) with PBD150 at a concentration of 2.4 mg (PBD150 lc) or 7.2 mg (PBD150 hc) per g of food pellets. Groups consisted of male and female mice ($n = 8-12$; control consisted of 5 females and 4 males, PBD150 lc consisted of 4 males and 4 females, PBD150 hc consisted of 6 males and 6 females). Data are expressed as mean \pm s.e.m. (* $P < 0.05$ versus control, one-way ANOVA followed by Tukey HSD).

(b) Immunohistochemical detection of A β plaques in 16-month-old control mice and of age-matched littermates treated for 10 months with PBD150, as described in **a**. Top, 3,3'-diaminobenzidine (DAB) staining of A β plaques with 4G8 and 6E10 antibodies. The reduced A β plaque burden was accompanied by diminished gliosis, as shown for the astrocytic (GFAP, red fluorescence) and microglial (bio-GSA, red fluorescence) labeling. The scale bar applies to all images. **(c)** The plaque load was significantly reduced, as shown by quantification of histochemical stainings. **(d)** Conditioned fear test performed at the end of the treatment

period. When only female mice were analyzed, there was significantly improved context fear memory (% immobile in context – novel) in mice treated with the high dose of PBD150 (44.2%) as compared with the control group (24.4%) and with the low dose PBD150 group (11.2%, $P = 0.0158$; ANOVA, $F_{2,13} = 3.901$, $P = 0.0471$, $n = 5-8$). Data are expressed as mean \pm s.e.m. (* $P < 0.05$ versus control, Fisher least-significant difference).



To evaluate the potential effect of glutaminy cyclase inhibition on animal behavior, we applied a conditioned fear procedure as employed recently to monitor age-dependent changes of context memory in Tg2576 mice¹⁸. In female mice, improvement of context memory was observed in the high-dose PBD150 group (44.2%), as compared with the control group (24.4%) and with the low-dose PBD150 group (11.2%, $P = 0.0158$) (ANOVA, $F_{2,13} = 3.901$, $P = 0.0471$; **Fig. 2d**). Only female mice were analyzed, because the constitution of the groups for behavioral analysis was inconsistent with respect to gender. Freezing behavior before conditioning or in a novel environment with or without a cued tone was not different between treated and untreated mice (with tone: untreated, 67.6%; low dose, 61.3%; high dose, 90.6%; $F_{2,13} = 2.488$, $P = 0.1217$; without tone: untreated, 47.5%; low dose, 56.6%; high dose, 34.3%; $F_{2,13} = 0.753$, $P = 0.4904$), indicating an effect of PBD150 specifically on context memory.

To determine the efficacy of PBD150 in mice with distinct plaque pathology, we orally treated 10-month-old female Tg2576 mice with PBD150 for 6 months in a third trial. A moderate reduction of cortical A $\beta_{3(pE)-42}$ (by 26% and 43% compared to 100% of the control group) was observed on treatment without effect on A β_{x-42} and A β_{x-40} peptides and on the total plaque load (**Supplementary Fig. 3** online). The microglial activation around plaques was reduced, as observed in the prophylactic treatment study (see **Fig. 2b**). Contextual fear conditioning showed a tendency toward dose-dependent improvement of cognition in the treated animals (**Supplementary Fig. 3**), although this improvement was not statistically significant. Freezing behavior before conditioning or in a novel environment with or without a cued tone was not different between treated and untreated mice (with tone: untreated, 71.5%; low dose, 61.0%; high dose, 60.2%; $F_{2,19} = 0.415$, $P = 0.6663$; without tone: untreated, 41.4%; low dose, 38.5%; high dose, 38.0%; $F_{2,19} = 0.038$, $P = 0.9628$).

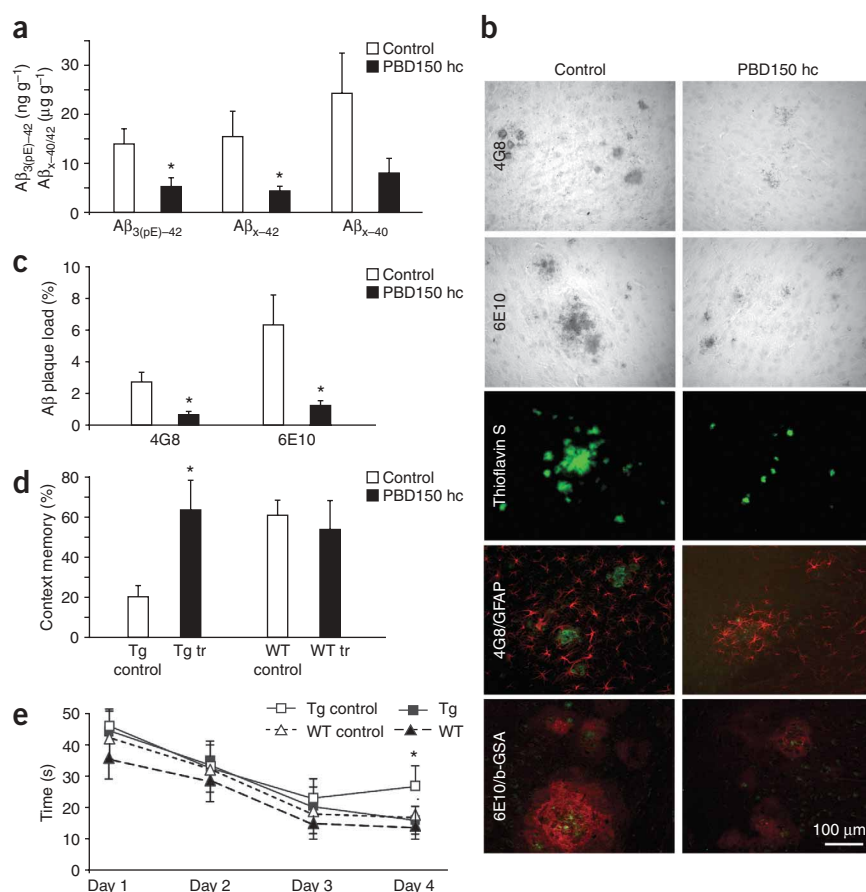
Taken together, the data of the three different studies in Tg2576 mice suggest that the *de novo* formation of A $\beta_{3(pE)-42}$ can be

influenced by glutaminy cyclase inhibition at any stage of the aggregation process, without substantial effect on previously formed deposits. This provides strong evidence for the concept of A $\beta_{3(pE)-42}$ acting as a seeding peptide species¹¹.

This conclusion was substantiated by PBD150 treatment of another transgenic mouse line, TASD-41, which is characterized by the neuron-specific overexpression of human APP751 with two familial Alzheimer's disease mutations (APP Swedish and APP London, APPsw/l mice). Because these mice develop A β plaques at 5 to 6 months of age, we treated them from months 4 to 7 with the high dose of PBD150 (7.2 mg per g food pellet), which was found to be efficient in Tg2576 mice. Similarly, PBD150 reduced the concentration of A $\beta_{3(pE)-42}$ by 58% and that of A β_{x-42} and A β_{x-40} by 61% and 54%, respectively (**Fig. 3a**). The plaque density in brains of TASD-41 mice was significantly diminished by 80% and accompanied by alleviated gliosis ($P < 0.05$; **Fig. 3b,c**).

PBD150 treatment resulted in a significant memory improvement of TASD-41 mice, but not of wild-type littermates, as measured by the freezing time in contextual fear conditioning ($P < 0.05$; **Fig. 3d**). After tone conditioning, the treated mice showed a tendency toward prolonged freezing, which, however, did not reach statistical significance (with tone: wild type untreated, 31.0%; wild type treated, 26.3%; TASD-41 untreated, 22.7%; TASD-41 treated, 47.3%; $F_{3,32} = 1.657$, $P = 0.1959$). In a Morris water maze, PBD150-treated TASD-41 mice showed reduced escape latency as compared with vehicle-treated mice, resulting in a performance that was virtually identical to that of wild-type littermates on the fourth day of training (**Fig. 3e**). Depending on the statistical analysis, the effect of treatment was significant at the fourth day of training (one-way ANOVA, followed by Newman-Keuls multiple comparison test). The effect lacked statistical significance, however, in factorial ANOVA analyzing the entire time of training. In an accompanying probe trial, all groups behaved similarly when the

Figure 3 Effects of glutaminyl cyclase inhibition on T ASD-41 mice. **(a)** Quantification of A β concentrations in the brains of 7-month-old T ASD-41 control mice and age-matched littermates treated for 3 months (prophylactic treatment) with PBD150 at a concentration of 7.2 mg (PBD150 hc) per g of food pellets. Groups consisted of male and female mice ($n = 4-5$). **(b)** Immunohistochemical detection of A β plaques in 7-month-old control mice and of age-matched littermates treated for 3 months as described in **a**. Top, DAB staining of A β plaques with 4G8 and 6E10 antibodies. The reduced A β plaque burden was accompanied by diminished gliosis, as shown for astrocytic (GFAP, red fluorescence) and microglial (bio-GSA, red fluorescence) labeling. The scale bar applies to all images. **(c)** The plaque load was significantly reduced, as shown by quantification of histochemical stainings. **(d)** Conditioned fear test performed at the end of the treatment period. There was significantly improved memory (percentage immobile in combined spatial and cued context – percentage in the novel environment) in T ASD-41 mice treated with PBD150 as compared with the control group ($n = 7-8$). Treatment of wild-type (WT) mice did not affect memory. Data are expressed as mean \pm s.e.m. ($*P < 0.05$ versus control, one-way ANOVA followed by Fisher least-significant difference). Male and female mice were analyzed. **(e)** Morris water maze of PBD150-treated and untreated T ASD-41 mice and wild-type littermates. Male and female mice were analyzed ($n = 7-8$). Data are expressed as mean \pm s.e.m. ($*P < 0.05$ versus control, one-way ANOVA followed by Newman-Keuls multiple comparison test). A factorial analysis applying two-way ANOVA did not reveal significance for treatment and treatment \times time interactions.



platform was removed (**Supplementary Fig. 4** online). PBD150 never affected the performance of wild-type mice or parameters such as the swimming speed, reflecting the specific effect of glutaminyl cyclase inhibition mediated via A $\beta_{3(pE)-42}$ reduction (**Fig. 3e**).

To prove the concept of seeding by pE-A β and to further exclude a nonspecific effect of PBD150, we generated transgenic *Drosophila* flies with neuron-specific expression of A β_{1-42} or A $\beta_{3(Q)-42}$ (**Fig. 4**). The expression constructs contained the A β sequence, which was

N-terminally fused to the prepro-sequence of murine thyroliiberin (TRH). Liberation of A β was accomplished by prohormone convertase processing in the secretory pathway (**Fig. 4a**). The generation of A β from these constructs was confirmed by ELISA and urea-PAGE western blotting following expression in S2 *Drosophila* cells (**Fig. 4b**). A 4-week treatment of transgenic flies with PBD150 led to a significant decrease of A $\beta_{3(pE)-42}$ ($P < 0.05$; **Fig. 4c**). On the other hand, total A β was not affected in flies expressing A β_{1-42} , suggesting that PBD150 specifically reduces pE-A β (**Fig. 4c**).

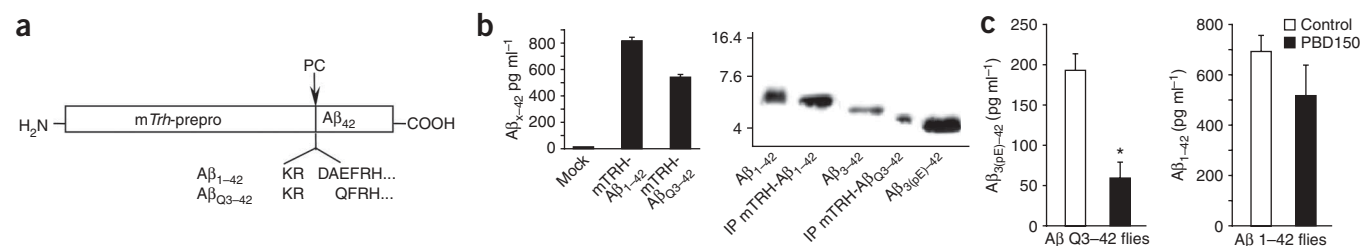


Figure 4 Glutaminyl cyclase inhibition diminishes A $\beta_{3(pE)-42}$ deposition in transgenic *Drosophila* flies. **(a)** Schematic representation of the constructs used for the generation of the N-terminal variants of A β in *Drosophila*. The expression constructs consisted of the A β sequence, which is fused to the C terminus of the murine TRH prepro-sequence. Processing of the preproprotein in the secretory pathway led to the release of A $\beta_{3(Q)-42}$, the direct precursor of A $\beta_{3(pE)-42}$ or of A β_{1-42} . **(b)** Expression of the A β constructs in S2 *Drosophila* cells. The expression led to significant increases in the A β concentrations in the conditioned media, as shown by immunoprecipitation and urea-PAGE followed by immunodetection of A $\beta_{3(pE)-42}$ and A β_{1-42} . **(c)** Treatment of transgenic *Drosophila* with PBD150. PBD150-supplemented agar (1 mM) was used for application. After 4 weeks of treatment, fly heads were collected and A β concentrations were determined by ELISA. A significant effect of treatment was observed with the flies expressing the precursor of A $\beta_{3(pE)-42}$. Data are expressed as mean \pm s.e.m. ($*P < 0.05$ versus control).

Previous work^{4,6,9,19} has suggested that N-terminally truncated and pE-modified A β contributes to the development of Alzheimer's disease, mainly by a boosted aggregation propensity^{11,20}. Such N-terminally truncated A β peptides are present at very early stages of Alzheimer's disease pathology^{4,10} and can be found in the cerebrospinal fluid (CSF) and plasma of individuals suffering from mild cognitive impairment several years before Alzheimer's disease diagnosis²¹. Notably, we found that only A $\beta_{3(pE)-42}$ brain tissue immunoreactivity was associated with Alzheimer's disease pathology, indicating that A $\beta_{3(pE)-42}$ probably contributes to amyloid deposition, thus influencing the progression of the disease (see Fig. 1). This has also been observed in early-onset Alzheimer's disease caused by presenilin mutations^{5,9}.

On the basis of the recently discovered capability of glutamyl cyclase to catalyze N-terminal pE formation from glutamic acid precursors^{13,14}, the upregulation of glutamyl cyclase in brains of individuals with Alzheimer's disease (Fig. 1) suggests that glutamyl cyclase is important for the generation of pE-A β peptides. Spontaneous N-terminal pE formation from glutamic acid, as has been recently suggested²², is very unlikely under physiological conditions, considering that the half life of glutamic acid is years to decades²³.

The coincidence of glutamyl cyclase overexpression, accumulation of pE-A β and progression of neurodegeneration in Alzheimer's disease strongly implies a disease-provoking function of A $\beta_{3(pE)}$. Inhibition of glutamyl cyclase represents a strategy for reducing A $\beta_{3(pE)-42}$ formation *in vivo*.

In contrast with our recent approach of injecting A $\beta_{3(E)-40}$ into rat brain²⁴, the Tg2576 and T ASD-41 mice showed relatively low levels of A $\beta_{3(pE)-42}$ (see Fig. 3), but high levels of A $\beta_{1-40/42}$ (refs. 25,26). In Tg2576 mice, we detected A $\beta_{3(pE)-42}$ by ELISA from 6 months of age onwards, and the first A $\beta_{3(pE)-42}$ immunoreactive plaques appeared at 12 months of age. During aging, A $\beta_{3(pE)-42}$ accumulated, but still represented only 0.1–0.5% of total A β . T ASD-41 mice developed plaques from 5 months of age onwards and had already revealed behavioral deficits at 6 months of age, which correlates to their relatively high levels of A β_{1-42} . In preceding experiments, we detected A $\beta_{3(pE)-42}$ at low concentrations, accounting for only 0.5% of the total A β . Therefore, these models allowed us to test the seeding hypothesis for A $\beta_{3(pE)-42}$. The reduction of insoluble A $\beta_{3(pE)-42}$ by 50% (~10 ng per g) resulted in the suppression of the prominent total A β by up to 75% (~30 μ g per g; Figs. 2–4), whose concentration is more than 1,000-fold higher than pE-A β . This finding provides strong evidence for A $\beta_{3(pE)-42}$ as a potential nidus of amyloidogenic aggregation^{11,24}. Direct evidence for the high seeding capacity of A $\beta_{3(pE)}$ was also obtained from *in vitro* co-aggregation of A $\beta_{3(pE)-40}$ and A β_{1-40} (see also Supplementary Fig. 5 online). This aggregation process was not affected by the glutamyl cyclase inhibitor PBD150 used in this study (Supplementary Fig. 5). In summary, all experimental data presented here are consistent with the hypothesis of pE-A β acting as a seeding peptide species in the amyloid cascade (Supplementary Fig. 6 online).

In addition, our results have implications for the inherited neurodegenerative amyloidoses familial British dementia and familial Danish dementia, which are caused by stop-codon or frame-shift mutations in the BRI gene (also known as ITM2B)²⁷. The so-called amyloid peptides ADan and ABri account for brain lesions that are similar to those seen in Alzheimer's disease. Virtually all of the deposited BRI peptides in these brains are modified by N-terminal pE. Apparently, these peptides also trigger A β deposition, acting as a seeding factor^{11,28}.

In mouse models with small amounts of A $\beta_{3(pE)-40/42}$ compared with Alzheimer's disease, glutamyl cyclase inhibition was shown to result in diminished A β plaque formation and gliosis, and improved

memory. If glutamyl cyclase inhibition is similarly efficacious in humans, this new approach may prove to be disease-modifying. In conclusion, prevention of pE formation at the N-terminus of peptides by inhibition of glutamyl cyclase represents a new therapeutic strategy for alleviating amyloidoses caused by the seeding of amyloidogenic peptides.

METHODS

Human brain tissue. The definite diagnosis of Alzheimer's disease for all cases used in this study was based on the presence of neurofibrillary tangles and neuritic plaques in the hippocampal formation and neocortical areas. Case recruitment and autopsy were approved by the Ethical Committee of Leipzig University (License# 063/2000), and informed consent was obtained from all subjects.

mRNA and western blot analysis for glutamyl cyclase. We carried out quantitative real-time PCR using the QuantiTect Primer Assay for QPCT (QT00013881, Qiagen) as well as the QuantiTect SYBR Green RT-PCR kit (Qiagen). Absolute transcript amounts were determined using external glutamyl cyclase standard DNA. We normalized against HPRT and GAPDH. For western blot analysis, we homogenized and ultrasonicated the tissue, and detected glutamyl cyclase using purified rabbit polyclonal antibodies that were raised against human glutamyl cyclase.

Cell culture. We cultured HEK293 cells in Dulbecco's modified Eagle's medium (10% fetal bovine serum). Cells were co-transfected with the APP695 variant APP-NLE²⁹ and human glutamyl cyclase using Lipofectamin2000 (Invitrogen) and were incubated for 24 h in the absence or presence of 0.1 μ M and 1.0 μ M of PBD150.

Animals. We housed Tg2576 mice (B6/SJL, human APPsw695-transgene) at a 12-h day/12-h night cycle with free access to tap water and food pellets supplemented with either no supplement (control), 2.4 mg PBD150 per g of pellet (low concentration) or 7.2 mg PBD150 per g of pellet (high concentration). Animals were treated for three different periods of time (Supplementary Fig. 1). Likewise, T ASD-41 mice^{26,30} (C57/Bl6 hybrid) were treated via food pellets supplemented with 7.2 mg PBD150 per g of pellet. Animal studies were approved by the local legal authorities 'Regierungspräsidium' of Leipzig (TVV40/04) and the 'Steiermärkische Landesregierung' (Departments 8C and 10A) of Graz (Authorizations 78JO 21_5 - 04 and 78JO 10_6 - 03).

Behavioral testing. For conditioned fear testing, we used two training trials. Mice were placed in an operant chamber, allowed to explore for 2 min and then given an auditory cue for 15 s and a foot shock for 2 s (1.5 mA unpulsed). The mice were returned to the same chamber (context) 24 h after training and freezing behavior (immobility) was recorded for 5 min. We transferred the mice to a novel environment 1 h later and freezing behavior (immobility) was recorded for 3 min. The auditory cue was then presented for 3 min and freezing behavior (immobility) was recorded. Freezing scores are expressed as a percentage for each portion of the test. The Morris water maze task was conducted in three trials on 4 consecutive days. The mouse had to find the hidden, diaphanous target during 1-min trials. After each trial, mice were allowed to rest on the platform for 10–15 s. Escape latency, pathway and presence of the mice in the platform quadrant were quantified. A probe trial, in which the platform was removed, was carried out on the fourth day of training (see Supplementary Methods online).

Immunochemical analysis of human and rodent brain samples. We quantified A β peptides in 2% SDS and formic acid fractions by sandwich ELISAs (IBL). We carried out immunohistochemical stainings, applying the A $\beta_{3(pE)}$ -specific antibody (Clone 6, mouse monoclonal antibody, dilution 1:2,500) and the A β -specific antibody (4G8 mouse monoclonal antibody, dilution 1:2,500, Calbiochem) using fixed human tissue (HOPE-fixation, DCS Innovative Diagnostic Systems). For immunodetection, we used a biotinylated mouse-specific IgG (BA 9200, Vector Laboratories), followed by diaminobenzidine staining (Vectastain ABC-Kit, Vector Laboratories). Immunohistochemistry in the mouse brain was performed using the antibodies 6E10 (Chemicon) and

biotinylated antibody 4G8 (Signet), coupled with secondary horseradish peroxidase-conjugated antibodies and the diaminobenzidine reaction. In dual fluorescent immunolabeling procedures, we detected microglial cells with biotinylated lectin *Griffonia simplicifolia* agglutinin isolectin B4 (bio-GSA, Sigma). Depending on the A β double-labeling procedure, we visualized astrocytes with mouse GFAP-specific or with rabbit GFAP-specific antibodies (both from Sigma). Brain sections were incubated with cocktails of primary antibodies from different species overnight at 4 °C and then visualized using fluorochromated secondary antibodies.

Generation of transgenic *Drosophila*. We cloned prepro-mTRH-A β constructs encoding A β ₁₋₄₂ and A β _{3(Q)-42} into a pUAST expression vector containing P element repeats and *white* as a marker gene. The insertion of the DNA into germ-line chromosomes was mediated by P element transposase. We then selected transgenic lines in the F2 generation. For transgene production, we used a *white*-isogenized *Drosophila* line. Males from five different transgenic lines expressing A β ₁₋₄₂ or A β _{3(Q)-42} were crossed to females of driver line P{GawB}elav^{C155} (Bloomington Stock 458). At the age ~50 d, we collected 100 transgenic flies and determined the A β content by ELISA.

Statistical analysis. We used one-way ANOVA followed by Tukey's honestly significantly different (HSD) test for analyzing the A β ELISAs. We evaluated the conditioned fear data by one-way ANOVA followed by *post hoc* analysis using Fisher protected least-significant difference and Scheffé's tests. For multiple comparisons, $P = 0.5/k$, with k being the number of comparisons that were considered to be significant (Bonferroni-Dunn test). For the Morris water maze data, we applied one- and two-way ANOVA followed by *post hoc* analysis using Newman-Keuls multiple comparison test if significance was obtained in ANOVA.

Note: Supplementary information is available on the Nature Medicine website.

ACKNOWLEDGMENTS

We thank K. Sowa, R. Jendrek, K. Schulz, M. Bornack, E. Scheel and M. Buchholz for technical assistance. The authors would like to express their gratitude to K. Hsiao (University of Minnesota) for kindly providing Tg2576 mice and E. Masliah (University of California, San Diego) for providing the TAD-41 mice. Thanks are due to T.C. Saido (Riken Brain Science Institute) for the gift of the APP-NLE vector. S. Winter maintained and analyzed organotypic brain slice cultures from Tg2576 mice. We are also grateful to J. Heins for statistical analysis and to M.T. Stubbs, K. Glund and M. Hartlage-Rübsamen for helpful discussion. This work was supported by German Federal Department of Education, Science and Technology BMBF grant #3013185 to H.-U.D.

AUTHOR CONTRIBUTIONS

T.H., S.S. and S.R. planned most of the experiments. S.S., H.C., T.H., A.K., D.S. and U.H. conducted most of the biochemical and cell biological investigations. S.S., A.K., W.J., M.F. and M.H. analyzed the human brain tissue. U.Z. and S.R. carried out the Tg2576 mouse experiments. M.P., B.H.-P. and M.W. performed the TAD-41 mouse experiments. D.M. conducted the behavioral analysis of Tg2576. C.L., T.R. and G.R. generated the transgenic *Drosophila* lines. S.R., S.S. and H.-U.D. designed the study and wrote the manuscript. H.-U.D. initiated the research and supervised the program.

COMPETING INTERESTS STATEMENT

The authors declare competing financial interests: details accompany the full-text HTML version of the paper at <http://www.nature.com/naturemedicine/>.

Published online at <http://www.nature.com/naturemedicine/>

Reprints and permissions information is available online at <http://npg.nature.com/reprintsandpermissions/>

- Hardy, J.A. & Higgins, G.A. Alzheimer's disease: the amyloid cascade hypothesis. *Science* **256**, 184–185 (1992).

- Iwatsubo, T. *et al.* Visualization of A β 42(43) and A β 40 in senile plaques with end-specific A β monoclonals: evidence that an initially deposited species is A β 42(43). *Neuron* **13**, 45–53 (1994).
- Iwatsubo, T., Mann, D.M., Odaka, A., Suzuki, N. & Ihara, Y. Amyloid beta protein (A β) deposition: A β 42(43) precedes A β 40 in Down syndrome. *Ann. Neurol.* **37**, 294–299 (1995).
- Saido, T.C. *et al.* Dominant and differential deposition of distinct β -amyloid peptide species, A β N3(pE), in senile plaques. *Neuron* **14**, 457–466 (1995).
- Russo, C. *et al.* Presenilin-1 mutations in Alzheimer's disease. *Nature* **405**, 531–532 (2000).
- Saido, T.C., Yamao, H., Iwatsubo, T. & Kawashima, S. Amino- and carboxyl-terminal heterogeneity of β -amyloid peptides deposited in human brain. *Neurosci. Lett.* **215**, 173–176 (1996).
- Naslund, J. *et al.* Relative abundance of Alzheimer A β amyloid peptide variants in Alzheimer disease and normal aging. *Proc. Natl. Acad. Sci. USA* **91**, 8378–8382 (1994).
- Liu, K. *et al.* Characterization of A β 11–40/42 peptide deposition in Alzheimer's disease and young Down's syndrome brains: implication of N-terminally truncated A β species in the pathogenesis of Alzheimer's disease. *Acta Neuropathol.* **112**, 163–174 (2006).
- Russo, C. *et al.* PE-modified amyloid β -peptides–A β N3(pE)–strongly affect cultured neuron and astrocyte survival. *J. Neurochem.* **82**, 1480–1489 (2002).
- Saido, T.C. Alzheimer's disease as proteolytic disorders: anabolism and catabolism of β -amyloid. *Neurobiol. Aging* **19**, S69–S75 (1998).
- Schilling, S. *et al.* On the seeding and oligomerization of pGlu-amyloid peptides (*in vitro*). *Biochemistry* **45**, 12393–12399 (2006).
- Miravalle, L. *et al.* Amino-terminally truncated A β peptide species are the main component of cotton wool plaques. *Biochemistry* **44**, 10810–10821 (2005).
- Schilling, S., Hoffmann, T., Manhart, S., Hoffmann, M. & Demuth, H.-U. Glutamyl cyclases unfold glutamyl cyclase activity under mild acid conditions. *FEBS Lett.* **563**, 191–196 (2004).
- Cynis, H. *et al.* Inhibition of glutamyl cyclase alters pE formation in mammalian cells. *Biochim. Biophys. Acta* **1764**, 1618–1625 (2006).
- Pohl, T., Zimmer, M., Mugele, K. & Spiess, J. Primary structure and functional expression of a glutamyl cyclase. *Proc. Natl. Acad. Sci. USA* **88**, 10059–10063 (1991).
- Sykes, P.A., Watson, S.J., Temple, J.S. & Bateman, R.C.J. Evidence for tissue-specific forms of glutamyl cyclase. *FEBS Lett.* **455**, 159–161 (1999).
- Buchholz, M. *et al.* The first potent inhibitors for human glutamyl cyclase: synthesis and structure-activity relationship. *J. Med. Chem.* **49**, 664–677 (2006).
- Jacobsen, J.S. *et al.* Early-onset behavioral and synaptic deficits in a mouse model of Alzheimer's disease. *Proc. Natl. Acad. Sci. USA* **103**, 5161–5166 (2006).
- Piccini, A. *et al.* β -amyloid is different in normal aging and in Alzheimer disease. *J. Biol. Chem.* **280**, 34186–34192 (2005).
- Pike, C.J., Overman, M.J. & Cotman, C.W. Amino-terminal deletions enhance aggregation of β -amyloid peptides *in vitro*. *J. Biol. Chem.* **270**, 23895–23898 (1995).
- Vanderstichele, H. *et al.* Amino-truncated β -amyloid42 peptides in cerebrospinal fluid and prediction of progression of mild cognitive impairment. *Clin. Chem.* **51**, 1650–1660 (2005).
- Hashimoto, T. *et al.* CLAC: a novel Alzheimer amyloid plaque component derived from a transmembrane precursor, CLAC-P/collagen type XXV. *EMBO J.* **21**, 1524–1534 (2002).
- Yu, L. *et al.* Investigation of N-terminal glutamate cyclization of recombinant monoclonal antibody in formulation development. *J. Pharm. Biomed. Anal.* **42**, 455–463 (2006).
- Schilling, S. *et al.* Inhibition of glutamyl cyclase prevents pGlu-A β formation after intracortical/hippocampal microinjection *in vivo/in situ*. *J. Neurochem.* **106**, 1225–1236 (2008).
- Kawarabayashi, T. *et al.* Age-dependent changes in brain, CSF, and plasma amyloid (β) protein in the Tg2576 transgenic mouse model of Alzheimer's disease. *J. Neurosci.* **21**, 372–381 (2001).
- Rockenstein, E., Mallory, M., Mante, M., Sisk, A. & Masliah, E. Early formation of mature amyloid- β protein deposits in a mutant APP transgenic mouse depends on levels of A β (1–42). *J. Neurosci. Res.* **66**, 573–582 (2001).
- Ghisso, J. *et al.* Chromosome 13 dementia syndromes as models of neurodegeneration. *Amyloid* **8**, 277–284 (2001).
- Tomidokoro, Y. *et al.* Familial Danish dementia: co-existence of Danish and Alzheimer amyloid subunits (ADAN AND A β) in the absence of compact plaques. *J. Biol. Chem.* **280**, 36883–36894 (2005).
- Shirogami, K., Tsubuki, S., Lee, H.J., Maruyama, K. & Saido, T.C. Generation of amyloid beta peptide with pE at position 3 in primary cortical neurons. *Neurosci. Lett.* **327**, 25–28 (2002).
- Hutter-Paier, B. *et al.* The ACAT inhibitor CP-113,818 markedly reduces amyloid pathology in a mouse model of Alzheimer's disease. *Neuron* **44**, 227–238 (2004).

Enhancing a Chemokine's Fate for Degradation: A Novel Therapy for Cardiovascular Disease

Holger Cynis¹, Torsten Hoffmann¹, Susanne Manhart¹, Katrin Gans¹, Martin Kleinschmidt¹, Jens-Ulrich Rahfeld¹, Reinhard Sedlmeier², Anke Müller², Sigrid Graubner², Ulrich Heiser¹, Astrid Kehlen¹, Daniel Friedrich¹, Raik Wolf¹, Paul H.A. Quax³, Mikael Thomsen¹, Stephan Schilling¹ & Hans-Ulrich Demuth¹

¹Probiodrug AG, Weinbergweg 22, 06120 Halle/Saale, Germany. ²Ingenium Pharmaceuticals, Fraunhoferstrasse 13, 82152 Martinsried, Germany. ³Gaubius Laboratory, TNO Quality of Life, P.O. Box 2215, 2301CE Leiden, The Netherlands

Correspondence should be addressed to S.S. (stephan.schilling@probiodrug.de)

One-sentence summary

The enhancement of proteolytic degradation of the chemokine CCL2 (MCP-1) by inhibition of glutaminyl cyclase represents a novel therapeutic approach for a treatment of atherosclerosis and restenosis.

Abstract

Compelling evidence suggests a pivotal role of monocyte chemoattractant protein 1 (MCP-1, CCL2) in development of cardiovascular/coronary heart disease and inflammatory disorders. Here, we report a novel approach to inhibit the MCP-mediated migration of monocytes. Inhibition of glutaminy cyclase (QC) prevents the formation of a pyroglutamate (pGlu) residue at the N-terminus of CCL2. The mechanism enables additional proteolytic pathways for N-terminal cleavage of MCPs, resulting in decreased *in vivo* half-life and rapid inactivation of the peptides. Dipeptidyl peptidase 4 represents the major degrading enzyme of the immature CCL2 in human serum. The approach was validated in two different animal models involving MCP-mediated inflammatory processes, thioglycollate-induced peritonitis in mice and cuff-induced accelerated atherosclerosis in the ApoE3*Leiden mouse model. Application of the QC-inhibitor PBD150 reduced infiltrating monocytes significantly in both models. Moreover, PBD150 improved lumen stenosis and alleviated common signs of atherosclerotic pathology in ApoE3*Leiden mice. The modulation of chemokine maturation by inhibition of QC represents a novel approach for the treatment of cardiovascular disease/restenosis and provides implications for neuroinflammatory disorders involving CCL2-activity, e.g. Alzheimer's disease.

Introduction

Cardiovascular disease (CvD) is the leading cause of death in the western hemisphere and compelling evidence suggests an underlying inflammatory disease caused by a number of risk factors, such as hyperlipidemia, smoking and diabetes (1-3). Among others, the chemokine CCL2 (MCP-1) was found to play an important role in the development of CvD (4) and a number of studies have underlined the crucial role of CCL2 for the development of atherosclerosis in animal models (5, 6).

Upon secretion, CCL2 binds to glycosaminoglycans of the extracellular matrix building up a chemokine gradient, which is important for the attraction of immune cells to sites of inflamed tissue (7, 8). Importantly, structure/activity studies revealed that an intact N-terminus is crucial for the ability of CCL2 to attract monocytes. Artificial elongation or truncation of CCL2 leads to a loss of function, albeit receptor interaction is still observed (CCR2) (9-12). On the basis of these observations, receptor antagonists were developed (13), demonstrating efficacy in reducing atherosclerosis in different animal experiments (14, 15).

Naturally, a pyroglutamate (pGlu) residue constitutes the N-terminus of all human MCPs, protecting the peptides against degradation, which, in turn, stabilizes chemotactic activity (16). N-terminal pGlu-residues have been described for a number of hormones and secreted proteins, such as thyrotropin-releasing hormone (TRH), gonadotropin-releasing hormone (GnRH) and fibronectin (17, 18). It has been already shown for TRH and GnRH, that the pGlu-residue exerts a stabilizing function or is important for the hormonal activity (19, 20). Immature CCL8 (MCP-2), possessing an N-terminal glutamine-proline (Gln-Pro)-motif has been shown to underlie cleavage by dipeptidylpeptidase 4 (DP4/CD26) (21). Interestingly, all known human MCPs (CCL2, 7, 8, 13) reveal such a Gln-Pro-motif, rendering the peptides potentially prone to cleavage upon suppression of N-terminal pGlu-formation.

The blocked N-terminus is post-translationally formed from a glutaminyl precursor by glutaminyl cyclase (E.C. 2.3.2.5, QC) (22, 23) and inhibition of QC has been shown to prevent pGlu-peptide formation in mammalian cells (24, 25). Consequently, here we evaluated inhibition of QC to modulate CCL2 activity. By prevention of pGlu-formation, CCL2 is destabilized and alternative, additional degradation pathways are enabled. The importance of the findings is supported by the impact on the atherosclerotic pathology in a model of cuff-induced accelerated atherosclerosis in ApoE3*Leiden mice dosing QC-inhibitor for 14 days. The results might open a field of novel, specific anti-inflammatory drugs for the treatment of CCL2-related disorders.

Results

QC-inhibition provokes alternative pathways for degradation of CCL2 *in vitro*

In order to show, that human CCL2 is protected against N-terminal truncation by aminopeptidases, the immature (glutaminyll-) and mature (pyroglutamyl-) recombinant peptide was incubated with different proteolytic enzymes. The resulting products were analyzed using Maldi-TOF MS. Aminopeptidase P (ApP) and Dipeptidylpeptidase 4 (DP4) were chosen as model proteases, cleaving either pre- or post-proline in the penultimate position at the N-Terminus of the peptides, respectively (Fig. 1A). The incubation of CCL2(Q¹-76) with recombinant human DP4 led to a rapid generation of CCL2(D³-76). However, pre-incubation of CCL2(Q¹-76) with recombinant human QC generating CCL2(pGlu¹-76) prevents N-terminal truncation (Fig. S1A). Similar results were obtained using ApP, liberating the N-terminal glutamine from CCL2(Q¹-76) but not pGlu from CCL2(pGlu¹-76) (Fig. S1B). In addition, human CCL7, 8 and 13 - also containing pGlu in their mature state - are protected from truncation by DP4. The unblocked N-termini of these peptides are, however, all susceptible to truncation due to their conserved Gln-Pro-motif (Fig. 1A, Fig. S2A-C). Since the pGlu-residue at the N-terminus of CCL2 is generated by QC, the recently developed QC-inhibitor PBD150 was implemented into the *in vitro* studies (24). In presence of QC and PBD150, the incubation of CCL2(Q¹-76) with DP4 led to N-terminal truncation, whereas pre-incubation of CCL2(Q¹-76) with QC and subsequent DP4 application protects against degradation. In addition, application of QC in combination with PBD150 prevented the pGlu-formation at the N-terminus of CCL2(Q¹-76), making the N-terminus accessible for cleavage (Fig. 1B).

Naturally, CCL2 is N-terminally cleaved by matrix metalloproteinase 1 (MMP-1) (26). In contrast to cleavage by DP4 or ApP, incubation of CCL2(Q¹-76) with human synovial fibroblast derived MMP-1 resulted in liberation of Gln-Pro-Asp-Ala, generating CCL2(I⁵-76).

The cleavage is independent from the N-terminal modification, since CCL2(pGlu¹-76) is also processed by MMP-1. However, a faster processing of CCL2(Q¹-76) could be observed, apparent after 2h and 4h of incubation (Fig. S1C).

The potential of suppressing the N-terminal pGlu-formation to destabilize CCL2 was further demonstrated by co-incubation of DP4 and MMP-1. Naturally, MMP-1 and DP4 coexist within the circulation, however, only MMP-1 is able to degrade mature CCL2 (Fig. S1C). Accordingly, co-incubation of DP4 and MMP-1 with CCL2(pGlu¹-76) resulted in detection of CCL2(I⁵-76). In contrast, the unblocked N-terminus allows both enzymes to degrade CCL2(Q¹-76), represented by the mass spectrometric detection of CCL2(I⁵-76) and CCL2(D³-76) (Fig. 1C). Thus, the unblocked N-terminus results in much faster degradation of CCL2. The effect becomes evident for CCL2(Q¹-76) after 2 hours, where the peptide is almost fully truncated, compared to the minimal turnover at the 2 hours time point for CCL2(pGlu¹-76), showing only a small portion of N-terminally truncated substrate (Fig. 1C).

Proline-specific dipeptidyl peptidases represent the major proteolytic activity degrading immature CCL2 in human serum

In order to characterize the stability of mature and immature CCL2, the peptide was incubated in human serum *ex vivo*. The resulting peptide pattern of CCL2(Q¹-76) revealed the presence of competing QC and protease activities, ending after 7 h with a ratio of approx. 60 % CCL2(D³-76) and 40 % CCL2(pGlu¹-76) (Fig. 2A). Importantly, CCL2(pGlu¹-76) was completely resistant to cleavage (Fig. 2B). The application of the DP4-inhibitor P32/98 to the serum suppressed an N-terminal cleavage of CCL2(Q¹-76), proving that immature CCL2(Q¹-76) is prone to alternative cleavage by DP4 or DP4-like activity in human serum (Fig. 2C). Concluding, QC-inhibition enables additional degradation pathways in the circulation resulting in a general destabilization and, in turn, perhaps to impaired chemokine function.

Truncation of CCL2 leads to diminished chemotactic function

The impact of N-terminal modification of CCL2 on its chemotactic potency was investigated using THP-1 monocytes in an *in vitro* assay for chemotaxis. In agreement with previous observations, the dose-response curves were bell-shaped. Here, CCL2(pGlu¹-76) and CCL2(Q¹-76) were found to be equally potent in attracting THP-1 monocytes, showing a maximum response at 50-100 ng/ml. However, the truncation of CCL2 by ApP (CCL2(P²-76)) and DP4 (CCL2(D³-76)) led to a shift of the dose-response curve to higher concentrations of CCL2 (500-1000 ng/ml), required to elicit the maximum response. Truncation of CCL2 by MMP-1 (CCL2(I⁵-76)) did not result in a shifted dose-response, but the maximum response was significantly reduced (Fig. 3), supporting previously published data (26).

In addition, the chemotactic potency of the other MCPs (CCL7, 8, 13) was compared to CCL2. The absence of the pGlu-residue does not grossly influence the chemotactic potency of CCL7 and CCL8 (Fig. S3B, C). In contrast, any alteration at the N-terminus of CCL13 diminished the chemotactic potential (Fig. S3D). A N-terminal truncation of CCL7, 8 and 13 by DP4 again reduced the activity to attract THP-1 monocytes (Fig. S4A-D).

Therefore, QC-inhibition prevents pGlu-formation at the N-terminus of CCL2 and the related chemokines resulting in general suppression of chemotaxis.

QC-inhibition reduces monocyte recruitment in a model of thioglycollate-induced peritonitis

In order to validate the presented concept *in vivo*, the effect of PBD150 treatment was evaluated in a model of thioglycollate-induced peritonitis in mice. The cellular composition of the peritoneal lavage fluid was determined with emphasis on infiltrating monocytes 4 h, 24 h and 72 hours after thioglycollate-challenge. PBD150 reduced the number of infiltrating monocytes to the peritoneum dose-dependently after 4 h (Fig. 4A). In addition, the presence

of Moma2-positive monocytes/macrophages was assessed 24 h and 72 h after thioglycollate application. QC inhibition reduced the number of Moma2-positive cells after 24 h significantly (Fig. 4B). A tendency to diminished numbers of Moma-2 positive cells was also observed 72 h after challenge (Fig. 4C). In addition to PBD150, several other inhibitors of QC attenuated the infiltration of monocytes to the peritoneum, effectively ruling out a compound-specific effect (not shown). Moreover, the application of PBD150 gave no evidence for an influence on the recruitment of granulocytes (Fig. 4D). Thus, the N-terminal destabilization of the MCPs by inhibition of QC has potential to directly effect the recruitment of monocytes *in vivo*.

PBD150 diminishes atherosclerosis-like pathology in ApoE3*Leiden mice.

The potential of QC-inhibition to ameliorate CCL-2 mediated disease conditions was further evaluated by treatment of ApoE3*Leiden mice. Accelerated atherosclerosis was triggered by cuff placement at the femoral artery of ApoE3*Leiden mice receiving a moderate western type of diet to reach plasma cholesterol levels of 12-15 mM. PBD150 was applied *via* the drinking water. Animals from a first group were sacrificed for the evaluation of cell adherence at and CCL2 expression in the vessel wall 2 days after cuff placement (early time point). In addition, another group of animals was sacrificed for investigating the effect of PBD150 on vascular remodelling, accelerated atherosclerosis and CCL2 expression at a late time point after 14 days.

Treatment of the mildly hypercholesterolemic ApoE3*Leiden mice with the QC-specific inhibitor PBD150 resulted in a profound reduction of total adhering cells by 45%, ($P < 0.05$) after 2 days. Specific analysis of adhering monocytes revealed an even stronger reduction by 67% ($P < 0.05$) at the cuffed vessel segments of the treated animals (Fig. 5A). A reduction of CCL2 expression was detected in the media and the intima of the vessel wall segment of the animals in the treated group 2 days after surgery (Fig. 5B,C). Analysis of the relative area of

the cross sections positive for CCL2 revealed a 52% ($P<0.01$) reduction of CCL2 expression in the media and a 36% ($P<0.001$) reduction in the intima (Figure 5C).

Apparently, the reduced adherence of monocytes after vascular surgery resulted in significant amelioration of lumen stenosis (Fig. 6A, D (arrows)) and neointimal area (Fig. 6B) after two weeks of treatment. Furthermore, the inhibitor reduced the area of the media (Fig. 6C) significantly. At the later time point of 14 days, when the neointima formation and accelerated atherosclerosis has progressed, the overall CCL2 expression is lower compared to the early time point (Fig. 6D). CCL2 did not differ between treated and untreated animals (Fig. 6E). Further analysis revealed tendencies to improvements in the intima/media ratio and remaining lumen (Fig. S5A,B). The treatment did not affect the total area within the outer diameter of the vessel segment (Fig. S5C) and the area of the intima (Fig. S5D).

Discussion

The results presented here introduce a novel mechanism to reduce the activity of CCL2 under different inflammatory conditions. In contrast to other approaches aimed to abolish CCL2 activity by, e.g. receptor antagonists or disruption of the MCP-gradient, the present trial focuses on influencing the maturation of the functionally important N-terminus of the MCPs. Importantly, the approach has proven efficacy in atherosclerosis-like pathology in a mouse model.

Several lines of evidence support a pivotal role of MCPs, in particular CCL2, in different disorders. For instance, the beneficial effect of an anti-CCL2 treatment strategy has been shown for pulmonary fibrosis and rheumatoid arthritis using CCL2 k.o. animals or applying a dominant negative CCR2 receptor antagonist (27, 28). In addition, cross-breeding of tg2576 mice, a model for Alzheimer's disease, with CCL2 over-expressing mice revealed a dramatic aggravation of plaque pathology (29). Therefore, an anti-CCL2 treatment might also be beneficial in diseases of the central nervous system. Especially in atherosclerotic and related restenotic models, the connection between circulating CCL2 and severity of the lesions has been proven (14, 15). According to a widely accepted hypothesis, CCL2 is the central mediator for monocyte infiltration in the vessel wall, initiating a cascade of events finally resulting in the formation of atherosclerotic lesions (30, 31). In this regard, anti-CCL2 therapies have been already proven efficacy in animal models with atherosclerosis-like pathology (6, 15, 32). With respect to reducing the CCL2 activity, the approach to modulate the pathways of maturation, in turn, facilitating the cleavage by ubiquitous protease(s) of the circulation represents a novel strategy. An reduction of the half-life of CCL-2 provides also potential advantage over specific receptor antagonists, since activation of additional CCL2-receptors(s), which have been described recently (33), would be influenced.

The finding that immature CCL2 undergoes cleavage by DP4 is in line with the potential role of DP4 to modulate plasma chemokine and hormone activity. For example, it has been shown that DP4 cleavage influences the activity of regulated upon activation, normal T-cell expressed, and secreted (RANTES) (16) or the incretins glucose-dependent insulintropic polypeptide (GIP) and glucagon-like peptide 1 (GLP-1) (34). The notion, that also human MCPs (CCL2, 7, 8, 13) might be potential DP4 substrates has been neglected due to the presence of an N-terminal pGlu-residue (16, 21). Caused by QC-inhibition and reduced N-terminal maturation, however, MCPs are rapidly inactivated by taking advantage of circulating proteolytic enzymes, such as DP4 or DP4-like enzymes. Thus, the concept is particularly based on expression of the potential degrading enzymes at the inflamed tissue, e.g. the vessel wall. In this regard, DP4 might turn out as the central degrading enzyme due to the ubiquitous expression and its abundance on epithelial tissue and smooth muscle cells (35, 36). Moreover, additional proline-specific aminopeptidases are present in plasma, e.g. ApP and fibroblast activation peptide (FAP), providing several different pathways for CCL2 inactivation upon an inhibition of pGlu-formation.

The specificity of CCL2 for monocytes offers the chance to interfere selectively with disease conditions related to chemotaxis and avoiding general suppression of immune function, which is supported here by the thioglycollate –induced peritonitis model (Figure 5). Moreover, besides MCPs, only human fractalkine has been described to contain an N-terminal pGlu residue. An important function of the moiety has not been described, permitting a specific suppression of MCP function by QC inhibition. Along these lines, up-regulation of QC and CCL2 has been reported in macrophages upon stimulation (37). The coincidence of CCL2 and QC expression thus further supports the crucial role of QC activity in CCL2 maturation. The suppression of QC activity following stimulation of CCL2 release, by, for instance coronary angioplasty, might therefore turn out as primary field for drug development. The plasma concentration of circulating CCL2 correlates with the development of restenosis

after coronary angioplasty (38). Normalizing CCL2 within 14 days appeared to be sufficient to prevent restenosis and improve patients condition prognosis (38).

Summarizing, compelling evidence suggests an underlying inflammatory response in the vast majority of acute and chronic diseases. Among others, CCL2 has been shown to be a major player in a number of disease conditions, stimulating monocyte migration, maturation and regulating the expression of other cytokines like IL-1, IL-6 and TNF- α (39, 40). Apparently, chemokines and cytokines operate as a network, reduction of one species has been shown to influence several others simultaneously, as for instance demonstrated in CCL2 knock out mice (41). These and our findings of the presented study support a novel anti-inflammatory strategy by inhibition of QC to alleviate atherosclerosis/restenosis and potentially Alzheimer's disease.

Figure Legends

Fig. 1. Absence of the N-terminal pGlu-residue renders MCPs susceptible to protease cleavage. (A) Alignment of the N-terminal sequences of CCL2, CCL7, CCL8 and CCL13. All human MCPs contain an N-terminal pyroglutamyl residue and display cleavage sites for ApP (1) and DP4 (2). In addition, CCL2 is processed by MMP-1 (3). (B) N-terminal degradation of human CCL2(Q¹-76) and CCL2(pGlu¹-76) by DP4. CCL2(pGlu¹-76) was generated from CCL2(Q¹-76) by QC catalysis. In addition, CCL2(Q¹-76) was incubated with human QC and the QC-specific inhibitor PBD150 (QC-I) followed by DP4 application. (C) Mass spectra after incubation of CCL2(pGlu¹-76) and CCL2(Q¹-76) with MMP-1 and DP4 at indicated time points.

Fig. 2. Serum-DP4 truncates immature CCL2 lacking the N-terminal pGlu-residue. Mass spectra after different incubation times of CCL2(Q¹-76) (A), CCL2(pGlu¹-76) (B) and CCL2(Q¹-76) in combination with DP4-inhibitor P32/98 (C) in human serum. The results suggest DP4 as a primary enzyme for the degradation of N-terminally immature CCL2 within the circulation.

Fig. 3. N-terminal truncation of CCL2 impairs its chemotactic function. The chemotactic potency of N-terminal variants of human CCL2 was evaluated in trans-well assays. The following peptides were applied to attract THP-1 monocytes: (Q¹-76) (closed circles), CCL2(pGlu¹-76) (open squares), CCL2(P²-76) (open triangles), CCL2(D³-76) (closed squares) and CCL2(I⁵-76) (open circles).

Fig. 4. QC-inhibition reduces the infiltration of monocytes to the peritoneum in a model of thioglycollate-induced peritonitis. (A) Relative numbers of monocytes in the peritoneal

lavage fluid 4 h after thioglycollate-challenge. A significant reduction of monocytes was observed after treatment with PBD150. In addition, Moma2-positive cells were decreased by PBD150 24h (B) and 72h (C) after thioglycollate-challenge. (D) Number of infiltrating granulocytes to the peritoneum in absence or presence of PBD150 treatment measured over a time period of 72 h. The dosage is outlined in the experimental section (ANOVA; *, P<0.05).

Fig. 5. Histopathological analysis of the cuffed vessel segments 2 days after cuff placement.

(A) Monocyte adhesion and total adhering cells 2 days after cuff placement.

Adhering and infiltrating cells per cross section in absence (black bars) or presence (open bars) of PBD150 treatment. The total number of adhering cells per cross section was counted in the cross section of the cuffed femoral arteries. Within the total population of adhering cells, a specific staining for monocytes/macrophages was applied using marker AIA31240 to identify the adhering and infiltrating monocytes (*, P<0.05, Student's *t*-test). (B) shows an example for CCL2- immunohistochemical staining of lesions after 2 days (black arrows). (C) In addition, the CCL2-positive area was calculated in cross sections within the media and neointima in absence (black bars) and presence (open bars) of PBD150 treatment (**, P<0.01, ***, P<0.001; Student's *t*-test).

Fig. 6. Morphometric analysis of the cuffed vessel segments 14 days after cuff placement. (A)

Degree of lumen stenosis in %, (B) neointima formation in μm^2 and (C) media thickness in μm^2 of the cuffed vessel segments of mice sacrificed after 14 days, treated in absence (black bars) and presence (open bars) of QC-inhibitor PBD150 (*, P<0.05; Student's *t*-test). (D) shows an example for CCL2 immunohistochemical staining of lesions 14 days after cuff-placement. The reduced lumen stenosis is illustrated by the black arrows. (E) The CCL2-positive area 14 days after cuff-placement was calculated in cross sections within the media and neointima in absence (black bars) and presence (open bars) of PBD150 treatment.

References and Notes

1. P. Libby, P. M. Ridker, A. Maseri, *Circulation* 105, 1135-1143 (2002).
2. P. Libby and P. Theroux, *Circulation* 111, 3481-3488 (2005).
3. R. Ross, *Am.Heart J.* 138, S419-S420 (1999).
4. I. F. Charo and M. B. Taubman, *Circ.Res.* 95, 858-866 (2004).
5. L. Gu et al., *Mol.Cell* 2, 275-281 (1998).
6. J. Gosling et al., *J. Clin.Invest.* 103, 773-778 (1999).
7. E. K. Lau et al., *J.Biol.Chem.* 279, 22294-22305 (2004).
8. A. E. Proudfoot et al., *Proc.Natl.Acad.Sci.U.S.A.* 100, 1885-1890 (2003).
9. P. Proost et al., *J Immunol.* 160, 4034-4041 (1998).
10. Y. J. Zhang, B. J. Rutledge, B. J. Rollins, *J.Biol.Chem.* 269, 15918-15924 (1994).
11. S. Masure, L. Paemen, P. Proost, J. Van Damme, G. Opdenakker, *J. Interferon Cytokine Res.* 15, 955-963 (1995).
12. S. Hemmerich et al., *Biochemistry* 38, 13013-13025 (1999).
13. Y. Zhang and B. J. Rollins, *Mol.Cell Biol.* 15, 4851-4855 (1995).
14. M. Usui et al., *FASEB J* 16, 1838-1840 (2002).
15. E. Mori et al., *Circulation* 105, 2905-2910 (2002).
16. J. Van Damme et al., *Chem. Immunol.* 72, 42-56 (1999).
17. B. Blomback, *Methods Enzymol.* 11, 398-411 (1967).
18. A. C. Awade, P. Cleuziat, T. Gonzales, J. Robert-Baudouy, *Proteins* 20, 34-51 (1994).
19. R. E. Morty, P. Bulau, R. Pelle, S. Wilk, K. Abe, *Biochem.J.* 394, 635-645 (2006).
20. G. N. Abraham and D. N. Podell, *Mol.Cell Biochem.* 38, 181-190 (1981).
21. E. Van Coillie et al., *Biochemistry* 37, 12672-12680 (1998).
22. W. H. Fischer and J. Spiess, *Proc.Natl.Acad.Sci.U.S.A.* 84, 3628-3632 (1987).
23. S. Schilling et al., *J.Biol.Chem.* 278, 49773-49779 (2003).
24. M. Buchholz et al., *J.Med.Chem.* 49, 664-677 (2006).
25. H. Cynis et al., *Biochim.Biophys.Acta* 1764, 1618-1625 (2006).
26. G. A. McQuibban et al., *Blood* 100, 1160-1167 (2002).

27. I. Inoshima et al., *Am.J.Physiol.Lung Cell.Mol.Physiol.* 286, L1038-L1044 (2004).
28. J. H. Gong, L. G. Ratkay, J. D. Waterfield, I. Clark-Lewis, *J.Exp.Med.* 186, 131-137 (1997).
29. M. Yamamoto et al., *Am.J.Pathol.* 166, 1475-1485 (2005).
30. S. Kitamoto, K. Egashira, A. Takeshita, *J.Pharmacol.Sci.* 91, 192-196 (2003).
31. Y. Sheikine and G. K. Hansson, *Ann.Med.* 36, 98-118 (2004).
32. L. Boring, J. Gosling, M. Cleary, I. F. Charo, *Nature* 394, 894-897 (1998).
33. A. D. Schecter et al., *J.LeucocyteBiol.* 75, 1079-1085 (2004).
34. H.-U. Demuth, C. H. McIntosh, R. A. Pederson, *Biochim.Biophys.Acta* 1751, 33-44 (2005).
35. M. D. Gorrell, V. Gysbers, G. W. McCaughan, *Scand.J.Immunol.* 54, 249-264 (2001).
36. A. M. Lambeir, C. Durinx, S. Scharpe, M. De, I., *Crit.Rev.Clin.Lab.Sci.* 40, 209-294 (2003).
37. T. Chikuma, K. Taguchi, M. Yamaguchi, H. Hojo, T. Kato, *J.Chromatogr.B Analyt.Technol.Biomed.Life Sci.* 806, 113-118 (2004).
38. F. Cipollone et al., *Arterioscler.Thromb.Vasc.Biol.* 21, 327-334 (2001).
39. Y. Jiang, D. I. Beller, G. Frendl, D. T. Graves, *J.Immunol.* 148, 2423-2428 (1992).
40. O. Dewald et al., *Circ.Res.* 96, 881-889 (2005).
41. A. M. Ferreira et al., *Cytokine* 30, 64-71 (2005).

The technical assistance of Kathrin Czislik, Sandra Torkler, Katja Kaschik and Stephan Reich is gratefully acknowledged. In addition, we thank Leona Wagner for helpful discussion. Prof. H.-U. Demuth serves also as CSO of Probiodrug AG and holds stock of the company.

Figure 1.

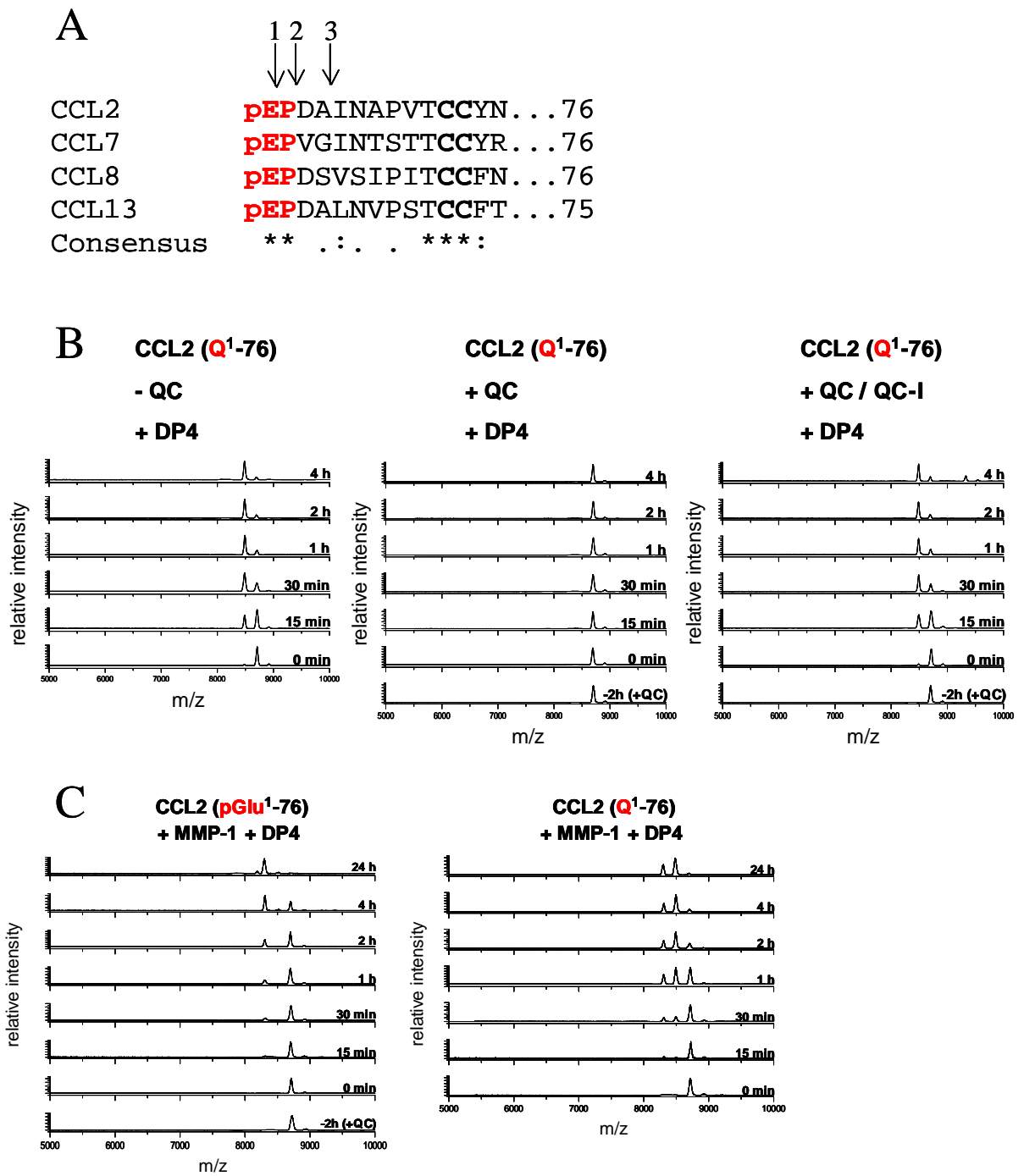


Figure 2.

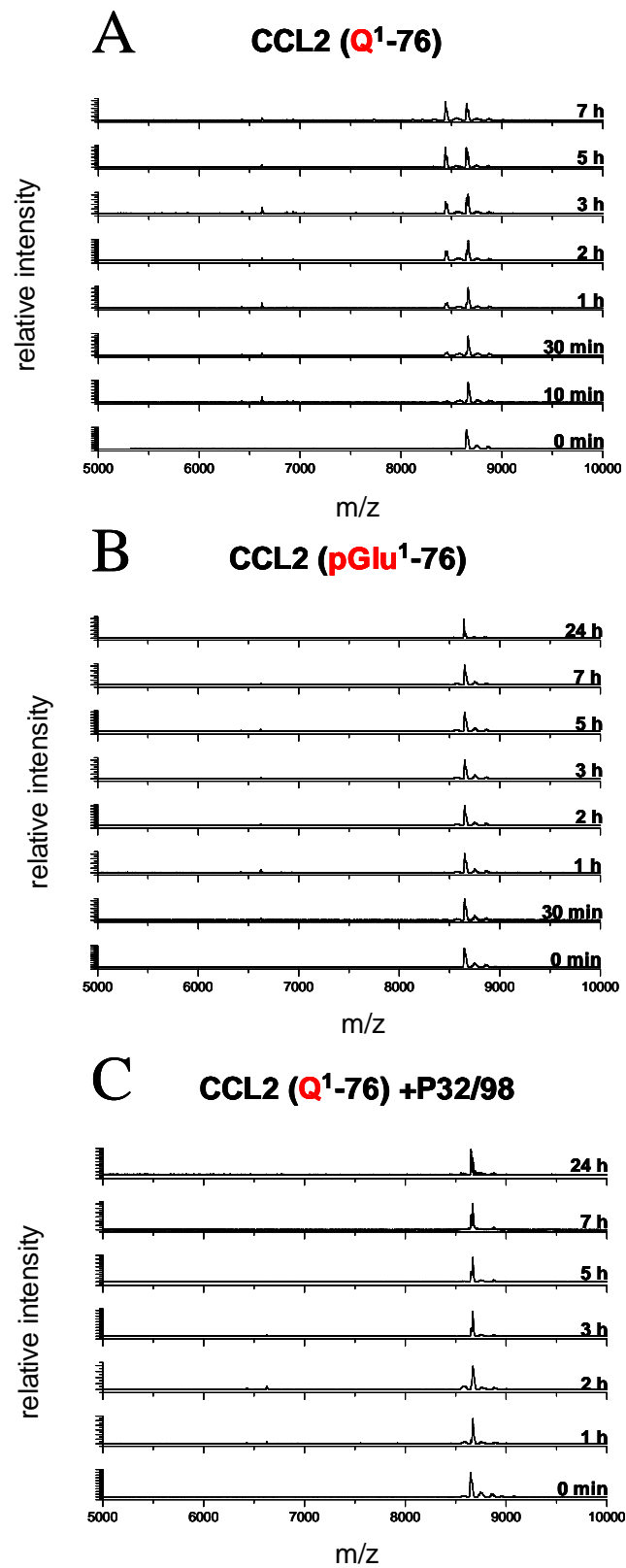


Figure 3.

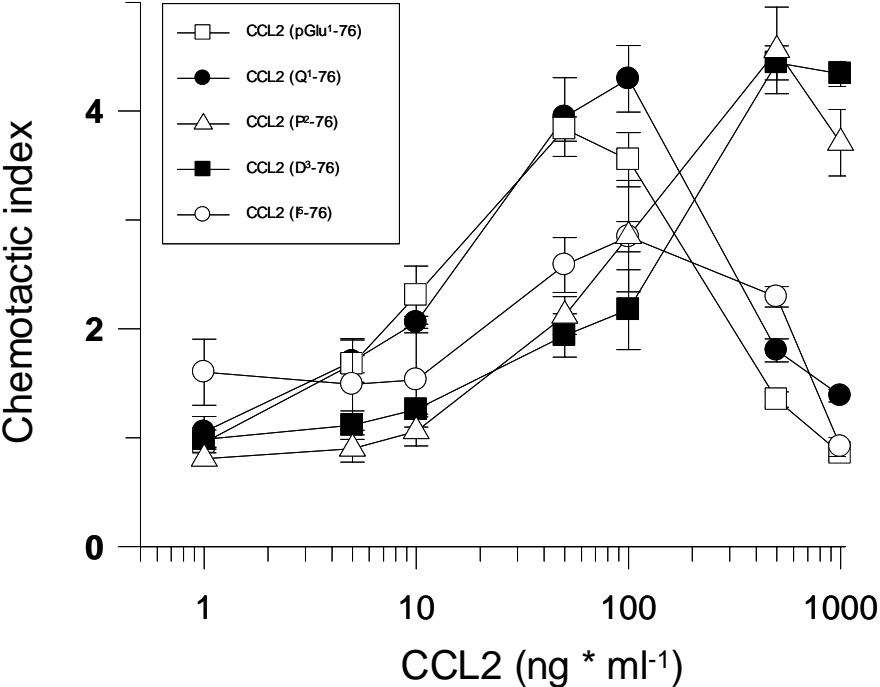


Figure 4.

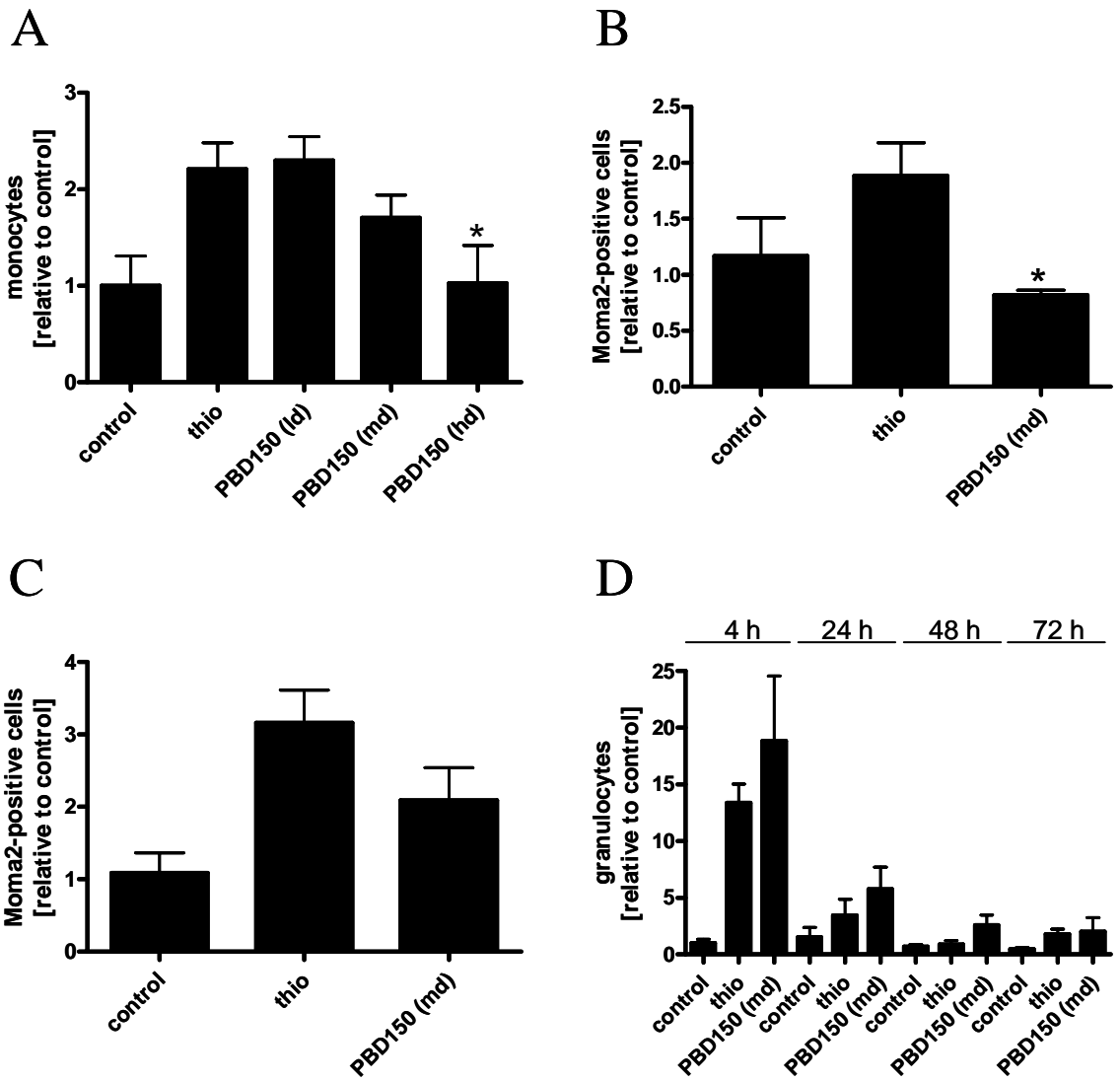
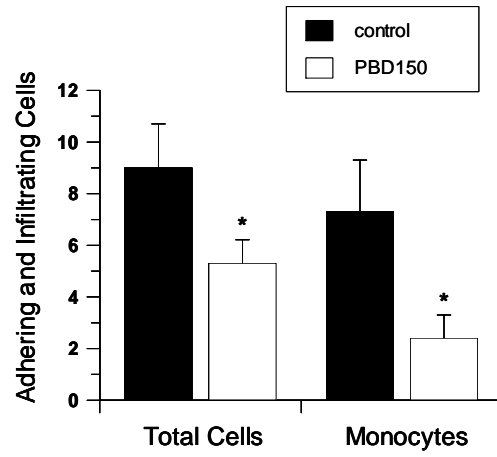
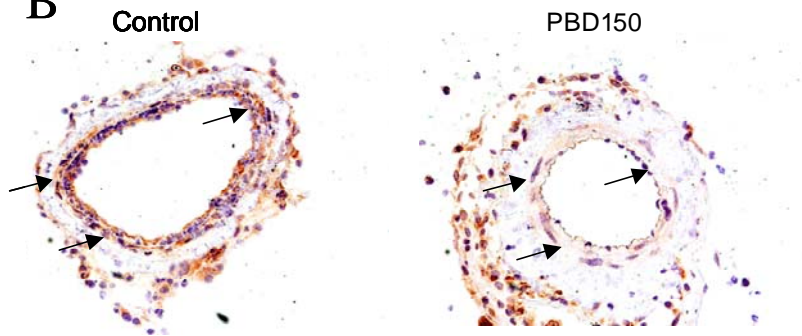


Figure 5.

A



B



C

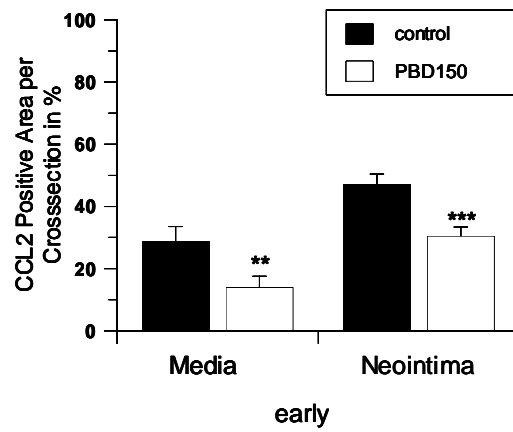
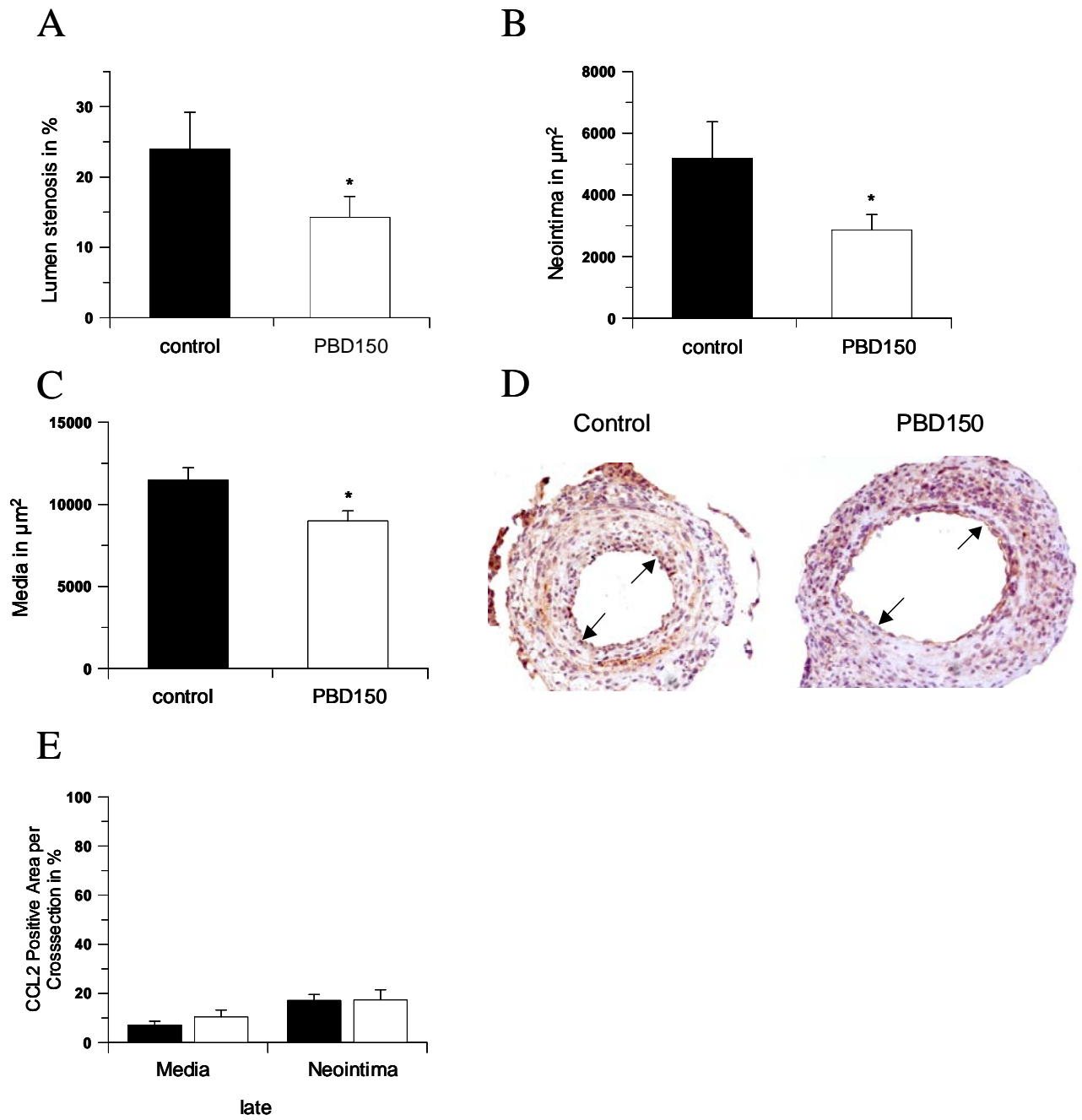


Figure 6.



Supporting Online Material for

Enhancing a Chemokine's Fate for Degradation: A Novel

Therapy for Cardiovascular Disease

Holger Cynis, Torsten Hoffmann, Susanne Manhart, Katrin Gans, Martin Kleinschmidt, Jens-Ulrich Rahfeld, Reinhard Sedlmeier, Anke Müller, Sigrid Graubner, Ulrich Heiser, Astrid Kehlen, Daniel Friedrich, Raik Wolf, Paul H.A. Quax, Mikael Thomsen, Stephan Schilling & Hans-Ulrich Demuth¹

* To whom correspondence should be addressed. E-mail: stephan.schilling@probiodrug.de

This PDF file includes

Materials and Methods

Fig. S1 to S5

References

Materials and Methods

TransWell chemotaxis assay

Human acute monocytic leukaemia cell line THP-1 was cultured in RPMI1640, 10 % FBS, in a humidified atmosphere of 5% CO₂ at 37°C. The chemotactic assay was performed using 24-well TransWell plates with a pore size of 5 µm (Corning). 600 µl of chemoattractant solution were applied to the lower chamber. Serum-free RPMI was applied as negative control. THP-1 cells were harvested and resuspended in RPMI1640 in a concentration of 1*10⁶ cells / 100 µl and applied in 100 µl aliquots to the upper chamber. Cells were allowed to migrate towards the chemoattractant for 2 h at 37°C. Subsequently, cells from the upper chamber were discarded and the lower chamber was mixed with 50 µl 70 mM EDTA in PBS and incubated for 15 min at 37°C to release cells attached to the membrane. Afterwards, migrated cells were counted using a cell counter system (Schärfe System, Reutlingen). The chemotactic index was calculated by dividing cells migrated to the stimulus from cells migrated to the negative control.

N-terminal degradation of human CCL2 by DP4, ApP, MMP-1 and human serum

Recombinant human CCL2, carrying an N-terminal glutaminy residue (Peprotech, Rocky Hill) was dissolved in 25 mM Tris/HCl pH 7.6 in a concentration of 10 µg/ml. The CCL2 solution was either pre-incubated with recombinant human QC (1) (0.6 µg/ml) for 2 h at 30°C and subsequently incubated with DP4 (2) or ApP (R&D Systems, Wiesbaden) or incubated with proteases without QC.

The MMP-1 proenzyme from human rheumatoid synovial fibroblasts (Calbiochem, Nottingham) was activated using 25 mM p-aminophenylmercuric acetate (APMA), dissolved in 0.1 N NaOH at 37°C for 3h in an APMA:enzyme-ratio of 1:10. For analysis of cleavage of CCL2(pGlu1-76), a preincubation with QC was performed as described above.

In addition to the cleavage by recombinant proteases, human CCL2 (Peprotech) was dissolved in 25 mM Tris/HCl, pH 7.6 in a concentration of 100 µg/ml and incubated with human serum (1:50 in 25 mM Tris/HCl, pH 7.6). In addition, the incubation of CCL2(Q¹-76) was carried out in the presence of 9.6 µM DP4-inhibitor isoleucyl-thiazolidide (P32/98) (3). All samples were analyzed using Maldi-TOF-MS after the indicated times.

Maldi-TOF-MS

Matrix-assisted laser desorption/ionization mass spectrometry was performed using the Voyager De Pro (Applied Biosystems, Darmstadt, Germany) in a linear mode. 5µl of the samples from the degradation experiment was mixed and co-crystallized with 5 µl of matrix solution (Sinapinic acid 20 mg/ml in acetonitrile / 0.1 % TFA in water, 50 :50 (v/v)), 1µl of this solution was spotted on the sample plate and air dried. The analytes were ionized by a nitrogen laser pulse (337 nm) and accelerated under 20 kV with a time delayed extraction before entering the time-of-flight mass spectrometer. Detector operation was in the positive ion mode ranging from 2000 to 20000 amu. Insulin and myoglobin solutions (Sigma Aldrich, Schnellendorf) were used for calibration in this range according to the instructor's manual from Applied Biosystems. Each spectrum represents the sum of at least 6x 100 laser pulses.

Thioglycollate-induced peritonitis in mice

The experiments were approved by the animal well fare committee of the administration department of the state Saxony-Anhalt (approval number: 203.h-42502-2-856probio). C57/Bl6J mice were purchased from Charles River Laboratories (Kisslegg, Germany). For each experiment, the mice were age- and sex-matched. An intraperitoneal injection of 25 ml/kg body weight of sterile 8% (w/v) thioglycollate (Sigma-Aldrich) was used to induce peritonitis. At different time points before and after thioglycollate application, mice were injected i.p. with 70 µmole/kg (low dose, ld), 140 µmole/kg (medium dose, md) and 280

$\mu\text{mole/kg}$ (high dose, hd) of QC-inhibitor PBD150 (molecular weight PBD150: 356,9 g/mole). For lavage of the peritoneum, the animals were anesthetized using 2% isofluran. Peritoneal exudates were collected by washing the peritoneum with 8 ml of sterile PBS at two time points (4 and 24 hours) after thioglycollate injection. The cells were collected by centrifugation and stained according to the manufacturer's instructions for BD Trucount tubes (BD Trucount tubes; catalog no. 340334; BD Biosciences, Franklin Lakes, NJ). Cells were blocked with CD16/32 (Caltag) and stained with Ly6G-PE (Miltenyi, Auburn, CA) /F4/80-APC (Caltag/Invitrogen, Carlsbad, CA) as well as IgG1-PE (BD)/IgG2a-APC (Caltag) as isotype controls for 15 min. After staining, cells were lysed with BD FACSLyse (BD) in the dark at room temperature for 15 min. Moma2-FITC (Acris, Herford) positive cells were stained using the inside stain kit from Miltenyi. Flow cytometric analysis was performed on a BD FACSCalibur (BD, Franklin Lakes, NJ) based on 5000 beads per sample as reference standard.

*Cuff-induced accelerated atherosclerosis in ApoE3*Leiden mice*

After approval by the TNO animal well fare committee, 30 male ApoE3Leiden mice (4) (age 12 weeks) were fed a mildly hypercholesterolemic diet for 3 weeks prior to surgical cuff placement. Thereafter, the mice underwent surgical non-constricting cuff placement (day 0) and were divided into 2 groups, matched for plasma cholesterol levels. The mice either received control (acidified) drinking water or drinking water containing the QC inhibitor 1-(3-(1H-imidazol-1-yl)propyl)-3-(3,4-dimethoxyphenyl)thiourea hydrochloride (5) in a concentration of 2.4-mg/ml. 7 days after start of treatment, the inhibitor concentration was reduced to 1.2 mg/ml. 5 Mice of each group were sacrificed after 2 days for analysis of monocyte adhesion and infiltration, and 10 mice were sacrificed after 2 weeks for histomorphometric analysis to quantify the inhibition of accelerated atherosclerotic lesions and neointima formation.

Surgical procedure of cuff placement

At the time of surgery, mice were anaesthetized with an intraperitoneal injection of 5 mg/kg Dormicum, 0.5 mg/kg Domitor and 0.05 mg/kg Fentanyl. This cocktail gives complete narcosis for at least one hour and can be quickly antagonized with Antisedan 2.5 mg/kg and Anexate 0.5 mg/kg. A longitudinal 1 cm incision was made in the internal side of the leg and the femoral artery is dissected for 3 mm length from the femoral nerve and femoral vein. The femoral artery is looped with a ligature and a non-constrictive fine bore polyethylene tubing (0.4 mm inner diameter, 0.8 mm outer diameter, length 2 mm) is longitudinally opened and sleeved loosely around the femoral artery. The cuff is closed up with two ligature knots. The skin is closed with a continued suture. After surgery, the animals were antagonized and placed in a clean cage on top of a heating pad for a few hours.

Sacrifice of the animals

For histological analysis, animals were sacrificed either 2 days or 14 days after cuff placement. The thorax of the anaesthetized animals was opened and a mild pressure-perfusion (100 mmHg) with 4% formaldehyde was performed for 3 minutes by cardiac puncture. After perfusion, a longitudinal 2 cm incision was made in the internal side of the leg and the cuffed femoral artery was harvested as a whole and fixed overnight in 4% formaldehyde and processed to paraffin.

Analysis of monocyte adhesion and CCL2 expression

Adhesion of leukocytes in general and monocytes/macrophages in particular to the activated endothelium of the cuffed vessel wall was investigated by microscopic analysis of cross sections harvested 2 days after cuff placement. The number of adhering and/or infiltrating leukocytes in general, identified as adhering cells at the luminal side of the vessel segment,

and monocytes/macrophages in particular was counted and illustrated as cells per cross-section or as defined areas per cross section. Monocytes were identified by specific immunohistochemical staining using AIA31240 antibody, recognizing monocytes and macrophages. In addition on these sections a specific immunohistochemical staining for CCL2 was performed.

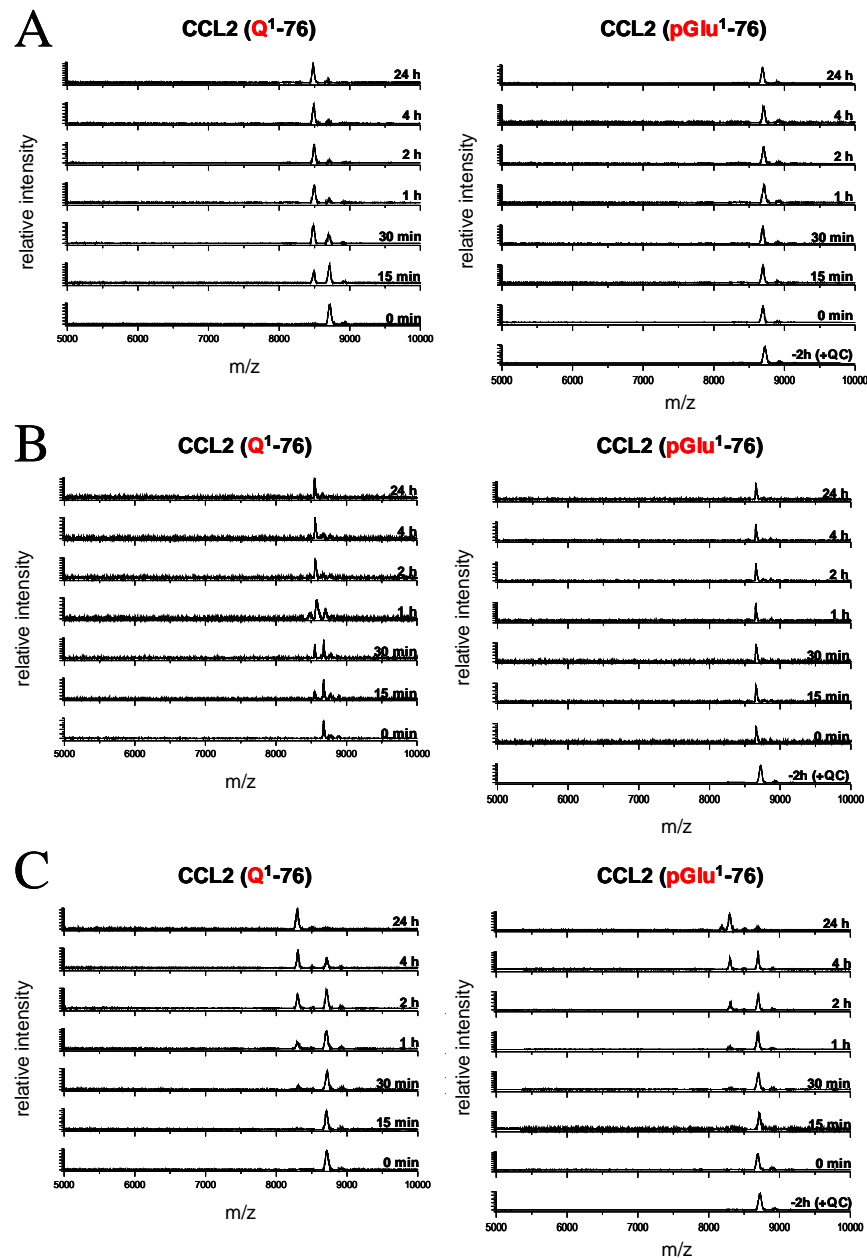
Analysis of vascular remodeling and accelerated atherosclerosis

Vessel wall remodelling, accelerated atherosclerosis and neointima formation were analyzed morphometrically in all mice sacrificed after 14 days. A full comparison between the two groups was performed for all relevant vessel wall parameters (neointima formation, vascular circumference (i.e. outward remodelling), media thickness, lumen stenosis). Accelerated atherosclerosis was analyzed by immunohistochemical staining for macrophages in the lesion area by AIA31240 antibody. The sections were also stained for CCL2.

Statistical analysis

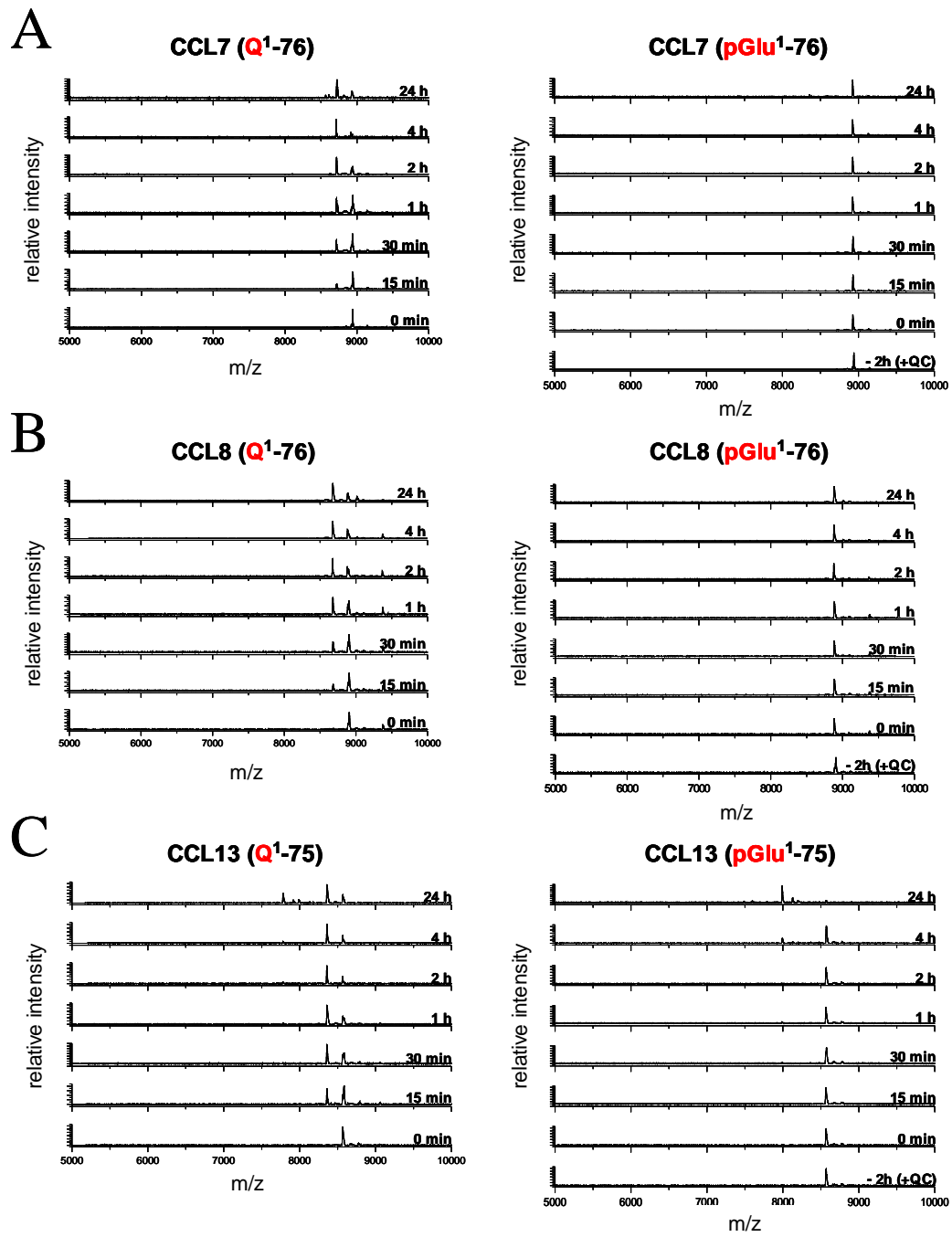
Statistical analysis was performed using Student's *t*-test or one-way ANOVA using Excel from Microsoft or Graph pad prism 4 from Graphpad Software Inc., respectively.

Figure S1:



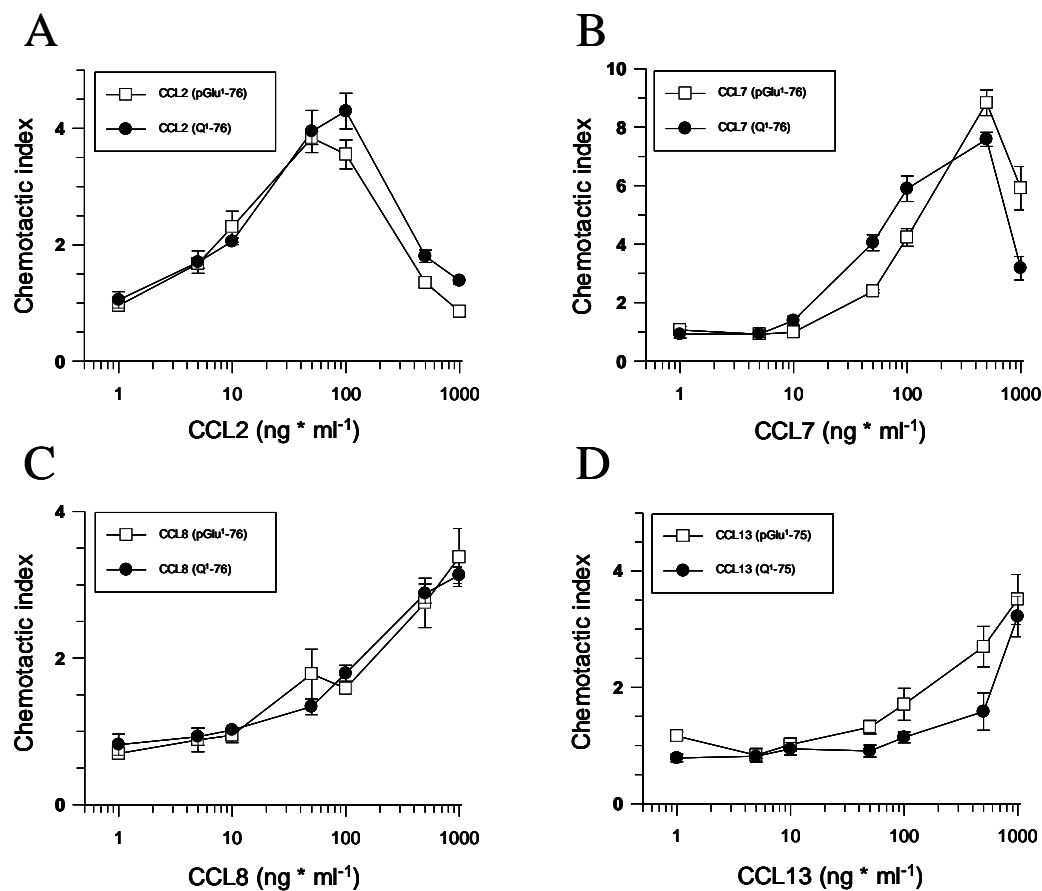
(A) Maldi-TOF mass spectra showing the degradation of CCL2(Q¹-76) by DP4 only in case of an unblocked CCL2(Q¹) N-terminus. Pyroglutamic acid, constituting the native N-terminus, protects CCL2(pGlu¹-76) against truncation by DP4. (B) Maldi-TOF mass spectra illustrating the N-terminal truncation of CCL2(Q¹-76) by ApP. Again, CCL2(pGlu¹-76) is protected against cleavage. (C) CCL2 is cleaved by MMP-1, irrespective of the N-terminal amino acid.

Figure S2:



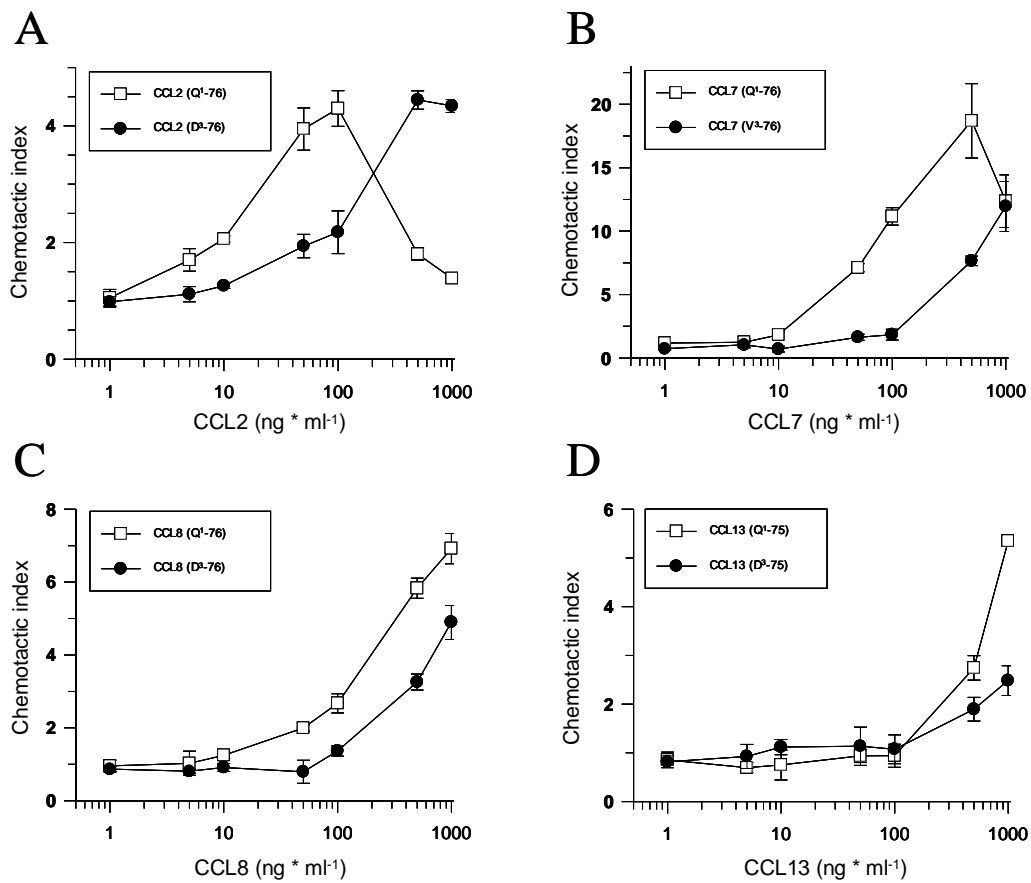
Mass spectra of the time course of the degradation of human (A) CCL7, (B) CCL8 and (C) CCL13 by DP4 in absence and presence of an N-terminal pGlu-residue. Only peptides with an N-terminal glutaminy residue are accessible for cleavage by DP4.

Figure S3:



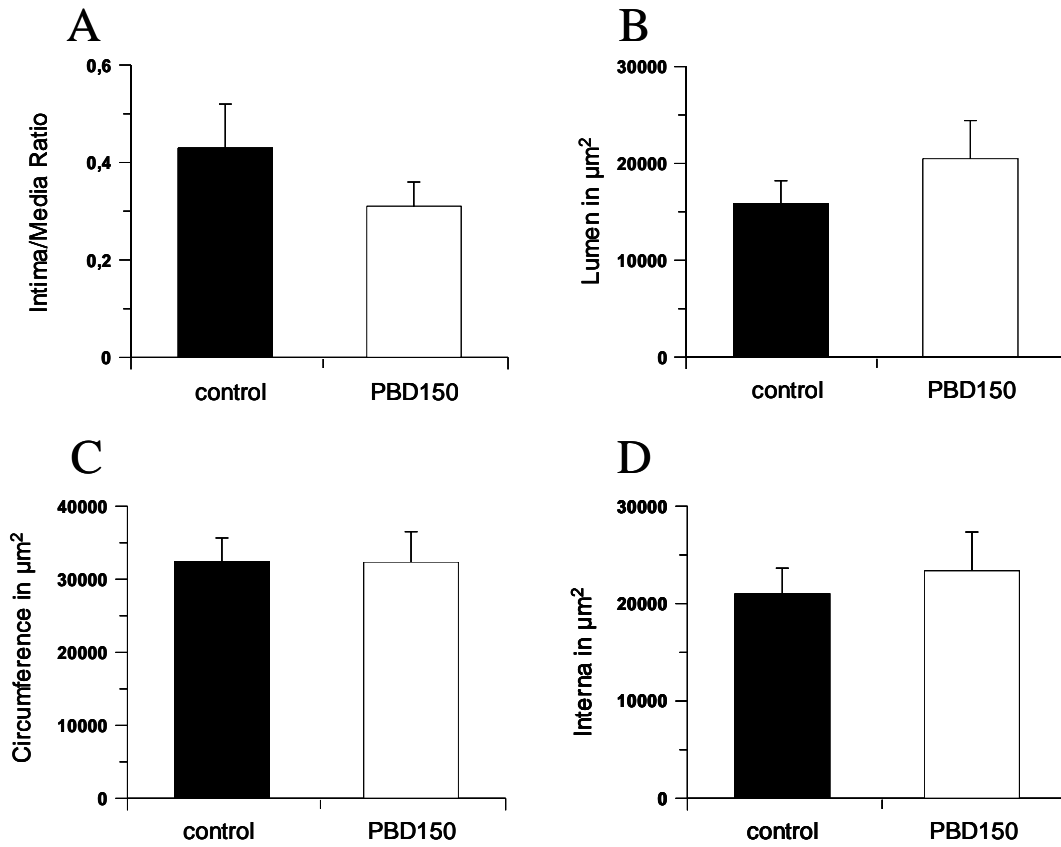
Comparison of the potency of (A) CCL2, (B) CCL7, (C) CCL8 and (D) CCL13 to attract THP-1 monocytes subject to the presence of an N-terminal pGlu-residue. The chemotactic index was determined in trans-well assays.

Figure S4:



Comparison of the ability of (A) CCL2, (B) CCL7, (C) CCL8 and (D) CCL13 starting with N-terminal amino acid Q¹ or D³ to attract THP-1.

Figure S5:



Morphometric quantification of (A) the intima /media ratio, (B) remaining lumen in μm^2 , (C) the circumference of the cuffed vessel segments in μm^2 and (D) the area of the interna in μm^2 , depending on PBD150 treatment.

References

1. S. Schilling et al., *Biochemistry* 41, 10849-10857 (2002).
2. M. Engel et al., *Proc.Natl.Acad.Sci.U.S.A.* 100, 5063-5068 (2003).
3. R. A. Pederson et al., *Diabetes* 47, 1253-1258 (1998).
4. J. H. Lardenoye et al., *Circ.Res.* 87, 248-253 (2000).
5. M. Buchholz et al., *J. Med. Chem.* 49, 664-677 (2006).

Danksagung

Mein besonderer Dank gilt Herrn Prof. Dr. Hans-Ulrich Demuth für die Überlassung dieses überaus interessanten Themas, das mir entgegengebrachte Vertrauen und die umfassende Unterstützung bei der Realisierung dieser Arbeit.

Bei Herrn Prof. Dr. Milton T. Stubbs bedanke ich mich herzlich für die Bereitschaft, diese Arbeit an der Martin-Luther-Universität Halle-Wittenberg zu betreuen.

Herrn Dr. Stephan Schilling bin ich zu großem Dank für wertvolle Diskussionen und tatkräftige Unterstützung verpflichtet.

Den MitarbeiterInnen der Probiodrug AG, insbesondere der Arbeitsgruppe Enzymologie, sowie Frau PD Dr. Astrid Kehlen, Herrn Dr. Torsten Hoffmann, Herrn Dr. Jens-Ulrich Rahfeld und Herrn Dr. Ingo Schulz danke ich für die angenehme Zusammenarbeit, stete Hilfsbereitschaft und Unterstützung.

Meiner Familie, besonders meiner Frau Kathrin, danke ich für das Verständnis und das in mich gesetzte Vertrauen, welches maßgeblichen Anteil am Gelingen der vorliegenden Arbeit hatte.

Lebenslauf

Angaben zur Person

Name: Holger Cynis
Geburtsdatum/-ort: 05.09.1978, Wippra
Staatsangehörigkeit: deutsch
Familienstand: verheiratet

Ausbildung

1985-1988 Teiloberschule Bräunrode
1988-1991 Polytechnische Oberschule „Nguyen duc Soat“, Grossörner
1991-1997 Gymnasium „Am Markt“, Hettstedt, Abschluss: Abitur
1997-1999 Wehrdienst
1999-2001 Grundstudium Biologie, Martin-Luther-Universität Halle-Wittenberg
2001-2004 Hauptstudium Biologie, Martin-Luther-Universität Halle-Wittenberg, Abschluss 09/2004 Diplom-Biologe, Diplomarbeit: „Expression von humanem Amyloid Precursor Protein in Glutaminyl-Cyclase exprimierenden Säugerzelllinien“, Institut für Genetik, Prof. Dr. G. Reuter
2002-2004 Probiodrug AG, wissenschaftliche Hilfskraft
2004-2006 Studium Medizin, Martin-Luther-Universität Halle-Wittenberg
seit 10/2004 Probiodrug AG, wissenschaftlicher Mitarbeiter
seit 10/2006 Promotionsstudent, Martin-Luther-Universität Halle-Wittenberg
seit 2006 Assoziierter Promotionsstudent „Marie Curie Ph.D. Graduate School – Neurodegeneration in Alzheimer’s disease (NEURAD)“
seit 10/2007 Gastwissenschaftler Universität von Kalifornien, San Diego (UCSD)

Erklärung

Hiermit erkläre ich an Eides statt, dass ich die vorliegende Arbeit selbständig und ohne fremde Hilfe verfasst, andere als die angegebenen Quellen und Hilfsmittel nicht benutzt und die den benutzten Werken wörtlich oder inhaltlich entnommenen Stellen gekennzeichnet habe.

Die Arbeit wurde nur an der Naturwissenschaftlichen Fakultät I der Martin-Luther-Universität eingereicht.

Die der Dissertation angefügten Publikationen umfassen den Inhalt der eigenen Arbeiten und wurden vollständig oder in den entsprechenden Teilgebieten von mir verfasst.

Halle (Saale), den 26.01.2009

A handwritten signature in black ink, appearing to read "Volker E." followed by a stylized flourish or scribble.